LEABHARLANN CHOLÁISTE NA TRÍONÓIDE, BAILE ÁTHA CLIATH | TRINITY COLLEGE LIBRARY DUBLIN
Ollscoil Átha Cliath | The University of Dublin

Terms and Conditions of Use of Digitised Theses from Trinity College Library Dublin

Copyright statement

All material supplied by Trinity College Library is protected by copyright (under the Copyright and Related Rights Act, 2000 as amended) and other relevant Intellectual Property Rights. By accessing and using a Digitised Thesis from Trinity College Library you acknowledge that all Intellectual Property Rights in any Works supplied are the sole and exclusive property of the copyright and/or other IPR holder. Specific copyright holders may not be explicitly identified. Use of materials from other sources within a thesis should not be construed as a claim over them.

A non-exclusive, non-transferable licence is hereby granted to those using or reproducing, in whole or in part, the material for valid purposes, providing the copyright owners are acknowledged using the normal conventions. Where specific permission to use material is required, this is identified and such permission must be sought from the copyright holder or agency cited.

Liability statement

By using a Digitised Thesis, I accept that Trinity College Dublin bears no legal responsibility for the accuracy, legality or comprehensiveness of materials contained within the thesis, and that Trinity College Dublin accepts no liability for indirect, consequential, or incidental, damages or losses arising from use of the thesis for whatever reason. Information located in a thesis may be subject to specific use constraints, details of which may not be explicitly described. It is the responsibility of potential and actual users to be aware of such constraints and to abide by them. By making use of material from a digitised thesis, you accept these copyright and disclaimer provisions. Where it is brought to the attention of Trinity College Library that there may be a breach of copyright or other restraint, it is the policy to withdraw or take down access to a thesis while the issue is being resolved.

Access Agreement

By using a Digitised Thesis from Trinity College Library you are bound by the following Terms & Conditions. Please read them carefully.

I have read and I understand the following statement: All material supplied via a Digitised Thesis from Trinity College Library is protected by copyright and other intellectual property rights, and duplication or sale of all or part of any of a thesis is not permitted, except that material may be duplicated by you for your research use or for educational purposes in electronic or print form providing the copyright owners are acknowledged using the normal conventions. You must obtain permission for any other use. Electronic or print copies may not be offered, whether for sale or otherwise to anyone. This copy has been supplied on the understanding that it is copyright material and that no quotation from the thesis may be published without proper acknowledgement.

Investigation of the Role of RACK1 in T lymphocyte Migration

By

Christine Rudolph

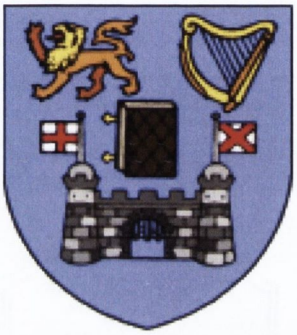

A dissertation submitted in partial fulfilment for the degree of

Doctor in Philosophy (Molecular Medicine)

Under the supervision of Aideen Long, Ph.D. at

Trinity College Dublin

2012

TRINITY COLLEGE
2 4 MAY 2013
LIBRARY DUBLIN

Thesis 9829

Declaration

I declare that this thesis has not been submitted as an exercise for a degree at this or any other university and it is entirely my own work. I agree to deposit this thesis in the University's open access institutional repository or allow the library to do so on my behalf, subject to Irish Copyright Legislation and Trinity College Library conditions of use and acknowledgement.

Christine Lynn Rudolph

Summary

Induction of the immune response and production of pro-inflammatory cytokines results in the upregulation of ICAM-1 expressed on endothelial cells. Binding of ICAM-1 to the β_2 integrin receptor LFA-1 on T cells induces T cell polarisation allowing the cell to migrate between endothelial cells to the site of injury or inflammation. Transendothelial migration involves the rearrangement of the cellular cytoskeleton, a process dependent on translocation of Protein Kinase C (PKC) isotypes. Receptor for Activated C Kinase 1 (RACK1) is a scaffolding protein which directs the subcellular localisation and activity of PKC, where it phosphorylates specific substrates in response to different stimuli. RACK1 has been shown to interact with membrane-bound receptors, including the cytoplasmic domain of β integrin, thus linking PKC to integrin-mediated signal transduction and implicating a role for RACK1 in integrin-mediated immune cell adhesion and migration. Recent studies on RACK1 suggest that this adaptor protein plays an essential role in migratory capacity in all cell types where it is expressed. Despite its apparent dominant role in cell migration, the role of RACK1 in the context of immune cell migration has been widely overlooked. This thesis aimed to characterise RACK1 and any potential regulatory function in integrin-mediated immune cell migration. To investigate the function of RACK1 in mediating immune cell migration, four projects have been pursued.

PKC is a family of serine/threonine kinases involved in signal transduction pathways that mediate a number of downstream events, including remodelling of the cellular cytoskeleton, regulation of gene expression, and immune responses. Several studies have reported the translocation of PKC isozymes in response to integrin activation. Therefore, the first study presented in Chapter 3 characterised the expression of RACK1 in association with cytoskeletal components and key polarity proteins in resting and polarised migrating T cells. Immunocytochemistry data indicated RACK1 translocates from a cytosolic, peripheral distribution in resting cells to the leading edge of polarised migrating cells. In addition, RACK1 partially co-localised with cytoskeletal elements, including filamentous actin and the microtubule network, and atypical PKC ζ, a key polarity regulator. Furthermore, suppression of RACK1 by siRNA prevented PKC ζ translocation to the leading edge of LFA-1-mediated migrating T cells. Altogether, these results implicate a role for RACK1 in lymphocyte polarity during directional cell migration.

The second project described in Chapter 4 details the functional analysis of RACK1 in T cell polarisation and migration. Silencing RACK1 by siRNA reduced cell polarisation, but enhanced integrin-mediated SDF-1α-stimulated chemotatic migration. Conversely, overexpression of RACK1 inhibited integrin-mediated chemotatic migration. In addition, analysis of time-lapse microscopy indicated a reduction in speed and persistence of random cell migration on the integrin ligand ICAM-1 in RACK1-deficient cells as compared to control cells. Knockdown of RACK1 did not significantly affect integrin-mediated adhesion to the integrin ligand ICAM-1. Therefore, our findings indicate RACK1 is required for SDF-1α-mediated lymphocyte migration on

ICAM-1 by influencing velocity and directionality but in a manner that is independent of LFA-1 integrin activation or adhesion.

In order to further examine the molecular mechanisms by which RACK1 regulates immune cell migration, Chapter 5 details the comparative proteomic approach employed to determine proteins associated with RACK1 in resting and integrin-mediated migrating T cells. Several protein hits were identified by mass spectrometric analysis and the endogenous interaction with RACK1 was confirmed by immunoassays. In addition, RACK1 was found to be enriched in both the cytosolic and cytoskeletal fractions following LFA-1 activation suggesting an increase in RACK1 expression during cell migration. Furthermore, RACK1 was identified to associate with the distal ends of polymerised MTs in association with MT stabilising plus-end binding proteins, implicating a role in MT stability during cell migration.

Finally, the putative association between RACK1 and the motor protein non-muscle myosin heavy chain IIA (NMHC-IIA) and the functional implications of this interaction in immune cell migration were explored in the fourth study in Chapter 6. Full length and NMHC-IIA-derived truncation mutants were generated to use in conjunction with a RACK1 peptide array to determine domain-specific interactions. The direct interaction between RACK1 and NMHC-IIA was confirmed with the use of a RACK1 peptide array. The putative binding sites for NMHC-IIA on RACK1 were identified by peptide substitution arrays and *in-silico* interaction modelling, which revealed three candidate regions within the RACK1 sequence that contribute to a NMHC-IIA binding interface, specifically residues that are exposed on the outer β-strand of the propeller blades WD2, WD3, and WD4 of RACK1. Consistent with reports that chemokine receptors localise to the leading edge of chemokine-stimulated lymphocytes, we found that RACK1 co-localised with NMHC-IIA in association with filamentous actin and the chemokine receptor CXCR4 in SDF-1α-stimulated polarised T cells. While, knockdown of RACK1 expression slightly affected the surface levels of expression of CXCR4, suppression of RACK1 did not significantly affect myosin activity by mediating the phosphorylation of myosin light chain Ser19. Future work is necessary to elucidate the functional implications of this interaction and other RACK1-mediated protein complexes to further define the role of RACK1 in regulating directional cell migration. Nevertheless, this study demonstrated RACK1 directly interacts with NMHC-IIA and may link actomyosin complexes to the leading edge in association with chemokine receptors, providing an essential chemo-mechanical link between extracellular signalling and motor protein contractility required for directional cell migration.

The results from this study indicate RACK1 is required for T cell polarisation and altered levels of RACK1 expression are detrimental to controlled cell migration and chemotaxis. In accordance with previous observations, silencing of RACK1 by siRNA enhanced the chemotatic migration of T lymphocytes, while overexpression of RACK1 inhibited SDF-1α-stimulated chemotaxis. Altogether, the results described in this dissertation have demonstrated a novel role for RACK1 through its interaction with the MT cytoskeleton, established polarity protein PKC ζ, and the motor protein NMHC-IIA in regulating immune cell migration.

Dedication

This work is dedicated to my mom and dad for their unconditional love and constant support.

And to Paul for your absolute belief in me. You were nothing that I could have expected and everything I could have hoped for.

Acknowledgements

I would like to thank my supervisor, Aideen Long, for her guidance, patience, optimism, and encouragement over these last four years. Thank you for giving me this opportunity and a place in your lab in which to explore and grow intellectually. Thank you for your continuous guidance throughout this project and for taking the time to shred my thesis to pieces and help me put it back together in a more cohesive manner.

I would like to thank everyone in the Cell and Molecular Biology Group past, present, and future:

Past- For their words of wisdom and sage advice and for setting such high levels of research excellence. To Dara for challenging me to expand my knowledge of lymphocyte biology. To Eugene for always offering valuable advice and useful suggestions. To Ruchika for her cheerfulness and encouraging words. And to Seow Theng for her patience and willingness to help.

Present- Thanks for making the lab an entertaining and intellectually stimulating place to work. Thanks for all your honest and humbling scrutiny of my data at Tuesday morning lab meetings and for sharing all the highs and lows of research...for celebrating the big milestones (publications, passing the transfer viva, presentation awards) and for the little things...like sitting out on the grass because it is actually sunny and Kenny's or the Pav on a Friday.

To Mike for his constant help from beginning to end and for putting up with all my T cell related questions...I am indebted. To Antje for our discussions- scientific and non-scientific. To Denise for always being willing to lend a hand with an experiment and all our chats from planning our weddings to terrors of the GNIB and everything in between. To Cormac for always playing his Ipod in the lab and expanding my musical tastes, or was it the other way around? To Anne-Marie and Fran for mixing it up and not studying T cells. And to all my fellow labmates for helping to make the research presented in this thesis possible.

I am also indebted to my collaborators Patrick Kiely and David Adams for making the myosin interaction work possible. I am in awe of your knowledge of RACK1.

A special thanks to Tony D. and Connla for all their help with the IN Cell and salvaging my experiment just when I was ready to start W.A.G.E. To Jen and Tanya for their

assistance with the confocal. To Tony R. for letting me 'borrow' all his lab equipment. And to Catherine Botting for the mass spec work.

Future- For they may continue my work, in which case Good Luck (you'll need it)!

I owe my deepest gratitude to everyone a part of the Ph.D. in Molecular Medicine Program, especially to Ross McManus, Sheila Walshe, and all of the professors on the course, for without whom this entire endeavour would not exist. I would like to heartily thank my mentors, Padraic Fallon and Henry Windle, for their invaluable advice, support, and encouragement throughout this research project. Thank you to the HRB for providing me with the financial assistance to carry out this research project and attend conferences abroad.

A special thanks to all my fellow Ph.D. students on the course. To Chris for being such a great friend and for essentially teaching me everything I know about genetics (even if it was over a Bulmers at the Pav). To Ruth and Fiona for providing an experienced ear for any doubts about writing a thesis, and to Darragh for just being a computer whiz.

Thanks to everyone in the reading room, you have made my time in the IMM (while not faster) vastly more enjoyable. To Ben for always making me laugh and forget about writing for a while. And to my girls Sinead, Ciara, Jill, and Cat for their constant distraction at work and our crazy nights out- London Round 2?

And, finally, thanks to my other family, Rita and Brendan and Daniel, for your kind words and encouragement. For pampering Paul and I when we came home to visit, it was always great to escape to the country and forget about science for a while, or sending down food with Paul when I was stuck in lab or writing. Thank you for all your support!

Table of Contents

Declaration i

Summary ii

Dedication iv

Acknowledgements v

Table of Contents vii

List of Figures xv

List of Tables xviii

Abbreviations xix

Keywords xxiii

1 General Introduction 5

1.1 Role of T Lymphocytes in the Immune Response 5

1.2 T cell Development 5

1.3 T cell Activation 6

1.4 T cell Migration 10

1.5 T cell Migratory Phenotype 11

1.5.1 The leading edge 13

1.5.2 The main cell body 13

1.5.3 The uropod 13

1.6 Molecular Mechanisms of T cell Migration 16

1.6.1 Induction of Cell Polarisation 16

1.6.2 Generation of Membrane Protrusions at the Leading Edge 17

1.6.3 Formation of Cell-Substratum Contact Sites 17

1.6.4 Forward Movement of the Cell Body and Retraction of the Uropod 17

1.7 T cell Signalling 18

1.8 PKC: A Key Signal-Transducing Enzyme 18

1.9 Identification of the RACK Family of Proteins 20

1.9.1 RACK1 22

1.9.2 RACK1 Protein Interactions 24
1.10 T cell Integrins 25
1.10.1 Features of LFA-1 structure 26
1.10.2 Activation of LFA-1 on T cells 29
1.10.3 LFA-1 Activation Induces Conformational Change 32
1.10.4 Distribution of LFA-1 in Migrating T cells 35
1.10.5 LFA-1 Ligands in T cells 38
1.10.6 LFA-1 Signalling in T cells 41
1.10.7 Integrin-Mediated T cell Migration 42
1.11 Composition and Regulation of Cytoskeletal Elements in T cells 45
1.11.1 Actin Cytoskeleton 46
1.11.2 Microtubule Network 48
1.11.3 Intermediate Filaments 49
1.11.4 Non-muscle Myosin II 51
1.12 Chemokine-stimulated Directional Cell Migration 53
1.13 Regulation of T cell Polarisation 57
1.14 Clinical Relevance 60
1.15 Research Objectives 62
2 Materials and Methods 67
2.1 Antibodies and Reagents 67
2.2 Constructs and siRNA 67
2.3 Cell Culture 67
2.3.1 Culture of Human Jurkat Leukemic T Cells 67
2.3.2 Culture of Human HuT78 T Cells 68
2.3.3 Human Embryonic Kidney (HEK) 293 Cells 68
2.4 Isolation and Expansion of Peripheral Blood T Lymphocytes 68
2.5 Transfection 69
2.5.1 Electroporation Methods 69
2.5.2 Calcium Phosphate Transfection 74

2.6 Bacterial Transformation for the Expansion of pEGFP-RACK1 74
2.7 High Content Analysis 75
2.8 *In vitro* T Cell Migration Assay 78
2.8.1 *In Vitro* Haptokinetic Migration Assay: Hut78 T cells 78
2.8.2 *In Vitro* Chemokinetic Migration Assay: Primary T cells 79
2.8.3 Live Cell Tracking of LFA-1-dependent T cell Motility 81
2.9 Plate-bound ICAM-1 Cell Adhesion Assay for HuT78 T Cells 81
2.10 Plate-bound ICAM-1 Cell Adhesion Assay for Primary T Cells 82
2.11 Transwell Chemotaxis Assay 83
2.12 Chemokine-induced Cell Polarisation Assay 84
2.13 Treatment with Inhibitors 84
2.14 Flow Cytometry 85
2.15 Preparation of Cellular Protein Extracts 85
2.16 Calculation of Protein Concentration of Lysates 86
2.17 Acetone Precipitation of Cell Lysates 86
2.18 Preparation of Cell Lysates for Detection of MLC phosphorylation 87
2.19 Sodium Dodecyl Sulphate Polyacrylamide Gel Electrophoresis (SDS-PAGE) 87
2.20 Immunoblot Analysis 87
2.21 Stripping of Western Blot Membranes 89
2.22 Densitometric Analysis 89
2.23 Immunocytochemistry 89
2.23.1 Cell Permeabilisation and Blocking 89
2.23.2 Immunofluorescence Staining 90
2.23.3 Confocal Microscopy 90
2.24 Detergent Extraction Assay 90
2.25 Immunoprecipitation 91
2.26 Coomassie Brilliant Blue Staining of SDS-PAGE Gels 93
2.27 Silver Staining of SDS-PAGE Gels 93
2.28 Mass Spectrometry and Analysis 94

2.29 *In Silico* Gene Ontology Analysis with PANTHER 95
2.30 Generation of FLAG Fusion Proteins 95
2.30.1 Amplification of Full Length (FL) MYH9 95
2.30.2 Bacterial Transformation of FL MYH9 99
2.30.3 Sequencing of FL MYH9 99
2.30.4 Design and Generation of NMHCIIA- Derived Fragments 102
2.30.5 Polymerase Chain Reaction 105
2.30.6 DNA Gel Electrophoresis 105
2.30.7 Topoisomerase Cloning 106
2.30.8 Restriction Digest 109
2.30.9 Recombination into Mammalian Expression Vector 111
2.30.10 Expression and Purification of FLAG Fusion Proteins 111
2.31 RACK1 Peptide Array 112
2.32 Statistical analysis 113
3 Characterisation of RACK1 Expression in Resting and Migrating T Cells 117
3.1 Introduction 117
3.2 Objectives 120
3.3 Results 123
3.3.1 RACK1 Translocates to the Leading Edge of LFA-1-Induced Migrating T Cells 123
3.3.2 RACK1 Partially Associates with Actin and MT Cytoskeleton in T Cells 126
3.3.3 Investigation of RACK1 in Association with Candidate Cytoskeletal Associated Elements 129
3.3.4 SDF-1α Activation Induces Translocation of RACK1 to the Leading Edge of Migrating T Cells 133
3.3.5 RACK1 Associates with Polarity Regulator Par 3 in Integrin-activated Polarised T cells 136
3.3.6 RACK1 Associates with PKC ζ at the Leading Edge of LFA-1-induced Migrating T cells 138

3.3.7 Suppression of RACK1 Affects PKC ζ Distribution and Recruitment to Leading Edge in T cells 140

3.4 Discussion 144

3.4.1 Conclusion 148

4 Functional Analysis of RACK1 in Integrin-Mediated T cell Migration 151

4.1 Introduction 151

4.2 Objectives 154

4.3 Results 156

4.3.1 KD of RACK1 Decreases T Cell Polarisation HuT78 T cell Line 156

4.3.2 Investigation of KD of RACK1 on ICAM-1 Adhesion Assay in the HuT78 T cell Line 161

4.3.3 Inhibition of RACK1 Expression Enhances SDF-1α-stimulated Chemotaxis in HuT78 T cell Line 166

4.3.4 Optimisation of siRNA Transfection of Primary T Cells 171

4.3.5 KD of RACK1 Reduces Cell Polarisation in Primary T Cells 171

4.3.6 KD of RACK1 Decreases Speed and Persistence of Migration in Primary T Cells 175

4.3.7 Depletion of RACK1 Does Not Affect Adhesion to ICAM1 in Primary T Cells 178

4.3.8 Inhibition of RACK1 Expression Enhances SDF-1α-stimulated Chemotaxis in Primary T Cells 180

4.3.9 Overexpression of RACK1 Inhibits SDF-1α-Stimulated Chemotaxis in Primary T Cells 182

4.4 Discussion 184

4.4.1 Conclusion 189

5 Identification of RACK1-associated Proteins by a Proteomic Approach 193

5.1 Introduction 193

5.2 Objectives 194

5.3 Results 197

5.3.1 Isolation of RACK1 Immunoprecipitates 197

5.3.2 Categorisation of Proteins Identified by Mass Spectrometry 200

5.3.3 Validation of Mass Spectrometry by Immuno-assay Studies 202

5.3.4 Investigation of Cytoskeletal Components and Associated Proteins in Resting and Migrating Lymphocytes 206

5.3.5 RACK1 Associates with Polymerised MTs and MT Plus-end Binding Proteins in LFA-1-induced Migrating T cells 211

5.4 Discussion 222

5.4.1 Cytoskeletal Proteins 222

5.4.2 Signal Transduction 223

5.4.3 Transcription Regulation 224

5.4.4 RNA maturation, protein biosynthesis 224

5.4.5 Metabolic Enzymes 224

5.4.6 Molecular Chaperones 225

5.4.7 Validation of Mass Spectrometry 225

5.4.8 Analysis of Cytosolic and Cytoskeletal Fractions Following Detergent Extraction in T cells 226

5.4.9 RACK1 Localises to the Distal Ends of Polymerised MTs in T cells 227

5.4.10 Examination of NMHC-IIA Interaction with RACK1 in T cells 228

5.4.11 Conclusion 229

6 RACK1 Associates with NMHC-IIA in T Cells 233

6.1 Introduction 233

6.2 Objectives 236

6.3 Results 237

6.3.1 RACK1 Associates with NMHC-IIA in Resting and LFA-1-induced Migrating T lymphocytes 237

6.3.2 Generation of Full Length and NMHC-IIA-derived FLAG Fusion Proteins 238

6.3.3 Evidence for the Direct Interaction between RACK1 and NMHC-IIA 249

6.3.4 RACK1 Translocates to the Actin-rich cap in Association with NMHC-IIA and Chemokine Receptor CXCR4 in SDF-1α-Activated T cells 257

6.3.5 The Effect of KD of RACK1 on CXCR4 Cell Surface Expression in SDF1α-1-stimulated Jurkat T cells 259

6.3.6 The Effect of KD of RACK1 on Localisation of NMHC-IIA, RMLC, and pMLC ser19 in SDF-1α-stimulated PBTLs 261

6.3.7 Investigation of the Effect of Suppression of RACK1 on Phosphorylation of Myosin Light Chain at Ser19 261

6.4 Discussion 264

6.4.1 Conclusion 267

7 Discussion and Conclusion 271

7.1 Contribution of this Study to the Understanding of T lymphocyte Migration 271

7.2 Importance of RACK1 in Lymphocyte Polarisation and Migration 273

7.3 The Contribution of High Content Analysis to the Study of Lymphocyte Biology 278

7.4 Identification of RACK1-associated Proteins in Lymphocytes 278

7.5 Importance of Mapping Protein Binding Domains on RACK1 for the Study of RACK1-interacting Proteins and Associated Complexes 281

7.6 Future Directions 282

7.7 Importance of this Study in the Societal Context 284

7.8 Translational Benefits 286

7.9 Conclusion 286

8 References 287

APPENDIX 323

Appendix 1 325

Chapter 5 Supplementary Data 325

Chapter 6 Supplementary Data 351

Appendix 2 355

Sources of Reagents and Antibodies 355

Addresses 360

Appendix 3 362

REAGENTS AND BUFFERS 362

A. Cell Culture Reagents 362

B. Cell Lysis Reagents 363

C. SDS-PAGE Reagents 366

D. Western Blot Buffers 367

E. High Content Analysis 368

List of Figures

Figure 1.1: Two independent signals are required for lymphocyte activation. 9
Figure 1.2: Scanning electron micrograph of a T lymphocyte. 12
Figure 1.3: Schematic diagram of a polarised migrating T cell. 15
Figure 1.4: The scaffolding protein RACK is a PKC isoform-specific receptor. 21
Figure 1.5: Ribbon diagram of RACK1. 23
Figure 1.6: Ribbon diagram of LFA-1. 28
Figure 1.7: The three conformations of LFA-1. 34
Figure 1.8: Expression and Activation Status of LFA-1 Integrin. 37
Figure 1.9: ICAM Structure and Integrin Binding. 40
Figure 1.10: Lymphocyte Transendothelial Migration. 44
Figure 1.11: Actin and Microtubule Network Dynamics. 50
Figure 1.12: Actomyosin Complex. 52
Figure 1.13: Organisation of the actin and microtubule cytoskeleton during T cell migration. 59
Figure 2.1: Graphical illustration depicting the process of RNAi. 73
Figure 2.2: High Content Analysis through the use of an automated microscope. 77
Figure 2.3: A generalised model of LFA-1-mediated T cell migration. 80
Figure 2.4: N-Terminal pFLAG-CMV. 98
Figure 2.5: Location of Primers Designed for Sequencing and Determining Plasmid Orientation. 101
Figure 2.6: Schematic diagram of MYH9 cDNA deletion mutants. 104
Figure 2.7: The PCR8 entry vector containing Spectinomycin using in the TA/TOPO cloning technique. 108
Figure 2.8: Restriction maps of the entry vector PCR8 containing the each deletion mutant gene insert were generated in Vector NTI. 110
Figure 3.1: Induction of T cell Polarisation and Migration. 122
Figure 3.2: Expression of RACK1 in resting and LFA-1-mediated migrating T cells. 125
Figure 3.3: IF Staining of RACK1 and actin and MT cytoskeleton in resting and in LFA-1-induced migrating T cells. 128
Figure 3.4: IF staining of RACK1 and putative RACK1-associated proteins in resting and in LFA-1-induced migrating T cells. 132
Figure 3.5: RACK1 translocates to the leading edge in association with F-actin and the growing ends of polymerised MTs. 135

Figure 3.6: Par3 does not have a polarised localisation in migrating T cells but does associate with RACK1 in resting and LFA-1-mediated migrating T cells. 137
Figure 3.7: IF Staining of RACK1 with PKC isozymes in resting and LFA-1-induced migrating T cells. 139
Figure 3.8: Suppression of RACK1 is Associated with a Decreased Variation in PKC ζ Subcellular Distribution. 141
Figure 3.9: KD of RACK1 is Associated with a Decreased Variation in PKC ζ Subcellular Distribution. 143
Figure 4.1: Experimental flow-chart for analysis of T cell migration using IN Cell HCA platform. 155
Figure 4.2: Suppression of RACK1 results in reduced LFA-1-mediated cell polarisation in HuT78 T cells. 158
Figure 4.3: Optimisation of ICAM-1 Adhesion Assay in T cells. 163
Figure 4.4: KD of RACK1 did not affect adhesion to ICAM-1 in T cells. 165
Figure 4.5: Optimisation of Transwell Chemotaxis Assay in T cells. 168
Figure 4.6: Suppression of RACK1 Enhances Chemotatic Migration, but not random migration in T cells. 170
Figure 4.7: Polarisation Assay in PBTLs. 173
Figure 4.8: Depletion of RACK1 reduced speed and persistence of T cell chemokinetic migration. 177
Figure 4.9: KD of RACK1 does not affect SDF1 stimulated T cell adhesion to ICAM1. 179
Figure 4.10: Suppression of RACK1 Enhances Chemotatic Migration, but not random migration in primary T cells. 181
Figure 4.11: Overexpression of RACK1 inhibits SDF-1α-stimulated chemotaxis in primary T cells. 183
Figure 5.1: Experimental schema employed for identification of RACK1-associated proteins. 196
Figure 5.2: Coomassie Blue and silver nitrate staining of protein samples from resting and LFA-1-induced migrating T cells. 199
Figure 5.3: RACK1 Proteomics Data. 201
Figure 5.4: Validation of Mass Spectrometry Data for Candidate Protein by Immuno-assays. 205
Figure 5.5: Analysis of TritonX-100 soluble and insoluble extracts of resting and LFA-1-induced migrating T cells. 210
Figure 5.6: RACK1 Localises to the Plus-ends of MTs in T cells. 213
Figure 5.7: RACK1 Associates with CLIP -115 and -170 at the leading edge of LFA-1-stimulated migrating HuT78 T cells. 215

Figure 5.8: RACK1 Associates with IQGAP at the leading edge of LFA-1-stimulated migrating HuT78 T cells. 216
Figure 5.9: RACK1 associates with CLASP1 at the distal ends of polymerised MTs. 218
Figure 5.10: RACK1 does not associate with CLASP2 at the distal ends of polymerised MTs. 219
Figure 5.11: RACK1 Associates with NMHC-IIA at the Leading Edge and the Uropod of LFA-1-stimulated migrating T cells. 221
Figure 6.1: Non-muscle Myosin IIA 240
Figure 6.2: Generation of NMHC-IIA-derived Truncation Mutants. 242
Figure 6.3: NMHC-IIA-derived FLAG Fusion Proteins. 244
Figure 6.4: FLAG-NMHC-IIA Binds Endogenous RACK1. 246
Figure 6.5: Expression of NMHCIIA-derived deletion mutants in HEK293 cells. 248
Figure 6.6: RACK1 Interacts with Full length NMHC-IIA. 250
Figure 6.7: RACK1 Peptide Substitution Arrays. 252
Figure 6.8: Repetitive Sequences Involved in Interaction with NMHC-IIA. 254
Figure 6.9: Putative NMHC-IIA Binding Sites on RACK1. 256
Figure 6.10: RACK1 Localises to Actin-rich Cap in Association with NMHCIIA and membrane-bound CXCR4 in SDF-1α-Activated Cells. 258
Figure 6.11: KD of RACK1 does not affect chemokine receptor CXCR4 internalisation in response to SDF-1α. 260
Figure 6.12: Effect of suppression of RACK1 on phosphorylation of MLC at serine 19 (pMLC ser19). 263
Figure 7.1: Controlled T cell migration requires a regulated cellular expression of RACK1. 277

Appendix 1 Figure 1: Categorisation of proteins identified by mass spectrometry analysis of RACK1 immuno affinity purified proteins by Gene Ontology. 345
Appendix 1 Figure 2: Co-localisation of RACK1 with NMHC-IIA, CLIP-115 and -170, CLASP1 and CLASP2 at the leading edge of LFA-1-stimulated migrating T lymphocytes. 350
Appendix 1 Figure 3: Presentation of the key residues implicated in the NMHC-IIA interaction on the RACK1 homodimer. 354

List of Tables

Table 1.1: Known Mechanisms of LFA-1 Integrin Activation in Immune Cells 31
Table 2.1: Sequencing Primer Name and Base Composition. 100
Table 2.2: Primer Name and Base Composition used to generate NMHCIIA derived fragments from full length MYH9. 103
Table 4.1: Morphology parameter measurements based on F-actin staining for transfected HuT78 T cells (N=4). 160
Table 4.2: Morphology parameter measurements based on F-actin staining for transfected PBTLs (N=3). 174

Appendix 1 Table 1: RACK1 IP Mass Spectrometry Results 325
Appendix 1 Table 2: Summary of RACK1 Proteomics Data 347
Appendix 1 Table 3: RACK1 Peptide Array Results 351
Appendix 2 Table 4: Reagents 355
Appendix 2 Table 5: Antibodies 359
Appendix 3 Table 6: Components of the resolving gel solution for SDS-PAGE 366
Appendix 3 Table 7: Components of the stacking gel solution for SDS-PAGE 366
Appendix 3 Table 8: IN Cell Parameters (Adapted from Product User Manual, 2006). 368

Abbreviations

aa: amino acid

AKT (PKB): Protein Kinase B

APC: Antigen Presenting Cell

ATCC: American Type Culture Collection

BSA: Bovine Serum Albumin

CFTR: cystic fibrosis transmembrane conductance regulator

CHO: Chinese hamster ovary

CLASP: CLIP Associated Protein

CLIP: Cytoplasmic Linker Protein

CTLA-4: Cytotoxic T Lymphocyte Antigen 4

DAG: Diaglycerol

DMEM: Dulbecco's Modified Eagle Medium

ECM: Extracellular matrix

ERM: ezrin/radixin/moesin

FAK: Focal Adhesion Kinase

FITC: Fluorescein isothiocyanate

FL: Full length

GAP: GTPase-activating protein

GDI: GDP-Dissociation Inhibitor

GDP: Guanosine Diphosphate

GEF: Guanine Exchange Factor

GFP: Green Fluorescent Protein

GNB2L1: Guanine Nucleotide Binding protein (G protein), beta polypeptide 2-like 1

GPCR: G-protein Coupled Receptor

GRKs: G protein Regulatory Kinases

GTP: Guanosine Triphosphate

GαH: goat anti- rhICAM-1 coating antibody

Gβ: β subunit of heterotrimeric G-protein

h: hour

HCA: High Content Analysis

HEK293: Human Embryonic Kidney 293 Cells

HEV: High endothelial venules

HUVEC: Human Umbilical Vein Endothelial Cell

ICAM-1: Intercellular Adhesion Molecule-1

IEGF: integrin EGF-like

IF: Immunofluorescence

IFN-ɣ: interferon gamma

IGF-1R: Insulin growth factor 1-receptor IP: Immunoprecipitation

IL-1: interleukin-1

JAK: Janus kinase

JAM-1: Junctional adhesion molecule 1

KHDRBS1: KH domain containing, RNA binding, signal transduction associated 1

LB: Luria-Bertani

LFA-1: Lymphocyte Function- Associated Antigen-1

mAb: monoclonal antibody

MAP: MT-associated protein

MAPK: Mitogen-Activated Kinase

MFI: Mean Fluorescence Intensity

$MgCl_2$/EGTA: Magnesium Chloride/ Ethylene Glycol Tetraacetic Acid

MHC: Major Histocompatibility Complex

MLC: Myosin Light Chain

MLCK: Myosin Light Chain Kinase

MT: Microtubule

MTOC: Microtubule Organising Centre

NMDAR: N-methyl-D-Aspartate receptor

NMHC-IIA: Non-muscle Myosin Heavy Chain IIA

NMII: Non-muscle Myosin II

PAGE: Polyacrylamide Gel Electrophoresis

PBS: Phosphate buffered saline

PBTL: Peripheral Blood T Lymphocyte

PDLIM2: PDZ and LIM domain protein 2

PE: Phycoerythirin

PFA: Paraformaldehyde

PH: pleckstrin homology

PHA: Phytohaemagglutin

PI3K: Phosphatidylinositol 3-kinase

PIP2: Phosphatidylinositol 4,5-bisphosphate or PtdIns(4,5)P2

PKC: Protein Kinase C

PLC: Phospholipase C

PLL: Poly-L-lysine

PMA: Phorbol myristate acetate

pMLC: Phosphorylated MLC

PP2A: Protein phosphatase 2A

PSI: plexin-semaphorin-integrin

PVDF: Polyvinylidene Fluoride

Pyk-2: Protein Tyrosine Kinase-2

RACK1: Receptor for Activated C-Kinase-1

RGS: Regulator of G protein Signalling

rhICAM-1: recombinant human ICAM-1

RISC: RNA-inducing silencing complex

RNAi: RNA interference

RT: room temperature

SD: Standard Deviation

SDF-1: Stromal Cell Derived Factor-1

SDS: Sodium Dodecyl Sulphate

SEM: Standard Error of the Mean

siRNA: small interfering RNA

TBS/T: TBS with 1% Tween

TBS: Tris Buffered Saline

TCR: T cell receptor

TNF-α: tumour Necrosis Factor-α

VCAM-1: Vascular Cell Adhesion Molecule-1

WASP: Wiskott-Aldrich syndrome protein

WD: Tryptophan, Aspartic Acid

Keywords

RACK1

NMHC-IIA

T lymphocyte

Integrin-mediated immune cell migration

CHAPTER ONE

General Introduction

1 General Introduction

1.1 Role of T Lymphocytes in the Immune Response

T cells, a type of white blood cell known as lymphocytes, are an integral branch of the acquired immune system and play an essential role in cell-mediated immunity. An effective immune response depends on the circulation of T cells through the blood stream and into the lymphatic system where they are activated by antigen presenting cells (APCs), such as B lymphocytes and dendritic cells. Upon activation by APCs, the T cell undergoes maturation and clonal expansion and releases critical cytokines that promote proliferation of the cell-mediated immune response (von Andrian and Mackay 2000; Billadeau et al. 2007; Jacobelli et al. 2004a). Activated lymphocytes extravasate through the endothelial wall to areas of inflammation in a highly orchestrated process known as transendothelial migration. The fundamental molecular mechanisms underlying T lymphocyte development, activation, and migration will be discussed in the following sections.

1.2 T cell Development

T cells originate from haematopoietic stem cells in the bone marrow. These progenitor cells migrate to the thymus via the bloodstream and undergo expansion producing a large population of immature thymocytes (Schwarz and Bhandoola 2006). The earliest thymocytes express neither CD4 nor CD8 receptors, and are therefore classed as double-negative (CD4-/CD8-) cells (Germain 2002). The thymocytes undergo a series of developmental changes in the thymus, including somatic recombination, the rearrangement of the genes encoding the α/β or γ/δ chains forming the T cell receptor (TCR), to generate a pre-TCR (von Boehmer and Fehling 1997; Robey and Fowlkes 1994). Importantly, this pre-TCR is generated randomly and creates a vast array of antigen-specific immature T lymphocytes with each thymocyte, therefore, recognising only one specific antigen (Aifantis et al. 1999). Moreover, the TCR resembles a membrane-bound Fab fragment of an antibody, in that it is a disulfide-linked heterodimer, with each chain containing an immunoglobulin constant-like domain and an immunoglobulin variable-like domain, which forms the site for antigen recognition. As they progress through their development, signal transduction pathways initiated by the pre-TCR promote the expression of CD4 and CD8 co-receptors generating double-positive thymocytes.

The following selection process is dependent on the major histocompatibility complex (MHC), which present antigens to T cells necessary for an effective immune response. MHC genes include highly polymorphic sites, which determine T cell antigen recognition. Thymocytes undergo positive selection, which selects for T cells capable of interacting with MHC. Double-positive thymocytes ($CD4^+/CD8^+$) move deep into the thymic cortex where they are presented with MHC and peptide complexes on the surface of cortical cells. Only those thymocytes that have an affinity to the MHC molecule will be able to survive. All other thymocytes will die by apoptosis. In a process known as negative selection, double-positive thymocytes interact with epithelial and dendritic antigen-presenting cells (APCs) in the thymus and are subjected to selection based on their ability to bind "self"-peptides, or antigens present in the body (Germain 2002). "Self"-reactive thymocytes are ligated in the thymus resulting in cell death by apoptosis. Clonal deletion ensures these thymocytes do not mature and respond to activation by tissues present within the body. This selection process is an important component of immunological tolerance and prevents the maturation of self-reactive T cells capable of inducing autoimmune diseases in the host. The vast majority of all thymocytes undergo death during this process.

The remaining cells mature into single positive CD4+ or CD8+ T cells and exit the thymus into the bloodstream as naïve T lymphocytes and await activation in response to a specific foreign antigen. The CD4+ or CD8+ T cell phenotype corresponds generally, but not exclusively, with the T helper cell or cytotoxic T cell, respectively. T helper cells regulate the function and activity of other immune cells by producing a range of cytokines such as interleukin-2 (IL-2) in response to antigenic activation. Cytotoxic T cells, on the other hand, are involved in a wide number of functions in the immune system including the elimination of virally infected cells (von Andrian and Mackay 2000; Rochman et al. 2009).

1.3 T cell Activation

T cell activation by TCR-mediated recognition of antigens results in cytoskeletal-based rearrangements and integrin activation that convert the round cell morphology to a polarized phenotype. Although the specific mechanisms of activation vary slightly between different types of T cells, the "two-signal model" in CD4+ T cells applies to most. Activation of CD4+ T cells occurs through the engagement of both the TCR and CD28 receptor on the T cell by the MHC peptide and B7 family members on the APC, respectively (Smith-Garvin et al. 2009). Concomitant interaction is required for an

effective immune response; in the absence of CD28 co-stimulation, TCR signalling alone results in anergy, or induction of antigenic tolerance. This mechanism helps prevent accidental T cell activation by immature cells as B7 is present only on mature APCs. In addition, the presence of cytokines, such as IL-1, immobilised on endothelial cells in blood vessels promote the activation of T cells (Campbell and Butcher 2000; Rochman et al. 2009; Smith-Garvin et al. 2009).

In the two-signal model, the first signal is the TCR on the T cell interacting with the peptide-bound MHC complex on the APC (Figure 1.1). The partner APC is usually a dendritic cell in the case of naïve responses, although B-cells and macrophages can also be important APCs. T cell activation only occurs if the TCR is specific to that MHC-peptide complex. Therefore, the TCR will only recognise a particular combination of peptide-bound MHC. The co-recognition of peptide and MHC molecule is known as MHC restriction because the MHC molecule is said to restrict the ability of the T cell to recognise antigen. Initially, naïve T-cells, which have never encountered antigen, must determine whether antigen is present and whether it poses a threat to the body. The ability of the TCR to distinguish "self" from "non-self" by recognition of a specific foreign antigen is one of the cornerstones of immunological specificity (Kane et al. 2000).

The antigen-specific activation of these effector T cells is aided by co-receptors that distinguish between the two classes of MHC molecule; cytotoxic T cells express the CD8 co-receptor that binds MHC class I molecules, whereas T helper cells express the CD4 co-receptor with specificity for MHC class II molecules. The peptides presented to CD8+ T cells by MHC class I molecules are eight to nine amino acids in length; whereas, the peptides presented to CD4+ cells by MHC class II molecules are longer, as the ends of the binding cleft of the MHC class II molecule are open. However, the most important difference between MHC classes is dependent not on its structure but the source of bound peptides. The two classes of MHC molecule are recognised by different functional classes of T cell. MHC class I molecules bearing viral peptides are recognized by cytotoxic T cells, which then kill the infected cell. MHC class II molecules bearing peptides derived from pathogens taken up into vesicles are recognized by T helper cells. It is assumed that in most cases very few MHC molecules are loaded with antigenic peptide. Moreover, because of the low affinity of the TCR for specific antigenic peptides and the limited amounts of antigen-bound MHC II molecules on the APC, the threshold for cellular activation may not be reached. In order to attain this activation threshold, a number of co-stimulatory molecules facilitate the interaction T cell/ APC interaction. Furthermore, the CD4 or CD8 co-receptors on the T cell help to stabilise this interaction

by binding to the non-polymorphic regions on the MHC molecule (Dustin and Chan 2000).

A second stimulatory signal is required for T cell activation, which is delivered by interaction between the APC co-stimulatory molecule B7 and T cell CD28. In addition, interactions between adhesion receptors on T cells such as lymphocyte function associated antigen-1 (LFA-1) and its corresponding ligand on the APC, in particular intercellular adhesion molecule-1 (ICAM-1), also serve to stabilize the interaction between the T cell and APC (Zecchinon et al. 2006). The T cell response to antigen is also under control of inhibitory signalling through cytotoxic T lymphocyte antigen 4 (CTLA-4). CTLA-4 has higher affinity than CD28 for B7, resulting in the inhibition of T cell activation and proliferation (Evans et al. 2009).

The activated T cell undergoes clonal expansion whereby the differentiated effector cells will all express receptors with identical specificity to the parent cell. Moreover, T cell activation results in the formation of highly ordered complex structures containing receptors, lipid rafts, cytoplasmic signalling molecules, and cytoskeletal proteins. Activation of the T cell initiates a number of biochemical pathways in the cell that ultimately lead to the expression of genes that control specific cellular responses, including growth, differentiation, and secretion of cytokines (Appelbaum 2001). Many of these biochemical events initiated during T cell activation have only been discovered in the last decade.

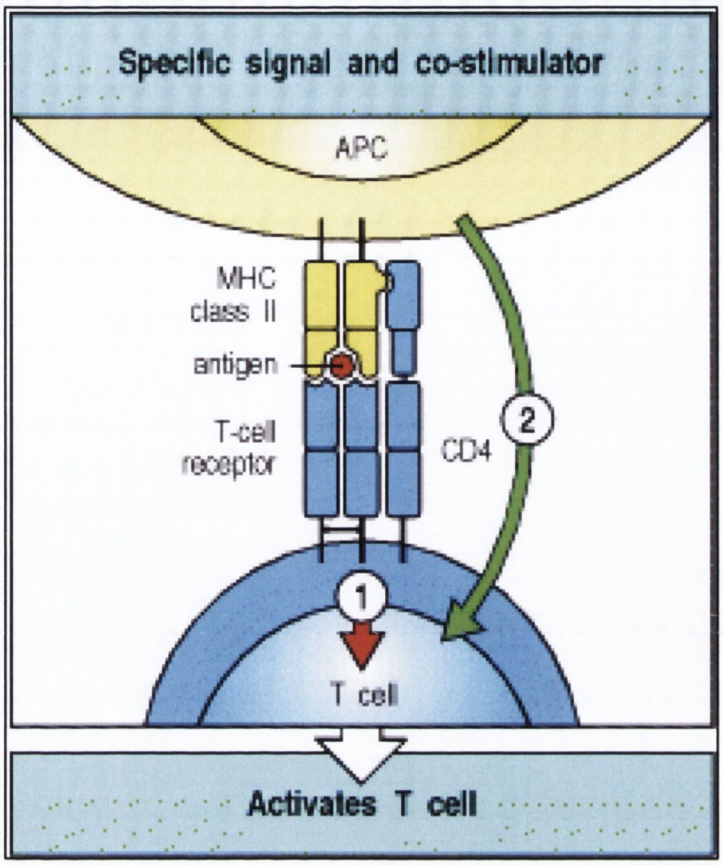

Figure 1.1: Two independent signals are required for lymphocyte activation.

In addition to binding of the peptide-MHC complex by the TCR and, in this example, the CD4 co-receptor (arrow 1), activation of naive T cells requires a second signal the co-stimulatory signal (arrow 2), which is delivered by interaction between the APC co-stimulatory molecule B7 and T cell CD28 (Adapted from Janeway et al. 2001).

1.4 T cell Migration

Cell motility is crucial in several aspects of normal physiology, including embryonic development, angiogenesis, wound healing, and immune surveillance, and is therefore tightly regulated. Since migration is fundamental throughout physiology, dysregulation of cell motility can lead to a number of pathological events, such as invasion and tumour metastasis. Cell migration is regulated by a complex array of cytoskeletal and signalling molecules that orchestrate cross-talk between diverse signalling pathways to achieve directed cell movement. The principles determining the migration of different cell types may result from their differences in origin, size and shape, function of adhesion receptors, and environmental factors, including the extracellular matrix.

Lymphocytes, including T cells, perform many functions depending on their maturation and activation status. The single most important feature that governs T cell activity is the inherent ability of both naïve and activated cells to migrate along a chemotactic gradient, which enables them to extravasate from the bloodstream to non-lymphoid tissues (Cose 2007; Cose et al. 2006; Jin et al. 2008; Westermann et al. 2001; Woodland and Kohlmeier 2009). The infiltration of effector T cells to sites of infection and injury is an integral step in the immune system response to inflammation and pathogen invasion (Bradley 2003; Mora and Von Andrian 2006). Moreover, in contrast to the normal delay in acquired immunological response, memory T cells present in peripheral tissues can act as a first line defence in secondary pathogen invasions (Woodland and Kohlmeier 2009). Unlike other non-haematopoietic migrating cells, which exhibit slow yet highly directional migration, T lymphocytes display a rapid and directionally unpredictable mode of migration. *In vivo* and *in vitro* live cell imaging indicates T cells migrate between 10 and 40 mm/min (Mempel et al. 2004; Miller et al. 2003). In fact, these studies have demonstrated T cells migrate approximately 100 times faster than non-haematopoietic cells. Certainly, studies on fibroblasts and endothelial cells have generated a vast amount of information about integrin-mediated migration. In particular, adherent cell migration is largely adhesion-dependent involving the formation of focal adhesions consisting of integrins associated with cytoskeletal components. Moreover, this type of cell migration requires the formation of stress fibers that are necessary for actomyosin force generation and subsequent translocation. T cells, however, lack traditional focal contacts, adhesions, and stress fibers (Smith et al. 2007a; Smith et al. 2005). T cell integrins are not organised into focal contacts, but rather exhibit increased lateral mobility, which may be fundamental for fast migration. Moreover, immune cells have

evolved a speed-oriented mode of migration, whereby the dynamics of integrin turnover in T cells must differ from that of slower moving cells.

1.5 T cell Migratory Phenotype

Polarisation of T lymphocytes in response to chemokine signalling is believed to be an important prerequisite for efficient migration by facilitating both directional movement and providing the necessary forces to propel the cell forward (Gómez-Moutón and Mañes; Krummel and Macara 2006; Russell 2008). The polarised morphology of migrating T cells is induced by chemotactic and adhesive stimuli and has been proposed as mechanism for crawling along the endothelium (Johnston and Butcher 2002; Jacobelli, Chmura, et al. 2004; Debes et al. 2006). Unlike typical cell migration, T cells exhibit a highly polarised 'hand mirror' morphology characterised by a flattened leading edge followed by a large cell body comprised of the nucleus, which narrows into a 'handle-like' tail termed the uropod. This migrating phenotype allows T cells to move much faster than most non-hematopoietic cells. The polarised morphology of a migrating T cell is illustrated Figure 1.2, which depicts a scanning electron micrograph T lymphocyte crawling along the endothelium.

The plasma membrane of migrating T cells is hypothesised to be divided into lipid microdomains that are continually recycled around the cell periphery. These lipid rafts contain a number of membrane receptors, which recruit associated secondary messengers that induce alternative signalling pathways in the appropriate subcellular locations. Furthermore, the polar distribution of chemokine receptors and leukocyte integrins organised in complex lipid raft microdomains not only act as molecular markers to define T cell polarity, but also give mechanistic insight into T cell migration (Barreiro et al. 2007; Evans et al. 2009; Gomez and Billadeau 2008; Smith et al. 2007b). Indeed, lipid rafts have been shown to be essential for the generation and maintenance of the morphologic, biochemical, and functional polarity of T lymphocytes (Millán et al. 2002).

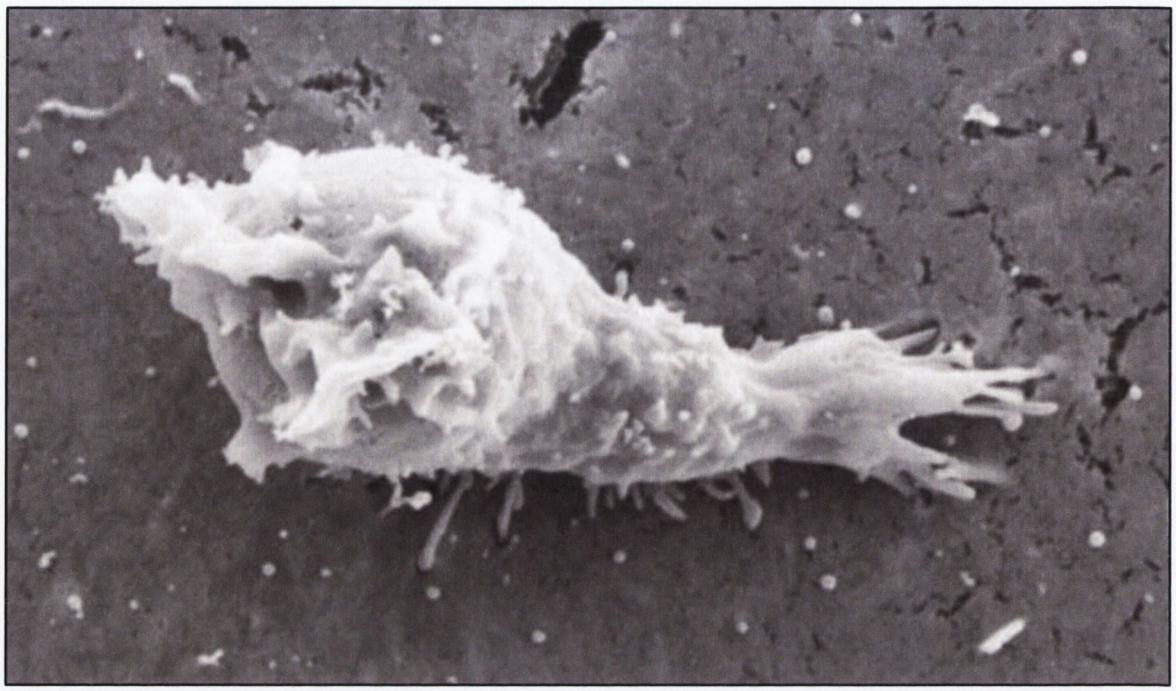

Figure 1.2: Scanning electron micrograph of a T lymphocyte.

The T cell crawling along a cytokine-stimulated endothelial cell illustrates the migratory morphology: forward stretching lamellipodium, cell body with invasive filopodia, and trailing uropod (Adapted from Shulman et al. 2009).

1.5.1 The leading edge

The leading edge of a migrating T cells is a membrane protrusion pointing in the direction of migration. The leading edge is characterised by a forward extending lamellipodia and finger-like invasive filopodia. Each protrusion type requires the coordination of a wide spectrum of signalling molecules and regulators of cytoskeletal dynamics (Ridley 2011). During migration, the dynamic leading edge facilitates rapid directional changes characteristic of T cells in response to external stimuli (Smith et al. 2007a; Smith et al. 2003). Formation of the leading edge, or lamellipodium, and assembly of chemosensory receptors is critical for sensing chemokine gradients and promoting integrin-mediated adhesion and generating forward movement. The leading edge is enriched in transmembrane receptors that bind chemokine ligands expressed on the surface endothelial cells or sense gradients of soluble mediators, or chemoattractants. These include CXCR4, CCR2, and CCR5, which have been shown to respond to complex chemoattractant gradients that induce directed T cell migration and guide lymphocytes to areas of inflammation (Campbell and Butcher 2000; Gómez-Móuton et al. 2001; Jin et al. 2008; Mañes et al. 2001). Chemokine-induced integrin activation and cytoskeletal remodelling in directed T cell migration is discussed in more detail in section 1.12.

1.5.2 The main cell body

The rounded morphology of the cell body, which contains the nucleus and centrosome provides a centre of attachment, allowing firm adhesion to the substratum and stability during migration (Evans et al. 2009; Smith et al. 2007a). Although traditionally believed to move over endothelial cells as flattened bodies (Ley et al. 2007), recent evidence suggests lymphocytes use ventral adhesive filopodia along the cell body to rapidly crawl and scan endothelial cells via a millipede-like locomotion. By using an *in vitro* model of lymphocyte adhesion and migration across cytokine-activated human umbilical vein endothelial cells (HUVEC), Alon and colleagues (2009) also demonstrated that under the stress of shear flow, the number of ventral invasive filopodia and membrane protrusions triples in crawling T cells compared to shear-free conditions.

1.5.3 The uropod

The tail, or trailing uropod, is a membrane protrusion at the rear of the cell formed during T cell migration that projects above the substrate surface. A number of functions for the

uropod have been proposed, including increasing evidence that it can participate in adhesive events (Gomez and Billadeau 2008; Smith et al. 2007a). For instance, despite the term 'trailing', the uropod is thought to both anchor the cell and generate contractile forces, propelling the cell forward (Smith et al. 2007a). The uropod also functions as a membrane exit point for newly synthesized proteins and as a reservoir for unengaged receptors, which are continually recycled to the leading edge in order to form new projections and adhesions in response to a chemokine gradient (Fabbri et al. 2005; Millán et al. 2002). Therefore, Millán and colleagues argue the uropod in not merely a 'storage depot', but a rather specialised region involved in T lymphocyte recruitment and aggregation.

In addition, the uropod has been shown to serve as a point of attachment for succeeding cells, promoting T cell interaction when crossing the vasculature (del Pozo et al. 1998). Friedman and colleagues (2006) demonstrated the ability of the uropod to attach to chemokine-bound endothelial cells. This observation prompted the backward vantage point theory, in that, it primes the T cell to rapidly scan the surface of the APC and to either become activated or disengaged if no appropriate stimulating peptide is located.

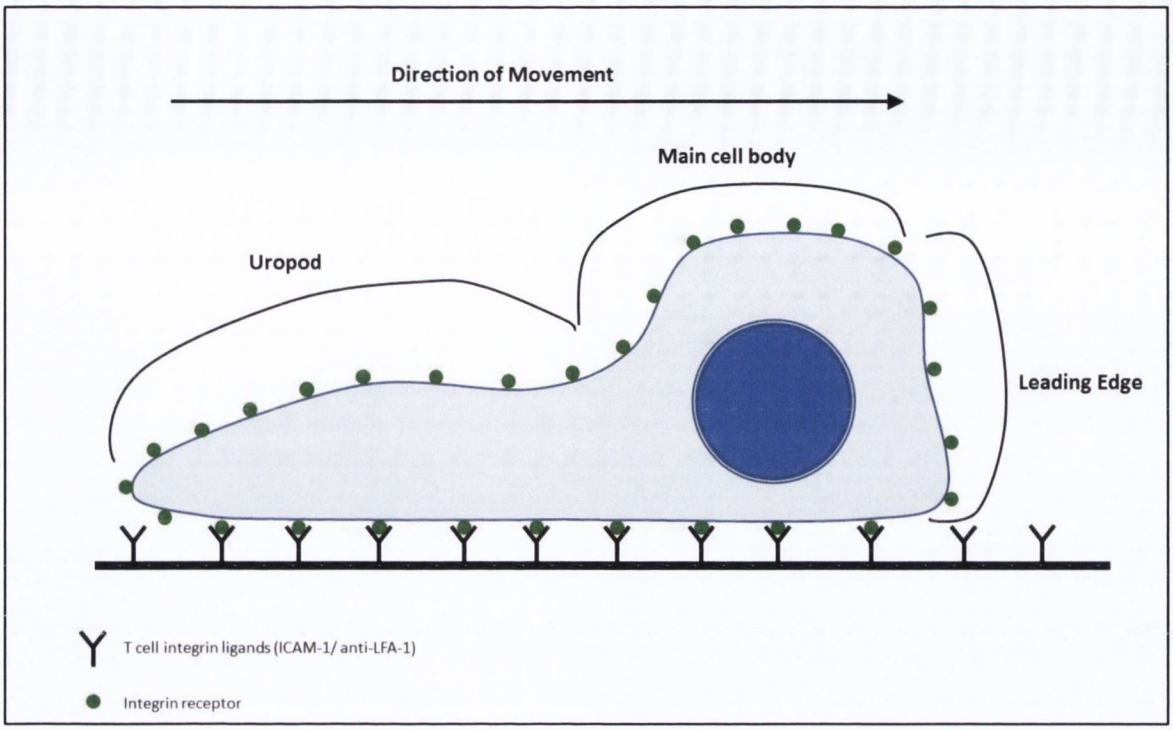

Figure 1.3: Schematic diagram of a polarised migrating T cell.

Migrating T cells display a highly polarised morphology or "hand-mirror" shape with three distinct compartments including the leading edge, main cell body, and uropod.

1.6 Molecular Mechanisms of T cell Migration

The circulation of naïve T cells between the bloodstream and lymphatic system depends on their ability to respond to chemoattractant gradients and interact with adhesion molecules, which anchor the cell in preparation for crossing the endothelium. All secondary lymphoid organs except the spleen have a specialised endothelial cell layer known as high endothelial venules (HEVs). HEV cells express a particular subset of ligands, which enable elevated levels of lymphocyte extravasation (Evans et al. 2009).

Activated T cells must undergo a similar process to extravasate into inflamed tissue. Although, it involves different adhesion molecules and chemoattractants, which attract activated effector T cells. This tightly regulated process allows tissue-specific homing of distinct T cell populations within the body (Engelhardt and Wolburg 2004; Hogg et al. 2003). Generally, T cell mobility is classified as amoeboid-like and is driven by protrusions, or membrane blebbing, of actin-rich pseudopodia at the leading edge, working in concert with contractile forces at the rear of the cell (Jacobelli et al. 2004a). T cell migration can be viewed as a multi-step process incorporating four sequential stages, which are described in the following sections.

1.6.1 Induction of Cell Polarisation

Upon ligand and receptor engagement, a multitude of signalling cascades is initiated causing an asymmetrical distribution of signalling components and cytoskeletal elements within the cell generating a polarised phenotype. Cell surface molecules, including chemokine receptors, co-stimulatory molecules, and adhesion receptors, engage their ligands in the microenvironment and contribute to establishing and maintaining cell polarity (Gómez-Móuton et al. 2001; Krummel and Macara 2006). Activation of cell surface proteins induces polarisation of the actin and microtubule cytoskeleton and vesicle traffic relative to an anterior/posterior axis, which is thought to stabilise lymphocyte polarity. Regulation and maintenance of T cell polarity by the actin and microtubule cytoskeleton is discussed further in section 1.13. In addition, a family of polarity proteins in T cells that includes proteins scribbled (Scrib), lethal giant larvae (Lgl) and discs large (Dlg) together with partitioning defective (Par) proteins have been shown to establish cell polarity. The Par polarity proteins form a complex comprised of Par 3, Par 6, and atypical Protein Kinase C (PKC) (Betschinger et al. 2003). Furthermore, as discussed in the previous section, it is clear that the lipid raft-mediated transport system is essential for generating and maintaining the biochemical and functional polarity of T

lymphocytes (Gómez-Móuton et al. 2001; Russell and Oliaro 2006; Sánchez-Madrid and del Pozo 1999). Ultimately, the successful response of a T cell is dependent on the proper formation of functional polarity. Therefore, loss of polarity regulators or directional cues may interfere with T cell activation.

1.6.2 Generation of Membrane Protrusions at the Leading Edge

Once polarity has been established, the second phase of migration starts with the protrusion of the plasma membrane from the front of the cell. The forward thrust of membrane protrusions (forward stretching lamellipodia and invasive filopodia) is supported by active actin polymerisation at the leading edge followed by stabilisation of new membrane extensions by adhesive contacts (Evans et al. 2009; Lewis et al. 2008; Sánchez-Madrid and del Pozo 1999).

1.6.3 Formation of Cell-Substratum Contact Sites

After membrane extension has been formed, new points of contact are formed by T cell surface receptor engagement with their specific ligands. This involves adhesion molecules of the integrin family (Hogg et al. 2003). In rapidly migrating T cells, ligand binding triggers integrin clustering and recruitment of cytoskeletal proteins to cytoplasmic integrin domains. This prevents retraction of the newly extended membrane and provides mechanical link between receptor signalling and motor proteins responsible for generating tractional force required for cell movement (Rey et al. 2002).

1.6.4 Forward Movement of the Cell Body and Retraction of the Uropod

The final two stages of T cell migration involve the cytoplasmic flow of intracellular organelles into the protruding area of the cell and the retraction of the trailing uropod. The forward extending leading edge is supported by cytoskeletal reorganisation and cross-linking to integrins, while contractile forces concentrated at the rear project the cell body forward (Morin et al. 2008; Smith et al. 2007c; Sánchez-Madrid and Serrador 2009). The net result of this highly orchestrated process is directional movement of the cell and deviations within any of these molecular mechanisms can have a dramatic effect on cell migration.

1.7 T cell Signalling

Cells of multicellular organisms communicate with each other in order to coordinate growth and differentiation. Cells can react to environmental changes by transduction of extracellular signals to produce functional intracellular responses. Signal transduction is essentially a series of highly ordered and efficient post-translational modifications of proteins via phosphorylation/ dephosphorylation cascades performed by kinases and phosphatases, respectively, usually activated near the plasma membrane. These families of enzymes propagate the appropriate signal(s) from the membrane to the cytosol by tethering to specific non-enzymatic scaffolding proteins and activating defined cellular substrates. The signalling pathway ultimately results in activation of cytosolic transcription factors. Activated transcription factors can then enter the nucleus where they bind specific promoter sites and induce the expression of a number of genes. These newly assembled proteins can then illicit a functional cellular response. The initiation and regulation of these complex intracellular signalling pathways is gradually being elucidated through intensive and exhaustive research.

1.8 PKC: A Key Signal-Transducing Enzyme

PKC comprises a family of lipid-dependent serine/threonine kinases that differ with respect to activator and co-factor requirements, substrate specificity, tissue expression, and subcellular localisation. This diverse set of signalling enzymes have been shown to regulate a number of essential cellular processes including cell proliferation, apoptosis, survival and migration (Dempsey et al. 2000).

To date, twelve PKC isoforms have been identified. They have been divided into three subfamilies based on their co-factor requirements for full activation. Conventional PKCs (α, β1, β 2, and γ) are calcium- and lipid messenger diacylglycerol (DAG)-dependent. Receptor-stimulated hydrolysis of plasma membrane Phosphatidylinositol 4,5-bisphosphate, also known simply as PIP2, results in elevated intracellular levels of both calcium and DAG and induces PKC activation (Cameron and Parker 2010; Mellor and Parker 1998; Parker and Murray-Rust 2004). Stimulation with tumour promoter phorbol esters or hormones also results in an increase in intracellular concentrations of DAG and activation of PKCs. The second subgroup, or "novel" PKCs, (δ, ε, η, θ, and PKD) is defined by calcium-independent activation. The third subfamily comprises the DAG- and calcium-independent, or atypical PKCs (ι and ζ). Each PKC isoform displays distinct

tissue and subcellular distributions (Cameron and Parker 2010; Parker and Murray-Rust 2004).

Mounting evidence indicates a critical role for PKC in integrin-mediated events, including adhesion, spreading, migration, and focal adhesion formation and actin stress fibre assembly on various ECM substrates (Bertram and Ley 2011; Disatnik and Rando 1999; Ivaska et al. 2003; Lewis et al. 1996). Distinct PKC isoforms have been reported to be involved in integrin-mediated processes in different cell contexts, suggesting the mechanism of PKC regulation of integrin function is dependent on the cell type (Harper and Poole 2007; Laudanna et al. 1998; Ng et al. 1999).

PKC isozymes have also been widely implicated in tumourigenesis as altered levels of PKC expression have been linked to disease progression (Griner and Kazanietz 2007). For example, PKC α mediates β1 integrin endocytosis and recycling to the plasma membrane. Overexpression of PKC α accelerated integrin recycling and induced tumour metastasis in breast carcinoma cells (Ng et al. 1999). The importance of regulation of PKC and integrin cross-talk has also been demonstrated *in vivo*. One study, in particular, reported that overexpression of PKC α results in increased phosphorylation of the integrin signalling component paxillin and tumour progression in mice (Hu et al. 2011). In addition, to facilitating signal propagation downstream of integrin, PKC has also been implicated in mediating intracellular activation of integrin. For instance, epidermal growth factor-induced integrin-mediated migration was shown to be dependent on PKC activity, illustrating the role of PKC in integrin activation (Rabinovitz et al. 1999).

The importance of the physiological functions of PKC isoforms in immune cell signalling has also been established (Baier 2007; Tan and Parker 2003). Several PKC isoforms are highly expressed in lymphocytes including, PKC θ and α, which are required for T cell activation, differentiation, adhesion and motility (Altman and Villalba 2003; Baier 2003). However, despite considerable evidence describing the importance of PKC in integrin-mediated events, the molecular mechanisms of underlying the involvement and regulation of PKC in these processes in T cells have yet to be fully elucidated. PKC enzymatic activity is required for diverse cellular processes, and altered levels of activity can have devastating effects. Therefore, it is pertinent PKC expression and activity is strictly regulated.

Spatial and temporal organisation of signal transduction molecules is critical in maintaining an appropriate cellular response. Adaptor proteins recruit signalling molecules to specific subcellular locations, where they interact with select substrates.

Activated PKC isozymes are targeted to distinct subcellular locations by a family of WD repeat proteins known as RACKs. RACKs are not substrates for PKCs but rather interact only with activated PKC, hence, the name Receptor for Activated C Kinase (Mochly-Rosen et al. 1995; Schechtman and Mochly-Rosen 2001). Despite their initial discovery as a receptor for PKCs, these molecular scaffolds have been implicated in numerous signalling pathways and a myriad of protein interactions. These key signalling adaptor proteins are discussed in detail in the next section.

1.9 Identification of the RACK Family of Proteins

RACK proteins are members of the WD40 protein family, which also includes the G protein β-subunits. To date, there are three established RACK proteins: RACK1, RACK2, and RACK7. The understanding of the enigmatic RACK family of proteins has increased dramatically in recent years from their original identification as anchoring proteins for protein kinase (Ron et al. 1994) and have since been shown to regulate trafficking and activity of PKC (Csukai and Mochly-Rosen 1999; McCahill et al. 2002; Schechtman and Mochly-Rosen 2001). RACKs target activated PKC isozymes to distinct subcellular compartments, where they phosphorylate isozyme-specific substrates, suggesting each isoform mediates distinct cellular functions (Figure 1.4; Mochly-Rosen and Gordon 1998). Moreover, RACKs are isozyme specific; therefore, the site specificity of PKC function may be partly determined by the location of RACK. Thus, RACKs have been implicated in regulating signal transduction. This study focuses on the regulatory role of the RACK1 protein, specifically in the context of T cell migration.

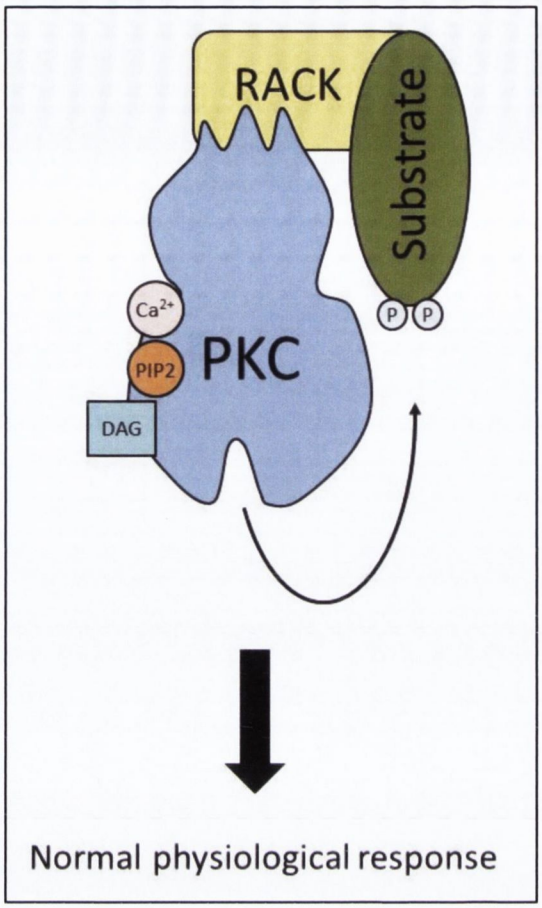

Figure 1.4: The scaffolding protein RACK is a PKC isoform-specific receptor.

RACK targets activated PKC isozymes to distinct subcellular compartments, where they phosphorylate isozyme-specific substrates.

1.9.1 RACK1

RACK1 is a 36-kDa protein encoded by the gene GNB2L1 (guanine nucleotide binding protein (G-protein), beta polypeptide 2-like 1), which is located on chromosome 5 (5q35.3) and consists of eight exons and seven introns (Wang et al. 2003). RACK1 belongs to the tryptophan-aspartate (WD-40) repeat family and therefore shares significant homology to the β subunit of G-proteins (Gβ), in which WD repeats were first identified (Adams et al. 2011; Stirnimann et al. 2010; Wall et al. 1995). This globular structure is composed of seven blades (WD1–7 regions), each containing a four-stranded antiparallel β-sheet, connected by loops (Figure 1.5; Adams et al. 2011; Nilsson et al. 2004; Sondek and Siderovski 2001; Ullah et al. 2008). These compact and multi-sided structural features facilitate protein-protein interactions.

Indeed, RACK1 has been reported to interact with a number of other WD repeat-containing proteins (Chen et al. 2004b). The WD repeat sequence of RACK1 is highly conserved in a diverse range of species (Adams et al. 2011), including plants (Kwak et al. 1997; Ullah et al. 2008) and genetically malleable species, such as *Drosophila melanogaster* and *Caenorhabditis elegans* (Bini et al.). Indeed, RACK1 is ubiquitously expressed in the tissues of humans, including the brain, liver, and spleen (Chou et al. 1999), suggesting that it has an important functional role in most, if not all, cells. Furthermore, RACK1 has been implicated in diverse physiological processes such as development, cell migration, central nervous system function, and circadian rhythm (Adams et al. 2011).

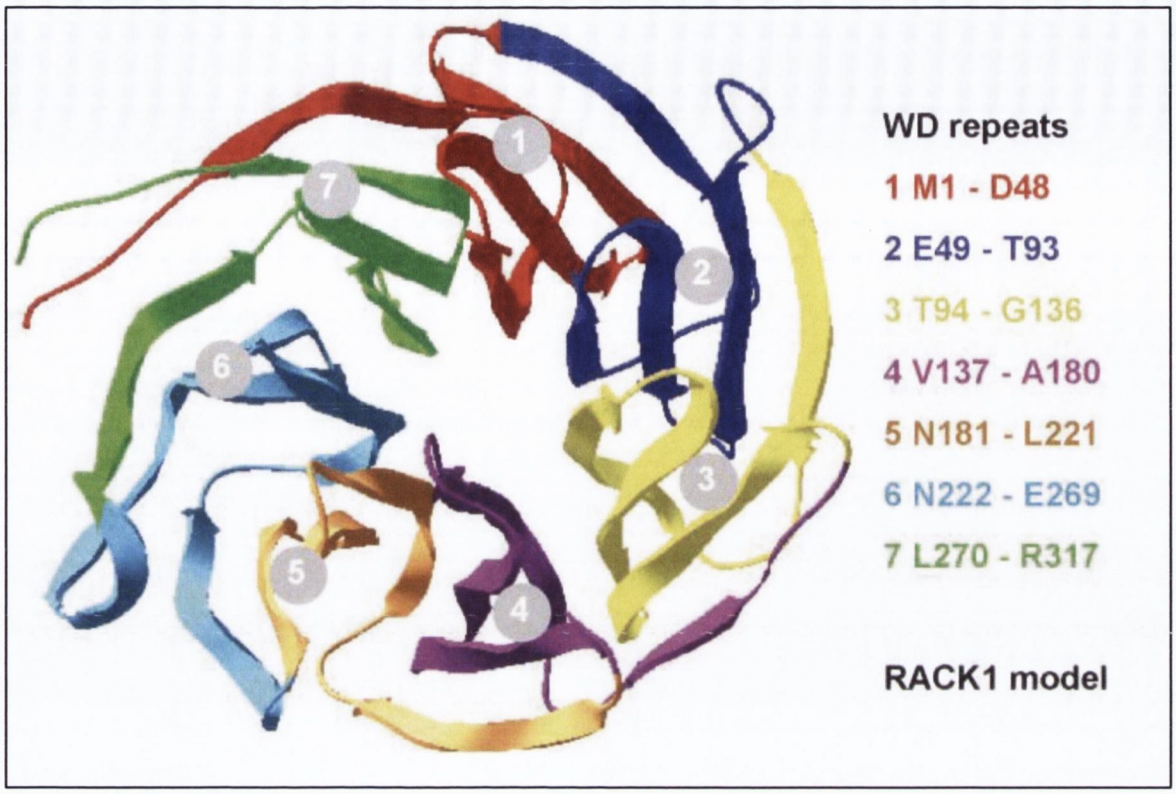

Figure 1.5: Ribbon diagram of RACK1.

RACK1 propeller blade model depicting the seven WD repeat sequences colour coded and numbered from the N terminus (Adapted from McCahill et al. 2002).

1.9.2 RACK1 Protein Interactions

As a scaffold protein, RACK1 integrates signalling inputs from distinct pathways and is critical for fundamental cellular activities such as cell proliferation, transcription and protein synthesis, as well as various neuronal functions. The compact and multi-sided structural features of RACK1 allow it to bind proteins through a wide array of protein domains. By controlling the interaction network between these different families of signalling proteins, RACK1 regulates a wide range of discrete signalling events at the level of several subcellular compartments such as the cytosol (Adams et al. 2011; McCahill et al. 2002), the endoplasmic reticulum (Qiu et al. 2010), and the nucleus (He et al. 2010; Neasta et al. 2012; Robles et al. 2010). In addition, translocation of RACK1 from one subcellular location to another has been shown to mediate various cellular responses following a stimulus. For instance, RACK1 accompanies PKC βII to its site of action in response to its activation.

Indeed, RACK1 has been shown to associate with several isoforms of PKC. RACK1 was originally identified through interactions with active "conventional" PKC isoforms (Csukai and Mochly-Rosen 1999; Mochly-Rosen et al. 1995; Mochly-Rosen and Gordon 1998; Ron et al. 1999). However, RACK1 has also been reported to interact with novel PKCs, e.g., PKC ε (Besson et al. 2002). These observations strongly support the notion that RACK1 may regulate cell processes other than those involving conventional PKCs. For example, binding of PKC βII to RACK1 is important for PKC-mediated translational control (Grosso et al. 2008). In addition, RACK1, in association with PKC ε, regulates the activity and stabilises the expression of the cyclic AMP-dependent cystic fibrosis transmembrane conductance regulator (CFTR) Cl channel in the apical plasma membrane of epithelial cells, which plays a key role in fluid homeostasis. Defects in CFTR channel activity or biosynthesis lead to the development of the disease cystic fibrosis (Auerbach and Liedtke 2007). In addition to associating with the serine/threonine PKCs, RACK1 is a molecular scaffold for protein tyrosine kinase Fyn (Yaka et al. 2002).

While RACK1 contains structural domains which present multiple protein-binding domains, many binding partners interact with RACK1 at the same site. This allows proteins to competitively bind RACK1 in a stimulus-dependent manner. For instance, Protein phosphatase 2A, or PP2A, and Insulin growth factor 1-receptor (IGF-1R) bind RACK1 in a mutually exclusive manner. IGF-1R binding induces PP2A to dissociate from RACK1 allowing it to bind β1 integrin, which is necessary for IGF-I integration and adhesion-mediated recruitment of other proteins to the complex to promote cell

migration. (Kiely et al. 2008). Binding of RACK1 to integrins also promotes the engagement of survival signalling pathways (De Toni-Costes et al. 2010), the mitogen-activated protein kinase (MAPK) pathway (Vomastek et al. 2007), and the recruitment of several PKC isoforms (Besson et al. 2002; Buensuceso et al. 2001; Lee et al. 2002). T cell integrins and associated signalling pathways are detailed in the following sections.

RACK1 also functions as a homodimer, thereby increasing its number of binding partners (Chen et al. 2005; Thornton et al. 2004). Moreover, the formation of a homodimer enables the simultaneous interaction of RACK1 with two binding partners that share the same binding site on RACK1. For instance, dimerization of RACK1 allows the concurrent interaction with both Fyn and the NR2B subunit of the N-methyl-D-Aspartate receptor (NMDAR), which engage overlapping residues of RACK1 (Yaka et al. 2002). Furthermore, RACK1 has also been shown to interact with ribosomal machinery, several cell surface receptors, and proteins within the nucleus (Grosso et al. 2008; He et al. 2002; Liliental and Chang 1998).

The protein liaisons that involve RACK1 seem to fall into two broad categories: constitutive, as with the cyclic AMP-specific phosphodiesterase PDE4D5 (Yarwood et al. 1999), and stimulus-dependent, as with PKC. RACK1 also plays a key role in modulating the enzymatic activity of its binding partners, either promoting or suppressing the activity of bound enzymes (Adams et al. 2011). Therefore, RACK1 is a key mediator of various pathways and contributes to numerous aspects of cellular function. Indeed, the accumulated data from a number of studies indicates RACK1 acts as a general scaffolding protein and interacts with a range of different cellular proteins including kinases, phosphatases, transcription factors, and the cytoplasmic domain of membrane proteins (Adams et al. 2011). Thus, as a result, RACK1 may have diverse, cell type-specific functions.

1.10 T cell Integrins

Integrins are αβ- heterodimeric cell surface receptors that mediate cell-cell and cell-extracellular matrix (ECM) interactions, critical for cell growth and development, haemostasis, and host defence (Arnaout et al. 2005; Skubitz 2002). T cells use integrins in essentially all of their functions, including migration in and out of lymph nodes and, following infection, migration into other tissues as well as formation of the immunological synapse between T cells and APCs (Hogg et al. 2003). T lymphocytes express at least 12 of the 24 known integrin heterodimers, depending on the subtype and maturation

state of the cell (von Andrian and Mackay 2000). The integrin lymphocyte function associated antigen (LFA)-1 ($\alpha_L\beta_2$) has the most abundant and widespread expression in T cells (Hogg et al. 2003). LFA-1 plays a prominent role in T cell signalling events that coordinate cellular responses, such as migration (Shimizu 2003).

Evidence suggests LFA-1, also known as CD11a/CD18, is expressed on virtually all leukocytes and many leukocyte-derived cells (Cabañas and Sánchez-Madrid 1999; Springer 1990a; Springer et al. 1987) and displays high-affinity adhesion to the β_2-integrin ligands (Zecchinon et al. 2006). The adhesion process is critical for a wide range of immunological processes, including cytolysis of target cells by complement-mediated membrane disruption, lymphocyte interaction and cross-stimulation, phagocytosis of complement-coated targets, and the regulation of leukocyte trafficking between the bloodstream and tissues (Zecchinon et al. 2006). In addition, the peripheral ring of the immunological synapse is comprised of LFA-1 where it mediates adhesion between T cells and APCs (Shimizu 2003). Under normal conditions, integrins (including LFA-1) are in inactive or non-ligand-binding conformation in circulating lymphocytes. Exposure to cytokines or chemokines and engagement of other cell-surface receptors and adhesion molecules results in rapid integrin activation and subsequent ligand binding (Denucci et al. 2009; Ebert et al. 2005; Hogg et al. 2003). The activation of LFA-1 on T cells is discussed in detail in section 1.10.2.

1.10.1 Features of LFA-1 structure

In recent years, experimental and conceptual advances in the integrin field, especially publication of the crystal structure, have furthered our understanding of the dynamic integrin structure (Arnaout et al. 2005). The structure of LFA-1 can be divided into three basic domains: the ligand binding domain, transmembrane domain, and cytoplasmic domain (Figure 1.6).

Both the α- and β-subunits of LFA-1 contain a large extracellular ligand binding domain. The extracellular region of the α-subunit comprises an N-terminal seven-bladed β-propeller domain followed by three β-sandwich domains (termed thigh, calf-1, and calf-2). It also contains a domain of about two hundred amino acids known as an inserted (I) domain, which is incorporated in the upper face of the β-propeller. In LFA-1, the α I domain is the major ligand-binding site. While, the β-subunit extracellular regions consists of an N-terminal cysteine rich PSI (plexin-semaphorin-integrin) domain, a single

β-sandwich hybrid domain, a β I-like domain, four integrin EGF-like (IEGF 1-4) repeats, and a β-tail domain (Evans et al. 2009).

The transmembrane segment is approximately 25-29 amino acids long. Glycosylation studies have demonstrated transmembrane segments are likely tilted or coiled inside the membrane (Armulik et al. 1999; Stefansson et al. 2004). Rearrangement of the inter-helical transmembrane interface is necessary for integrin activation as well as integrin-mediated signal transduction; however, there is still a lack of evidence as to how the transmembrane interface induces activation of the integrin (Adair and Yeager 2002; Gottschalk et al. 2002; Luo et al. 2004; Partridge et al. 2005).

The cytoplasmic tails of LFA-1 are small in size (<50 residues) relative to the extracellular domains, but are pivotal in transmitting the induction of high-affinity ligand binding and signalling functions of engaged LFA-1, which are described in detail in section 1.10.6 (Woodside et al. 2001). The assembly of protein complexes to the α- and β-subunit carboxy-terminal tails is necessary for integrin activation, as these interactions have been shown to stabilise the extended integrin conformation and provide a mechanical link to the cytoskeleton (Hogg et al. 2011).

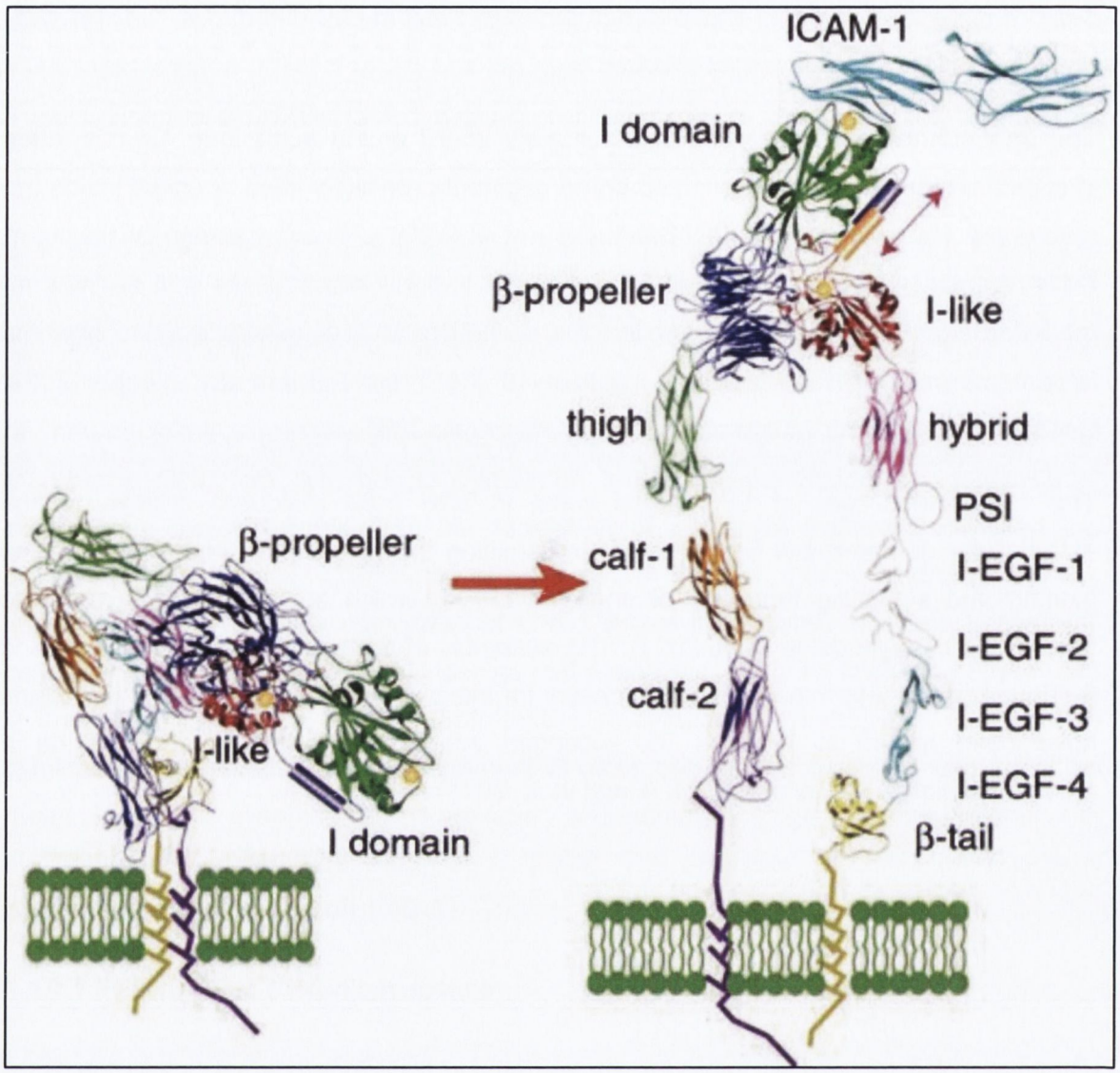

Figure 1.6: Ribbon diagram of LFA-1.

The structural domains of the α– and β–subunits of both the inactive, bent and extended conformations of LFA-1 integrin are depicted (Adapted from The Jin Lab Website).

1.10.2 Activation of LFA-1 on T cells

Because of their prominent role and functional implications in the immune response, T cell integrins are maintained in an inactive state on the cell surface of circulating leukocytes to prevent inappropriate binding to their ligands. Expression of the inactive form of LFA-1 in circulating peripheral blood T lymphocytes (PBTLs) is crucial in maintaining homeostasis, since constitutively active LFA-1 would cause instantaneous aggregation of circulating cells and clogging of the blood vessels as well as trigger an inappropriate immune response (Lub et al. 1995; Smith et al. 2007a). The activation of leukocyte integrins through stimulation of diverse receptors induces transformation of the integrin from a bent, resting form to an extended conformation, with at least two known states of ligand-binding activity. This highly regulated activation process is essential for T cell migration and the formation of an immunological synapse (Hogg et al. 2011).

LFA-1 activation status, and subsequent function, is triggered by signalling produced by ligation of other membrane receptors, such as the TCR. This ensures integrin activation is site specific and occurs only after a series of immune activation steps. These signals can also be triggered by the phorbol myristate acetate (PMA), or by substances that increase intracellular calcium levels (van Kooyk & Figdor 2000; van Kooyk et al. 1989; Dustin & T A Springer 1989; Lub et al. 1995).

Ligation of cell-surface receptors, such as the TCR or chemokine receptors, generates intracellular signals necessary for integrin activation and adhesive mechanisms. This is known as 'inside-out' signalling. Addition of the divalent cations Mn^{2+}/Mg^{2+} or activating antibodies that bind to the extracellular domain of LFA-1 cause conformational changes that also activate LFA-1 (Stewart et al. 1996). Furthermore, *in vitro* analysis of lymphocyte migration has demonstrated intracellular activation can also be induced by divalent cations or LFA-1 activating antibodies (Dransfield et al. 1992; Hogg et al. 2003).

Ligand binding can also trigger an enhanced affinity of leukocyte integrins. Activated integrins are also capable of inducing intracellular signal transduction pathways, known as 'outside-in' signalling (Abram and Lowell 2009; Hogg et al. 2003).

Increased affinity for ligand by conformational changes and avidity, or clustering of integrins on the cell surface, are necessary for successful integrin-mediated adhesion and locomotion Both mechanisms are highly regulated by a complex exchange of signalling events, binding of divalent cations, and association with the cytoskeleton and accessory molecules (Hogg et al. 2003; Stewart and Hogg 1996). For example, 'inside-

out' activation by addition of phorbol esters induces an increase in integrin lateral mobility and clustering through a cytoskeletal-dependent mechanism (Kucik et al. 1996). In order to control the activity of integrins during lymphocyte circulation, the integrins are constrained by the cytoskeleton. After antigen engagement of the TCR, integrins are released from their cytoskeletal constraints by the Ca^{2+}-dependent activation of a calpain-like enzyme, resulting in integrin clustering and increased adhesion (Leitinger and Hogg 2002; Stewart et al. 1998).The known mechanisms of LFA-1 activation in immune cells is displayed in Table 1.1.

However, since integrins cooperate with other receptors (e.g. TCR), its specific signalling function is difficult to ascertain. Moreover, while the cytoplasmic domains of integrins have been shown to be important in linkage to the cytoskeleton and recruitment of signalling molecules, they are short and lack enzymatic features. To overcome this, it is believed that LFA-1 associates with adaptor proteins, which mediate its interaction with the cytoskeletal network, cytoplasmic kinases, and G-coupled protein receptors to induce signal transduction (van Kooyk and Figdor 2000).

Table 1.1: Known Mechanisms of LFA-1 Integrin Activation in Immune Cells

Inside-out Activation	
TCR Ligation	Antigen or CD3 ligation activates TCR signalling, which induces cytoskeletal reorganisation and integrin avidity.
Chemokine Receptor Ligation	Chemokines activates signalling pathways downstream of the chemokine receptor, thereby influencing integrin affinity.
Phorbol Esters	DAG analogues that can activate PKCs directly and thus bypass TCR ligation; induces cytoskeletal reorganisation and integrin avidity.
Outside-in Activation	
Mg^{2+}, Mn^{2+}	Divalent Cations bind to α I domain to allow high affinity ligand binding.
Ligand	Ligand-binding activates signalling pathways downstream of LFA-1 to influence cytoskeletal reorganisation.
Activating antibodies	Antibodies that bind and activate LFA-1 ectodomain inducing high-affinity ligand binding, thereby activating downstream signalling of LFA-1 to influence cytoskeletal reorganisation.

1.10.3 LFA-1 Activation Induces Conformational Change

A basic model for LFA-1 activation has been developed from the structural data generated by electron microscopy and crystallography studies of integrins together with the use of monoclonal antibodies that recognize epitopes exposed only after LFA-1 activation. The functional implications of integrin activation on conformational changes has been discussed at length (Luo et al. 2007; Shimaoka et al. 2002; Takagi and Springer 2002). These studies have identified three predominant LFA-1 conformations that are thought to reflect different stages of activation. These include the inactive bent form, the extended form with a closed ligand-binding head that exhibits intermediate ligand affinity, and, finally, the active form, in which the hybrid domain has swung out, enabling the ligand-binding I domain of the α subunit to bind with higher affinity (Figure 1.7; Evans et al. 2009; Nishida et al. 2006).

Since the determination of these initial structures, an increasing number of studies on both the extracellular and cytoplasmic domains have established that the bent conformation represents the physiological low-affinity, inactive state, whereas 'inside-out' signalling and ligand binding trigger the extended conformation (Evans et al. 2009; Kim et al. 2003; Takagi et al. 2003; Takagi and Springer 2002; Xiao et al. 2004). The three conformations can be distinguished by their binding to specific monoclonal antibodies, which were designed to interact with the different epitopes as they become exposed (Figure 1.7). LFA-1-mediated arrest of rolling lymphocytes is triggered by chemokines expressed on the endothelium. This chemokine receptor signalling triggers the instantaneous conformational rearrangement of LFA-1 even in the absence of LFA-1 engagement (Shamri et al. 2005). The initial interaction of intermediate-affinity LFA-1 with its ligand has been proposed to induce the high-affinity conformation thereby stabilising adhesion, but the conformational switches are still not fully understood.

Interestingly, potent TCR signals alone are not capable of inducing the extended head piece of LFA-1, whereas LFA-1 interaction with surface-bound ligand does trigger the high-affinity conformation. While TCR activation can stimulate LFA-1 in the absence of sheer blood flow and internal mechanical forces, primary binding to surface-bound ligand is necessary to induce the high-affinity conformation, resulting in cell arrest and spreading on the endothelium (Alon and Dustin 2007; Evans et al. 2009; Feigelson et al. 2010). Moreover, recent data from *in vitro* sheer flow studies supports the theory that integrin activation is dependent on traction or translational motion. The authors reported the interaction of chemokine-stimulated LFA-1 with surface-immobilised but not soluble

ligand was able to trigger the adhesive, high affinity state of LFA-1 (Schürpf and Springer 2011). Furthermore, it was observed the presence of sheer flow increases the number of adhesive and invasive filopodia (Shulman et al. 2009). Nevertheless, T lymphocyte crawling and migration is dependent on chemokine triggering of high-affinity LFA-1 integrin under shear flow.

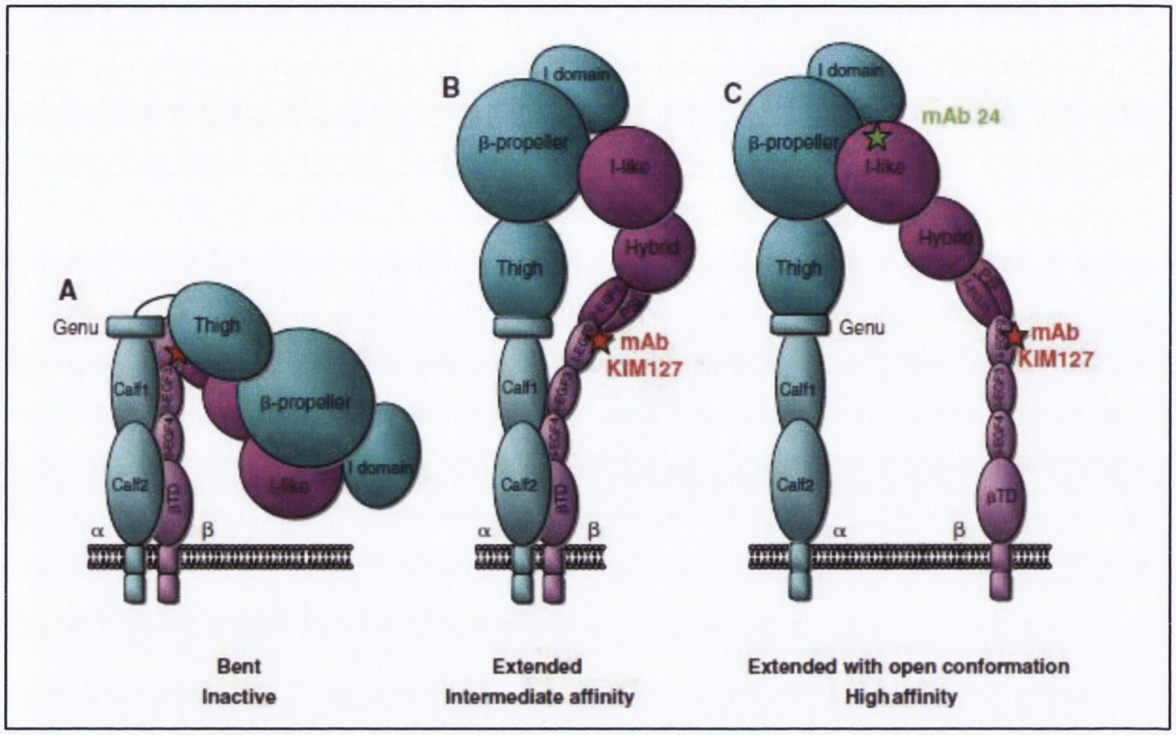

Figure 1.7: The three conformations of LFA-1.

The three conformations of LFA-1 include the inactive bent form (A), the extended form (B) with a closed ligand-binding head that exhibits intermediate ligand affinity recognised by monoclonal antibody (mAb) KIM127, and, the extended with open conformation (C), in which the hybrid domain has swung out, enabling the ligand-binding I domain of the α subunit to bind with higher affinity identified by mAb 24 (Adapted from Evans et al. 2009).

1.10.4 Distribution of LFA-1 in Migrating T cells

The distribution of LFA-1 in the membrane of migrating T cells varies across the cell surface. Confocal microscopy has demonstrated that cell surface expression of LFA-1 ranges from a low level at the cell's leading edge to a high level in the non-attached uropod at the rear. The formation and stability of the LFA-1 distribution pattern is dependent on the integrin-associated protein talin and differs from integrin-containing attachments displayed by other cell types (Smith et al. 2005). This uneven distribution of LFA-1 correlates with changes in morphology during cell migration (Evans et al. 2009).

Using probes for the two active conformations of LFA-1, it was observed there is at least three separate expression and activation zones of LFA-1 in the migrating T cell: intermediate affinity in the projecting lamellae at the leading edge, high-affinity LFA-1 in the midcell zone, and high levels of LFA-1 of unknown affinity in the uropod (Figure 1.8; Evans et al. 2009). This is in keeping with the report that the expression and activation status of integrin receptors varies across the polarised cell (Smith et al. 2005).

The rapidly protruding and retracting leading edge of the T cell expresses a low level of intermediate affinity LFA-1 (Smith et al. 2005; Stanley et al. 2008). This conformation of LFA-1 is speculated to allow the leading edge to participate in rapid, transient adhesive interactions than would high-affinity LFA-1. Moreover, it is suspected these weaker, temporary contacts made by intermediate affinity LFA-1 with its ligand are more susceptible to membrane remodelling and rapid shape change in response to chemoattractants during an immune response than highly stabilised contacts (Evans et al. 2009; Smith et al. 2007a). In order for the T cell to achieve forward momentum, the LFA-1 at the leading edge must communicate with the cytoskeleton through direct linkage or by signalling its reorganisation. The importance of this integrin-cytoskeletal link during T cell migration is discussed in detail in section 1.12.

In contrast, the elevated expression of high affinity LFA-1 the midcell focal zone provides firm adhesion and stability during migration (Smith et al. 2005). If the focal zone is immobilised by LFA-1 antibody binding, the leading edge remains motile, indicating that the generation of mechanical force at the leading edge is sufficient to propel the cell forward. This feature allows T cells to rapidly migrate within lymph nodes and inflamed tissue. However, once a T cell encounters an APC bearing appropriate antigen, then activated TCR provides addition 'stop' signals, resulting in cessation of migration (Smith et al. 2007a).

Despite expressing the highest level of LFA-1 in the migrating T cell, the involvement of the uropod has been somewhat neglected in models of T cell motility (Smith et al. 2005). This high level of LFA-1 is in keeping with the idea of the uropod acting as a reservoir or storage depot that recycles LFA-1 to the leading edge for migration to proceed. The mechanisms underlying this recycling process are not well understood but studies have implicated intracellular vesicle trafficking or lipid raft transport over the plasma membrane (Gómez-Móuton et al. 2001; Millán et al. 2002; Sánchez-Madrid and Serrador 2009). There is even published data suggesting that uropod resident LFA-1 has the potential to link into the actin cytoskeleton via human discs large-1 (Smith et al. 2007a).

Barreiro and colleagues (2007) discussed the functional significance of the dynamic redistribution of integrins during T cell migration. They proposed that because the T cell extends exploratory pseudopodia through the endothelial cell junction during extravasation, integrins are continually recycled in lipid rafts via endo/exocytosis to replenish regions of new protrusions and adhesions.

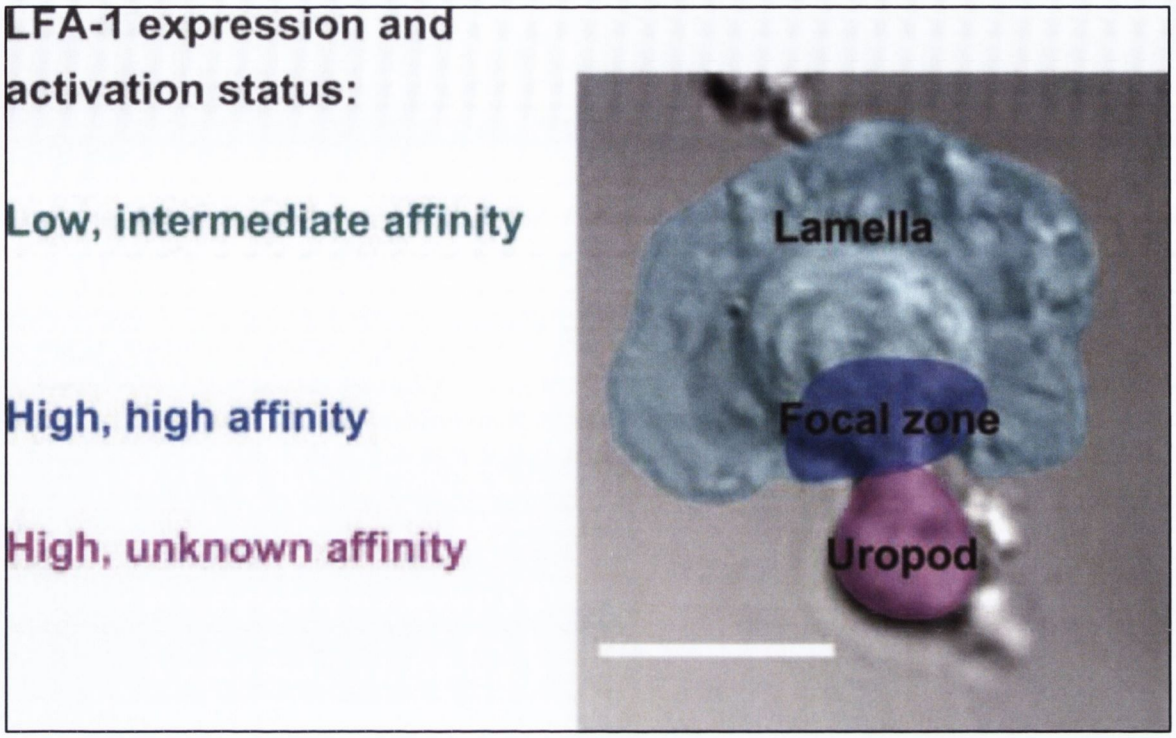

Figure 1.8: Expression and Activation Status of LFA-1 Integrin.

A model illustrating the differential expression and affinity conformations of LFA-1 during T cell migration in the forward stretching lamellipodium, midcell focal zone, and trailing uropod (Adapted from Smith et al. 2007a).

1.10.5 LFA-1 Ligands in T cells

The predominant cellular ligands for leukocyte integrins, such as LFA-1, are called intercellular adhesion molecules (ICAMs). They are members of the immunoglobulin superfamily, which contain characteristic Ig-domains composed of two β-sheets connected by a highly conserved disulphide bridge. ICAMs are type I transmembrane glycoproteins and have a large extracellular domain, which is composed of Ig-like domains, and a relatively short cytoplasmic tail (Gahmberg et al. 1997; Springer 1990a). To date, five ICAMs (ICAM-1 to ICAM-5) have been described. ICAM-1 and ICAM-3 each contain five Ig-domains, whereas ICAM-2 and ICAM-4 contain only two; ICAM-5 is unusually complex with its nine Ig-domains. Although all the ICAMs are structurally analogous and bind leukocyte integrins, each family member possesses a distinct function, cell signalling capacity, and expression pattern (Gahmberg et al. 1997; Hayflick et al. 1998; Long 2011). The distinct structures of the ICAMs are illustrated in Figure 1.9.

ICAM-1, also known as CD54, was originally characterised by Dustin and colleagues (1986) and is by far the most researched ICAM to date. ICAM-1 is the principal ligand for integrins and is expressed throughout the vasculature, lymph nodes, and tissue cells. It is an endothelial- and leukocyte-associated protein long recognised for its importance in stabilising cell-cell interactions and facilitating leukocyte endothelial transmigration during immune surveillance (Long 2011). ICAM-1 is a transmembrane protein possessing an N-terminus extracellular domain, a single transmembrane domain, and a C-terminal cytoplasmic domain. It is normally present in low concentrations in the membranes of leukocytes and endothelial cells, but is extensively upregulated in response to pro-inflammatory cytokines such as tumour necrosis factor-α (TNF-α), interferon gamma (IFN-ɣ), and interleukin-1 (IL-1) (Gahmberg et al. 1999; Hayflick et al. 1998; Springer 1990b). Activated leukocytes bind to endothelial-bound ICAM-1 via LFA-1, which facilitates transmigration of leukocytes across the vascular endothelium and extravasate into target tissues. Due to its prominent role during an inflammatory response, ICAM-1 has classically been assigned the function of intercellular adhesion. The functionally important integrin-binding site in ICAM-1 lies in the N-terminal domain (D1) with some contribution by the second domain (D2), which is shown in Figure 1.9 (Bella et al. 1998; Shimaoka et al. 2002; Staunton et al. 1990). Additionally, it has been shown that LFA-1 integrin ligation with ICAM-1 initiates intracellular signalling cascades involving a number of kinases resulting in pro-inflammatory effects such as leukocyte recruitment, which are discussed in the following section.

ICAM-2 (CD102) is also present on leukocytes and endothelial cells (Kotovuori et al. 1999). Although, unlike ICAM-1, ICAM-2 displays a more stable expression and is not easily induced *in vivo*. However, an upregulation of ICAM-2 has been reported in lymphomas (Renkonen et al. 1992). A major function of ICAM-2 may actually be its stimulatory action on leukocytes, in that, it has been shown to induce cytotoxicity as well as locomotion in an adhering leukocytes (Somersalo et al. 1995). The third family member, ICAM-3 (CD50), is constitutively expressed on leukocytes and functions not only as an adhesion molecule but also as a potent signalling molecule. Interestingly, it binds well to LFA-1 (Gahmberg et al. 1999). Certainly, its putative regulatory role in an immune response should be further explored. ICAM-4, more commonly referred to as the Landsteiner-Wiener (LW) blood group antigen, has also been shown to bind leukocyte integrins (Gahmberg et al. 1999). LW has been shown to contribute to erythrocyte adhesion during haematopoiesis. LW may also contribute to other intravascular processes, such as both venous and arterial thrombosis, due to its ability to interact with both activated platelets as well as leukocytes (Delahunty et al. 2006). The expression of ICAM-5, also known as telencephalin, is brain tissue-specific and is able to bind leukocyte β_2 integrins. As a novel cell adhesion molecule, ICAM-5 shares many structural similarities with the other members of Ig superfamily; however, ICAM-5 has several unique properties compared to the other ICAMs. With its nine extracellular Ig domains, ICAM-5 is the largest member of ICAM subgroup identified thus far. Whereas all the other ICAM members are expressed mostly by cells in the immune and blood systems, the expression of ICAM-5 is confined to the telencephalic neurons of the central nervous system and is involved in synapse formation in the telencephalon. Moreover, recent studies show that it is important for the regulation of immunological activity in the brain and for the development of neuronal synapses and signal transmission (Gahmberg et al. 2008; Yang 2012).

Additionally, increasing evidence suggests LFA-1 may bind to other proteins such as E-selectin (Kotovuori et al. 1993), type I collagen (Garnotel et al. 1995), and junctional adhesion molecule 1 (JAM-1) (Ostermann et al. 2002). The signalling events that occur after ligation of LFA-1 mediating the immune response are described in the next section.

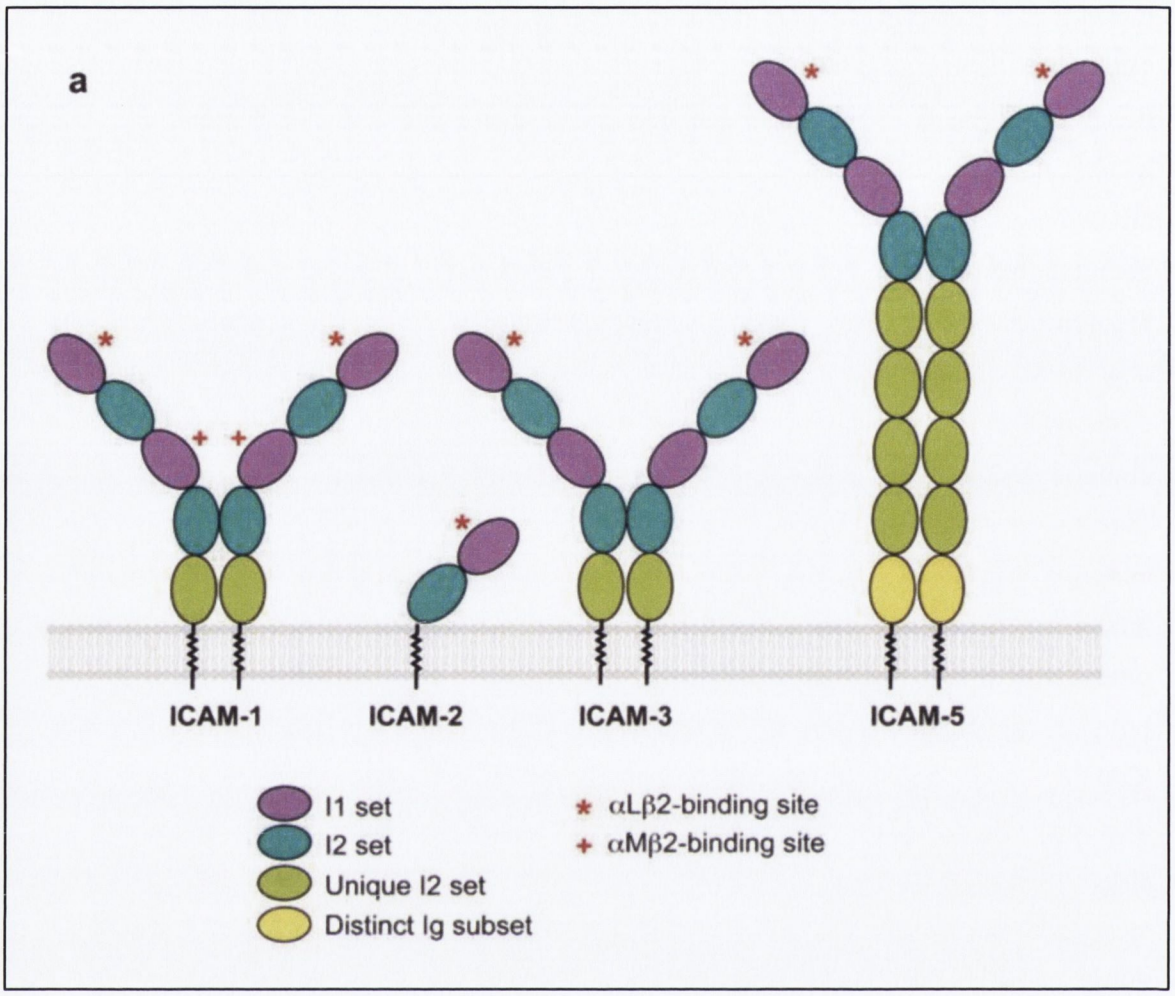

Figure 1.9: ICAM Structure and Integrin Binding.

Schematic diagram of ICAM-1, -2, -3, and -5. The domains are colour coded, and integrin-binding sites are shown (Adapted from Luo et al. 2007).

1.10.6 LFA-1 Signalling in T cells

Integrins can transmit information about the chemical and mechanical qualities of the surrounding environment into the cell as well as reveal the internal status of the cell to the periphery, allowing rapid and flexible responses to stimuli, including changes in cell morphology. As mentioned in the previous section, ligation of cell surface receptors with chemokines, cytokines, and foreign antigens initiates an intracellular signalling cascade altering integrin adhesion mechanics. This dynamic feature of integrins allows immune cells to rapidly adapt to their environment and is central to maintaining an appropriate immune response.

Integrins are also capable of signalling, and the pathways dedicated to the molecular mechanisms necessary for cell locomotion have been of recent interest. Ligation to ICAM-1 on the endothelium activates LFA-1 leading to T cell arrest and spreading. Integrin ligation induces polarised signal transduction cascades resulting in cytoskeletal reorganisation and a polarised distribution of signalling molecules. In addition, the LFA-1/ICAM-1 interaction mediates dynamic adhesions between the lymphocyte and endothelial cell during transmigration (Hogg et al. 2011; Hogg et al. 2004) Moreover, ligation of T cell integrins induces several intracellular signalling pathways in cells that alter gene expression, and thus influences cell survival, differentiation, morphology, and migration (Giancotti and Ruoslahti 1999). Although integrins themselves do not have any catalytic activity, signals are transmitted through a complex interplay of integrin cytoplasmic domain adaptor proteins and signalling molecules (Luo et al. 2007).

Signalling events that directly follow LFA-1 engagement include recruitment and initiation of several kinases, which phosphorylate and thus activate target proteins in a signalling cascade. These include tyrosine kinases, such as zeta-chain-associated protein kinase 70 (ZAP-70) (Soede et al. 1998), the proline-rich protein tyrosine kinase (Pyk-2) (Rose et al. 2003), and focal adhesion kinase (FAK) (Giannoni et al. 2003; Kanner et al. 1993; Rodríguez-Fernández 1999) and serine-threonine kinases, such as PKC (Buensuceso et al. 2005; Soriani et al. 2006) and MAPK (Perez et al. 2003). For instance, in addition to mediating T cell adhesion and migration, LFA-1 signalling contributes to T cell activation and differentiation through cytohesin-1-mediated signalling of MAPK pathway (Perez et al. 2003).

Even more, signals initiated by engagement of one integrin can alter the function of a second integrin, a process termed integrin trans-regulation or cross-talk. A form of trans-

regulation relevant to the immune response has been demonstrated between two integrins essential for leukocyte migration, alpha-4/beta-1 integrin and LFA-1. Specifically, alpha 4/beta 1 engagement with ligand vascular cell adhesion molecule (VCAM)-1 triggers β2-integrin-dependent cell adhesion and migration (Chan et al. 2000; Rose et al. 2001). Moreover, tyrosine kinases have been shown to mediate this integrin cross-talk, whereby paxillin binding to the cytoplasmic domain of the alpha-4 subunit stimulates LFA-1-dependent T cell migration by enhancing the activation of Pyk-2 and FAK (Rose et al. 2003).

Moreover, while PKC is generally associated with chemokine-triggered 'inside-out' integrin activation, PKC isoforms have also been implicated in 'outside-in' signalling responses (Buensuceso et al. 2005; Soriani et al. 2006). However, the substrates of these PKC isoforms are unknown. Nevertheless, the functional implications of their roles in 'inside-out' and 'outside-in' signalling pathways warrant further investigation.

It is now established that integrins can transduce biochemical signals from the extracellular environment to the cell interior leading to profound changes in T cell behaviour (Abram and Lowell 2009; Arnaout et al. 2005). Most of the signalling pathways activated by integrins have been identified through the analysis of biochemical events that are triggered by integrin engagement and by the identification of proteins that associate with focal adhesion complexes. Information on the functions of such proteins has aided our understanding of their role in integrin-mediated signalling. These LFA-1-dependent signalling pathways control the function and, in particular, the migration of T cells. Integrin-mediated migration across the endothelium during an immune response is discussed in the following section.

1.10.7 Integrin-Mediated T cell Migration

The study of leukocyte integrin mechanics and signalling provides a detailed understanding of the processes involved in integrin-mediated T cell migration. This section describes the journey of an antigen-activated T cell from the lymph node to the site of inflammation. The migration of mature T cells is guided by chemotactic interactions to target vasculature (Alon and Shulman 2011; Ebert et al. 2005; Thelen and Stein 2008). Carbohydrate ligands on the circulating lymphocytes transiently bind to selectin molecules on endothelial wall with marginal affinity. This causes the leukocytes to slow down and begin rolling in a process known as rolling adhesion. Lymphocyte rolling is further slowed by chemokines secreted by cells within the inflamed tissue.

When chemokines adhere to their cognate receptors on the T cell, 'inside-out' signalling activates cell surface integrins, including LFA-1, to adhere to endothelial-bound ICAM-1 leading to lymphocyte arrest. Upon firm adhesion to ICAM-1, LFA-1 induces several signalling cascades resulting in cell polarisation, allowing the cell to undergo transendothelial migration (TEM) from the vasculature. This process is depicted in Figure 1.10. In addition to ICAM-1-mediated migration between endothelial cells (paracellular route), *in vivo* studies have shown that leukocytes can also migrate through an endothelial cell (transcellular route). This process has been demonstrated in both inflammatory scenarios *in vivo* (Feng et al. 1998) and *in vitro* models (Carman and Springer 2004). Only a small minority of emigrating cells (approximately 5-20%) undergo transcellular migration, which involves lymphocyte passage through a vacuole-formed intracellular channel. Because this type of leukocyte migration is associated with areas of endothelial-cell thinning, it is predicted that it facilitates leukocyte migration by shortening the transmigration pathway (Engelhardt and Wolburg 2004; Ley et al. 2007).

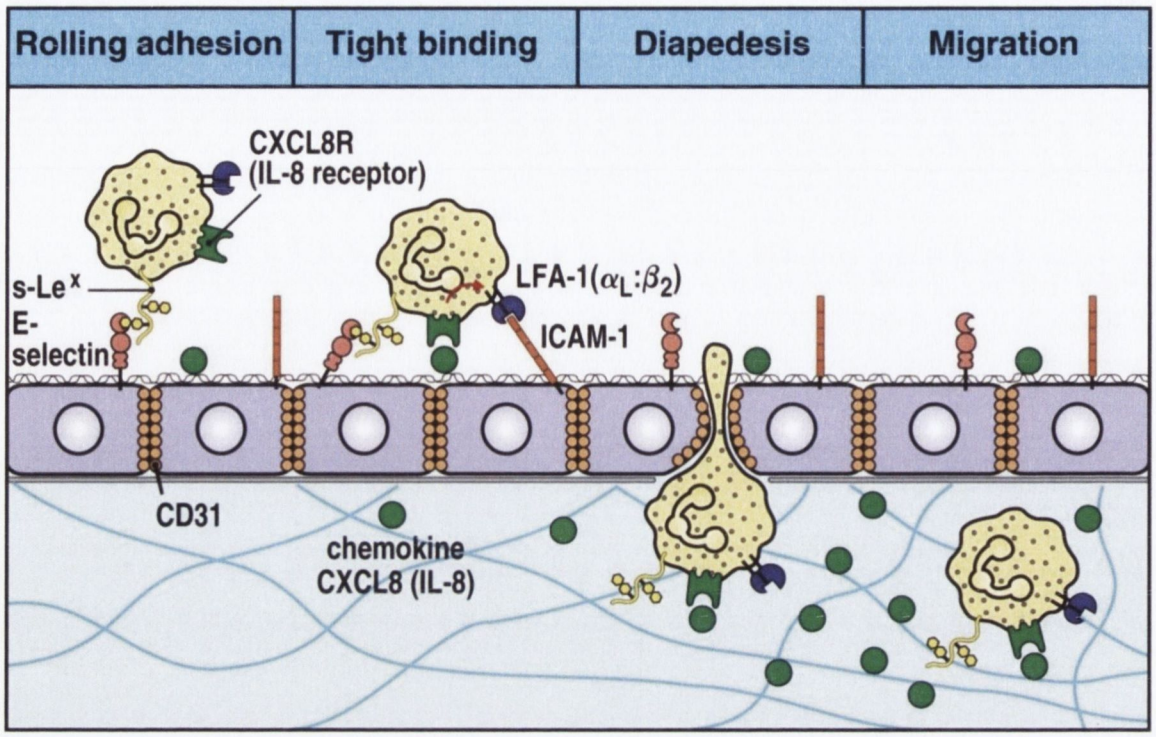

Figure 1.10: Lymphocyte Transendothelial Migration.

Illustration depicting the four steps of leukocyte transendothelial migration, including rolling adhesion, tight binding between LFA-1 and ICAM-1, diapedesis, and migration (Adapted from Janeway, Jr et al. 2001).

1.11 Composition and Regulation of Cytoskeletal Elements in T cells

The formerly distinct fields of lymphocyte signal transduction and cytoskeletal remodelling have recently become linked, as proteins involved in transducing signals downstream of lymphocyte antigen receptors have also been implicated in actin cytoskeleton remodelling, microtubule dynamics, and regulation of cell polarity. These discoveries have fuelled interest in understanding the role of the cytoskeleton as an integral component of lymphocyte activation (Miletic et al. 2003). The spatial and temporal distribution of integrins requires a precisely controlled cellular cytoskeleton, whose dramatic reorientation is tightly regulated by a number of signalling molecules and adaptor proteins. Actin-regulatory proteins associated with T cell activation facilitate downstream signalling events and effector functions to control actin dynamics in response to external stimuli. Activation of diverse cell surface receptors induces several signalling cascades regulating actin-regulatory proteins, thereby, directing T cell morphology. Complex interactions between external stimuli cell surface receptors and adhesion molecules initiate signalling pathways that trigger dynamic cytoskeletal rearrangements and subsequent motility in T cells (Burkhardt et al. 2008; Miletic et al. 2003; Samstag et al. 2003; Small and Kaverina 2003). Essentially, directed T cell migration is driven by a regulated and polarised turnover of the cytoskeleton.

The importance of cytoskeletal structure in cell migration was first recognized over forty years ago (Vasiliev et al. 1970). Further studies revealed a direct mechanistic link between the lymphocyte-specific components of the signal transduction pathways triggered by antigen and chemokine receptors and the downstream machinery that affect cytoskeletal reorganisation (Moissoglu and Schwartz 2006; Samstag et al. 2003; Vicente-Manzanares et al. 2002). It is now evident that dynamic remodelling the cytoskeleton plays a central role in T cell function, particularly T cell activation and migration. Although, a considerable degree of information has been amassed regarding the individual molecular components involved in migratory processes, the complex interplay of all the functional elements is still not fully understood. An increasing amount of evidence implicates cytoskeletal components in mediating early receptor-mediated intracellular signalling events.

The cytoskeleton is intimately involved in the dynamic regulation of the adhesive state of T cell integrins, in particular LFA-1 (Gomez and Billadeau 2008; Samstag et al. 2003; Small and Kaverina 2003; Stewart et al. 1998). It provides the matrix that enables recruitment and efficient formation of molecular signalling complexes. Numerous studies

have demonstrated that several signalling pathways initiated by LFA-1 activation require an intact cytoskeleton (Evans et al. 2011; Gundersen and Cook 1999; Hogg et al. 2004; Hogg et al. 2003; Pribila and Shimizu 2003; Samstag et al. 2003; Shimizu 2003; Small and Kaverina 2003; Stanley et al. 2008).

As mentioned in section 1.5.1, T cells respond to directional cues such as chemokine gradients via membrane receptors at the leading edge of the migrating cell. Inflammatory signals like chemokines attract migrating T cells by engaging membrane receptors. Localised receptor stimulation triggers polarised signalling cascades, which orients membrane protrusions at the leading edge. This polarised induction of cytoskeletal remodelling is required for directional migration. In addition, the cytoskeleton can also 'sample' its surrounding environment by supporting random membrane protrusions in the form of invasive filopodia (Alon and Feigelson 2002; Alon and Shulman 2011; Moissoglu and Schwartz 2006; Rikitake and Takai 2011). The interaction between the cell and its environment is dependent on cytoskeletal dynamics and dictates induction of lymphocyte effector functions versus lymphocyte anergy.

The cytoskeleton is composed of three distinct elements: actin microfilaments, microtubules, and intermediate filaments. The actin cytoskeleton is thought to provide protrusive and contractile forces, and microtubules to form a polarised network allowing organelle and protein movement throughout the cell. Intermediate filaments are generally considered the most rigid component, responsible for the maintenance of the overall cell shape (Ridley 2011). The function and regulation of all three cytoskeletal components in T cell migration will be discussed in the following sections.

1.11.1 Actin Cytoskeleton

The actin cytoskeleton is critically involved in cell motility and maintenance of cell shape and polarity. The cytoarchitecture of T cells rapidly transforms in response to extracellular stimuli depending on whether a cell is circulating within the bloodstream, migrating through tissues, or interacting with antigen-presenting cells (Burkhardt et al. 2008). The actin cytoskeleton exists as individual globular actin or G-actin which assembles into filamentous actin or F-actin, forming the microfilaments of the cytoskeleton. Actin filaments are a cytoskeletal component of all eukaryotic cells providing structural support and generating movements involved in cytoplasmic streaming, cell migration, cytokinesis, endocytosis, and secretion (Khaitlina 2001). The importance of cytoskeletal remodelling during lymphocyte activation was initially

recognised when research discovered the formation of a receptor cap and a uropod could be blocked by cytochalasins, inhibitors of actin polymerisation and elongation (Miletic et al. 2003).

Subsequent studies have established the importance of the actin cytoskeleton in T cell migration (Burkhardt et al. 2008; Etienne-Manneville 2004; Samstag et al. 2003; Vicente-Manzanares et al. 2009a). At the leading edge of the polarised migrating T cell, actin is organised in parallel bundles which form filopodia and in a dense meshwork that forms lamellipodia. In the cell body and uropod, filamentous actin forms contractile stress fibres responsible for the contraction of the cell body and retraction of the trailing edge. Actin polymerisation and depolymerisation is coordinated by a wide spectrum of signalling molecules and regulators in propelling T cells forward during migration (dos Remedios et al. 2003; Revenu et al. 2004; Samstag et al. 2003).

T cells have a directional axis of motility, and a fundamental driving force for the polarisation and migration of T cells is the dynamic remodelling of actin cytoskeletal elements. In most cell types that have been studied, remodelling is controlled by the Rho family of GTPases through a plethora of effector proteins. These Rho GTPases (such as Rac, Rho and Cdc42) which promote actin polymerisation (F-actin) and the formation of membrane protrusions at the leading edge of the cell (Gómez-Moutón and Mañes; Tybulewicz and Henderson 2009). Both Rac and Cdc42 localise to the leading edge of migrating cells where they promote F-actin-rich lamellipodia and filopodia, respectively (Ridley 2011). Overexpression of mutant forms of either GTPase results in loss of polarity and defective chemotaxis toward the chemokine SDF-1α (del Pozo et al. 1999). Downstream effectors of Rac and/or Cdc42 include the Wiskott-Aldrich syndrome protein, which induces actin nucleation via the Arp2/3 complex. In contrast to Rac and Cdc42, which promote actin nucleation, the GTPase RhoA activates a protein kinase, known as ROCK, that phosphorylates myosin light chains and, thus, increases the contraction of actin filaments (Laudanna et al. 1996; Wilkinson et al. 2005). Furthermore, as Rac often antagonizes Rho function (Leeuwen et al. 1997), the details of how these GTPases function in concert remains a mystery. The F-actin cytoskeleton is also modulated by other families of proteins including branching proteins (e.g. Arp2/3 complex), severing proteins (e.g. cofilin), capping proteins (e.g. gelsolin) and bundling proteins (e.g. plastins; Samstag et al. 2003).

1.11.2 Microtubule Network

Microtubules (MTs) are composed of polymers of alpha and beta tubulin heterodimers. They are found in the mitotic spindle and the cytoplasm where they contribute to cell shape and motility and provide anchoring and guiding for several protein complexes. Polymerised microtubules exist in equilibrium with free tubulin, and the regulation of microtubule formation and collapse is essential for assuming polarity and maintaining cell migration. Like actin filaments, microtubule formation is under dynamic regulation, resulting in MT retraction and extension during periods of catastrophe and rescue, respectively. As with actin filaments, microtubules can undergo treadmilling, with addition of tubulin heterodimers at the plus end and dissociation of tubulin heterodimers at the minus end. These dynamic processes are mediated by a large collection of MT-associated proteins (MAPs). Recent studies using green fluorescent protein (GFP) in living cells have shown that some MAPs accumulate specifically at the distal ends of growing microtubules. These plus-end binding proteins include cytoplasmic linker protein (CLIP)-170, CLIP-associated proteins (CLASPs), and the molecular motor dynein and are involved in MT treadmilling and linking the cell cortex to the plus ends of MTs, which are both necessary for cell migration (Watanabe et al. 2005).

The MT spindle is reorganised in T lymphocytes following antigen receptor activation. This MT network reorganisation is accompanied by the translocation of organelles important for protein secretion, such as the golgi apparatus (Watanabe et al. 2005). MTs nucleate from a region called the Microtubule-Organising Centre (MTOC), or centrosome, which regulates spindle formation. The MT spindle is orientated with the growing or 'plus ends' leading into the cytoplasm, while the 'minus ends' are anchored at the MTOC. The process of MT polymerisation requires GTP hydrolysis. The MT network is extremely dynamic and is constantly polymerising and depolymerising, or growth and shrinkage (Howard and Hyman 2003). In a polarised migrating T cell with a single leading edge, the MTOC and the Golgi apparatus are orientated behind the nucleus opposite to the direction of migration. This differs from most cell types where the MTOC reorients in front of the nucleus toward the direction of migration (Watanabe et al. 2005). This repositioning of the MTOC in an anti-polar position to the extending actin front is an essential determinant of the position of the uropod. It is hypothesised that this relocation of the MTOC in conjunction with the retraction of microtubule networks into the uropod facilitates transmigration through the polarised endothelium into inflamed peripheral tissues (Etienne-Manneville 2004; Ratner et al. 1997; Serrador et al. 1999; Sánchez-Madrid and Serrador 2009; Takesono et al. 2010). The polarity protein complex and

dynein motor protein activity have been implicated in the repositioning of the MTOC by engaging the distal ends of MTs (Etienne-Manneville et al. 2005; Krummel and Macara 2006). However, published reports suggest the apparent MTOC repositioning may actually be an illusion created by reorientation of the nucleus (Gomes et al. 2005). The mechanism of MTOC reorientation in T cells remains to be elucidated. Nevertheless, T cell migration is dependent on a delicate balance between extension and retraction of the MT network and rearrangement of cellular organelles.

1.11.3 Intermediate Filaments

Intermediate filaments are a family of related proteins that share common structural and sequence features. The domain structure of intermediate filaments molecules is conserved. Each protein has a non-alpha-helical (globular) domain at the N and C-termini, which surrounds the alpha-helical rod domain, which forms parallel dimers. The dimer is formed through the interaction of the rod domain to form a coiled coil. In contrast to actin and tubulin, which are globular proteins, intermediate filament proteins are fibrous (Herrmann et al. 2009). Intermediate filaments are putatively involved in absorbing mechanical stress and appear to play a vital role in cell plasticity, contractility, and rigidity (Herrmann et al. 2007; Wang and Stamenovic 2002). Mutations in the genes encoding intermediate filaments result in devastating diseases as diverse as muscular dystrophy and premature ageing (Eriksson et al. 2009). Despite most research focused on microfilaments or microtubules, the intermediate filaments protein vimentin, which is the major intermediate filament protein expressed in leukocytes, has been reported to control lymphocyte rigidity during chemokine-induced polarisation and migration (Brown et al. 2001). The authors demonstrated that intermediate filaments are a primary source of structural support in circulating human lymphocytes, but undergo a regulated collapse dependent on intact vimentin filaments required for TEM (Brown et al. 2001). More recently, vimentin has been implicated in lymphocyte adhesion and transmigration through endothelial cells (Nieminen et al. 2006).

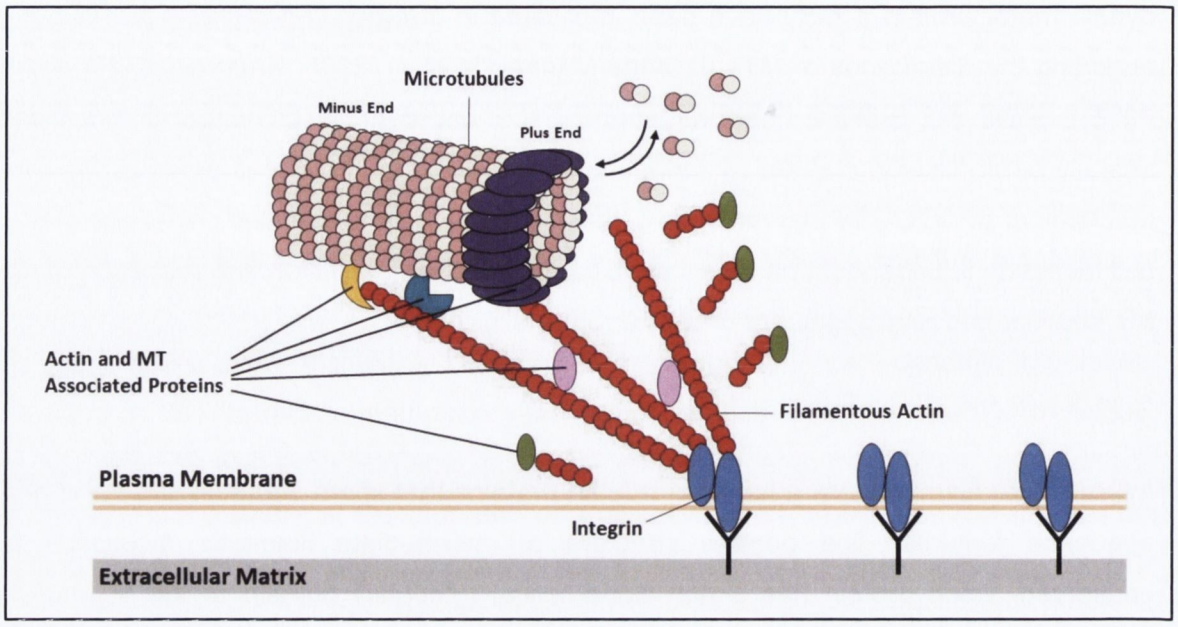

Figure 1.11: Actin and Microtubule Network Dynamics.

Polymerised MTs are guided along actin filaments in migrating cells. A number of actin- and MT-binding proteins influence the structure and organisation of the actin and MT cytoskeleton. Signal transduction cascades initiated by integrin activation target adaptor proteins that regulate cytoskeletal remodelling.

1.11.4 Non-muscle Myosin II

Myosins comprise a family of ATP-dependent motor proteins. Myosin is a force generating mechanoenzyme that is best known for its role in cell contractility and is required for cell spreading and cell migration. Although myosin was originally thought to be restricted to muscle cells, virtually all eukaryotic cells contain myosin isoforms. Myosins form a huge superfamily of genes whose protein products share the basic properties of actin-binding, ATP hydrolysis, and force transduction (Krendel and Mooseker 2005; Sellers 2000). The myosin superfamily is made up of several classes of myosins and has been implicated in diverse cellular functions including muscle contraction and protein transport. Extensive research has been done to identify the structure and function of myosins. The generic myosin structure consists of a *head domain*, which binds the filamentous actin and uses ATP hydrolysis to generate force and to "walk" along the filament towards the barbed end; the *neck domain*, which acts as a lever arm for transducing force generated by the catalytic motor domain and binding site for myosin light chains which have regulatory functions; and the *tail domain*, which mediates interactions with cargo molecules or other myosin subunits and is implicated in regulating motor activity (Sellers 2000; Syamaladevi et al. 2012).

The myosin II subfamily has the most members and includes skeletal, cardiac, and smooth muscle myosins, as well as non-muscle myosin II (NMII). NMII plays a role in a variety of cellular processes including cell migration, cytokinesis, cell adhesion and cell shape change (Conti et al. 2008). In addition, like all myosins, NMII can bind to actin and is involved in actin cross-linking and contractile function. NMII filaments are hexamers, consisting of two coiled-coil myosin heavy chains (MHC), two sets of myosin light chains (MLC), essential and regulatory. The MHC forms an amino-terminal globular motor domain, known as the myosin head, which contains an actin and ATP-binding site. The ATPase activity of the head enables a conformational change that moves actin filaments in an anti-parallel manner (Conti and Adelstein 2008; Goldman 1998). The tails of two MHC interact to form an extended α-helical coiled-coil rod domain that terminates in a short nonhelical tailpiece. NMII molecules assemble into bipolar filaments through interactions between their rod domains. Bipolar myosin filaments link actin filaments together in thick bundles that form actomyosin structures such as stress fibres (Vicente-Manzanares et al. 2009b). A schematic diagram depicting the association between NMII and actin filaments is shown in Figure 1.12.

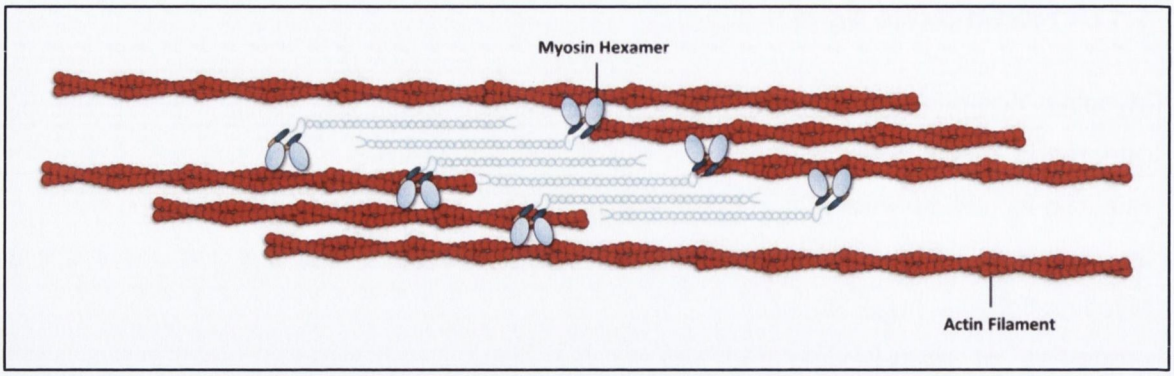

Figure 1.12: Actomyosin Complex.

Non-muscle myosin II is involved in actin filament rearrangement, which is necessary for processes such as cell adhesion, cell migration and cell division.

1.12 Chemokine-stimulated Directional Cell Migration

The arrest of leukocytes at target blood vessel sites depends on rapid conformational activation of β2 integrins through binding of endothelial-displayed chemokines to chemokine receptors (Alon and Shulman 2011; Shamri et al. 2005). As discussed in section 1.5.1, chemokine receptors present on the T cells recognise complex chemoattractant gradients that induce directed T cell migration and guide lymphocytes to areas of inflammation. These chemical signals, or cytokines, are then transmitted into the cells and result in activation of leukocyte integrins and actin remodelling machineries critical for leukocyte adhesion and motility across vascular barriers. Chemokines are a type of chemotatic cytokine. Primarily, chemokines are responsible for the directional migration, or chemotaxis, of leukocyte populations, where they coordinate the homing of lymphocyte populations to specific lymphoid tissues and the recruitment of lymphocytes to sites of infection or tissue damage (Ebert et al. 2005; Moser and Loetscher 2001; Ward and Westwick 1998).

One such chemokine very effective in activating T cells, inducing cytoskeletal reorganisation, cell polarisation, and promoting transendothelial migration is Stromal Cell Derived Factor 1 (SDF-1). SDF-1 is part of the chemokine family of C-X-C motif ligands and, thus, also referred to as CXCL12. SDF 1-alpha and 1-beta are small chemokine that belong to the intercrine family, members of which activate leukocytes and are often induced by pro-inflammatory stimuli such as lipopolysaccharide, TNF, or IL-1. SDF1 is expressed in two isoforms, SDF-1α and SDF-1β, by alternative splicing of the same gene (De La Luz Sierra et al. 2004). SDF-1α is expressed constitutively in a broad range of tissues and is strongly chemotactic for lymphocytes. During embryogenesis it directs the migration of hematopoietic cells from foetal liver to bone marrow and the formation of large blood vessels (Bleul et al. 1996). Stimulation with SDF-1α induces pleiotropic effects in T cells by activating multiple signalling pathways involved in hematopoietic cell trafficking and adhesion, lymphocyte homing, as well as tumour metastasis. SDF-1α is a potent chemoattractant and has roles in both inflammation and immune homeostasis (Bleul et al. 1996; Moser and Loetscher 2001).

Chemokines bind transmembrane chemokine receptors known as a G- protein coupled receptors (GPCRs). Because GPCRs span the plasma membrane, chemokines bound to the extracellular domain induce activation of the intracellular domain, thus, transmitting the chemical signal into the cell (Miller 2008). As the name implies, all GPCRs are intimately associated with a G (guanine nucleotide-binding) -protein complex, which is

activated by bound chemokine (Oldham and Hamm 2008). The heterotrimeric G proteins (α, β, γ) are a family of signal transducers that communicate signals from many hormones, neurotransmitters, and other signalling factors. The activated G protein triggers several distinct signalling cascades involving further effector proteins. These pathways interact with one another to form a network that regulates diverse cellular processes including transcription, motility, contractility, and secretion (Neves et al. 2002). These G-proteins act as a molecular switch, cycling between a GDP-bound inactive form and GTP-bound active form to transmit intracellular signals through an array of effector proteins (Neves et al. 2002; Oldham and Hamm 2008; Pitcher et al. 1998).

As stated previously, RACK1 shares significantly homology with the Gβ subunit of the heterotrimeric G protein. Gβ was identified as the anchoring protein of another translocating protein kinase, the G protein coupled receptor kinase (GRK). Gβ binds GRK following hormone binding to seven transmembrane receptors (Boguth et al. 2010; Pitcher et al. 1992). These findings suggest that there might be a family of WD-40 containing proteins that serve as selective anchoring proteins for different activated protein kinases.

Many chemokines act through GPCRs to activate small GTPases and promote directional cell migration (Etienne-Manneville and Hall 2002; Rickert et al. 2000). The activities of small GTPases are controlled both spatially and temporally by three kinds of regulators: guanine-nucleotide-exchange factors (GEFs), which promote the exchange of GDP for GTP; Rho GDP-dissociation inhibitors (GDIs), which interact with GDP-bound Rho GTPases and inhibit the exchange of GDP for GTP; and GTPase-activating proteins (GAPs), which enhance the intrinsic GTPase activities of Rho GTPases by hydrolysing GTP (Etienne-Manneville and Hall 2002; Siderovski and Willard 2005; Takai et al. 2001). Ligand-binding induces a conformational change in the GPCR, which allows it to act as a GEF. The GPCR can then activate an associated G-protein by exchanging its bound GDP for a GTP. Dissociation of the GTP-bound form can then trigger the initiation of a number of signal transduction pathways. For instance, binding of the chemokine SDF-1α to its chemokine receptor CXCR4 has been shown to activate the Janus kinase (JAK) /STAT pathway, phosphatidylinositol 3-kinase γ (PI3Kγ), and mitogen-activated kinase (MAPK) pathways (Chen et al. 2008; Ganju 1998; del Pozo et al. 1999; Rickert et al. 2000; Vila-Coro et al. 1999).

Among the pathways that regulate morphology of migrating cells, the small GTPases of the Rho family are particularly important in establishing cell polarity and in the formation

and disassembly of leading edge structures (Charest and Firtel 2007; Etienne-Manneville and Hall 2002; Nobes and Hall 1999; Tybulewicz and Henderson 2009). Chemokine-stimulated GPCRs transmit signals via multiple Rho GTPases, including Rac, RhoA, and Cdc42, which activate downstream effectors (e.g. WASp, Arp2/3) coordinating cytoskeletal rearrangement (Gallego et al. 2006; Miletic et al. 2003). Stimulation with SDF-1α elicits rapid translocation of PI3Kγ to the leading edge of cells, which in turn generates local accumulation of acidic phospholipids phosphatidylinositol-3,4,5-trisphosphate (PIP3; Rickert et al. 2000). PIP3 recruits pleckstrin homology (PH) domain-containing proteins, which are substrates of PKC, to the leading edge. In addition, it activates small GTPases, such as Rac and Cdc42, resulting in actin polymerisation, cell polarisation, and directional migration (Charest and Firtel 2007). Each Rho family member induces unique morphological changes that involve rearrangement of F-actin (Charest and Firtel 2007; Etienne-Manneville and Hall 2002; Ridley 1999). For instance, activation of Rho triggers the assembly of contractile actin-myosin bundles coupled to focal adhesion complexes. Rac has been shown to induce the assembly of a meshwork of actin filaments associated to the cell membrane, known as membrane ruffles or lamellipodia. And finally, Cdc42 activation induces the formation of filopodia, finger-like protrusions of the plasma membrane formed by F-actin bundles (Fukata et al. 2003; Nobes and Hall 1999; Ridley 2011; Ridley et al. 2003; Ridley 1999). There is also substantial cross-talk between the Rho family members (Heasman et al. 2010; Ridley 1999) and lymphocyte chemotaxis is likely to be controlled by these Rho GTPases in a spatially temporal coordinated manner. For instance, a RhoA-dependent signal at the trailing edge of cells counterregulates the excitatory signals generated by Gβγ-dependent activation of PI3K and Rac at the leading edge of cells (Xu et al. 2003).

The small GTPase Rho A is required for actomyosin- mediated detachment of the uropod through ROCK phosphorylation of MLC. Unlike in non-haematopoietic cells, where inhibition of RhoA facilitates rear release by disrupting focal adhesions, the function of RhoA in cell detachment appears to be a common feature in all migrating leukocyte (Ridley et al. 2003). Moreover, inhibition of the RhoA effector protein ROCK in T cells also results in a failure of the trailing edge to detach (Smith et al. 2003). The authors demonstrated that inhibition of ROCK by inhibitor Y-27632 blocks phosphorylation of Ser19 of MLC, which is required for the contraction of actomyosin. Thus, the RhoA/ROCK axis may function at the rear of the cell to disrupt adhesions mechanically by inducing actomyosin contraction. The enhanced adhesion of T cells that occurs upon ROCK inhibition may also be explained by the observation that inhibition of

RhoA or ROCK in T cells promotes integrin clustering, which suggests that RhoA/ROCK has a role in regulating integrin avidity (Rodríguez-Fernández et al. 2001). Furthermore, inhibition of either Rho A or ROCK does not block short-term actin polymerisation, but induces MT instability and abrogates lymphocyte migration and SDF-1α-mediated chemotaxis, suggesting the RhoA/ROCK axis plays a pivotal role in regulating cell morphology (Vicente-manzanares et al. 2002).

Even more, Rho family GTPases, which are key regulators of cell migration, affect microtubules, in addition to the actin cytoskeleton and adhesion (Watanabe et al. 2005). Rho family GTPases capture and stabilize microtubules through their effectors at the cell cortex, leading to a polarised microtubule array. For example, Vav-1 is a GEF for the GTPase Rac, and expression of active Rac in T cells causes LFA-1-mediated spreading and clustering (D'Souza-Schorey et al. 1998). When a T cell engages with an APC, the MTOC orients in the direction of the immunological synapse. Interestingly, in Vav-1-deficient T cells, there is a lack of LFA-1 function and the MTOC fails to polarise towards the immunological synapse suggesting this process is dependent on LFA-1 avidity (Ardouin et al. 2003; Hogg et al. 2004; Hogg et al. 2003; Smith et al. 2007a). In turn, microtubules have been shown to modulate the activities of Rho family GTPases (Fukata et al. 2003; Ren et al. 1999; Tybulewicz and Henderson 2009).

Integrins are linked to the cytoskeleton through integrin-adaptor proteins such as talin. Rho GTPases locally raise plasma membrane levels of the talin-activating phospholipid PIP2. Additional pools of GPCR-stimulated Rho GTPases together with other GPCR stimulated signalling molecules activate leukocyte integrins via integrin-scaffolding network proteins, such as talin (Bolomini-Vittori et al. 2009; Critchley 2009). Specifically, RhoA has been shown to regulate chemokine-induced 'inside-out' induction of LFA-1 head extension before ligand binding. However, it is not required for a variety of chemokine, including CXCL9, signals that rapidly strengthen LFA-1 adhesiveness to ICAM-1 bonds without the high-affinity extended LFA-1 conformation and integrin clustering (Pasvolsky et al. 2008). Chemokine-stimulated Rho GTPases have been shown to regulate the turnover of focal contacts of leukocyte integrins, induce the collapse of leukocyte microvilli, and promote polarised leukocyte crawling along the endothelium (Alon and Shulman 2011).

1.13 Regulation of T cell Polarisation

T cell migration relies on the generation of a polarised cell response. This is the result of two distinct phenomena: first, an 'intrinsic' cell polarisation enabling the cell to organise its membrane and cytoskeletal and signalling molecules in a polarised manner; and second, a direction-sensing mechanism, which allows a cell to orient its intrinsic polarity axis in response to extracellular cues. During T cell migration, direction sensing orients the cell towards a chemoattractant gradient; whereas intrinsic polarisation leads to simultaneous protrusive and contractile activities at opposite cellular locations. Several signalling cascades have already been described at the leading edge and trailing uropod that are required for T cell polarisation and chemotatic migration (Gérard et al. 2007; Heasman et al. 2010; Hogg et al. 2003; Takesono et al. 2010; Vicente-manzanares et al. 2002).

As discussed above, both actin and MT are required for T cell polarisation and migration. The organisation of the actin and MT cytoskeleton is arranged within two general regions in the polarised cell during cell migration. The first region is located at the leading edge of the cell and is comprised of actin-rich bundles organised into filopodia, a dense actin meshwork forming a protruding lamellipodia, and the plus-ends of polarised MT arrays. While, actin concentrates preferentially at the advancing front, the myosin motor protein and MTs are packed in the cell body and trailing uropod. This MT-rich region consists of a MT array radiating from the centrosome towards the plasma membrane and actin structures in the form of compact stress fibres, which are anchored to the substrate via focal adhesions. As described in section 1.4, due to the rapidly moving nature of migrating T cells, strong actin stress fibres and true focal adhesions do not appear to exist. Figure 1.13 illustrates the organisation of the actin and MT cytoskeleton in migrating cells.

There is a close relationship between actin and MT dynamics in many cellular processes, including migration. As a consequence, although their functions seem well defined, they are in fact overlapping, with actin playing a role in membrane trafficking and MTs being involved in coordinated protrusive and contractile forces, each process generally attributed to the other cytoskeletal component (Etienne-Manneville 2004). Moreover, there is accumulating evidence that cytoskeletal elements are also involved in regulating each other. This cytoskeletal crosstalk appears to be both direct and mediated by signalling molecules. For instance, MTs have been shown to modulate actin stress fibre formation suggesting it participates in actin dynamics (Etienne-Manneville 2004;

Gundersen and Cook 1999). In addition, MT plus-end binding proteins are involved in both the polarisation of the microtubules and the actin filaments (Galjart 2005; Watanabe et al. 2005).

Cell motility is a well-studied example where the interplay between actin and microtubules appears bidirectional (Etienne-Manneville 2004; Heasman et al. 2010; Ridley 2011; Ridley et al. 2003). Membrane fluctuations promoted by actin and/or MT dynamics promote sensing of the extracellular environment. The organisation of the MT array in a migrating cell presents similarities with that of actin filament polymerisation. Like actin, MT activity is polarised during cell migration, with different dynamics at the leading edge and retracting edges (Watanabe et al. 2005). Correlation between actin and MT organisation suggests that the two polymers are linked either directly or indirectly through intermediate proteins or signalling molecules. Thus, T cell polarity in migrating cells is determined by cooperation between the actin and MT cytoskeleton.

The contribution of MTs to T cell polarisation and migration is well established (Burkhardt et al. 2008; Samstag et al. 2003; Small et al. 1999; Small and Kaverina 2003; Takesono et al. 2010; Xu et al. 2005). In most migrating cells, MTs nucleate in the cell centre and adopt a general orientation in parallel to an axis given by the direction of cell movement. This process requires interpretation of intracellular positional information by the MT network, which must be able to distinguish their target regions at the cell front and rear from the rest of the cell. However, the molecular mechanism underlying this behaviour is not fully understood.

Various lines of evidence indicate that MTs exert their influence on cell polarity by affecting anchorage and protrusion through modulation in the activities of Rho-family GTPases (Palazzo et al. 2001; Small and Kaverina 2003; Watanabe et al. 2005). In addition, the MT array is generally aligned along the long axis of the migrating cell. The contribution of MTs on cell polarity was also attributed to their ability to selectively regulate the turnover of specific sets of substrate adhesions in a cell, to allow protrusion at the front, and promote retraction at the rear. The turnover of focal adhesions is necessary to remodel the cytoskeleton and to recycle components required for protrusion (Amano et al. 1997; Hogg et al. 2011; Smith et al. 2005; Totsukawa et al. 2004; Watanabe et al. 2005). Therefore, while chemotaxis appears to be dependent on localised stimulation of chemokine receptors resulting in a polarised activation of signal transduction pathways, the so-called 'intrinsic' polarity of the cell is probably established by the polarised MT array.

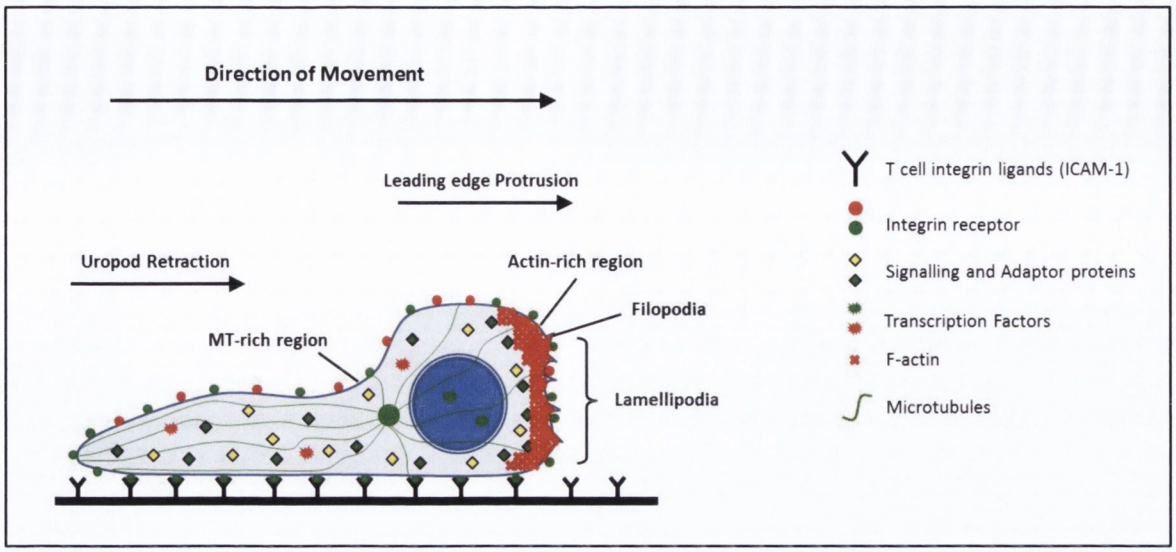

Figure 1.13: Organisation of the actin and microtubule cytoskeleton during T cell migration.

Two regions can be distinguished in a cellular protrusion. The first is an actin-rich region with filopodia comprised of actin bundles, a dense actin meshwork forming the protruding lamellipodia, and the plus-ends of extending MTs. The second is a MT-rich region, where MTs radiate from the MTOC forming a polarised array. Numerous signalling and adaptor proteins facilitate cytoskeletal reorganisation induced by integrin activation.

1.14 Clinical Relevance

The regulation of the systemic immune responses is critically dependent on the coordinated circulation and migration of lymphocytes. Integrating our knowledge thus far of the molecular mechanisms underlying T cell migration, allows researchers to understand the processes of an appropriate as well as abnormal immune response. The recruitment of T cells from the bloodstream into target tissues is crucial to mount an effective immune response against pathogenic microorganisms and viruses and to tissue injury caused by infection or wounding. Following clearance of infection or resolution of injury, T cell infiltration subsides and inflammation resolves without overt tissue damage. However, inappropriate inflammatory responses, such as failure of T cells to migrate or excessive T cell infiltration into tissues can result in life threatening consequences, such as chronic inflammatory diseases and autoimmune disorders as well as metastasis (van den Boorn et al. 2006; Christen and von Herrath 2005; Munn and Mellor 2006; Munn and Mellor 2003; Zehn and Bevan 2006). The pathology of some of these conditions characterised by excessive lymphocyte infiltration are discussed below.

Uncontrolled inflammation is a trademark of asthma and allergies. Asthma, a chronic inflammation of the airways, results from a persistent immune response to foreign materials (allergens) inhaled from the environment. The constant presence and activation of T cells in the airways of asthmatics causes excessive tissue damage, leading to hyper-reactivity of the airways to otherwise innocuous stimuli such as exercise, stress, and cold air (Nadeau et al. 2010; Robinson 2010). In rheumatoid arthritis, the constant destruction of joint tissue by inflammatory cells migrating into these compartments results in compromised limb function and crippling pain (Cooles and Isaacs 2011; Solomon 2010). Psoriasis, an inflammatory disease of the skin, is characterised by lymphocyte infiltration, keratinocyte proliferation, and the over production of pro-inflammatory cytokines and chemokines. The central role of T cell migration in the pathogenesis of this disease is well documented (Cather et al. 2003; Gottlieb 2005; Gottlieb et al. 2002; Lebwohl et al. 2003; Lebwohl 2003). New drugs that inhibit organ-specific homing cascades of populations of pathogenic T lymphocytes would permit the use of tissue-selective anti-inflammatory interventions.

An effective immune response is dependent on the ability of activated T cells to home to inflammatory sites and infiltrate target tissues. However, some pathological conditions arise from a deficiency in function lymphocyte migration. For instance, dynamic cytoskeletal rearrangement is essential for a polarised morphology and subsequent TEM

across the vasculature. The Wiskott–Aldrich Syndrome protein is a key regulator of the actin cytoskeleton, transmitting and integrating actin-regulating signals that are essential for multiple cell functions, including cell motility and induction of cell shape change as mentioned in section 1.11.1 (Burns et al. 2004; Thrasher 2002). Reduced or absent WASp expression may result in the primary immunodeficiency disorder Wiskott–Aldrich Syndrome (WAS), which is characterized by immune deficiency. As WASp is exclusively expressed in haematopoietic cells, defective function has been described in most immune cell lineages, giving rise to a complex combined cellular and humoral immune deficiency, resulting in susceptibility to severe and life-threatening infections (Ochs and Thrasher 2006). Studies of the effects of WASp deficiency *in vivo* have been assisted by the generation of two separate WASp knockout (KO) mouse models, both of which provide good models for the haematopoietic features of the human disease (Snapper et al. 1998; Zhang et al. 1999). At present, the only curative therapy is bone marrow or haematopoietic stem cell transplantation. Although, over the last decade good progress has been made in the development of corrective gene therapy for WAS (Candotti et al. 1999; Dupré et al. 2004).

A better understanding of this process could ultimately lead to treatments that selectively block excessive lymphocyte migration for immunosuppressive therapy for chronic inflammatory diseases as well as hypersensitivity reactions and graft rejection. Despite progress in understanding the mechanisms of T cell polarity and motility, there is still a limited understanding of the mechanisms that contribute to antigen-induced T cell arrest. Studies on T cell migration are yielding promising targets for new anti-inflammatory therapies, as the development of antagonists for integrin receptors, adhesion molecules, and cytoskeletal dynamics to subdue inflammatory diseases are among the most actively pursued areas in pharmaceutical research. Drugs that disrupt cell migration appear particularly promising in clinical trials and in many animal models of inflammatory disease. Cell migration inhibitors not only interfere with migration of cells to a tissue, but also can affect other necessary processes such as mediator release and angiogenesis and are likely to transform the current therapies for inflammatory diseases and cancers (Mackay 2008). For instance, efaluzimab is a recombinant, humanized monoclonal (mAb) that was approved in 2003 for the treatment of moderate to severe plaque psoriasis (Leonardi et al. 2008). Psoriasis is a chronic autoimmune disorder affecting the skin resulting from the infiltration and activation of T cells to the dermis, which triggers the release of cytokines, particularly tumour necrosis factor (TNF)-α (Cai et al. 2012). As previous discussed, the integrin LFA-1 is one of the important integrins for leukocyte

binding to the endothelium and subsequent migration through tissue. Therefore, efaluzimab acts as an immunosuppressant by targeting this integrin and inhibiting lymphocyte activation and cell migration out of blood vessels into tissues. However, despite being one of the most effective treatments for psoriasis to date, the drug was shown to be associated with fatal brain infections and withdrawn from the market in 2009 (Leonardi et al. 2008; Major 2010). While efaluzimab was highly specific and effective, it targeted an integrin required for generating an immune response against infectious disease. The current challenge in the development of new anti-inflammatory drugs is the identification of appropriate targets that are crucial in the inflammatory response but are otherwise dispensable for host defence against pathogens. Nevertheless, the concept of interference with T cell migration remains a common avenue for development of novel immuno-suppressants and the use of cell migration inhibitors for the treatment of inflammatory diseases and possibly cancers and infectious diseases is still promising (Mackay 2008).

Finally, the lack of studies that effectively elucidate the regulation of signalling cascades in T cell migration highlights the need of further experiments to decipher the exact role of regulatory mechanisms in T cell migration. Advances in this scientific field may enhance our understanding of the molecular mechanisms associated with disease progression and potentially identify early intervention strategies or develop more efficient and new cost effective therapies. Scaffolding proteins, such as RACK1, recruit a large number of signalling proteins and serve as molecular platforms for the assembly of signalling networks, thereby regulating the temporal and spatial distribution of signalling cascades. While the role of RACK1 in cell adhesion and migration is well documented, our understanding of the cell-type specific function and regulation is incomplete. Understanding the precise molecular mechanisms underlying it's regulatory role, whether positive or negative, in T lymphocyte migration could potentially lead to more promising and specific immunomodulation therapies in cases where cells excessively infiltrate into target tissues causing damage (such as in autoimmune disorders) or exhibit impaired migration (such as in patients with a compromised immune system).

1.15 Research Objectives

An effective immune response depends on the circulation of T cells through the lymphatic and circulatory systems, where they are activated by antigen-presenting cells. The migration of mature T cells is guided by chemotactic interactions to sites of inflammation and infection. T cell migration is a highly complex process dependent on

expression and activation of adhesion molecules, reorganisation of the cytoskeleton network, induction of molecular motors, reorientation of organelles, and phosphorylation-dependent signalling cascades.

The molecular scaffolding protein RACK1 has been implicated in regulating integrin-mediated adhesion and migration in all cell types investigated thus far. However, despite its apparent dominant role in cell migration, examination of the role of RACK1 in the context of immune cell migration has been widely overlooked. Although considerable evidence has demonstrated the importance of PKC in integrin-mediated events, the molecular mechanisms underlying the involvement and regulation of PKC activity in these processes in T cells are still not fully understood. Therefore, it is pertinent to investigate the putative regulatory role of RACK1 in integrin-mediated signalling events required for functional lymphocyte migration. The purpose of this thesis intended to characterise RACK1 any potential regulatory function in in integrin-mediated immune cell migration. Therefore, the following aims of this study were:

1.) To characterise RACK1 expression in resting and integrin-mediated and chemokine-induced polarised migrating T cells.
2.) To investigate the putative regulatory role of RACK1 in T cell polarity, adhesion, and motility.
3.) To identify and characterise proteins associated with RACK1 and the functional implications of these interactions in T cells.

CHAPTER TWO

Material and Methods

2 Materials and Methods

2.1 Antibodies and Reagents

A full list of reagents and antibodies and their sources are provided in tabular form in Appendix 3.

2.2 Constructs and siRNA

pEGFP-RACK1 (kind gift from Dr. Patrick Kiely, University of Limerick, Ireland) was previously described (Kiely et al. 2006; Kiely et al. 2002). RNA interference of RACK1 was performed using RACK1-specific siRNA (siGenome [GNB2L1]), consisting of a pool of RACK1 mRNA-specific siRNA designed using specific algorithms, in conjunction with a non-targeting control siRNA (siGenome). The Dharmacon SMARTpool technology reduces false negatives by targeting four mRNA regions at once with a single, highly functional reagent, for potency at low concentrations (Dharmacon, Lafayette, CO).

2.3 Cell Culture

Both primary and T cells lines were used in this study to characterise the role of RACK1 in integrin-mediated and chemotactic T lymphocyte migration. The cells were seeded in pre-warmed media and the cell number was monitored using a haemocytometer. Composition of cell culture media and associated buffers are provided in Appendix 3. The source and culture of immortalised Jurkat Leukemic and HuT78 lymphoma T cell lines as well as isolation of primary T cells is discussed in detail below.

2.3.1 Culture of Human Jurkat Leukemic T Cells

The Jurkat cell line [American Type Culture Collection (ATCC), Manassas, VA, USA] was established in the late 1970s from the peripheral blood of a 14 year old boy with T cell leukaemia. The cell line was cultured to maintain and preserve cell structure, function, and behaviour at 37°C and 5% CO_2 in a humidified atmosphere in T-25 or T-75 cm^2 flasks in RPMI-1640 with HEPES with 10 % v/v Foetal Bovine Serum (FBS), 50 U/ml penicillin, and 50 µg/ ml streptomycin. Cells were seeded at 1-2 x 10^5 cells/ ml and grown to 1 x 10^6 cells/ ml.

2.3.2 Culture of Human HuT78 T Cells

The Human cutaneous T lymphoma cell line, HuT78, (ATCC) was originally derived from peripheral blood of a white male with Sezary syndrome. Morphological features of HuT78 T cells include hyperconvoluted and large nucleoli (Bunn and Foss, 1996). HuT78 T cells are cultured under the same conditions as Jurkat T cells in similar flasks and culture temperatures but were grown in complete RPMI-1640 with HEPES which contains 10 % v/v FBS, 50 U/ml penicillin, and 50 µg/ml streptomycin as well as 1.5 mg/ml Sodium Bicarbonate and 1 mM Sodium pyruvate. Cells were seeded at 0.5 x 10^5 cells/ ml and grown to 0.5 x 10^6 cells/ ml.

2.3.3 Human Embryonic Kidney (HEK) 293 Cells

The human embryonic kidney cell line known as HEK 293 (American Type Culture Collection [ATCC], CRL-1573, Manassas, VA, USA) are adherent cells, frequently grown in cell culture and widely used in cell biology research. In addition, the cells are readily transfected and were utilised in this study for vector transfection and FLAG fusion protein expression. The cell line was cultured to preserve cell structure, function, and behaviour and maintained between 10% and 90% confluency at 37°C and 5% CO_2 in a humidified atmosphere in T-25 or T-75 cm^2 flasks in complete Gibco Dulbecco's Modified Eagle Medium (DMEM) with 10 % v/v FBS, 50 U/ml penicillin and 50 µg/ ml streptomycin. Cells were seeded at 0.5 x 10^5 cells/ ml and grown to 0.5 x 10^6 cells/ ml.

2.4 Isolation and Expansion of Peripheral Blood T Lymphocytes

Peripheral blood T lymphocytes (PBTLs) were isolated from healthy volunteers using the Lymphoprep™ method. Briefly, blood was collected into tubes containing anticoagulant such as EDTA or heparin. The blood was diluted with an equal volume of PBS. The diluted blood was carefully layered onto 20 ml of Lymphoprep™ solution. The two phases were not allowed to mix. The samples were centrifuged at 1200x*g* with no break for 20 min at room temperature. After centrifugation, the mononuclear cells, which form a distinct white band near the sample/medium interface, were removed using a Pasteur pipette without removing the upper layer. The harvested fraction was diluted with an equal volume of PBS and centrifuged at 250x*g* for 10 min at room temperature. The supernatant was removed and the pellet was washed five times with an excess volume of PBS to remove any contaminating platelets (a portion of the solution was analysed microscopically using a haemocytometer to check contaminating platelets, if any). The

cell suspension was incubated in a T-175cm^2 flask for 1-2 hours at 37ºC, and the monocyte and macrophage cell population was removed by allowing them to adhere to the plastic. The non-adherent cell population was expanded by culturing in RPMI 1640 medium containing 10% (v/v) heat inactivated FBS in the presence of 2 µg/ml phytohaemagglutin (PHA) in T-175 cm^2 flasks at a density of 2 x 10^6 cells/ml for 3 days. These cells were then maintained in culture medium supplemented with 20 ng/ ml IL-2. The cells were then washed three times with complete RPMI-1640. The cells were seeded into new flasks at a density of 1-2 x 10^6 cells/ml with 20 ng/ ml IL-2 for seven days at 37°C. After seven days, the PBTLs were harvested and used within one week while maintaining IL-2 concentration. The purity of the cells was typically >95% CD3+ T lymphocytes as detected by flow cytometry, with the proportion of T lymphocytes typically being 83% CD4+, 15% CD8+ and <1% CD4+/CD8+ (Lefort and Kim 2010).

2.5 Transfection

The process of introducing nucleic acids into eukaryotic cells by nonviral methods is defined as transfection. Using various chemical, lipid or physical methods, this gene transfer technology is a powerful tool to study gene function and protein expression in the context of a cell. Development of reporter gene systems and selection methods for stable maintenance and expression of transferred DNA have greatly expanded the applications for transfection (Groskreutz and Schenborn 1997).

Transfection is any method that allows introducing negatively charged molecules (e.g., phosphate backbones of DNA and RNA) into cells with a negatively charged membrane. Chemicals like calcium phosphate and cationic lipid-based reagents coat the DNA, neutralising or even forming an overall positive charge to the molecule, which facilitates the DNA: transfection reagent complex ability to cross the plasma membrane. Physical methods like microinjection or electroporation permeabilise the cell membrane and introduce DNA directly into the cytoplasm. In this study, electroporation was employed to transfect suspension cells, including both T cell lines and primary T cells. Whereby, the calcium phosphate transfection technique was utilised in transfecting the HEK cells. Both techniques are described in detail below.

2.5.1 Electroporation Methods

Electroporation was used to transfect suspension cells with both siRNA and vector DNA. In order to transiently suppress gene expression in T cells, synthetic double-stranded

RNA complementary to the mRNA was introduced into the cell through electroporation. The technique known as RNA interference (RNAi) takes advantage of a natural gene-silencing mechanism (Nellen and Lichtenstein 1993). The phenomenon of gene silencing by RNAi is central to a number of natural RNA-based silencing processes, and is a valuable tool in functional genomics, target validation, and gene-specific therapeutic research. Introduction of RNAi into different organisms induces both effective and specific post-transcriptional gene silencing by directly mediating degradation of homologous target RNAs (Scherer and Rossi 2003; Sharp 2001).

The sequence-specific, post-translational gene-silencing mechanism of double-stranded RNAi was originally described by Fire and colleagues (1998) and depends on hybridisation between the small interfering RNA (siRNA) and endogenous mRNA transcripts. The chemically synthesised siRNA enters downstream of the dicer enzyme and is recruited to the multi-subunit protein complex called the RNA-inducing silencing complex (RISC). The function of the sequence-specific siRNA is to guide the coding mRNA to be cleaved, resulting in mRNA degradation and gene silencing (Figure 2.1) (Elbashir et al. 2001). Therefore, RNAi can effectively and selectively block expression of theoretically any gene, allowing researchers to examine the result of protein suppression. A RACK1-specific siRNA as well as a non-targeting control siRNA, which is not complementary to any human transcript, was employed in order to examine the effects of knockdown on T cell migration. Transfection of the cells lines and primary cells was optimised using with two different electroporators and associated protocols.

(a) Transfection of HuT78 and Jurkat T cell lines with siRNA

In order to transiently suppress gene expression in the HuT78 and Jurkat T cell lines, the BTX ECM830 square wave electroporator (BTX Molecular Delivery Systems, Holliston, MA) was employed according to the following protocol.

Cells in logarithmic growth were seeded at 0.5 x 10^6 per transfection in 200 µl cold electroporation medium (RPMI with 20% FBS) in 2mM gap cuvettes. A final concentration of 500nM siRNA was added to the cell solution, which was then incubated for 5min at room temperature. Cells were then electroporated at 130V for a single 12 ms pulse. Cells were removed from the cuvette and washed in fresh RPMI and re-suspended at 0.5 x 10^6 cells/ ml and incubated in pre-warmed complete RMPI (section 2.3.2) at 37˚C for 24 hours. Transfection procedure was repeated after 24 hours (h) and cells were harvested for experimentation and assessment of knockdown 72 h after the initial transfection.

(b) Transfection of PBTLs with siRNA

In order to transiently suppress gene expression in PBTLs, two transfection reagents were used: (1) the Amaxa™ transfection kit (Lonza, Cologne, Germany) and (2) the Ingenio® (Mirus Bio, Madison, WA) transfection solution both in conjunction with the Amaxa™ nucleofector device (Lonza, Cologne, Germany).

(1) On day 5 of IL-2 stimulation, the cells were harvested and viable cells isolated using density gradient centrifugation using Lymphoprep™ solution by centrifugation at 1200g for 5 min with the brake set to 4. IL-2 stimulated PBTLs were washed in PBS and seeded at 2 x 10^6 cells per transfection in 100 µl Amaxa Human T Cell Nucleofector Solution. Cells were divided into two 4mM gap cuvettes. A final concentration of 500nM siRNA siRNA was added to the cell solution. Cells were electroporated with the Amaxa nucleofector device programme T-20, which is optimised for primary T cells. Cells were removed from the cuvette, re-suspended in 2ml pre-warmed complete RMPI (section 2.3.2), and incubated at 37°C for 24 h. Transfection procedure was repeated after 24 hours and cells were harvested for experimentation and assessment of knockdown 72 h after the initial transfection.

(2) On day 5 of IL-2 stimulation, the cells were harvested and viable cells isolated using density gradient centrifugation using Lymphoprep™ solution by centrifugation at 1200g for 5 min with the brake set to 4. IL-2 stimulated PBTLs were washed in PBS and seeded at 5 x 10^6 cells per transfection in 100 µl Ingenio® Electroporation solution pre-warmed to RT. A final concentration of 1000nM concentration of siRNA was added to the cell solution. Cells solution was then dispensed into Amaxa electroporation cuvettes and electroporated with the Amaxa nucleofector device using program T-07. Cells were removed from the cuvette, re-suspended in 2ml pre-warmed RMPI containing 10% FCS without antibiotics. IL-2 (20 ng/ml) was added 2-4 h after transfection and the cells were incubated at 37°C for 72 h. After 72 h, the cells were harvested, washed in sterile PBS, and resuspended in 100µL of Ingenio Electroporation solution. The same concentration of siRNA was added and the cells were electroporated as before using program T-07. IL-2 was again added 2-4 h after transfection and the cells were cultured for a further 48 h. The cells were then harvested for experimentation and assessment of knockdown. The PBTLs were typically serum

starved for 2 h in RPMI-1640 in 0.5% BSA prior to experimentation as the IL-2 activates many signalling pathways in the cell.

(c) Transfection with Plasmid DNA

Cells were seeded at 2 x 10^6 cells per transfection in 100 µl Amaxa Nucleofector Solution R. Cells were divided into two 4mM gap cuvettes. 2.5 µg of DNA was added to the cell solution. Cells were electroporated with programme V-01, which is optimised for T cells. Removed cells from cuvette and resuspended in 2 ml of complete RPMI. Cells were removed from the cuvette, re-suspended in 2ml pre-warmed complete RMPI (section 2.3.2), and incubated at 37°C for 24 h. Transfection procedure was repeated after 24 hours and cells were harvested after 24 h for experimentation. Where appropriate, transfection efficiency was measured by analysis of GFP expression by fluorescence microscopy.

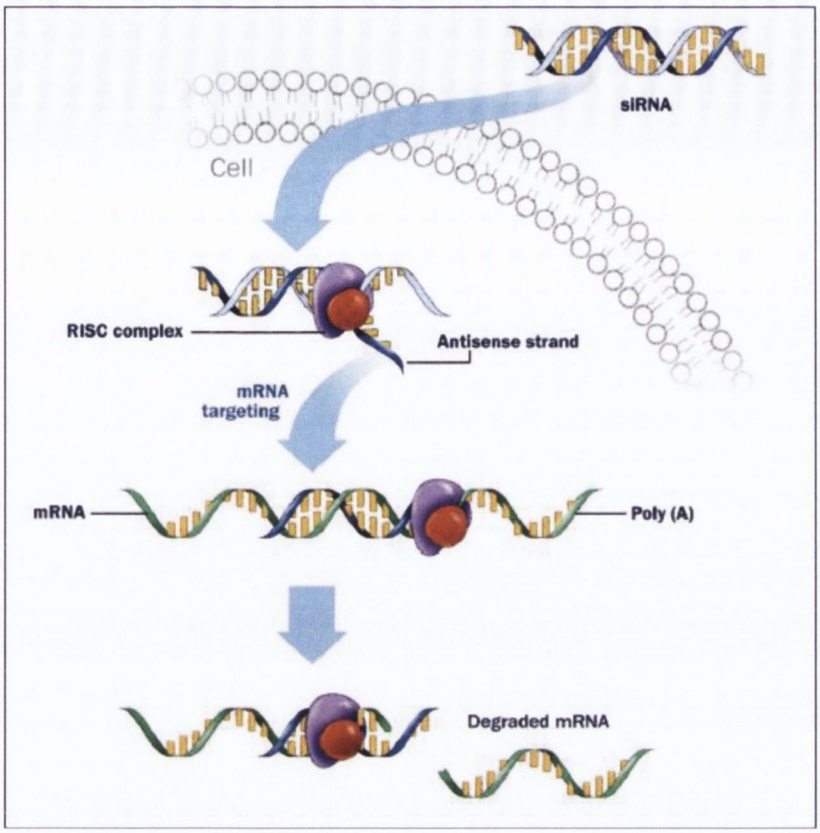

Figure 2.1: Graphical illustration depicting the process of RNAi.

Double stranded RNA complementary to the mRNA is introduced into the cell through electroporation. The mechanism depends on the ability of the siRNA to hybridise with the endogenous mRNA transcripts. The chemically synthesised siRNA enters downstream of the dicer enzyme and is recruited to the multi-subunit protein complex called the RNA-inducing silencing complex (RISC). The function of the sequence-specific siRNA is to guide the coding mRNA to be cleaved, resulting in mRNA degradation and gene silencing (Adapted from Nastech Pharmaceutical Company, Inc., 2008).

2.5.2 Calcium Phosphate Transfection

For the expression of FLAG fusion proteins (section 2.29), HEK293 cells were transfected using calcium phosphate transfection. The principal of the technique relies on DNA and calcium phosphate to form a coprecipitate, which adheres to the cell surface and is taken up by the cell, likely by endocytosis. The transfection technique was optimised using 30 µg control GFP (pmaxGFP, a green fluorescent protein from the copepod *Pontellina p.*, provided by the manufacturer, to measure transfection efficiency by fluorescent microscopy.

Cells were seeded at $20x10^6$ cells /10ml in serum-free medium 15 cm plates. The cells were pre-treated with 25uM Chloroquine and incubated for 5 min at 37°C, which inhibits lysosomal DNases by neutralizing vesicle pH. In a separate tube, 2X Hepes Buffered Saline (concentration (in H_2O): 10 g/l HEPES; 16 g/l NaCl; 0.74 g/l KCl; 0.27 g/l $Na_2HPO_4.2H_2O$; 2.0 g/l dextrose), calcium chloride, and 30 µg DNA were thoroughly mixed for 30 sec with a pipetting aid. After 5 min, the colour of the medium in the plates was checked to ensure an increase in pH; DNA was added drop wise and the cells were incubated for 24 hours at 37°C. The following day the medium was changed to fresh complete DMEM. After 48 hours, the cells were harvested for purification of FLAG fusion proteins (section 2.30.10).

2.6 Bacterial Transformation for the Expansion of pEGFP-RACK1

Competent *E. Coli* (DH5 Alpha) were transformed with EGFP-RACK1 plasmid, which contains an Ampicillin resistant gene, following manufacturer's instructions. Briefly, I heat shocked cells at 42°C for 30 sec, 250 µl SOC medium was then added to cells on ice, and *E. Coli* suspension was expanded in 2ml LB broth containing Ampicillin for 8 hours at 37°C in an orbital shaker. 1 ml of starter colony was then transferred to 20 ml LB broth containing Ampicillin at 37°C overnight in an orbital shaker. The bacterial cells were pelleted by centrifugation and the plasmid was then purified from *E. coli* by QIAprep Spin Miniprep Kit following manufacturer's instructions. The plasmid DNA was then quantified with the Multi-Sample Micro-Volume UV-Vis Spectrophotometer NanoDrop 800 (Thermo Scientific, NanoDrop, Wilmington, DE, USA). The DNA was stored at -20°C for short term or -80°C for long term storage.

2.7 High Content Analysis

High Content Analysis (HCA) or screening involves the use of an automated microscope to facilitate rapid, highly parallel biological research and drug discovery. High-content screening technology allows for the evaluation of multiple biochemical and morphological parameters in cellular systems in discovery research. Through combining the imaging of cells in microtiter plates with automated image analysis algorithms, researchers can acquire deeper knowledge on multiple biochemical or morphological pathways at the single-cell level.

In order to perform HCA on experiments, the cells were scanned using the automated microscope IN Cell Analyzer 1000 HCA platform [GE Healthcare, Buckinghamshire, England] shown in Figure 2.2, which offers high-throughput and high-content subcellular imaging and analysis. Images could then be analysed using IN Cell Investigator software [GE Healthcare]. The software is capable of measuring a variety of cellular data based on a number of protocols. For this research project, the automated microscope was primarily used to count cells and measure morphology of user-defined nuclear and cytoplasmic compartments. To demonstrate this process, the protocol for determining changes in cell morphology in response to a particular treatment will be detailed below.

HuT78 or Jurkat T cells were seeded at $1x10^5$ cells/ ml and primary T cells were seeded at $2x10^5$ cells/ ml in Nunc 96 well plates. The cells were treated with siRNA or chemical inhibitors and subjected to the *in vitro* LFA-1 induced T cell migration assay described in section 2.8. Because cell morphology was to be assessed, the cells were stained for cytoskeletal elements actin or tubulin. Plates were then scanned using the IN Cell Analyzer. A total of 15 fields per well were imaged under 10× magnification, and 10 fields per using 3 separate filters to capture the nucleus (blue) and two separate stains (green and red). Image analysis was performed using the InCell analysis software. The software is designed to analyse cells based on a protocol with two waves. The software detects cells for morphology analysis by nuclear stain (wave 1) thereby identifying cells and avoiding cell debris, with quantification of cellular morphologies and fluorescent intensities determined from one or more intracellular stains by wave 2 (e.g., α-tubulin or actin). Morphological and fluorescence intensity staining parameters were automatically recorded for every cell in the field, and these parameters were also automatically recorded numerically as average values per field and average values per well. Morphological and fluorescence intensity/distribution parameters that were measured included 1/ (form factor), cell area, cell gyration radius, cell/nuclear area, nuclear

displacement, cell intensity, nuclear intensity, intensity (nucleus and cytoplasm, N + C), IxA (nucleus and cytoplasm, N + C), intensity coefficient of variation (CV), and cell count. The definitions of these parameters are described in Appendix 3. The IN Cell HCA platform together with the selected morphology parameters has been previously validated for quantifying changes in T cell morphology (Freeley et al. 2010). The cells could also be classified into subpopulations by applying one or more filters, each of which is based on one or two user selectable fluorescence or morphology measures. Therefore, the morphology of the whole cell population could be assessed as a whole or as a sum of individual entities. While the degree of polarity of the cell is indicative of migration, in that, cell polarisation is required for successful T cell migration, cell polarisation does not give indication to the rate of migration. Measurements of speed and persistence of T cell migration were assessed using live cell tracking which is discussed in the section 2.8.3.

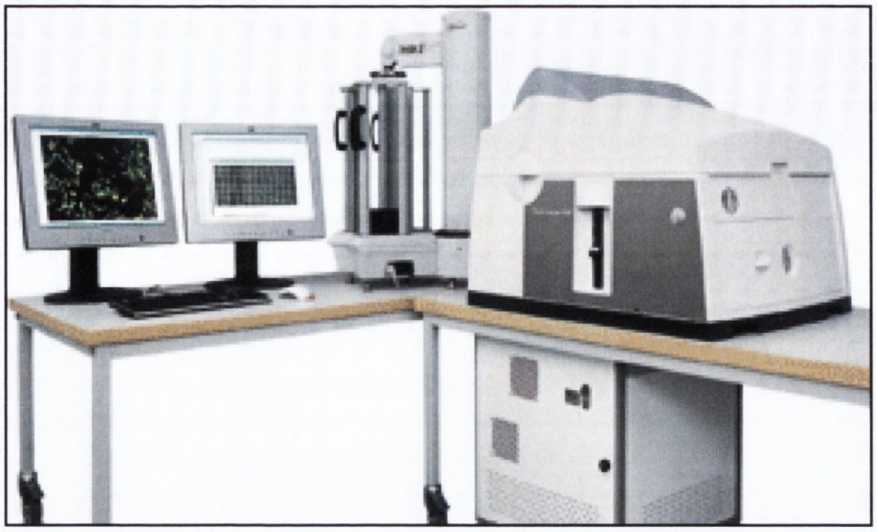

Figure 2.2: High Content Analysis through the use of an automated microscope.

The IN Cell Analyzer 1000 platform allows for the analysis of thousands of cells in hundreds of wells to determine the average effect on a single experiment.

2.8 *In vitro* T Cell Migration Assay

An *in vitro* model of T cell migration was used to induce migration following LFA-1 integrin activation as previously described (Verma et al. 2008; Volkov et al. 2001; Volkov et al. 1998). In this assay, immobilised, plate-bound recombinant human ICAM-1-Fc (rICAM-1-Fc) or antibodies raised against LFA-1 (anti-LFA-1) were utilised to stimulate T cells and induce haptokinetic cell migration, in that, the cells migrate across a 2-dimensional (2D) surface without additional stimuli. Haptokinetic cell migration across 2D surfaces consists of at least three processes: (i) protrusion of the leading edge for adhesive cell-substratum interactions followed by (ii) contraction of the cell body and (iii) detachment of the trailing edge. While *in vitro* haptokinetic migration is predominantly a function of adhesion and de-adhesion events lacking spatial barriers towards the advancing cell body, the biophysics of the tissues *in vivo* require a set of cellular strategies to overcome matrix resistance (Friedl and Bröcker 2000). Nevertheless, the *in vitro* migration assay allows researchers to measure the effect on a particular treatment on both cell polarisation and migration. In this assay, the polarised migrating T cells display a characteristic migratory phenotype. Moreover, the observed migratory phenotype *in vitro* closely mimics the *in vivo* equivalent. Matrix barriers force the cells to adapt their morphology and change shape in response to extracellular signals. This type of migration is investigated in the Transwell Migration Assay in section 2.11.

The plates were scanned using the automated microscope IN Cell Analyzer 1000 HCA platform as described in the previous section. The *in vitro* T cell migration assay was used to determine the effect of a particular treatment (i.e. transient suppression or overexpression) on T cell polarisation and migration in both the cell line HuT78 and primary T cells. The data are the mean of three independent experiments performed in triplicate +/- SEM.

2.8.1 *In Vitro* Haptokinetic Migration Assay: Hut78 T cells

The following techniques were optimised for Hut78 T cells:

(a) For induction of migration by anti-LFA-1:

Briefly, 96-well tissue culture plates were coated with 5ug/ml goat anti-mouse IgG diluted in sterile PBS and stored at 4°C overnight. The unbound antibody solution was removed and 1:1000 anti-LFA-1 (clone SPVL-7) in sterile PBS was added and incubated for 1-2 hours at 37°C. Again, the unbound antibody solution was removed and

HuT78 T cells (1 x 10^5 cells/ ml) were loaded onto pre-coated wells. The cells were incubated at 37ºC with 5% CO_2 for indicated times. Cells were fixed with a final concentration of 4% pre-warmed paraformaldehyde (PFA) for 15 min at 37˚C.

(b) For induction of migration by rhICAM-1-Fc:

Briefly, 96-well tissue culture plates were coated with 1:500 dilution of goat anti-human IgG (Fc specific) diluted in sterile PBS and stored at 4ºC overnight. The unbound antibody solution was removed and 1 µg/ml rhICAM-1-Fc was added and incubated for 1-2 hours at 37ºC. Again, the unbound ligand solution was removed and HuT78 T cells (1 x 10^5 cells/ ml) were loaded onto pre-coated wells. The cations magnesium chloride ($MgCl_2$) and EGTA at final concentration of 5 mM and 1.5 mM, respectively, were added to induce the active conformation of LFA-1 on the surface of T cells in the absence of chemokine. The cells were incubated at 37ºC with 5% CO_2 for indicated times. Cells were fixed with a final concentration of 4% pre-warmed PFA for 15 min at 37˚C.

(c) For non-migrating control (resting):

Briefly, 96-well tissue culture plates were coated with neat poly-L Lysine (PLL). PLL is synthetic polymer cation (Yavin and Yavin 1974). PLL is commonly used to coat tissue culture plates as an attachment factor, which improves cell adherency but does not activate the cells (Vancha et al. 2004). The unbound PLL solution was then removed and HuT78 T cells (1 x 10^5 cells/ ml) cells were seeded onto pre-coated wells. The cells were incubated at 37ºC with 5% CO_2 for indicated times. Cells were fixed with a final concentration of 4% pre-warmed PFA for 15 min at 37˚C.

2.8.2 *In Vitro* Chemokinetic Migration Assay: Primary T cells

In effect, Maxisorp 96-well tissue culture plates were coated with 3 µg/ml rICAM-1 and 1 µg/ml SDF-1α (CXCL12) diluted in sterile PBS and stored at 4ºC overnight. The unbound solution was removed and the wells were blocked with 0.5% BSA/ RPMI for 30m min at 37C. PHA/ IL-2-expanded PBTLs (1 x10^5 cells/ ml) were serum starved for 2h in 0.5% BSA/ RPMI and added to wells. The plates were centrifuged briefly at 10g for 15sec to ensure the cells settle on the bottom. The plates were then incubated at 37ºC with 5% CO_2 for indicated times. Cells were fixed with a final concentration of 4% pre-warmed PFA for 15 min at 37˚C. Cells were incubated on PLL-coated plates for control resting cells. Cells adhered to this surface without activation.

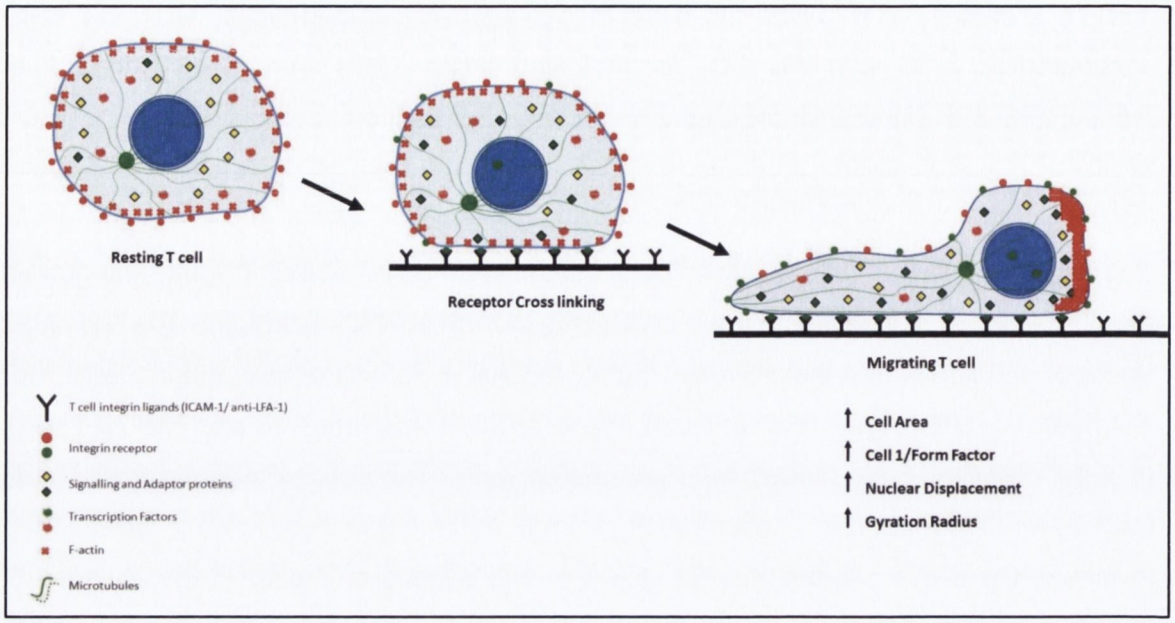

Figure 2.3: A generalised model of LFA-1-mediated T cell migration.

Upon receptor activation by immobilised activating antibody anti-LFA-1 or native ligand ICAM1, T cells acquire a polarised, migrating phenotype. This change in morphology is documented by measuring the validated morphology parameters including, cell area, cell 1/form factor, nuclear displacement, and cell gyration radius.

2.8.3 Live Cell Tracking of LFA-1-dependent T cell Motility

Optimal cell migration rate in a given direction is a function of speed and directional persistence (Dunn 1983). In order to determine the effect of treatment (i.e. protein knockdown or overexpression) on the speed and directional persistence of T cell migration, images of live cell migration of primary T lymphocytes were acquired by the automated microscope IN Cell Analyzer 1000. The *in vitro* 2D chemokinetic assay (section 2.8.2) was carried out in PBTLs and the microscope was set up to capture a brightfield image approximately every 30 seconds for 1 hour at 20X objective. The cells were maintained at 37°C for the length of acquisition. The images were then exported to .tif files and processed in Image J (version 1.44, National Institute of Health, Bethesda, USA) using the plugin MtrackJ (accessed at http://www.imagescience.org/meijering/software/mtrackj). Thirty cells were randomly selected and tracked over the course of an hour (120 frames). The average speed of migration was defined using the following equation:

$V = L/f$

Where L (μm) is the total cell path length and f is the number of frames (each frame interval is equal to 30 sec).

The average persistence of migration was defined using the following equation:

$P = \Delta x/L$

Where Δx (μm) is the net displacement of the cell and L (μm) is the total cell path length.

Therefore, if a cell travelled in a straight line its persistence would be equal to 1. However, if a cell travelled in an indirect course, its total distance travelled will be much greater than its net displacement and, therefore, its persistence would be less than 1.

The experiment was performed in duplicate and repeated in four separate donor T cell populations. The average speed and persistence of migration were calculated using Microsoft Excel 2011 (2010) and subsequently transferred to Graph Pad Prism (version 4) for statistical analysis and production of graphs.

2.9 Plate-bound ICAM-1 Cell Adhesion Assay for HuT78 T Cells

This ICAM-1 Cell Adhesion assay was optimised to quantify the effect of altered levels of RACK1 on affinity and avidity changes of LFA-1 adhesion to ICAM-1 in HuT78 T cells.

The assay was performed as described previously with minor modifications (Aoudjit and Vuori 2000). This assay involves seeding cells onto immobilised ICAM-1 and, after a series of washing steps, quantifying the number of adherent cells. This assay had not been previously performed in the laboratory and required a number of optimisation steps for use with the HuT78 T cell line. Nunclon 96-well tissue culture plates (Nunc) were coated with PLL, the ICAM-1 coating antibody goat anti-human IgG (Fc specific), ICAM-1, an antibody against LFA-1, anti-LFA-1 (clone SPVL-7), or uncoated. The wells coated with ICAM-1 and anti-LFA-1 had to first be coated with the coating antibody goat anti-human IgG (Fc specific) and goat anti-mouse IgG, respectively, overnight. The unbound coating antibodies were removed and 1 µg/ml rICAM-1-Fc or 1:1000 anti-LFA-1 in sterile PBS was added and incubated for 1-2 hours at 37ºC. PLL was also added to the appropriate well at this time. The unbound solution was removed and the cells were seeded at 1 x 10^4 cells/ well. The cells were either pre-treated with a final concentration of 50nM SDF-1α or divalent cations $MgCl_2$ and EGTA at final concentrations of 5 mM and 1.5 mM, respectively or untreated. The cells were incubated for 30min at 37°C and a prewash cell count was quantified by using the IN Cell Analyzer. The wells were washed three times with cation-free PBS, and the cells were then fixed and incubated with cell-permeable Hoechst nuclear stain (1nM). The postwash cell number was quantified by using the IN Cell Analyzer.

2.10 Plate-bound ICAM-1 Cell Adhesion Assay for Primary T Cells

This ICAM-1 Cell Adhesion assay was optimised to quantify the effect of altered levels of RACK1 on affinity and avidity changes of LFA-1 adhesion to ICAM-1 in Primary T cells. Conventional integrin adhesion assays involve cell incubation with the immobilised integrin, a series of washing steps to remove unattached cells, and a final cell count. Due to the number of cells detaching from the plate during the washing steps in the previous method, an adhesion assay previously described using reverse centrifugation was used instead of the washing steps (Konstandin et al. 2006) with some modifications. This ensured even removal of unattached cells, while attached cells remain on the plate.

Maxisorp 96-well tissue culture plates (Nunc) were coated with 1:500 dilution of goat anti-human IgG (Fc specific) diluted in sterile PBS and stored at 4ºC overnight. The unbound antibody solution was removed and 1 µg/ml rhICAM-1-Fc was added and incubated for 1-2 hours at 37ºC. PLL was also added to the appropriate well at this time. The unbound solution was removed and the plates were washed once with cation-free PBS. The cells were seeded at 1 x 10^4 cells/ well with or without a final concentration of

50nM SDF-1α or LFA-1-activating cations $MgCl_2$ and EGTA at final concentration of 5 mM and 1.5 mM, respectively. The cells were incubated for 30min at 37°C and then underwent reverse centrifugation at 10xg for 30sec to remove unbound cells. The cells were then fixed in 4% final PFA and incubated for 15 min with cell permeable Hoechst nuclear stain (1nM). The cells were quantified using the automated microscope IN Cell Analyzer 1000 HCA platform and normalised to the input cell count.

2.11 Transwell Chemotaxis Assay

In contrast to the 2D *in vitro* T cell Migration Assay, the Transwell Chemotaxis Assay was used to assess the effect of treatment (i.e. protein knockdown or overexpression) on 3D chemotactic migration. As mentioned in section 2.8, when cells come into contact with a matrix barrier, the cells adapt their morphology and change shape in response to extracellular signals, such as the presence of chemokine. Chemotaxis assays were performed in using a modified Boyden chamber (Boyden 1962). T cells were loaded into an upper chamber with an ICAM-1-bound porous membrane barrier and chemokine was added to the lower chamber. The transwell migration assay is an *in vitro* system which incorporates three important T cell functions necessary for transendothelial migration. These are the ability of the chemokine-stimulated T cells to bind, polarise, and migrate through an ICAM-1-bound filter. In general, the most important requisite is to calibrate the incubation time of the assay both to the model cell and the ligand to be evaluated. For instance, too short of incubation time results in limited number of cell migrating to the lower chamber, while too long of time perturbs the concentration gradients and measures more chemokinetic than chemotactic responses.

This assay utilised Millicell Hanging Cell Culture Insert made of polyethylene terephthalate (Millipore, Billerica, MA, USA). 5.0μM and 3.0μM pore size inserts were used for HuT78 and PBTLs, respectively. The membrane of the inserts were coated with goat anti-human antibody (1:500) and incubated at 4°C overnight. The next day the wells were washed 3X with PBS and coated with 1 μg/ml rhICAM-1. T cells were seeded at 1-2 $x10^5$ cells/ 100ul/ transwell, resuspended in serum free RPMI + 0.5% BSA, and serum starved for 2 hours before loading onto transwell filters. RPMI + 0.5% BSA with 10nM (50 ng/ ml) SDF-1α or without (no stimulus control) was added to the lower chamber. The cells were incubated for 3 hours at 37°C. The cells from the lower chamber were harvested and transferred to a poly-L-lysine pre-coated 96 well plate. The cells were fixed with a final concentration of 4% pre-warmed PFA for 15 min at 37°C, stained with Hoechst nuclear stain for 15 min at room temperature, and counted using the automated

microscope on IN Cell Analyser. The cells that successfully migrated to the lower chamber were counted and normalised to the number of cells loaded onto transwell (the input). It should be noted that unlike other chemotaxis methods, which include cells bound to the bottom of the filter by pelleting cells by centrifugation in the final cell count (Curnock et al. 2003), only cells which successfully migrated into the lower chamber and detached from the membrane were counted. The averages were obtained for duplicate transwells and the data was normalised to the input.

2.12 Chemokine-induced Cell Polarisation Assay

The Chemokine-induced Cell Polarisation Assay was used to evaluate the effects of a particular treatment on T cell polarisation, protein phosphorylation status, and cell surface expression of the chemokine receptor CXCR4 in response to SDF-1α. The cells were stimulated with a uniform concentration of solubilised SDF-1α in suspension, which binds its cognate receptor CXCR4 and induces cell polarisation. T cells were seeded at 5 $x10^5$ cells/ ml and serum starved for 2 hours prior to experiment in serum free RPMI + 0.5% BSA. The cells were then stimulated for indicated times with 100ng/ ml SDF-1α under discontinuous stirring conditions for the times indicated or left untreated. The activation was stopped by centrifugation for 30 sec at 850x*g* on a benchtop centrifuge.

For immunofluorescence microscopy analysis, the supernatant was discarded and the cells were then fixed with 4% final PFA, permeabilised with 0.5% Triton X-100 if necessary, and stained with protein-specific antibodies in solution. The cells were then loaded onto a 96 well glass bottom plate suitable for confocal microscopy pre-coated with PLL. Two drops of DAKO fluorescent mounting medium was added and at least 10 images were acquired for each well with a 63X oil immersion objective (section 2.23).

For Western blot analysis, the supernatant was discarded and the cells were lysed in 1X SDS sample buffer containing 1mM DTT and briefly sonicated for 10 sec. Finally, the samples were boiled for 5 min and were stored at -20°C or prepared for SDS-PAGE (section 2.19).

For analysis by flow cytometry, see section 2.14.

2.13 Treatment with Inhibitors

When indicated, the cells were pre-incubated with the following pharmacological inhibitors: the cytoskeletal inhibitors 5 μM Nocodazole for 40 min and 10 μM

Cytochalasin D for 40 min; the phosphatase inhibitors 300 nM okadaic acid for 20 min and 100nM Calyculin A for 30min; 20 μM ROCK inhibitor Y-27632 and 20 μM MLCK inhibitor ML-7 for 60min prior to experimentation; and 30 μM PKC pseudosubstrate inhibitor for 30min prior to experimentation.

2.14 Flow Cytometry

Flow cytometry was used to determine the effects of a particular treatment on cell surface expression of receptors, such as CXCR4. Jurkat T cells were seeded at 5 $x10^5$ cells/ ml and serum starved for 2 hours prior to experiment in serum free RPMI + 0.5% BSA. The cells were then stimulated for indicated times with 100 ng/ ml SDF-1α under discontinuous stirring conditions for the times indicated or left untreated. The activation was stopped by centrifugation for 30 sec at 850x*g* on a benchtop centrifuge. The cells were washed once with ice-cold PBS and then stained with Phycoerythirin (PE)-labelled antibodies against cell surface receptors in 1% BSA/ PBS and incubated for 30 min on ice. The cells were then washed twice in 1% BSA/ PBS and fixed in 1% PFA on ice. The cells were immediately analysed by flow cytometry or stored for up to 24 hours at 4°C.

The samples were measured with the DAKO CyAn ADP (Advanced Digital Processing) (Beckman Coulter Diagnostics Limited, Lismeehan, Co. Clare, Ireland) benchtop flow cytometer capable of analysis of up to 50,000 cells per second. The CyAn ADP LX 7 Colour model is equipped with 488 nm and 633 nm solid state lasers. The nine parameters available include FSC, SSC, and seven fluorescent channels (FL1-FL7) with five fluorescent channels available from blue laser and two from red laser excitation. The CyAn ADP is operated through the DAKO Summit Software. The results were analysed using associated the Dako Summit (version 4.3) software to generate histograms. The data then underwent statistical analysis and was graphed using Graph Pad Prism.

2.15 Preparation of Cellular Protein Extracts

T cells were harvested and pelleted by centrifugation at 3000x*g* for 5 min at room temperature and resuspended in ice-cold Cell Lysis Buffer (components of cell lysis buffers are provided in Appendix 3) at approximately 10 x 10^6 T cells/ 1 ml buffer. Unlysed cells, nuclei, and detergent-insoluble material were removed by centrifugation at 14,000x*g* for 5 minutes at 4°C in a bench-top centrifuge. Supernatant lysates were transferred to fresh tubes and stored on ice.

2.16 Calculation of Protein Concentration of Lysates

The protein concentration of the cell lysates was calculated by first preparing 1:2 and 1:5 dilutions for each cell lysate sample in distilled water. A 2 mg/ml solution of BSA was prepared in distilled water and used as a protein standard in this assay. The BSA stock was diluted in distilled water to give final concentrations of 1000 µg/ml, 750 µg/ml, 500 µg/ml, 250 µg/ml, and 125 µg/ml. The BSA standards and samples were loaded (10 µl) in a 96 well plate in triplicate and 300 µl of Coomassie Bradford protein dye was added. The plate was incubated at room temperature for 20 min. The colour change was correlated to the protein concentration with a dark blue reflecting the highest protein quantity. The plate was then analysed by the Versa Max Microplate Reader and the dye absorbance was measured at 590 nm. A standard curve of absorbance measurements versus BSA protein concentration was generated in Microsoft Excel. The slope of the trend line on the graph, setting the y-intercept (*b*) to zero, was calculated to yield the equation $y=mx + b$.

The average of each triplicate was calculated and used to compute the corrected absorbance values of the cell lysate samples. The corrected absorbance values (y) along with the slope (m) were entered into the equation produced by the standard curve in order to determine the protein concentrations (x) of the cell lysate samples. Cell lysates were normalised for equal protein content as indicated for particular immuno-blotting or affinity precipitation experiment and final volumes were adjusted with lysis buffer. Protein samples were boiled at 100°C for 5 min with equal volume 2X SDS sample buffer (Appendix 3) and centrifuged briefly (1 min) to remove any insoluble solids.

2.17 Acetone Precipitation of Cell Lysates

If the cell lysate needed to be concentrated before separating by gel electrophoresis, the cell lysate samples were resuspended in 5x volume of ice cold acetone for 30 min at -20°, and followed by centrifugation at 16,000x*g* for 5 minutes at 4°C. Supernatant was aspirated and precipitated protein was allowed to air dry for 1 min, and then resuspended at 50 µg of protein in 20 µl of 1X SDS sample buffer.

2.18 Preparation of Cell Lysates for Detection of MLC phosphorylation

The following protocol was previously used to detect phosphorylated MLC Ser19 (Ludwig et al. 2010) with some minor modifications. Briefly, cells were pelleted by centrifugation and rinsed twice in ice-cold PBS. Cellular proteins were then lysed with 100 µl/sample of ice-cold RIPA buffer (Appendix 3) supplemented with 50 mM phosphatase inhibitor NaF for 30 min. Lysates were then precipitated with three volumes of methanol and equal volume of chloroform at RT. The samples were then pelleted by centrifugation at top speed on a benchtop centrifuge. The upper aqueous phase was removed and discarded. Three volumes of methanol were added and the samples were inverted several times. The samples were then pelleted by centrifugation and allowed to air dry. The pellets were dissolved in 1X SDS sample buffer containing 1mM DTT, boiled for 5 min, and subjected to 15% SDS-PAGE.

2.19 Sodium Dodecyl Sulphate Polyacrylamide Gel Electrophoresis (SDS-PAGE)

The SDS-PAGE protocol was followed according to the Atto gel electrophoresis system (ATTO Corporation, Japan). The polyacrylamide gel was used at varying concentrations of acrylamide depending on the molecular weight size of the protein to be analysed. The components of the gel for each acrylamide percentage are provided in tabular form in Appendix 3 Table 6.

The gel was poured between the glass plates and allowed to set and overlaid with the stacking gel (Appendix 3 Table 7). Once gel was set, 200 ml of SDS-PAGE Running Buffer contained in final concentrations the following: 3.02 g TRIZMA, 18.8 g Glycine, 10 mls of 10% w/v SDS, and distilled water was poured into the gel electrophoresis system. The protein extract samples and molecular weight marker were loaded into the wells and the gels were run at 200V and 40 mAmps for approximately 1.5 h. Both unstained molecular weight markers and pre-stained molecular weight markers were used in this study.

2.20 Immunoblot Analysis

Once the gel electrophoresis was complete, Western blotting was carried out for the transfer of electrophoresed proteins to polyvinylidene fluoride (PVDF) membrane using

the semi-dry transfer technique according to the manufacturer's instructions (ATTO Corporation, Japan). The PVDF membrane (0.45 µm) was activated by soaking it in methanol for 1 min. The membrane was then immersed in transfer buffer containing in final concentration the following: 48 mM Trizma Base, 39 mM Glycine, 0.04 w/v SDS and 20 % Methanol. A gel sandwich was made by placing five sheets of Whatmann 3 mm filter paper (pre-soaked in transfer buffer) on the anode of the Western blotting apparatus. The PVDF membrane was then placed on top of the filter papers and kept moist by flooding it with transfer buffer. The gel was then placed on top of the PVDF membrane and any air bubbles between the gel and membrane were carefully removed. Another 5 sheets of Whatmann 3 mm filter (pre-soaked in transfer buffer) were placed on top of the gel. The cathode was lowered carefully onto the gel sandwich and any excess transfer buffer remaining on the anode was removed with paper towels to prevent the apparatus from short-circuiting. Western blotting was performed for 1 h at 100 mAmp/ 200 V per gel at room temperature. The unstained molecular weight markers were then removed from the membrane and stained with Coomassie stain to highlight protein bands.

Following Western blotting, non-protein bound sites on the PVDF membrane were blocked in blocking buffer containing: 5 % w/v milk powder in TBS/T, containing 1X TBS with 0.1% v/v Tween-20 for 1 hour at room temperature with constant gentle agitation. The PVDF membrane was washed three times with TBS/T (5 min washes) at room temperature. Each of the PVDF membranes was incubated with appropriate antibody to protein of interest diluted in 5% BSA/TBS containing 0.05% Sodium Azide overnight at 4° with gentle agitation. The PVDF membrane was again washed three times with TBS/T at room temperature to remove any unbound antibody. Each PVDF membrane was then incubated with an HRP- conjugated anti-mouse or anti-rabbit antibody (diluted to 1:2000) in 5% BSA/TBS for 1 hour at room temperature with gentle agitation. Afterwards, the PVDF membrane was washed three times with wash buffer at room temperature to remove any unbound protein.

In a process known as Enhanced Chemiluminescence (ECL), the membranes were incubated in HRP development solution for 60 sec as previously described (Haan and Behrmann 2007), in which 4-Iodophenolboronic acid is used instead of p-Coumaric acid (Appendix 3). The PVDF membranes were aligned with Coomassie stained molecular weight markers, placed between two sheets of acetate paper, and taped to the film cassette. The PVDF membrane was exposed with Kodak X-OMAT S film in the darkroom for various times. The film was developed with an automated film developer

(CURIX 60, AGFA, Type 9462/100/140, Agfa-Gevaert AG, Munich, Germany), which submerges film in developing solution and for 1 min, fixation solution for 1 min, and finally rinsed with distilled water and allowed to air dry.

For immunoblot analysis of phosphorylated proteins with the use of phospho-specific antibodies, the phosphatase inhibitor sodium fluoride (NaF) at final concentration of 50 mM was added to the lysis buffer, blocking buffer, and the primary and secondary antibody incubations as previously described in Sharma and Care, 2002.

2.21 Stripping of Western Blot Membranes

In some experiments where indicated, the PVDF membrane that was exposed to film was stripped of its primary and secondary antibodies and re-probed with different antibodies. This procedure was carried out by incubating the PVDF membrane in Western blot stripping solution at 50°C for 30 min (Appendix 3). The membrane was removed from the stripping solution and washed 5 times in TBS/T. Blocking of the membrane, incubation with primary and secondary antibodies, and detection by ECL was performed as described above.

2.22 Densitometric Analysis

Densitometric analyses of the Western blots were performed by using the gel analysis option of Image J software (version 1.44, National Institute of Health, Bethesda, USA). The relative values of the samples were determined by normalising each sample to the respective control samples (actin loading control) of each experiment.

2.23 Immunocytochemistry

2.23.1 Cell Permeabilisation and Blocking

In order to prepare cells for immunofluorescence staining and subsequent microscopy, cells were seeded in a Lab-Tek II 8 well chamber slide (Nunc) or Matrical 96-well glass bottom plates (0.17mm; PAA, UK) suitable for confocal microscopy. Fixation and blocking methods were optimised for each protein-specific antibody. Cells were treated with a fixation agent such as paraformaldehyde (PFA), methanol, or acetone and then washed with PBS and permeabilised with 0.3% Triton-X100 in PBS for 10 min at room temperature. The cells were then blocked with 3% BSA in PBS for 30 min at room

temperature. For experiments which included staining of RACK1, PHEM buffer (60 mM PIPES, 25 nM Hepes, 10 nM EGTA, 20mM $MgCl_2$; pH 6.9) was used instead of PBS.

2.23.2 Immunofluorescence Staining

Immunofluorescent staining was performed on cells fixed to an 8-well chamber slide or 96 well glass bottom plate (0.17mm; PAA, UK) suitable for confocal microscopy. First, the protein-specific, or primary antibody, was diluted according to manufacturer's instructions in 5% BSA/PBS and added to permeabilised and BSA-blocked cells for 1 h at room temperature. Then, unbound antibody was aspirated and cells were washed three times with PBS/0.05% Tween. Next, a secondary antibody, or fluorescently-labelled antibody against the primary antibody, and Hoechst nuclear stain were both diluted 1:2000 in 5% BSA/PBS and added to the cells for 30 min at room temperature. Again, unbound antibody was aspirated and cells were washed three times with PBS/0.05% Tween. For experiments staining for RACK1, PHEM (60 mM PIPES, 25 nM Hepes, 10 nM EGTA, 20mM $MgCl_2$; pH 6.9) was used instead of PBS; cells were washed with PHEM, without added Tween. The plastic attachment was removed from the chamber slide and a glass cover slip was mounted using DAKO fluorescent mounting medium. For the 96 well glass bottom plate, two drops of fluorescent mounting medium were added to each well. Negative controls with only secondary antibody were included to ensure that visualised patterns of protein localisation were the result of primary and secondary antibody binding and not the result of non-specific secondary antibody binding.

2.23.3 Confocal Microscopy

The cells were imaged using a Zeiss confocal workstation attached to a Zeiss LSM510 laser scanning microscope (Carl Zeiss, Thornwood, NY) using 10X, 20X, 40X, and 63X oil immersion objectives and the following three lasers: Diode, Argon, and DPSS with excitation wavelengths of 405, 488, 561 nm, respectively. The images were obtained, processed and analysed using Zeiss LSM Data Server software version 4.2.0.121 available for download on the Zeiss website. At least twenty images were acquired for each treatment and representative images are shown in the results sections.

2.24 Detergent Extraction Assay

In the detergent extraction assay, T cells were exposed to the mild detergent TritonX-100, which solubilises membrane proteins and preferentially preserves the nucleus, actin

and microtubule cytoskeleton, and cytoskeletal-associated proteins. The following protocol was developed in the laboratory to study MT-associated proteins and is based on two previously described methods: western blot analysis (Ohanian et al. 2005) and immunofluorescence analysis (Steindler et al. 2004) with minor modifications. After the LFA-1-induced migration assay, the cells were extracted with 0.05% Triton X-100/PHEM buffer at room temperature for 5 min. After incubation with TritonX-100, two fractions were recovered: triton-soluble (cytosolic) and triton-insoluble (cytoskeletal).

For immunofluorescence microscopy analysis, the cells were extracted with TritonX-100 instead of fixed and the triton-soluble fraction was discarded and the remaining insoluble fraction was stained with protein-specific antibodies. Two drops of DAKO fluorescent mounting medium was added and at least 10 images were acquired for each well with a 63X oil immersion objective (section 2.23).

For Western blot analysis, after detergent extraction the resting cells were pelleted by centrifugation at 700g for 5 min. The triton-soluble fraction was removed and the triton-insoluble fraction was then resuspended in 2% SDS/ PBS buffer. After detergent extraction of migrating cells, the triton-soluble fraction was removed and the triton-insoluble fraction was solubilised on addition of 2% SDS/ PBS buffer. Both of the insoluble fractions were sonicated briefly for 10 sec. All samples were then acetone precipitated, boiled for 5 min in 1X SDS sample buffer containing 1mM DTT, and stored at -20°C or prepared for SDS-PAGE (section 2.19). For experiments which included staining of RACK1, PHEM buffer (60 mM PIPES, 25 nM Hepes, 10 nM EGTA, 20mM $MgCl_2$; pH 6.9) was used instead of PBS.

2.25 Immunoprecipitation

In order to isolate protein from whole cell lysate, the lysate is incubated with a protein-specific antibody conjugated to agarose beads which are then separated from the lysate by centrifugation and analysed by Western blot in a process known as immunoprecipitation (IP). For the immunoprecipitation of RACK1 and associating proteins, I employed a protocol optimised to preserve membrane- and cytoskeletal-associated proteins (described previously in Kiely et. al., 2006) and is described below. In addition, I employ the Dynabeads Protein G kit, which utilises superparamagnetic iron impregnated, 4% agarose beads 2.8 µm in diameter, and have recombinant Protein G (approx. 17 kDa) covalently coupled to their surface that bind immunoglobulin via the Fc

region and a magnetic rack, instead to ensure multi-protein complexes are preserved during the IP process.

Cells were seeded at $20x10^6$ in T-175 flask coated with anti-LFA-1 or left uncoated. The cells were incubated for 3 hours at 37°C. Cells were lysed in 1 ml ice cold cell lysis buffer containing 1 mM EGTA, 1 mM EDTA, 10 mM Tris-HCl (pH 7.4), 150 mM NaCl, 1% sodium deoxycholate plus the tyrosine phosphatase inhibitor sodium orthovanadate (1 mM), and the protease inhibitors PMSF (1 mM) and leupeptin (10 µg/ ml). The IP is performed at 4°C to avoid protein complex dissociation and minimize enzymatic activity. The Dynabeads kit protocol was followed to manufacturer's instructions. Briefly, 50 µl (1.5 mg) protein G agarose bead slurry was aliquoted into microcentrifuge tubes, storage buffer (PBS, pH 7.4, containing 0.01% Tween-20 and 0.09% sodium azide) was separated by magnetic rack and discarded. Primary antibody was added to 200 µl of the antibody binding and washing buffer, which was included in the kit. The antibody solution was added to the tubes and incubated for 10 min with gently mixing on a daisy wheel at room temperature. Unbound antibody was separated by magnetic rack and discarded. The cell lysates were then added to tubes and incubated on a daisy wheel at 4°C for 1-2 hours.

The antibody control contained agarose beads + 5 µg normal mouse IgM/ normal rabbit IgG + 500 µl whole cell lysate. The IP contained agarose beads + protein-specific antibody (typically 1-10 µg of antibody according to manufacturer's instructions) + 500ul whole cell lysate. The antibody used to immunoprecipitate RACK1 is an IgM, which has a weak affinity to protein G; therefore, in RACK1 IP experiments, 5 µg of goat α-mouse IgM Fab fragment was pre-incubated with the beads. The tubes were then placed on magnetic rack and unbound protein was transferred to a fresh tube for future analysis. The beads were washed 3 times with 200 µl washing buffer included in the kit. The tubes were placed on the magnet between each wash, supernatant discarded, and bead conjugate was resuspend by gentle pipetting. The Dynabeads-antibody-antigen complex was resuspended in 100 µl washing buffer and transferred to a clean tube. The protein was then eluted from beads with 20 µl elution buffer included in the kit and boiled for 5 min with equal volume 4X SDS sample buffer containing 1mM DTT. The tubes were placed on the magnetic rack to separate eluted protein from beads and loaded onto gel for analysis by SDS-PAGE (section 2.19).

2.26 Coomassie Brilliant Blue Staining of SDS-PAGE Gels

Coomassie brilliant blue stain binds non-specifically to proteins and is commonly used to stain protein gels (Wilson 1983). Because the dye does not bind to the polyacrylamide gel, proteins will be detected as blue bands surrounded by clear gel zones once washed in a destaining solution. In addition, Coomassie brilliant blue stain is reversible and can be completely removed after incubation in destaining solution. The gel can then be stored in acetic acid or water, photographed, or dried to maintain a permanent record. The following protocol was previously described (Sasse and Gallagher 2004).

After separation of proteins by gel electrophoresis, the polyacrylamide gel was fixed in a solution containing 150 ml 50% methanol + 5% acetic acid and incubated for 2h on an orbital shaker. The fixing solution was removed and the gel was incubated in Coomassie blue stain containing 50% (v/v) methanol, 0.05% (w/v) Coomassie brilliant blue R-250, 10% (v/v) acetic acid, and 40% H_2O for 4h on an orbital shaker. The staining solution was removed and the gel was washed in fixing solution. The gel was then incubated in destaining solution for 2h on an orbital shaker. The destaining solution was removed and fresh destaining solution was added to the gel. This process was repeated until the destaining solution was clear and bands became distinguished from the background. The gel was temporarily stored in 7% (v/v) aqueous acetic acid or water. The gel was then placed in a clean clear plastic bag, photographed, and stored at 4°C.

2.27 Silver Staining of SDS-PAGE Gels

Silver staining relies on differential reduction of silver ions, which is the basis for photographic processes. A highly sensitive photochemical silver staining technique permits the detection of polypeptides in gels at subnanogram levels (Chevallet et al. 2006). The following protocol was adapted from a protocol employed at the Proteomics Resource Center (Rockefeller, NY [http://proteomics.rockefeller.edu/ms_silverStaining]) and is compatible with subsequent analysis by mass spectrometry. The entire procedure was carried out in clean glassware (Pyrex dish 14.5 cm x 20 cm).

After separation of proteins by gel electrophoresis, the polyacrylamide gel was fixed in a solution containing 150 ml 50% (v/v) methanol + 5% (v/v) acetic acid for 20 min. Next, the gel was washed in a solution containing 150 ml 50% methanol for 10 min. Then, the gel was washed in water for 10 min. The gel was incubated with solution containing 150 ml 0.02% (w/v) sodium thiosulfate for 1 min. and rinsed with water twice for 1 min. The

gel was submerged in a solution containing in 150ml 0.1% (w/v) silver nitrate with 0.08% formalin (37%) for 20 min and then rinsed with water twice for 1 min. The gel was then incubated with a solution containing 150ml 2% (w/v) sodium carbonate with 0.04% (v/v) formalin (37%) until the desired intensity of staining occurred. The gel was then washed in 150ml 5% acetic acid for 10 min and subsequently washed in water for 5 min. Finally, the gel was incubated in a preserving solution containing 150ml water and 13.2ml glycerol (100% v/v) for 20 min or for permanent storage at 4°C.

2.28 Mass Spectrometry and Analysis

RACK1 immunoprecipitation samples were further analysed by peptide sequencing (mass spectrometry) to identify putative binding partners for RACK1. Mass spectrometry (MS) is an analytical technique that measures the mass-to-charge ratio of charged particles. MS is both qualitative and quantitative. It is used to determine particle mass, to resolve the chemical structures of molecules, and in this study, to identify the peptide composition of a sample. The MS principle consists of ionizing chemical compounds to generate charged molecules or molecule fragments and measuring their mass-to-charge ratios (Sparkman, 2000). The samples were analysed by Dr. Catherine Botting at the Biomolecular Sciences Mass Spectrometry and Proteomics Facility at the University of St. Andrew's (Glasgow, UK).

Matrix-assisted laser desorption/ionization time-of-flight (MALDI-TOF) mass spectrometry analysis following tryptic digestion of polyacrylamide gel pieces was used to identify protein hits. In addition, two or more mass analysers, which sort the ion masses by applying electromagnetic fields, were employed for tandem mass spectrometry (MS/MS). The search parameters are as follows: fixed modifications Carbomidomethyl (C) and variable modifications Oxidation (M), monoisotropic mass values, unrestricted protein mass, peptide mass tolerance ± 0.2 Da, fragment mass tolerance ± 0.2 Da, 1 max missed cleavages, and instrument type was set to default. The peptide summary report was then analysed using Mascot software (www.matrixscience.com), searching the NCBInr 040310 database, and limiting search results with a significance threshold of $p < 0.05$. The results yielded several high mascot scores and identified probable protein hits based on the frequency of peptides identified specific for a known protein in *Homo sapiens*. The results were then organised in Microsoft Excel by order of decreasing mascot score for each segment analysed. The results from the RACK1 IP were cross-checked against peptide results from the control IP to discount any non-specific proteins immunoprecipitated with the control IgG

antibody. Candidate proteins were selected for validation of the mass spectrometry analysis by confirming endogenous interaction with RACK1 by immuno-assays.

2.29 *In Silico* Gene Ontology Analysis with PANTHER

The PANTHER classification system (Pathway version 2.5; www.pantherdb.org) is a unique online resource that classifies genes/gene products by their molecular function, using published scientific experimental evidence as well as evolutionary relationships to predict function in the absence of direct experimental evidence. The PANTHER database was designed for high-throughput analysis of protein sequences. Genes and gene products are classified by expert biologist into family and subfamilies of shared function, which are then categorised by molecular function and biological process ontology terms (Thomas et al. 2003). Therefore, data from microarray analysis or mass spectrometry can be mapped as comparative data or to a reference list (e.g. *H. sapiens*).

2.30 Generation of FLAG Fusion Proteins

In order to further investigate the functional implication of the interaction of NMHCIIA with RACK1, full length and deletion mutants of NMHCIIA were generated. The fusion proteins were then used in conjunction with a RACK1 peptide array to identify the binding domain for NMHC-IIA on RACK1.

A shuttle clone (OCABo5050H124D) containing the *MYH9* gene, which encodes NMHC-IIA, was obtained from ImaGenes (Source BioScience Ltd., Nottingham, UK), which possessed Spectinomycin resistance. In order to purify plasmid from *E. coli*, I used the QIAfilter Plasmid Midi Kit and followed manufacturer's instructions. Briefly, I incubated *E. coli* containing plasmid DNA overnight at 37°C in an orbital shaker. After 12 hours, the bacteria was spread onto Luria-Bertani (LB) broth agarose plates containing Spectinomycin and incubated at 37°C overnight. I selected a single colony and inoculated LB broth containing Spectinomycin for 8 hours at 37°C, and then transferred a proportion of the starter colony to a larger volume for overnight incubation. Finally, the plasmid was purified from the *E. coli* using the QIAfilter Plasmid Midi Kit as above.

2.30.1 Amplification of Full Length (FL) MYH9

The shuttle clone, or entry vector, containing the full length *MYH9* gene was recombined into a high level mammalian expression vector with CMV promoter containing an Ampicillin resistance gene with an N-terminal FLAG epitope cloned in the multiple

cloning site (Figure 2.4) using Gateway Cloning Technology (Invitrogen, Carlsbad, CA). The Gateway Technology provides a quick and highly efficient way to move genes into a multiple vector system for functional analysis and protein expression. The Gateway Cassette is a unique sequence, which is cloned into a destination plasmid. The gene in the entry plasmid (which possesses Spectinomycin resistance) is flanked by attL sites, whereas the Gateway cassette in the destination plasmid (which possesses Ampicillin resistance) is flanked by attR sites. These sites will recombine and exchange the sequences within the attL and attR sites upon addition of Clonase. This process is known as an LR reaction (Invitrogen, Gateway Technology Manual, 2003). Following the LR reaction protocol between the entry and the destination vectors, the desired gene is inserted in place of the Gateway cassette. One advantage of the technology is that it allows recombination of a gene of interest from the entry vector into many different destination vectors by a single LR reaction.

Gateway LR Clonase II enzyme mix contains the enzymes bacteriophage lambda recombination proteins Integrase (Int) and Excisionase (Xis) and the *E. coli*-encoded protein Integration Host Factor (IHF) as well as the reaction buffer in one solution. The reaction catalyses the *in vitro* recombination between an entry clone (containing a gene of interest flanked by *att*L sites) and a destination vector (containing *att*R sites) to generate an expression clone. The attL × attR reaction is mediated by Gateway® LR Clonase™ II enzyme mix is schematically represented below.

*att*L1-gene-*att*L2 × *att*R1-*ccd*B-*att*R2

(entry clone) (destination vector)

Where attL and attR are the recombination sites, ccdB is the F plasmid-encoded gene that inhibits growth of E. coli (death-cassette gene), and gene represents any DNA segment of interest. The bacteriophage lambda recombination proteins preferentially recombine the death cassette gene with the gene of interest in the correct orientation in the destination vector.

The recombination reaction was performed according to manufacturer's instructions. Briefly, the following components were combined in a microcentrifuge tube: 1-7 µl entry clone (50-150 ng), 1 µl Destination vector (150 ng/µl), TE buffer (pH 8.0) to 8 µl total reaction volume. Meanwhile, the LR Clonase™ II enzyme mix was thawed on ice vortexed briefly twice (2 seconds each time). To each sample (Step 1, above), 2 µl of LR Clonase™II enzyme mix was added to the reaction and mixed well by vortexing briefly

twice and collecting by microcentrifugation. The reaction was incubated at 25°C overnight. Then, 1 µl (2 µg) Proteinase K, which is included in the kit, was added to terminate the reaction and was incubated for 10 min at 37°C. This reaction was carried out for full length MYH9 and pENTR-gus (an entry clone containing the Arabidopsis thaliana β-glucuronidase, or gus, gene) was used as a positive control in the LR reaction and was included in the kit.

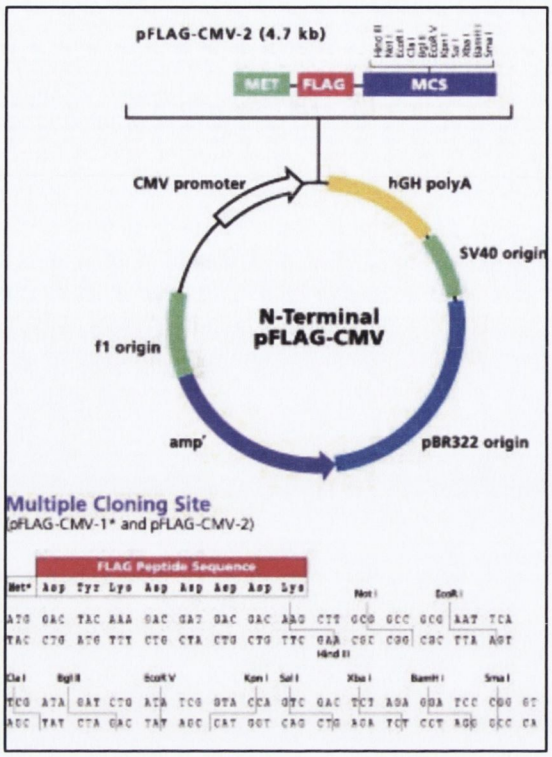

Figure 2.4: N-Terminal pFLAG-CMV.

High level mammalian expression vector containing CMV promoter, multiple cloning site with N-terminal FLAG epitope, and ampicillin resistance gene.

2.30.2 Bacterial Transformation of FL MYH9

The expression vector was then transformed into competent *E. coli* (DH5 Alpha) following manufacturer's instructions. Briefly, the *E. coli* cells were thawed on ice and the Clonase reaction product was added to the cells. The cells were then heat shocked at 42°C for 30 sec. The cells were then put on ice, 250 µl SOC medium was added, and the bacterial cell suspension was incubated at 37°C with shaking. After 1 hour, 150 µl of bacterial cell suspension was dispensed on LB broth and agarose plates containing Ampicillin and incubated at 37°C overnight. Five single colonies were then selected and expanded at 37°C overnight in LB broth containing Ampicillin. The bacterial cells were pelleted by centrifugation and the plasmid was then purified from *E. coli* by QIAprep Spin Miniprep Kit following manufacturer's instructions. The plasmid DNA was then quantified with the Multi-Sample Micro-Volume UV-Vis Spectrophotometer NanoDrop 800.

2.30.3 Sequencing of FL MYH9

Using Vector NTI to map the gene insert and the primer design function, a reverse primer (primer B1) was designed to recognise a region near the start of the gene in order to sequence a fragment of the DNA and confirm plasmids with correct orientation of the gene insert. Sequencing primers were also generated with forward primers overlapping approximately every 800 base pairs for the full length 6kb gene again using Vector NTI and UCSC *In-Silico* PCR browser to ensure the melting temperature was between 55°C and 65°C (Table 2.1). Fragments were then sequenced by Source BioScience (Nottingham, UK) and aligned to the cDNA of MYH9 using Vector NTI Align X software to confirm it was identical to the original clone sequence. The reverse primer B1 was designed to determine the plasmid with the gene insert in the correct orientation (Figure 2.5).

Plasmids containing the gene insert in the correct orientation were then transformed into competent *E. coli* DH5 Alpha cells. Briefly, I heat shocked cells at 42°C for 30 sec, SOC medium was then added to cells on ice, and bacteria was incubated in orbital shaker at 37°C. The cells were then dispensed onto LB + agarose plates containing Ampicillin overnight at 37°C. The following day, single colonies were selected and grown for 8 hours at 37°C in 2ml LB broth containing Ampicillin; 1ml of the broth was then used to inoculate 250 ml of LB Broth containing Ampicillin and grown at 37°C overnight. Finally, the plasmid was purified from bacteria cells by Qiafilter Plasmid Maxi kit.

Table 2.1: Sequencing Primer Name and Base Composition.

Primer Name	Base Composition
Seg2_F1	GTATGATGCAAGACCGAGAA
Seg3_F1	ACACTGACCAGGCGTCCATG
Seg4_F1	ACAAAGCTGACGAGTGGCTG
Seg5_F1	AGCGAGACCTGAAGATCACC
Seg6_F1	AGGACCAGAACTGCAAGCTG
Seg7_F1	GAAAGCAAACCTCGAGAAGG
Seg8_F1	TACGACAAGCTGGAGAAGAC
Seg9_F1	TCTCGTGAGGAGATCCTGGC
Seg1_B1	TGGTGTTCTCCGTCTTGCCA

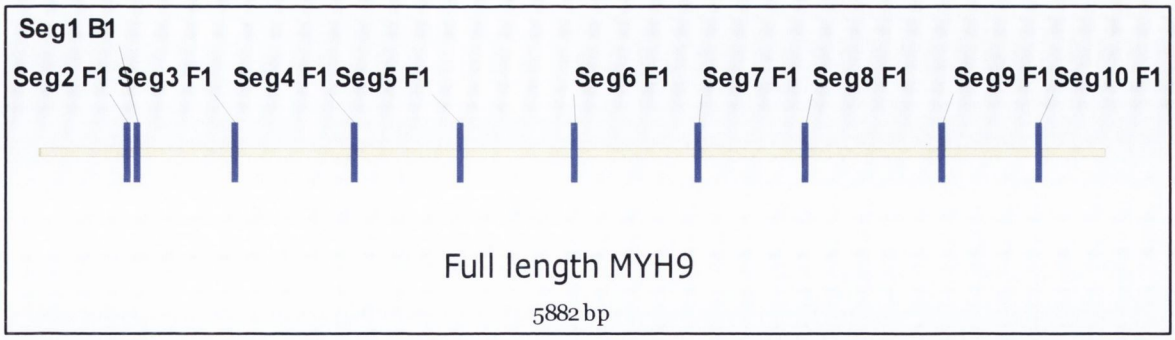

Figure 2.5: Location of Primers Designed for Sequencing and Determining Plasmid Orientation.

The location of sequencing primers (F2-10) for 6kb MYH9 open reading frame and full length plasmid orientation primer (B1) are depicted.

2.30.4 Design and Generation of NMHCIIA- Derived Fragments

In addition to generating a full length MYH9 FLAG fusion protein, I designed and generated three NMHC-IIA-derived fragments. The research and design of the three deletion mutants is discussed in detail in Chapter 5. Mutant deletion constructs were generated via PCR-based methods. The full length mammalian *MYH9* gene contains 1960 amino acids (aa), consisting of five core domains: the motor head which binds filamentous actin, the IQ domain which interacts with myosin light chains, the unknown domain, the coiled-coil tail, which is responsible for the dimerization and conformation of myosin heavy chain, and the globular tail, which is involved in NMHC-IIA subcellular localisation. The delta C mutant lacks the globular, or non-helical, tail (aa 1-1919), the delta motor mutant lacks the motor head and IQ domain (aa 796-1960), and the delta N mutant lacks the motor head, IQ domain, and unknown domain but with an intact coiled-coil and globular tail (aa 838-1960).

Primer pairs were designed to selectively amplify derived fragments from the MYH9 gene (Table 2.2) using the primer design function in Vector NTI Advanced (version 10.1) in conjunction with the UCSC *In-Silico* PCR browser (http://genome.csdb.cn/cgi-bin/hgPcr) to ensure the melting temperature was between 55°C and 65°C. The custom oligonucleotides were purchased from Sigma Aldrich and used to selectively amplify the NMHC-IIA derived deletion mutants described in the next section. Three reverse primers (MYH9_B1, B2, and B3) were designed to amplify the delta motor and delta N deletion mutants, but the MYH9_B2 primer was determined to yield the best amplification results by DNA gel electrophoresis and was used to generate the deletion mutants (Figure 2.6).

Table 2.2: Primer Name and Base Composition used to generate NMHCIIA derived fragments from full length MYH9.

Primer Name	Base Composition
MYH9_F1	ATGGCACAGCAAGCTGCC
MYH9_B1	CTATATTCGGCAGGTTTGGC
MYH9_B2	GGAGAAGAGGCTTATTCGGCAG
MYH9_B3	TGTCCATCCATCTCAGGCTGC
Delta N_F1	CAGGTGAGCCGGCAGGAG
Delta Motor_F1	GAAAGCATTTGCCAAGCG
Delta C_B1	CTAGTTCTTTAGGGAGCTGACTTC

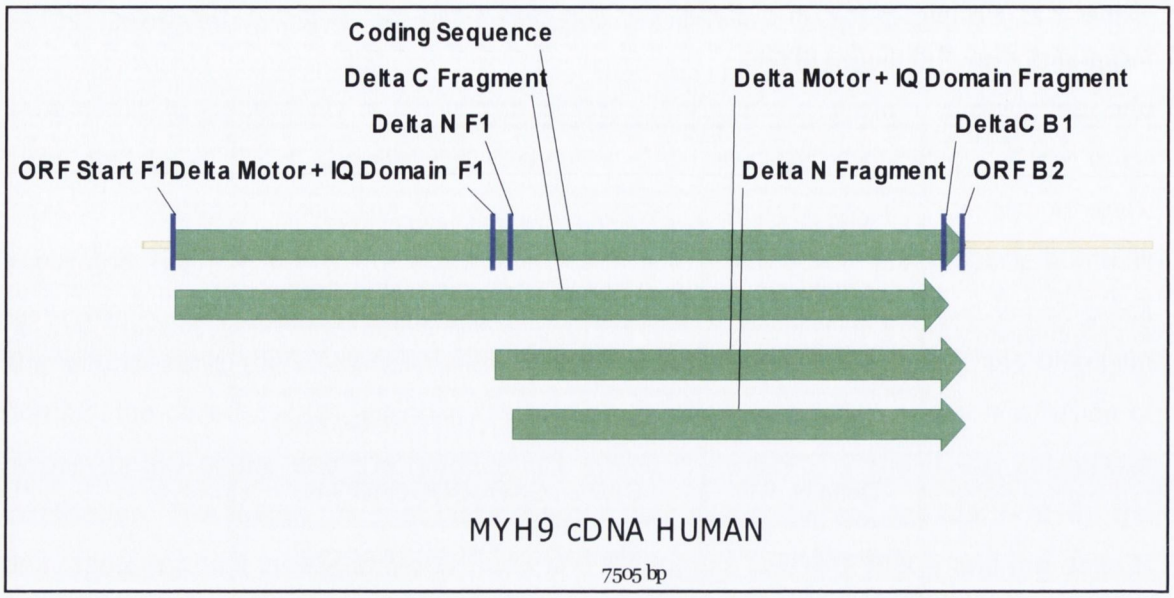

Figure 2.6: Schematic diagram of MYH9 cDNA deletion mutants.

The location of deletion mutant primers on the full length MYH9 open reading frame and the corresponding deletion mutants.

2.30.5 Polymerase Chain Reaction

The polymerase chain reaction (PCR) is a scientific technique in molecular biology to amplify a single or a few copies of a piece of DNA across several orders of magnitude, generating thousands to millions of copies of a particular DNA sequence (Bartlett and Stirling, 2003). The technique was originally developed by Mullis and colleagues (1985) and is now a common and often indispensable technique used in medical and biological research labs for a variety of applications, including DNA cloning for sequencing, DNA-based phylogeny, and functional analysis of genes. The method relies on thermal cycling, or repeated cycles of heating and cooling of the reaction. First, separation of the two strands in a DNA double helix at high temperature in a process called DNA melting, and then, at a lower temperature, enzymatic replication of the DNA. Primers (short oligonucleotides) complementary to the target region along with a heat-stable DNA polymerase, an enzyme originally isolated from the bacterium *Thermus aquaticus,* can selectively amplify the target DNA (Saiki et al. 1988). As PCR progresses, the DNA generated is itself used as a template for replication, setting in motion a chain reaction in which the DNA template is exponentially amplified. PCR can be extensively modified to perform a wide array of genetic manipulations.

For this study, Phusion Taq High-Fidelity PCR Master Mix was utilised and PCR was carried out following manufacturer's instructions. Briefly, the reaction conditions are as follows: 1X Phusion High-Fidelity PCR Master Mix with HF Buffer (containing 20 units/ ml Phusion DNA polymerase, 0.2 mM each dNTP, and 1X Phusion HF Buffer), DNA template, 0.5 µM primers and 3% DMSO (optional) in a total reaction volume of 50 µl. The reaction was performed with and without DMSO and the reaction combination that yielded the best amplification results was used in future experiments.

2.30.6 DNA Gel Electrophoresis

The amplicons were then separated by DNA gel electrophoresis to ensure DNA bands of the correct size. Using an electric field, the DNA was separated through an agarose gel. When the electric current is applied, the larger molecules move more slowly through the gel while the smaller molecules move faster toward the anode as DNA is negatively charged. The different sized molecules form distinct bands on the gel. The distance a band travels is approximately inversely proportional to the logarithm of the size of the molecule.

5X DNA loading dye was added to the samples. The samples were loaded onto a 0.8% or 1% agarose gel samples alongside a DNA ladder, which was used to determine band size. The gel was submerged in DNA gel cassette in 1XTBE (Tris-acetate buffer pH 8.0 and 1mM EDTA pH 8.3) diluted from 10X with distilled water and containing 5% ethidium bromide. The gel was electrophoresed at 100 V for 45 min. The gels contain ethidium bromide, which intercalates DNA, and were then visualised by UV transilluminator and photographed under ultraviolet light using a Bio-Rad Gel Documentation System (Bio-Rad Laboratories GmbH, München, Germany). DNA bands of the correct size were purified from the gel using the Qiagen Gel Purification kit following manufacturer's instructions. The quantity of DNA was then measured using the Multi-Sample Micro-Volume UV-Vis Spectrophotometer NanoDrop 800. The measured samples were then re-amplified by PCR. The PCR products were separated by gel electrophoresis and bands of the correct size were again purified from the gel using the Qiaquick Gel Extraction kit following manufacturer's instructions and measured.

2.30.7 Topoisomerase Cloning

The DNA fragments were then cloned into an entry vector with a technique known as Topoisomerase Cloning. The TA TOPO Cloning technique is a specific cloning method that relies on the ability of adenine (A) and thymine (T), which are complementary base pairs on different DNA fragments to hybridize and, in the presence of ligase, become ligated together. The PCR product was amplified using Phusion Taq DNA polymerase, which preferentially adds an adenine to the 3' end of the product, and incubated at 72°C for 20 min in a salt solution. The reaction contained the following to yield 20 µl reaction volume: 16 µl PCR product, 1 µl Taq enzyme, 2 µl PCR buffer/ MgCl2, and 1 µl 10 mM dNTP.

Next, the PCR amplified inserts were cloned into linearized entry vectors that have complementary 3' thymine overhangs. The following topoisomerase reaction was performed using the pCR8/GW/TOPO vector kit (Spectinomycin resistant) at room temperature for 1 hour (Figure 2.7). The reaction contained the following to yield a 6 µl reaction volume: 4 µl PCR/TOPO product, 1 µl salt solution, and 2 µl vector. The vector (total 6 µl) was then transformed into competent *E. coli* following manufacturer's instructions. Briefly, the cells were heat shocked at 42°C for 30 sec, 250 µl SOC medium was then added to cells on ice, and bacteria was incubated in orbital shaker at 37°C. After 1 hour, 150ul of bacteria suspension was dispensed on to LB broth and agarose plates containing Spectinomycin and incubated the plates at 37°C for 12 hours. Five

single colonies were then selected from each plate and inoculated 2ml LB broth containing Spectinomycin and incubated in the orbital shaker at 37°C for 8 hours. Next, the bacterial cells were pelleted by centrifugation and the plasmids were purified using Qiagen miniprep. Finally, the plasmid DNA was quantified by Multi-Sample Micro-Volume UV-Vis Spectrophotometer NanoDrop 800.

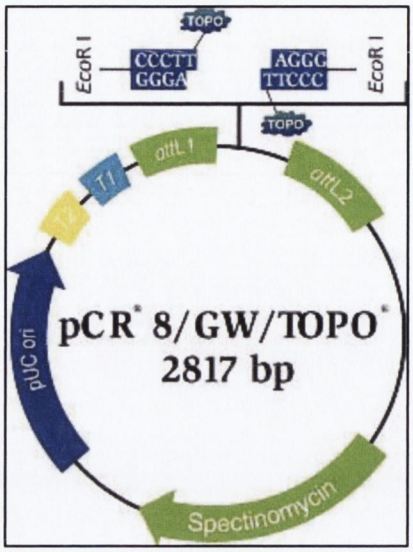

Figure 2.7: The PCR8 entry vector containing Spectinomycin using in the TA/TOPO cloning technique.

The PCR8 vector obtained from Invitrogen contained complementary 3' Thymine overhangs, a Spectinomycin resistance gene for robust *E. coli* selection, and Gateway cloning system was used to create an entry clone for the MYH9 deletion fragments using the TA TOPO Cloning technique.

2.30.8 Restriction Digest

The purified plasmid then underwent a method known as restriction digest, an enzymatic technique used for cleaving DNA molecules at specific sites, ensuring that all DNA fragments that contain a particular sequence have the same size. The cleavage method makes use of an important class of DNA-cleaving enzymes isolated primarily from bacteria. These enzymes are called restriction endonucleases or enzymes, which are able to cleave DNA molecules at the positions containing a short sequence of bases, known as restriction sites. Each restriction enzyme has a specific restriction site in which it cleaves DNA allowing one to choose the enzyme(s) necessary for the digest. These *recognition sequences* are typically four, six, eight, ten, or twelve nucleotides long. Because there are only so many ways to arrange the four nucleotides which compose DNA (Adenine, Thymine, Guanine and Cytosine) into a four- to twelve-nucleotide sequence, recognition sequences tend to occur by chance in any long sequence. Moreover, almost all artificial plasmids include a multiple cloning site that contains dozens of restriction enzyme recognition sequences within a very short segment of DNA. This allows the insertion of almost any specific fragment of DNA into plasmid vectors (Williams 2003). Furthermore, a restriction digest allows one to select plasmids with correct insert orientation by choosing an enzyme that asymmetrically cleaves the gene insert.

Restriction maps of the entry vector PCR8 containing the each deletion mutant gene insert were generated in Vector NTI and restriction enzymes sites were identified using NEBcutter V2.0, an online resource at http://tools.neb.com/NEBcutter2/, for enzymes BmtI and SphI. BmtI and SphI would fragment the vector backbone and the gene insert, respectively (Figure 2.8). The double digest was performed using 1 µl of plasmid DNA, 1 µl of each enzyme, and 2 µl NEBuffer 2, containing 10 mM Tris-HCl, 50 mM NaCl, 10 mM $MgCl_2$, 1 mM Dithiothreitol at pH 7.9, for 3 hours at 37°C. The resulting digested DNA was then selectively amplified using PCR and the amplicons were separated by gel electrophoresis, stained with Ethidium Bromide and photographed under ultraviolet light using a Bio-Rad Gel Documentation System.

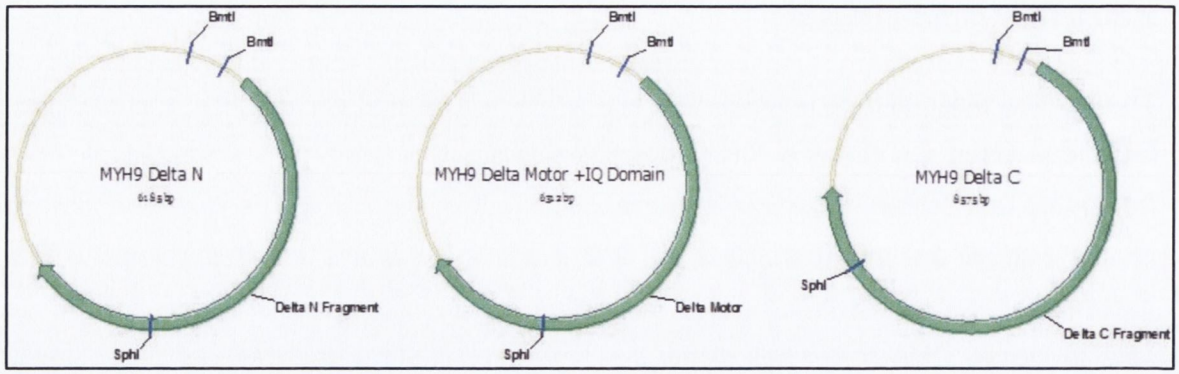

Figure 2.8: Restriction maps of the entry vector PCR8 containing the each deletion mutant gene insert were generated in Vector NTI.

Restriction enzymes sites were identified for enzymes BmtI and SphI, which fragment the vector backbone and the gene insert, respectively.

2.30.9 Recombination into Mammalian Expression Vector

Plasmids with DNA bands of the correct size after double digest were identified and subsequently recombined into high level mammalian expression vector pCMV containing a CCBD death cassette with Chloramphenicol resistance gene, Ampicillin resistance gene on the vector backbone, and an N-terminus FLAG tag cloned in the multiple cloning site using Gateway LR Clonase II enzyme following manufacturer's instructions. This reaction was carried out for each of the three deletion mutants and pENTR-gus was used as a positive control in the Clonase reaction and was included in the kit.

Plasmids containing deletion mutants in the correct orientation as determined by sequencing were then transformed into competent *E. coli* (DH5 Alpha) cells, single colonies were selected and amplified, and the plasmids were purified from bacteria cells (section 2.30.2). The NMHC-IIA-derived fragments were then sequenced using a primer designed for the backbone sequence of the expression vector (pCMV_F1) near the gene insert site (provided by Source BioScience) in order to sequence a fragment of the DNA and confirm plasmids with correct orientation of the gene insert. The sequencing primers used to sequence the FL MYH9 was also used to sequence the deletion mutants (Table 2.1). Sequenced fragments were then aligned to the cDNA of the *MYH9* gene using Vector NTI Align X software to confirm sequence identity.

Plasmids containing the gene insert in the correct orientation were then transformed into competent *E. coli* DH5 Alpha cells and the plasmid was purified from bacteria cells by Qiafilter Plasmid Maxi kit (section 2.30.3). Both the full length and deletion mutant plasmid DNA were used to transfect HEK293 cells (section 2.5.2), and the exogenously expressed proteins were purified by immunoprecipitation method described in the next section.

2.30.10 Expression and Purification of FLAG Fusion Proteins

To ensure adequate protein expression, the cells were harvested 24h and 48 h after calcium phosphate transfection (section 2.5.2) and lysed in RIPA buffer (Appendix 3). The protein was separated by SDS-PAGE (section 2.19) and blotted for anti-FLAG antibody to check for expression of FLAG fusion protein, anti-NMHCIIA for endogenous myosin, and anti-β actin as a loading control.

Once the calcium phosphate transfection was optimised, the FLAG fusion proteins were expressed in ten 15cm plates to yield sufficient protein for future experiments. After 48h,

the cells were harvested and lysed in High Salt (HS) Buffer (Appendix 3) and the protein was immunoprecipitated with anti-FLAG M2 magnetic beads, which are superparamagnetic iron impregnated, 4% agarose beads with an average diameter of 50 µm following manufacturer's instructions. Purified protein was measured by BSA assay and stored at -20°C.

2.31 RACK1 Peptide Array

The purified NMHC-IIA protein was overlaid onto a RACK1 peptide array. This work was done in collaboration with Dr. Patrick Kiely (University of Limerick, Ireland). Peptide libraries of overlapping 18-mer peptides (each peptide was shifted to the right by 4 amino acids) covering the entire sequence of RACK1 were produced by automatic SPOT synthesis as previously described (Kramer and Schneider-Mergener 1998) and synthesised on continuous cellulose membrane supports on Whatman 50 cellulose using Fmoc (N-(9-fluorenyl) methoxycarbonyl) chemistry with the AutoSpot-Robot ASS 222 (Intavis Bioanalytical Instruments) (Frank 2002; Frank and Overwin 1996). The interaction of the spotted RACK1 peptides with recombinant NMHC-IIA was determined by overlaying the cellulose membranes with 10 µg/ml of recombinant protein, as previously described (Kiely et al. 2008).

Briefly, the membrane was bathed in 100% ethanol for 5 min, equilibrated in 1x TBS-T for 10 min, and blocked in 5% milk in 1X TBS with 0.1% v/v Tween-20 (TBS/T) for 1 hour at room temperature. 10µg/ml of recombinant protein or IP-control was added in 1% milk in TBS/T and incubated at 4°C overnight with constant shaking. The following day the membrane was washed three times for 5min with TBS/T and incubated with rabbit antisera (NMHCIIA and FLAG) for 2 hours. The membrane was wash three times in TBS/T and incubated with secondary anti-rabbit antibody coupled with horseradish peroxidase for 1 hour at room temperature with constant shaking. The membrane was washed three times with TBS/T. The membrane was analysed by ECL (section 2.11.6). The overlay was repeated twice.

Once the binding site of NMHC-IIA on the full-length RACK1 array was determined, specific alanine scanning substitution arrays were generated using the same synthesis procedure. In cases where the parent amino acid was alanine, it was substituted for aspartate. The binding of FLAG-NMHC-IIA to the 18-mer single mutated peptides was measured by densitometry and presented as a percentage of the binding of FLAG-NMHC-IIA to the control "parent" peptide. A minimum of a 60% decrease of the binding

compared with the parent peptide was applied to identify amino acids critical for the interaction (Kiely et al. 2009; Kiely et al. 2008).

2.32 Statistical analysis

Quantitative data are presented as mean ± SEM of number (N) of experiments. The statistical significance of differences between experimental groups was assessed with Student's t test. For comparison of two or more groups, *p*-values were calculated using two-way ANOVA. In all cases $p < 0.05$ was considered to be statistically significant. Data was first analysed in Microsoft Excel (2010) and subsequently transferred to Graph Pad Prism (version 4) for statistical analysis and production of graphs.

CHAPTER THREE

Characterisation of RACK1 Expression in Resting and Migrating T Cells

3 Characterisation of RACK1 Expression in Resting and Migrating T Cells

3.1 Introduction

Cell migration is tightly regulated by a complex array of cytoskeletal and signalling molecules that orchestrate cross-talk between diverse signalling pathways to achieve directed cell movement. Lymphocyte migration and adhesion are essential for a functional immune system in the ability to fight disease/infection and maintain homeostasis. The polarisation of migrating T cells is induced by chemotactic and adhesive stimuli. These extracellular signals trigger a coordinated multi-step process required for T cell migration, including the extension of a protrusion in the direction of movement, formation of adhesions that stabilise the leading edge, translocation of the cell body, and disassembly of adhesive points and release of the uropod at the rear of the cell.

Migrating cells have a polarised morphology with an asymmetrical distribution of signalling molecules and the cytoskeleton. Complex interactions between external stimuli cell surface receptors and adhesion molecules initiate signalling pathways that trigger dynamic morphological changes and subsequent motility in T cells (Hogg et al. 2011; Hogg et al. 2004; Smith et al. 2007a). This induction of cell polarisation requires morphological and functional changes resulting in a bipolar asymmetric shape of T cells, which is mediated by the recruitment of surface receptors, signalling complexes, and cellular organelles to discrete areas of the plasma membrane (Vicente-Manzanares et al. 2002). For instance, polarised T cells are characterised by a leading edge, in which chemokine receptors and activated integrins (such as LFA-1) are clustered, and a uropod at the back, in which ICAM-1/3 and CD44 accumulate (del Pozo et al. 1995). Furthermore, directional cell migration is driven by a regulated and polarised turnover of the actin and MT cytoskeleton.

Circulating T cells are covered in short microvilli containing parallel bundles of highly dynamic actin filaments. In order to facilitate tethering and rolling along vessel walls and to minimize nonspecific adhesion, adhesion molecules of different affinity are segregated. Low-affinity L-selectin is located at the tips of the extended microvilli, while receptors involved in tight adhesion, including LFA-1, are excluded from microvilli (Burkhardt et al. 2008; Samstag et al. 2003; Vicente-Manzanares et al. 2009a). The

presence of chemokines displayed on the endothelium triggers rapid microvillar collapse via Rac1-mediated dephosphorylation-induced inactivation of the ezrin/radixin/moesin (ERM) family of actin regulators (Nijhara et al. 2004). In addition, integrin avidity is upregulated through a process involving release of integrins from the cortical actin cytoskeleton (Burkhardt et al. 2008; Vicente-Manzanares et al. 2009a). This leads to the arrest of the lymphocyte on the endothelium and, ultimately, migration across the vascular endothelium (Alon and Feigelson 2002; Shulman et al. 2009).

Smith and colleagues (2007) reported that LFA-1 binding to ICAM-1 was correlated with the induction of actin polymerisation, and the reorganisation of cytoskeletal architecture was essential for T cell adhesion and spreading. The authors also observed that disruption of the actin cytoskeleton inhibits LFA-1-induced T cell migration and adhesion. Moreover, Lub and colleagues (1997) discovered that disrupting the interaction between LFA-1 and the actin cytoskeleton induced clustering of high affinity LFA-1 and strong binding to ICAM-1, subsequently reducing migratory speed and formation of new projections. This would suggest the actin cytoskeleton is involved in both the controlled induction of integrin clustering and release of focal adhesions. This is thought to facilitate rapid migration as older focal adhesion points are continually replaced by new membrane protrusions at the leading edge.

The constant polymerisation and depolymerisation of the actin network is orchestrated by the coordinated functions of numerous actin-binding proteins. These actin-binding proteins facilitate the organisational function of the actin network. One actin-binding protein required for actin network formation is α-actinin, which forms head-to-tail dimers, cross-linking actin filaments into bundles and connecting the actin cytoskeleton to the cell membrane (Khaitlina 2001). Interfering with the LFA-1/α-actinin and α-actinin/actin complexes resulted in a decrease in spreading and rate of migration, suggesting that the intermediate affinity LFA-1 at the leading edge is linked directly to the actin cytoskeleton via α-actinin (Stanley et al. 2008).

Similar to the actin cytoskeleton, the microtubule network is also required for migration in T cells, in that, migration is altered following disruption of the MT cytoskeleton (Gundersen and Cook 1999). In migrating T cells, MTs have been shown to directly interact with the integrin LFA-1 (Moissoglu and Schwartz 2006; Volkov et al. 2001). LFA-1 engagement promotes translocation of PKC βI and PKC δ to the MTOC of the migrating T cell. PKC βI also co-localises with MTs, and PKC βI associates with a LFA-1-cytoskeletal complex enriched with tubulin required for T cell migration (Volkov et al.

1998). Moreover, T cells lacking PKC βI cannot migrate on ICAM-1 or develop a polarised MT array, which indicates that it is required for LFA-1-activated T cell motility. Indeed, re-introduction of PKC β1 to PKC β1-deficient cells restored motility (Volkov et al. 2001). In addition to PKC β1 and δ, integrin activation also induces the activation and translocation to the membrane of PKC ζ, which is necessary for LFA-1-mediated adhesion and migration (Giagulli et al. 2004; Trucy et al. 2006).

In addition to PKC, integrin-mediated activation in T cells induces the translocation of a number signalling molecules involved in regulating polarity. In various cell types and species, the conserved protein complex, termed the partitioning defective (Par), consisting of a core of Par3, Par6, and atypical PKC (PKC ζ), has been shown to regulate cell polarity (Etienne-Manneville et al. 2005; Real et al. 2007). Further implicating their putative role in controlling T cell polarity, the polarity proteins Par 3 and PKC ζ were reported to localise differentially throughout polarised T cells (Gérard et al. 2007; Ludford-Menting et al. 2005). The spatial and temporal regulation of key signalling molecules is crucial in mediating cell adhesion and migration. The polarised distribution of polarity proteins, specifically PKC ζ, suggests the receptor for PKC, RACK1, which targets PKC isozymes to distinct subcellular locations, also redistributes in migrating T cells. Certainly, RACK1 affects the subcellular distribution and function of numerous proteins and, as a result, plays an essential role in regulating signalling pathways in many key biological processes (McCahill et al. 2002). For example, RACK1 has been shown to associate with activated PKC βII in response to phorbol esters and direct its subcellular location (Ron et al. 1999). Moreover, there are no conclusive reports that the subcellular location of RACK1 is controlled by post-translational modifications of RACK1 itself. Little is known about post-translational modifications of RACK1 apart from phosphorylation, which is emerging as an important factor that modulates RACK1 protein-binding. However, no studies have directly shown the effect of phosphorylation on RACK1 translocation. Thus, the movement of RACK1 around the cell is most likely influenced by the particular cohort of proteins associated with RACK1 at any one time.

As cell motility is critical for mounting an effective immune response, understanding the molecular mechanisms underlying T lymphocyte polarisation and migration in normal and aberrant immune response is essential to understanding and developing novel treatments for uncontrolled inflammation, T cell lymphomas, and auto immune disorders. However, the complex nature of signalling cascades in T cell migration and highlights the need for further experiments to decipher the exact role of regulatory mechanisms in T cell migration.

3.2 Objectives

The scaffolding molecule RACK1 has been implicated in regulating adhesion and migration in all cell types investigated thus far. However, examination of RACK1 in the context of regulating integrin-mediated migration in T cells has been widely overlooked. Several polarity complex proteins, including PKC ζ, have been implicated in T cell migration and translocate to the leading edge upon integrin activation. As RACK1 is known to interact with members of the PKC family, it was hypothesised that induction of LFA-1 also induced RACK1 translocation. Therefore, the aim was to characterise the expression of RACK1 in resting and LFA-1-stimulated T cells. By employing the *in vitro* 2D model of LFA-1-mediated T cell migration described in section 2.8, a polarised migratory phenotype was induced in T cells. This model allows the investigation of protein subcellular localisation and any changes in distribution in response to LFA-1 activation in both the HuT78 T cell line and primary T cells. Furthermore, whether RACK1 is indeed functionally required for chemokine-induced T cell polarisation is unknown. Therefore, a chemokine-induced cell polarisation model described in section 2.12 was also employed. Stimulation with SDF-1α stimulation triggers cytoskeletal remodelling and a polarised morphology enabling the examination of proteins implicated in regulating cell polarity. Recent advances in imaging technology have begun to uncover when and how the cytoskeleton, signalling molecules, and adhesion molecules are asymmetrically distributed during migration. Therefore, high resolution laser scanning confocal microscopy in conjunction with immunocytochemistry was used to examine the subcellular localisation of RACK1 in resting and polarised migrating T cells. Furthermore, because the localisation of the cytoskeletal network is well documented in LFA-1-stimulated cells (Freeley et al. 2010; Verma et al. 2009), RACK1 expression was explored in association with cytoskeletal elements and candidate signalling molecules. Identifying proteins associated with RACK1 in resting and migrating cells will further elucidate the function of RACK1 in integrin-mediated immune cell migration.

In this chapter, there were four objectives:

1.) Characterise the expression of RACK1 in resting and LFA-1-induced migrating T cells.
2.) Investigate co-localisation of RACK1 with the actin and MT cytoskeleton in LFA-1-induced and chemokine-stimulated polarised migrating T cells.
3.) Investigate association of RACK1 with candidate polarity proteins during LFA-1-mediated migration in T cells.

4.) Determine the functional implications of these interactions by suppressing RACK1 expression.

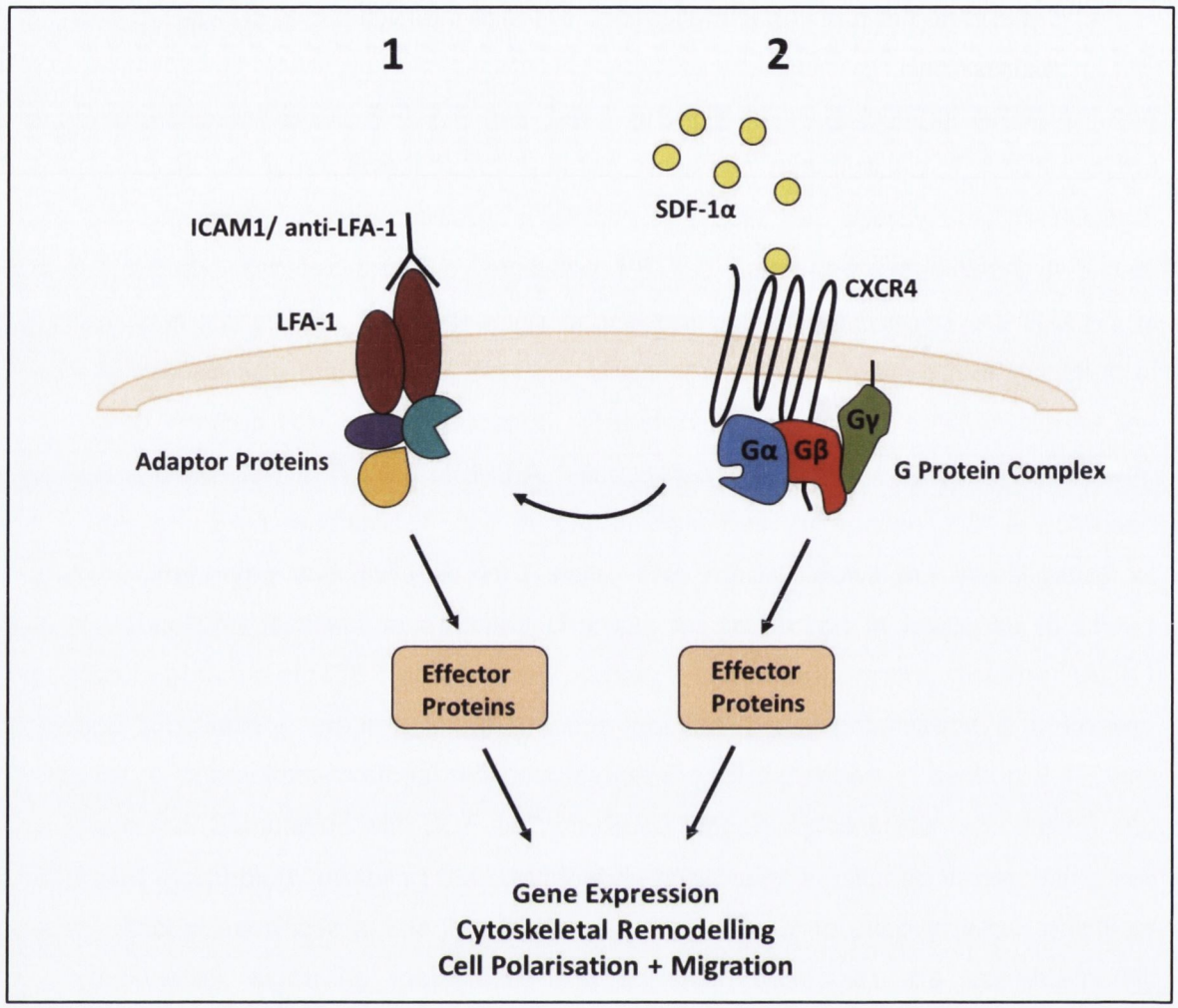

Figure 3.1: Induction of T cell Polarisation and Migration.

T cell polarisation and migration was induced by (1) haptokinetic migration: LFA-1 integrin activation by native ligand ICAM1 or anti-LFA-1 or (2) chemokinetic migration: CXCR4 chemokine receptor activation by SDF-1α triggering signalling pathways resulting in cytoskeletal remodelling and cell migration.

3.3 Results

3.3.1 RACK1 Translocates to the Leading Edge of LFA-1-Induced Migrating T Cells

The subcellular localisation of RACK1 in resting and LFA-1-induced migrating T cells was investigated by immunocytochemistry (section 2.23.2) using fixed and live cell fluorescent microscopy. Fixation and immunofluorescent staining techniques were optimised for characterising RACK1 expression in T cells at 63X by confocal microscopy and at 10X and 20X by pseudo-confocal microscopy on the In Cell Analyser 1000. The first objective was to investigate the subcellular localisation of RACK1 in resting and LFA-1-induced migrating T cells through fixed and live cell analysis. The results from immunofluorescence analysis of RACK1 expression indicate that RACK1 translocates from a cytosolic, peripheral distribution in resting cells to the leading edge of LFA-1-stimulated migrating T cells (Figure 3.2A). RACK1 is also localised at the rear of the trailing uropod in polarised cells. This anterior/posterior distribution was induced in as little 20 min of LFA-1 stimulation and was consistent in all polarised cells. Furthermore, RACK1 was completely omitted from nuclear regions and the neck of the polarised cell as confirmed by high resolution confocal microscopy.

The expression of RACK1 in primary T cells was also examined to verify the results obtained from the T lymphoma cell line. LFA-1-stimulated or unstimulated PBTLs were PFA-fixed and stained with RACK1-antibody and Hoechst nuclear stain. The results from expression analysis in primary cells confirmed the subcellular localisation data obtained in HuT78 T cells, in that, RACK1 displayed a resting peripheral distribution and translocated to the leading edge of polarised cells upon integrin activation (Figure 3.2B). The results obtained from primary T cells validated the use of HuT78 T cells for analysis of RACK1 in further immunocytochemistry experiments.

In addition, transfection of cells with EGFP-RACK1 construct was optimised to confirm the subcellular localisation of RACK1 in T cells through fixed and live cell imaging by laser scanning confocal microscopy. RACK1-specific expression of EGFP-RACK1 was compared to the negative pmaxGFP control, which yields a non-specific expression pattern. Expression of EGFP-RACK1 showed a very similar subcellular distribution as the immunofluorescent staining in resting and LFA-1-stimulated migrating T cells (Figure 3.2C). As expected, the leading edge localised RACK1-specific EGFP was very different compared to the EGFP-control, which exhibited a non-specific localisation generally

distributed throughout the cell (Figure 3.2D). Expression of EGFP-RACK1 indicated RACK1 was also present in the region behind the nucleus in the neck of the cell in addition to the leading edge and trailing uropod. This may be artefact due to an over-abundance of RACK1 in the cell with the combined exogenous expression of the EGFP-RACK1 construct and endogenous RACK1. Indeed, the endoplasmic reticulum and golgi apparatus, which are responsible for the translation and assembly of newly expressed proteins, are located in this region. Nonetheless, the results from the expression of EGFP-RACK1 clearly indicate the enrichment of RACK1 in the forward extending lamellipodia and uropod in LFA-1-polarised migrating T cells.

While live cell imaging results were acquired with a laser scanning confocal microscope, the exposure level of the laser to obtain quality images resulted in rapid cell death. It may have been possible to image the cells using a spinning disc confocal microscope. Unfortunately, high resolution live cell imaging of RACK1 was not possible due to limited access of this type of fluorescent microscopy. Nonetheless, the cells expressing EGFP-RACK1 were imaged at a lower resolution at 20X on the IN Cell semi-confocal microscope. The results indicated that RACK1 subcellular localisation is very dynamic and continually recycles around the periphery of resting cells (supplementary videos). Certainly the live cell analysis verified the dynamic polarised redistribution of RACK1 in response to LFA-1 stimulation during directional migration.

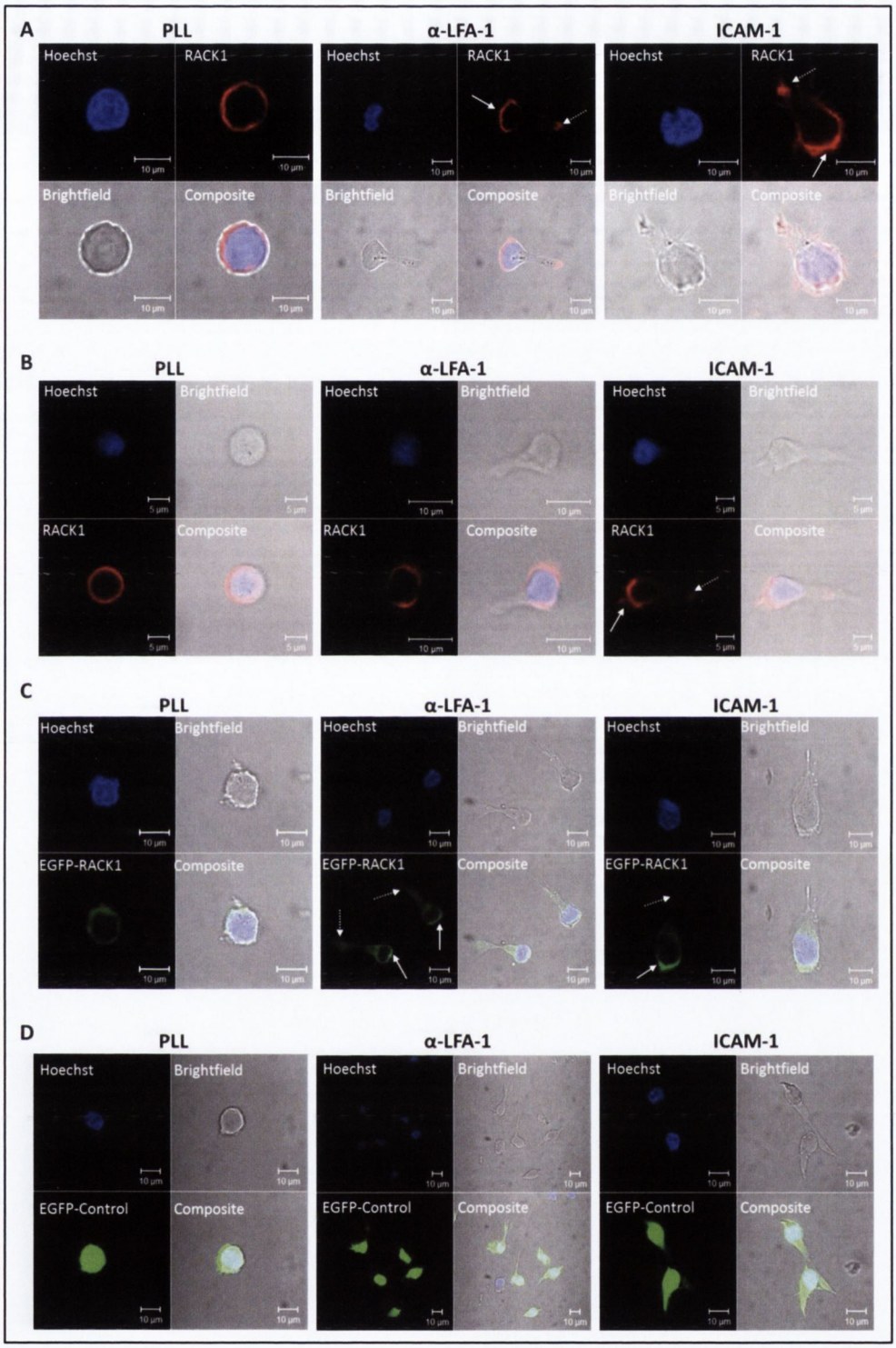

Figure 3.2: Expression of RACK1 in resting and LFA-1-mediated migrating T cells.

(A) IF staining of RACK1 in resting and LFA-1-induced migrating HuT78 T cells. (B) IF staining of RACK1 in resting and LFA-1-induced migrating primary T cells. (C) Expression of pEGFP-RACK1 and (D) EGFP-control in fixed resting and LFA-1-induced migrating HuT78 T cells. All images were acquired by confocal microscopy with 63X objective. Solid arrows indicate the leading edge and dashed arrows indicate the trailing uropod of the polarised cell.

3.3.2 RACK1 Partially Associates with Actin and MT Cytoskeleton in T Cells

Actin was stained with the fungal-derived phallotoxin Phalloidin, which binds filamentous actin, originally identified by Heinrich Wieland in the 1930s (Wieland and Faulstich 1978). As it prevents actin depolymerisation and is toxic to the cell, it cannot be used for live cell analysis. However, a fluorescent conjugate of the toxin is readily used in fixed cell analysis for visualising individual actin filaments *in vitro* (Cooper 1987). First, the *in vitro* LFA-1-mediated migration assay used to induce the phenotypic polarised morphology of migrating T cells was validated through IF staining of the actin and MT cytoskeleton. The polarised phenotype of migrating T cells was characterised by broad forward spreading lamellipodia with extending filopodia microspikes and a trailing uropod. This polarised phenotype is in accordance with independent research on *in vitro* induction of migration in T cells by LFA-1 activation (Freeley et al. 2010; Porter et al. 2002; Smith et al. 2007a; Smith et al. 2005).

Here, in accordance with previous data from colleagues, filamentous actin was localised to the plasma membrane and microvillar extensions in resting cells. RACK1 displays a peripheral ring-like appearance and was completely excluded from the actin-rich microvilli. Integrin activation by anti-LFA-1 or ICAM-1 induced translocation of RACK1 to the leading edge where actin undergoes active polymerisation in the formation of new protrusions in the migrating cell. RACK1 appeared to localise immediately behind the F-actin-rich front (indicated by white arrow in Figure 3.3A). RACK1 was primarily localised in the lamellipodium or region in front of the nucleus; although, a more detailed evaluation revealed the scaffolding protein was also present in some extending filopodia in association with F-actin.

RACK1 did appear to partially co-localise with the MT network in both resting and LFA-1-activated migrating T cells. Both RACK1 and alpha-tubulin have a membrane-associated peripheral distribution in resting cells, and RACK1 co-localised with a subset of tubulin at the leading edge in migrating cells. RACK1 and alpha tubulin associated at the base of extending filopodia, with RACK1 localised to the growing ends of MTs (indicated by white arrow in Figure 3.3B). Further evaluation of the expression pattern indicated RACK1 localised to the region where the plus ends of MT spindle and polymerised actin converge at the leading edge. While the MT spindle extends the entire length of cell, it originates from the MTOC. RACK1 did not appear to localise to the MTOC or cytosolic mitotic spindle as RACK1 association with tubulin was limited to the plasma membrane.

Interestingly, both RACK1 and the MT network were excluded from the nuclear region. Taken together, these data indicated RACK1 localises to the junction between the growing ends of polymerised MTs and filamentous actin at the leading edge of the polarised migrating T cell.

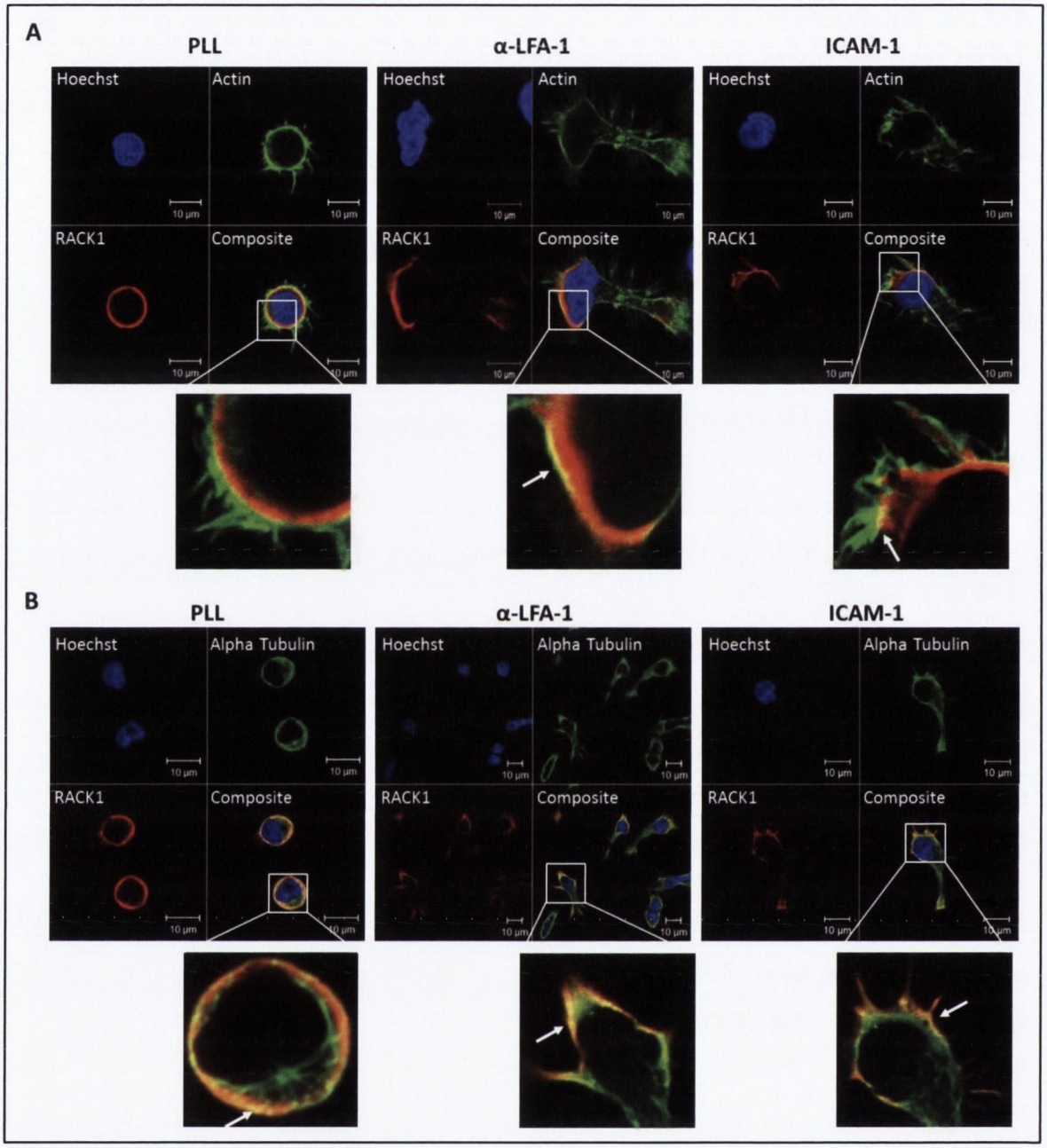

Figure 3.3: IF Staining of RACK1 and actin and MT cytoskeleton in resting and in LFA-1-induced migrating T cells.

(A) High resolution microscopy of HuT78 T cells stained with RACK1-specific antibody and TRIC-conjugated Phalloidin for F-actin. White arrows indicate RACK1 localisation behind the actin-rich front. (B) High resolution microscopy of HuT78 T cells stained with RACK1- and alpha tubulin-specific antibody. White arrows indicate RACK1 localisation at the growing ends of MTs. All images were acquired by confocal microscopy with 63X objective.

3.3.3 Investigation of RACK1 in Association with Candidate Cytoskeletal Associated Elements

In order to further examine the putative role in actin reorganisation, the localisation of RACK1 with candidate cytoskeletal-associated proteins in T cells was assessed by immunocytochemistry. Due to the partial co-localisation of exhibited by RACK1 with MTs, the association of RACK1 was examined with acetylated alpha tubulin, which is associated with stable MT structures (Westermann and Weber 2003). In addition, because RACK1 appeared to localise behind the filamentous actin front, its association was also examined with proteins implicated in actin organisation, including the actin-binding protein profilin, the actin-associating protein PDLIM2, and the actin cytoskeletal structural protein β spectrin.

Despite association with both the actin and MT cytoskeleton in migrating T cells, RACK1 did not appear to co-localise strongly with any of the candidate cytoskeletal elements, including MT acetylated, which localises to stabilised MT tubulin, or the actin-bundling protein profilin (data not shown). The next candidate protein was PDLIM2, an actin-associated protein belonging to a subfamily of proteins containing a PDZ and a LIM domain (Torrado 2004; Xiao et al. 2011). PDZ domains are reported to have multifunctional protein–protein interaction motifs and are involved in the assembly of protein complexes and have been shown to be associated with the plasma membrane (Fanning and Anderson 1999; Harris and Lim 2001; Hung and Sheng 2002). While, LIM domains are cysteine-rich zinc finger motifs normally found in transcription factors, kinases, and scaffolding proteins. LIM domain-containing proteins have been reported to have vital roles in cytoskeletal organisation and cell development (Bach 2000; Dawid et al. 1995; Kadrmas and Beckerle 2004). In addition, it was discovered that many proteins containing the LIM domain in their C-terminal, such as PDLIM2, have functional roles related to the cytoskeleton and signal transduction pathways (Khurana et al. 2002). Moreover, a recent study reported that PDZ and LIM domain-containing proteins interact with and are essential to the normal development and function of the actin cytoskeleton (Pomies et al. 2007). PDLIM2 has also been reported to directly interact with actin crosslinking components, such as α-actinin, filamin A, and myosins in corneal and lung cell extracts (Torrado 2004). The authors proposed such interactions suggest a role for PDLIM2 in maintaining the architecture and mechanics of the actin network. Therefore, PDLIM2 may act as an adapter protein to multiple mechanical components, providing stability and fidelity to the actin cytoskeleton. In addition, PDLIM2 was recently reported

as an Insulin-like Growth Factor (IGF)- regulated protein that promotes cell adhesion and migration, while suppressing anchorage-independent growth in non-transformed and cancerous cell lines (Loughran et al. 2005). In addition, the study determined that PDLIM2 co-localises with the actin structural protein alpha-actinin and β1-integrins at the distal end of stress fibres at focal adhesions in MCF-7 breast carcinoma cells. Due to its putative role in cytoskeletal remodelling and integrin adaptor protein functions and association with the plasma membrane, it was hypothesised LFA-1 activation may also induce PDLIM2 translocation to the leading edge in migrating T cells. Thus, the subcellular distribution of the actin-associated scaffolding protein PDLIM2 was assessed in relation to RACK1 in resting and migrating T cells. Somewhat surprisingly, PDLIM2 displayed an even distribution in both resting and integrin-activated polarised T cells and did not co-localise with RACK1. Moreover, PDLIM2 did not strongly associate with filamentous actin in the lamellipodia or extending filopodia in polarised migrating T cells. The actin-associated scaffolding protein did not appear to be enriched at the plasma membrane in either resting or polarised migrating cells, but it did localise to the nuclear membrane.

β Spectrin is a cytoskeletal protein that forms α- and β-spectrin heterotetramers form as part of a submembrane meshwork lining the intracellular side of the plasma membrane. It is required for the maintenance of the structure of the cytoskeleton and the integrity of the plasma membrane (Bennett and Gilligan 1993). The distribution of β Spectrin in the plasma membrane has also been shown to influence the fluidity of the lipid membrane (Langner et al. 1992). β Spectrin is part of the spectrin family of proteins, which also includes the actin-associated protein alpha-actinin. All of the family members consist of spectrin repeats, which are important interaction sites for the assembly of multi-protein structures involved both in cytoskeletal architecture and large signal transduction complexes (Djinovic-Carugo et al. 2002). In addition, the β Spectrin protein is also comprised of protein-protein and membrane interaction motifs, as well as a PH domain, which are known to bind phosphoinositides, such as PI3K, and drive stimulus-dependent membrane recruitment (Broderick and Winder 2005; Lemmon et al. 2002). RACK1 has been shown to concomitantly engage both PKC and β Spectrin, thereby mediating the interaction between PKC and its substrate (Rodriguez et al. 1999). Although this interaction was demonstrated by *in vitro* experiments with RACK1 and the recombinant PH domain of β Spectrin, no future studies have examined the functional implications of this association. PKC and β Spectrin have also been reported to translocate to TritonX-100-insoluble cytoplasmic aggregates distant from the plasma membrane in activated

lymphocytes (Di et al. 1997). The stimulus-dependent subcellular translocation of PKC and β Spectrin has not yet been studied in lymphocytes. Therefore, it was hypothesised RACK1 may be recruited to the plasma membrane in association with PKC and β Spectrin in response to LFA-1-induced T cell migration.

IF staining indicates β Spectrin has an even cytoplasmic distribution in resting cells but has an enriched distribution at the leading edge in association with RACK1. However, due to suboptimal staining for β Spectrin despite a number of optimisation methods for fixation and staining, suboptimal staining for β Spectrin precluded further analysis on association with RACK1 in T cells. Certainly, the immunocytochemistry experiment should have been repeated using a different commercial antibody as well as determination of association in T cells by co-immunoprecipitation had time permitted.

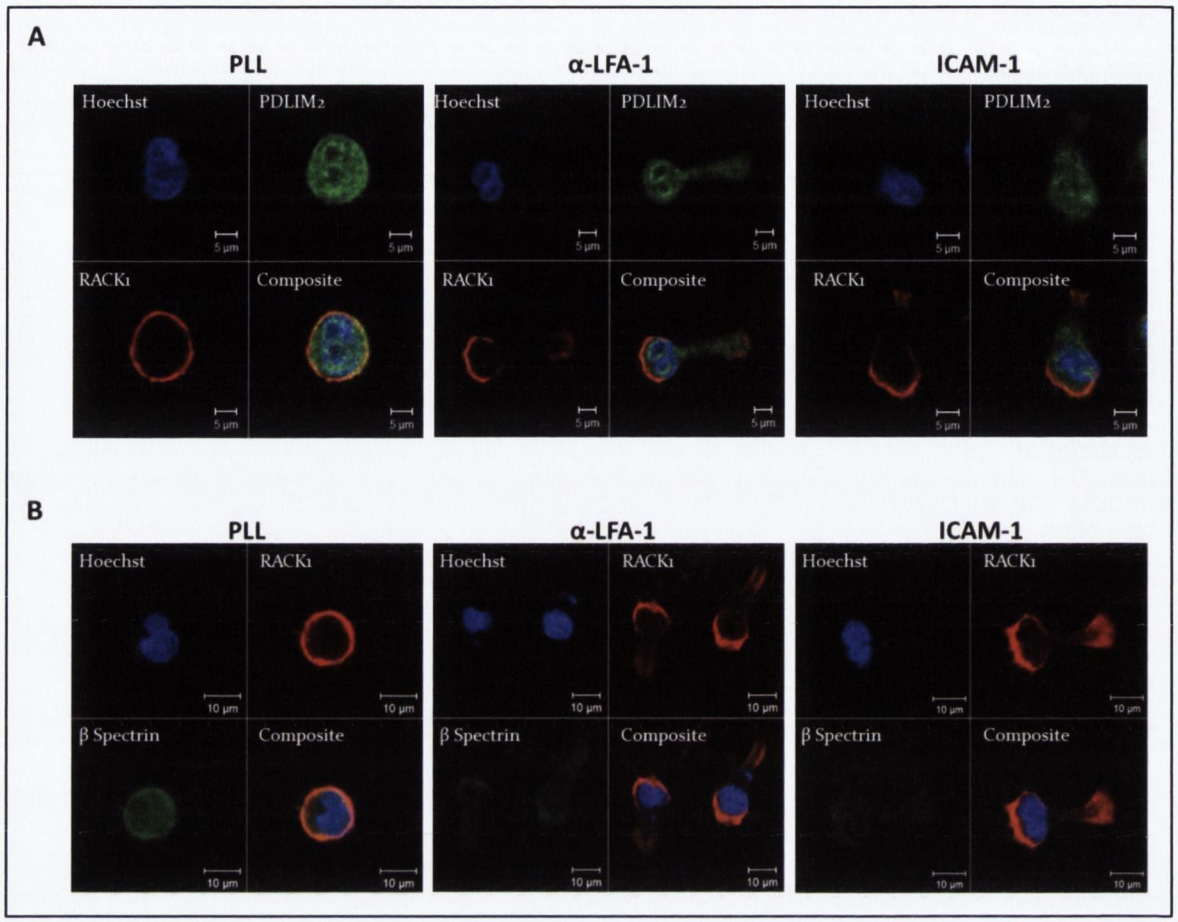

Figure 3.4: IF staining of RACK1 and putative RACK1-associated proteins in resting and in LFA-1-induced migrating T cells.

High resolution confocal microscopy of HuT78 T cells stained with RACK1- and PDLIM2-specific antibody (A) and β Spectrin-specific antibody (B) in resting and in LFA-1-induced migrating T cells. All images were acquired by confocal microscopy with 63X objective.

3.3.4 SDF-1α Activation Induces Translocation of RACK1 to the Leading Edge of Migrating T Cells

SDF-1α binds to its cognate cell surface G protein-coupled receptor CXCR4 and induces cytoskeletal reorganisation by Rho GTPases, including RhoA, Rac1, and CDC42, allowing the cell to infiltrate inflamed tissues (Kucia et al. 2004; Patrussi and Baldari 2008; Ridley 2011) and is a good model for *in vitro* cell polarisation. RACK1 has a putative role in directing signal transduction and may act as a scaffold for the formation of a multi-protein complex involved in propagating the signal induced by SDF-1α receptor binding. Whether RACK1 translocates to the leading edge of chemokine-induced polarised T cells is still unknown.

The following objective was to examine the expression of RACK1 in SDF-1α-activated T cells in association with the actin cytoskeleton/microtubule network reorganisation. HuT78 T were activated with SDF-1α for 5 min, 20 min, or 60 min or left untreated. The cells were then fixed, permeabilised, and stained in solution for actin, alpha tubulin, and RACK1 and analysed by high resolution confocal microscopy. SDF-1α activation rapidly induces F-actin accumulation at the leading edge and reorientation of the MT spindle and MTOC behind the nucleus of polarised T cells, consistent with previous studies in neutrophils and T cells (Ratner et al. 1997; Takesono et al. 2010; Thelen and Stein 2008; Vicente-manzanares et al. 2002; Volkov et al. 2001).

RACK1 distributed towards the periphery of the cell in unstimulated T lymphocytes but was not strongly co-localised with F-actin. Stimulation of the cells with SDF-1α resulted in a striking redistribution of RACK1 to the leading edge of the cell where it localised in the lamellipodia and behind the actin-rich front (Figure 3.5A). Formation of pseudopods begins to form and cell budding, as indicated by actin polymerisation, in as little as 5 min after activation by SDF-1α. By 1 hour after activation by SDF-1α, RACK1 had translocated to the leading edge of migrating cells behind active actin polymerisation. This re-distribution of RACK1 to the leading edge was observed as early as 5 minutes after SDF-1α stimulation. By 20 min after stimulation, RACK1 displayed an anterior-posterior distribution similar to LFA-1-polarised migrating cells and was observed for up to 1h after SDF-1α stimulation. Similar to integrin activated cells, RACK1 also localised to the trailing uropod in SDF-1α activated cells.

In addition, RACK1 interaction with the microtubule network was also analysed in chemokine-induced migrating HuT78 T cells by immunocytochemistry. Within the first 5

min after SDF-1α stimulation, there appeared to be no change in the distribution of the microtubule network as both RACK1 and alpha tubulin remain in a peripheral distribution. However by 20 min, the cell assumes the polarised morphology phenotypic of a migrating T cell. By 1hr, the MTOC had reoriented behind the nucleus, and the once resting peripheral tubulin distribution is transformed into a microtubule spindle spanning the length of the newly polarised cell. A subset of RACK1 simultaneously translocated to the leading edge of the polarised cell and partially co-localises with alpha tubulin. RACK1 and alpha tubulin appeared to be in association during both resting and polarised states (Figure 3.5B). The phenotype of SDF-1α activated HuT78 T cells as well as the subcellular localisation of the actin and microtubule cytoskeleton and RACK1 has now been characterised.

Nevertheless, with all T lymphoma cells, there is a caveat to using HuT78s for a chemokine-induced polarisation assay. For instance, as described in section 1.12, actin polymerisation is localised to the leading edge forming an 'actin cap' in chemokine-induced polarised T cells. It was noted that induction of polarisation was achieved in response to SDF-1 in several cells; however, the actin-rich cap was not readily formed in all cells in the microscopic field. This may be due to the HuT78 T cell line, which, unlike other Sezary Syndrome cells from cutaneous T cell lymphomas, expresses CD26. This cell surface receptor binds and cleaves SDF-1α, thereby suppressing subsequent chemokine stimulation and chemokine-induced migration (Narducci et al. 2006). Therefore, the chemokine-induced polarisation assays were repeated in primary cells, which have been shown to more readily respond to SDF-1α activation *in vitro* assays and more accurately represent chemokine activation *in vivo*.

In order to confirm the chemokine-induced polarised distribution of RACK1, the experiment was repeated in PBTLs. Stimulated PBTLs formed an actin-rich front at the leading edge of the cells in response to SDF-1 after 5 min and the majority of cells in the microscopic field were polarised by 20 min (Figure 3.5C). The PBTLs are much smaller compared to HuT78 cells and do not display an extended uropod or 'tadpole shape'. Indeed, RACK1 translocates to the leading edge in association with the 'actin-cap'. In addition, the MT spindle was reorganised and the MTOC was reoriented behind the nucleus as observed in HuT78 cells. Again, RACK1 did not appear to strongly co-localise with the MT network besides the growing ends of the MT network at the leading edge (Figure 3.5D). These data suggest that RACK1 may be involved in regulating cell polarity in both integrin-activated and chemokine-induced polarised T cells.

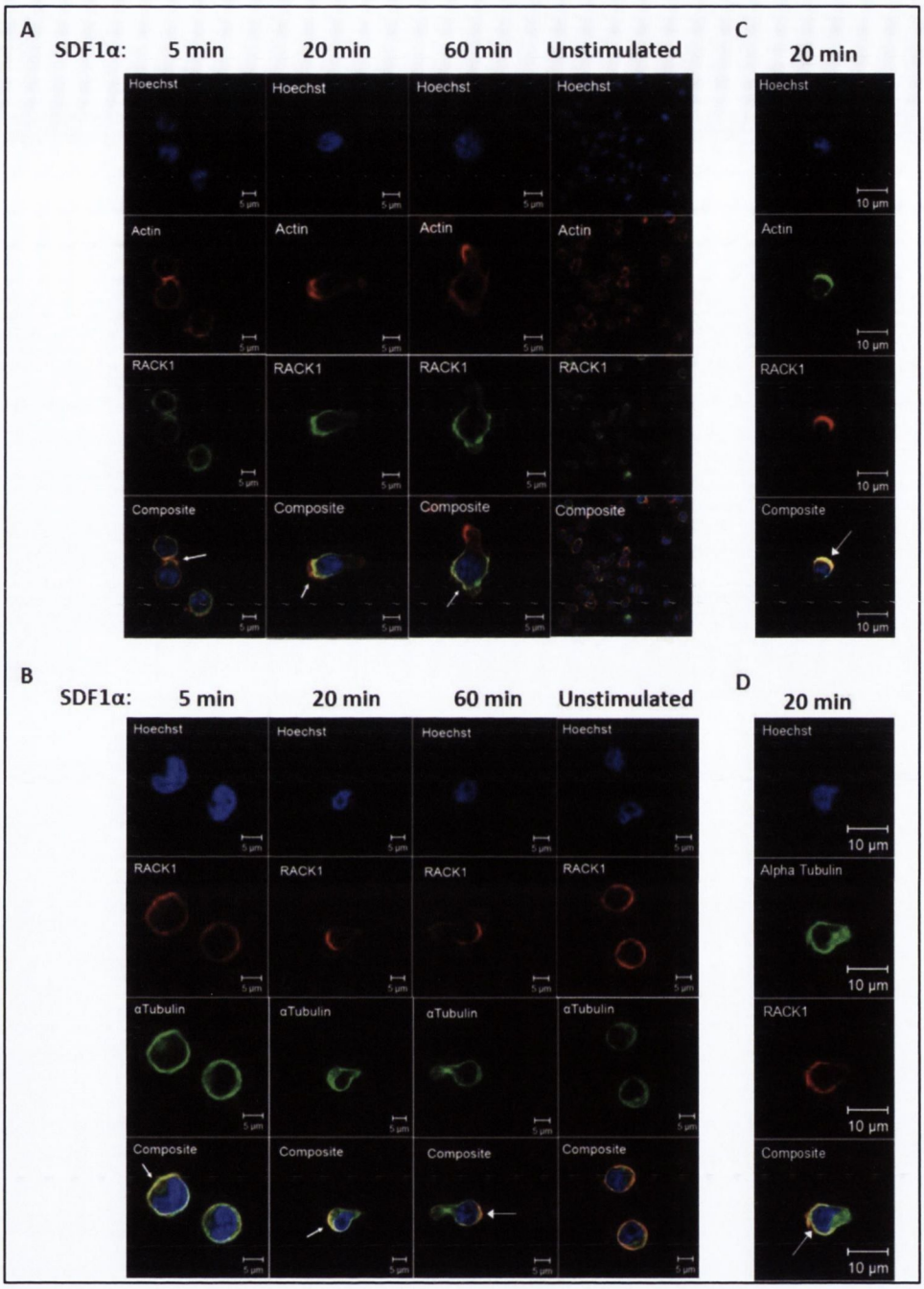

Figure 3.5: RACK1 translocates to the leading edge in association with F-actin and the growing ends of polymerised MTs.

(A) High resolution microscopy of HuT78 cells stimulated with SDF-1α for indicated time points or left unstimulated. Cells were stained with RACK1-specific antibody and TRITC-conjugated Phalloidin. (B) Same as A, but cells stained with RACK1-and alpha tubulin-specific antibody. (C) Primary T cells were stimulated with SDF-1α for 20 min and stained with RACK1-specific antibody and TRITC-conjugated Phalloidin. (D) Same as C, but cells stained with RACK1-and alpha tubulin-specific antibody. All images acquired by confocal microscopy with 63X objective. White arrows indicate areas of co-localisation.

3.3.5 RACK1 Associates with Polarity Regulator Par 3 in Integrin-activated Polarised T cells

The preponderance of evidence implicating RACK1 in regulating cell migration and the polarised distribution of RACK1 in LFA-1-stimulated migrating cells suggests a role in cell polarity. The polarity protein Par 3 has been implicated in the induction of cell polarisation required for such process as cell division and migration; however, its role in immune cell migration has yet to be fully understood. Recent evidence indicates that Par 3 also translocates to the leading edge of chemokine-induced polarised T cells (Gérard et al. 2007). Thus, the next objective was to determine the subcellular localisation of Par 3 in association with RACK1 in integrin-activated migrating T cells.

Unfortunately, the Par 3-specific antibody from Zymed Laboratories (Invitrogen, USA), which has been used to detect Par 3 in other cell types (Gérard et al. 2007), yielded a cytosolic granular appearance in both resting and migrating T cells. Optimisation for immunocytochemistry was performed using different antibody concentration and fixation techniques but was unsuccessful. Therefore, the results suggest that either Par 3 is evenly distributed throughout the cell and the localisation is not altered in the polarised state or the staining is non-specific. The speckled appearance of the immunofluorescence staining as well as lack of co-localisation with RACK1 would suggest that the antibody staining in non-specific. However, this commercially available antibody has been employed in previous published studies on the expression of Par 3 in T lymphoma cells, and the data suggest the antibody is specific to Par 3. Because of the key role Par 3 plays in cell polarity, it is pertinent to characterise Par 3 expression in polarised migrating T cells in response to integrin activation.

Therefore, while the immunofluorescence co-stain did not yield optimal staining results for Par 3, it was still possible to ascertain an interaction between RACK1 and Par 3 by co-immunoprecipitation (co-IP). The results indicate that in both resting and migrating T cells lysed with NP40, both isoforms of Par 3 (predicted molecular weights 150 and 180 kDa) co-immunoprecipitated with RACK1. However, the 180 kDa isoform of Par 3 that associated with RACK1 was enriched in the migrating state. Interestingly, only the 150 kDa isoform is detected in the resting and migrating whole cell lysates. Both the immunofluorescence co-stain and co-immunoprecipitation results are shown in Figure 3.6.

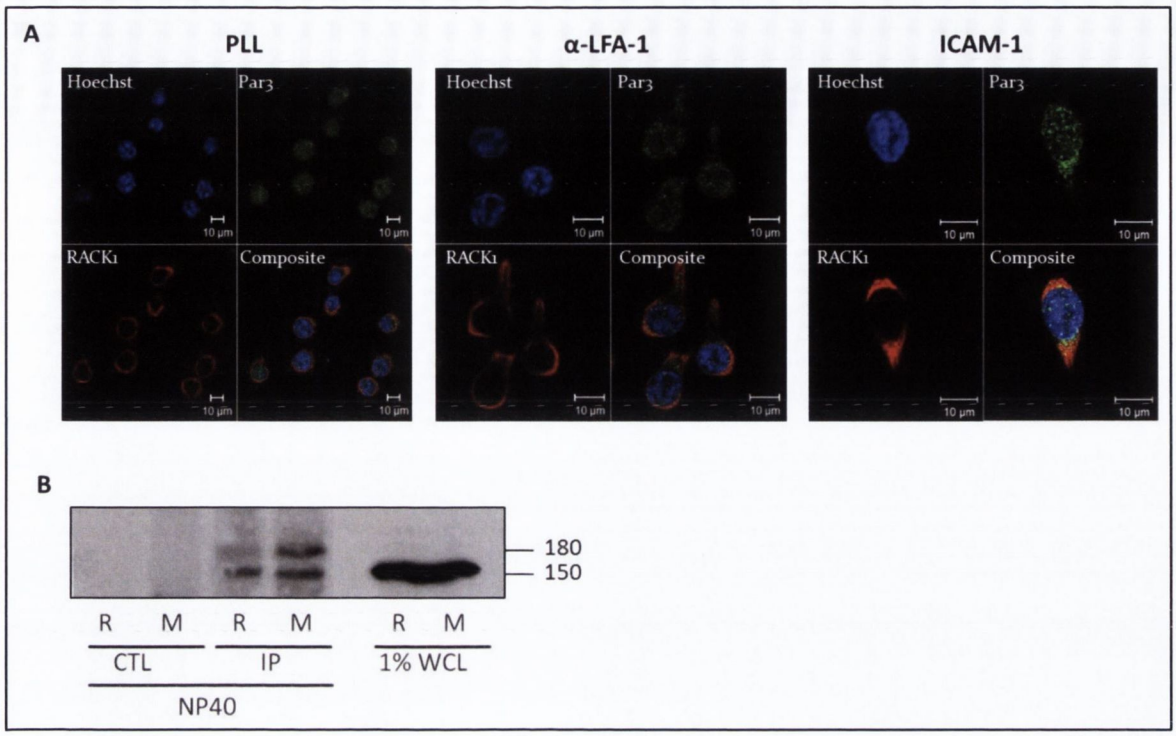

Figure 3.6: Par3 does not have a polarised localisation in migrating T cells but does associate with RACK1 in resting and LFA-1-mediated migrating T cells.

(A) High resolution confocal microscopy of HuT78 T cells stained with RACK1- and Par 3-specific antibody. All images acquired by confocal microscopy with 63X objective. (B) Cells were lysed with cell lysis buffer containing 1%NP40 and RACK1-associated complexes were immunoprecipitated with RACK1-specific antibody and immunoblot probed with Par 3 antibody.

3.3.6 RACK1 Associates with PKC ζ at the Leading Edge of LFA-1-induced Migrating T cells

Due to its role in directing the subcellular localisation of activated PKC, the next study sought to investigate which PKC isoforms associate with RACK1 in LFA-1-stimulated migrating T cells. Our group has previously determined the PKC isoforms expressed in lymphocytes. In addition, through the use of isoform-specific antibodies and GFP constructs, the subcellular localisation of the PKC isoforms expressed in lymphocytes was identified, including PKC α,β,δ, ε, ζ, η, and θ, following LFA-1 activation. Our group has previously demonstrated PKC βI associates with MTs in LFA-1-induced migrating T cells (Volkov et al. 1998), while PKC ζ, an established polarity protein (Real et al. 2007), has been reported to redistribute to the leading edge in association with the actin-rich front in SDF-1α-induced polarised T cells (Gérard et al. 2007). Moreover, Furthermore, none of the other PKC isozymes display a distribution pattern similar to RACK1 in T cells; therefore, PKC βI and ζ were examined in association with RACK1 in polarised migrating T lymphocytes.

In accordance with previous observations (Volkov et al. 1998), PKC β1 translocated from a resting cytosolic distribution to the MTOC (Figure 3.7A. However, a significant portion of the PKC isozyme remained distributed throughout the cell. As PKC β1 does not translocate to the leading edge, RACK1 does not strongly co-localise with the PKC isoform. The atypical PKC ζ translocated to the leading edge in association with RACK1 in polarised migrating T cells (Figure 3.7B). Moreover, while RACK1 was primarily localised to the forward extending lamellipodia, PKC ζ was distributed throughout the cell but enriched at the leading edge. RACK1 appeared to associate with a small subset of PKC ζ in resting cells, and upon integrin activation, both proteins translocated to the leading edge.

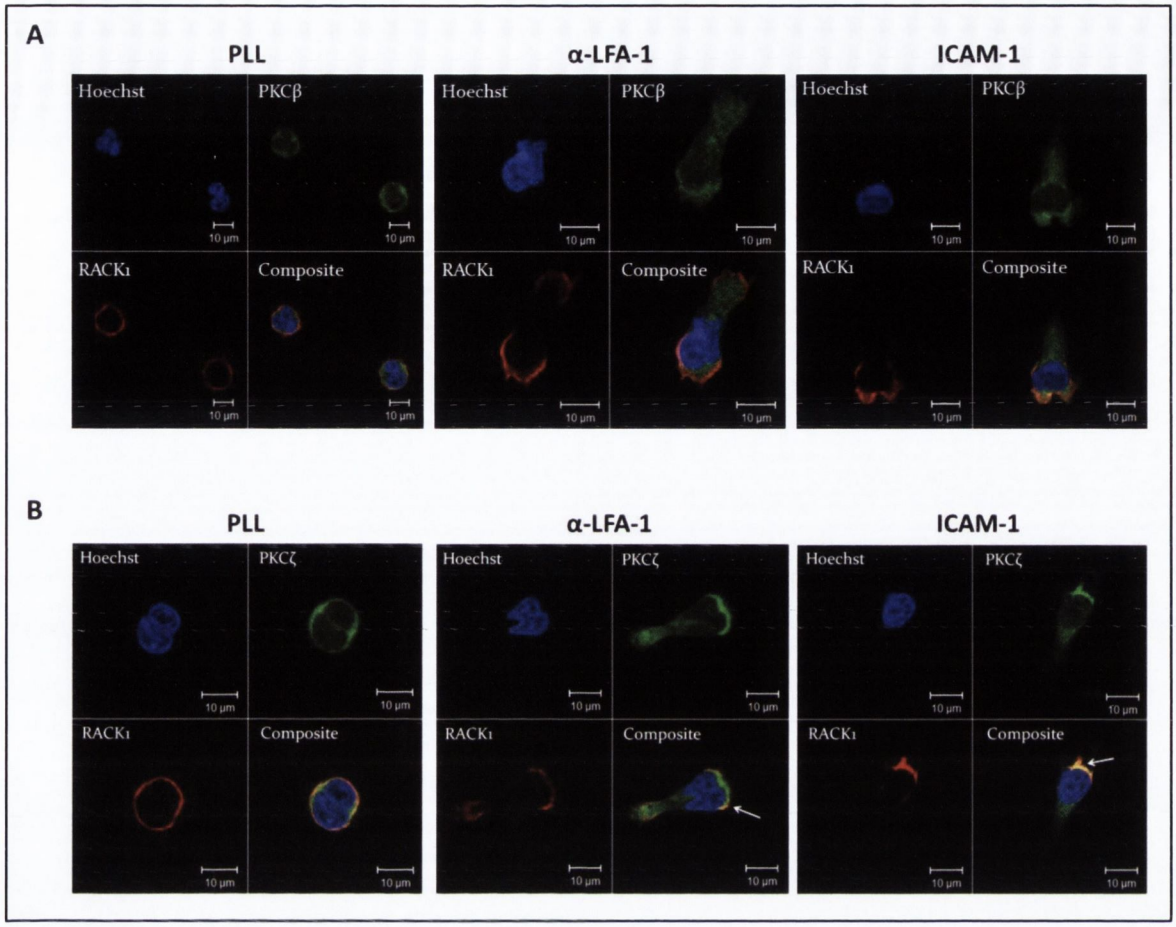

Figure 3.7: IF Staining of RACK1 with PKC isozymes in resting and LFA-1-induced migrating T cells.

(A) High resolution confocal microscopy of HuT78 T cells stained with RACK1- and PKC β1-specific antibodies (A) and with RACK1- and PKC ζ-specific antibodies (B). All images were acquired by confocal microscopy with 63X objective. White arrow indicates RACK1 and PKC ζ co-localisation at the leading edge of the migrating cell.

3.3.7 Suppression of RACK1 Affects PKC ζ Distribution and Recruitment to Leading Edge in T cells

Due to strong association exhibited by RACK1 and PKC ζ at the leading edge of polarised migrating T cells, it was hypothesised that RACK1 may target PKC ζ to the leading edge upon integrin activation. RACK1 was depleted by siRNA and any change in the subcellular distribution of PKC ζ was assessed by high content image analysis and confocal microscopy. HuT78 T cells were transfected with RACK1-specific or non-targeting control siRNA and stimulated with rhICAM-1 and divalent cations to induce integrin LFA-1 activation or unstimulated. The cells were stained with IF-conjugate antibodies against PKC ζ and RACK1. The fluorescence intensity of RACK1 was measured on the IN Cell Analyzer automated microscope, and RACK1-deficient had a significant decrease in fluorescence intensity of RACK1 compared to control cells. Knockdown of RACK1 expression compared to control cells was confirmed by Western Blot of whole cell lysates probed for RACK1 and validated the use of measuring fluorescence intensity to determine knockdown (Figure 3.8A and C). Results from the immunoblot indicated approximately 90% transfection efficiency, while measuring the IF intensity yielded slightly lower transfection efficiency at approximately 70%. This may have been due to background intensity. Changes in the distribution of PKC ζ was measured by Cell Intensity Coefficient of Variance (CV) in RACK1-deficient and control cells. Cells that display homogenous staining of a particular protein or stain have low Cell Intensity CV values, while cells with localised or polarised distribution of a particular protein or stain have higher Cell Intensity CV values. Following LFA-1 activation, the Cell Intensity CV of PKC ζ is increased representing an increase in the variation of its subcellular distribution. RACK1-deficient T cells displayed a significant decrease in Cell Intensity CV of PKC ζ in polarised migrating cells compared to the control cells (Figure 3.8B). Interestingly, suppression of RACK1 also significantly affected the Cell Intensity CV in resting cells. These results suggest that RACK1 is required for the localisation of PKC ζ at the leading edge of the cell.

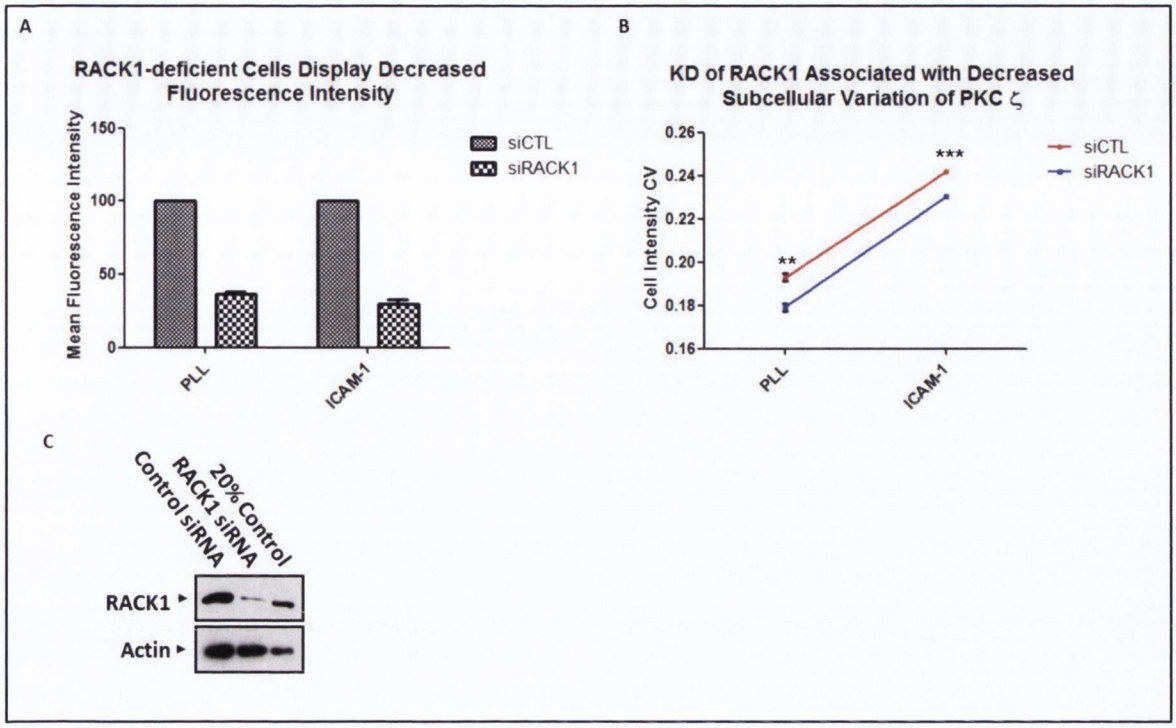

Figure 3.8: Suppression of RACK1 is Associated with a Decreased Variation in PKC ζ Subcellular Distribution.

(A) Mean Cell Fluorescence Intensity of RACK1 in resting and ICAM-1-stimulated HuT78 T cells stained with a RACK1-specific antibody. Intensity values normalised relative to secondary antibody control (background fluorescence). The mean and SEM of N=3 performed in triplicate is shown. (B) Cell Intensity CV of PKC ζ in resting (PLL) and LFA-1-induced migrating (ICAM1) RACK1-deficient (siRACK1) and control (siCTL) T cells. The mean and SEM of N=3 performed in triplicate is shown. ** denotes $p<0.001$ and *** $p<0.0005$ (C) Immunoblot shown is representative of protein knockdown achieved in HuT78 T cells 72 hours after transfection with RACK1-specific siRNA.

High resolution confocal analysis clearly demonstrated the effect of KD of RACK1 on PKC ζ subcellular distribution in migrating T cells (Figure 3.9). In RACK1-deficient cells, PKC ζ is more diffusely localised around the cell compared to the enrichment at the leading edge in control cells. The effect of KD of RACK1 on PKC subcellular localisation is apparent in both resting and LFA-1-mediated migrating T cells. These effects can be observed by analysis of RACK1-depleted cells exhibiting different levels of RACK1 expression. In cells expressing a sufficient level of RACK1, PKC ζ was still redistributed to the leading edge in association with RACK1. However, in cells exhibiting no observable level of RACK1, PKC was not localised at the leading edge of polarised migrating T cells. Together, these data indicate RACK1 is required for PKC ζ localisation at the leading edge in polarised migrating T cells.

Furthermore, in order to evaluate the effect of PKC ζ activity on the subcellular distribution of RACK1, cells were treated with the PKC ζ isozyme-specific pseudosubstrate inhibitor, which suppresses PKC ζ activity (Braun and Mochly-Rosen 2003). RACK1 only interacts with activated PKC (Adams et al. 2011; McCahill et al. 2002; Mochly-Rosen et al. 1995); therefore, RACK1 should not bind PKC in the presence of the pseudosubstrate inhibitor. HuT78 T cells were stimulated with LFA-1 or unstimulated. The cells were stained with IF-conjugate antibodies against PKC ζ and RACK1. The fluorescence intensity and Cell Intensity CV of RACK1 was measured on the IN Cell Analyzer automated microscope. There was no statistically significant effect on the expression or subcellular distribution of RACK1 in resting or migrating T cells treated with the pseudosubstrate inhibitor (data not shown).

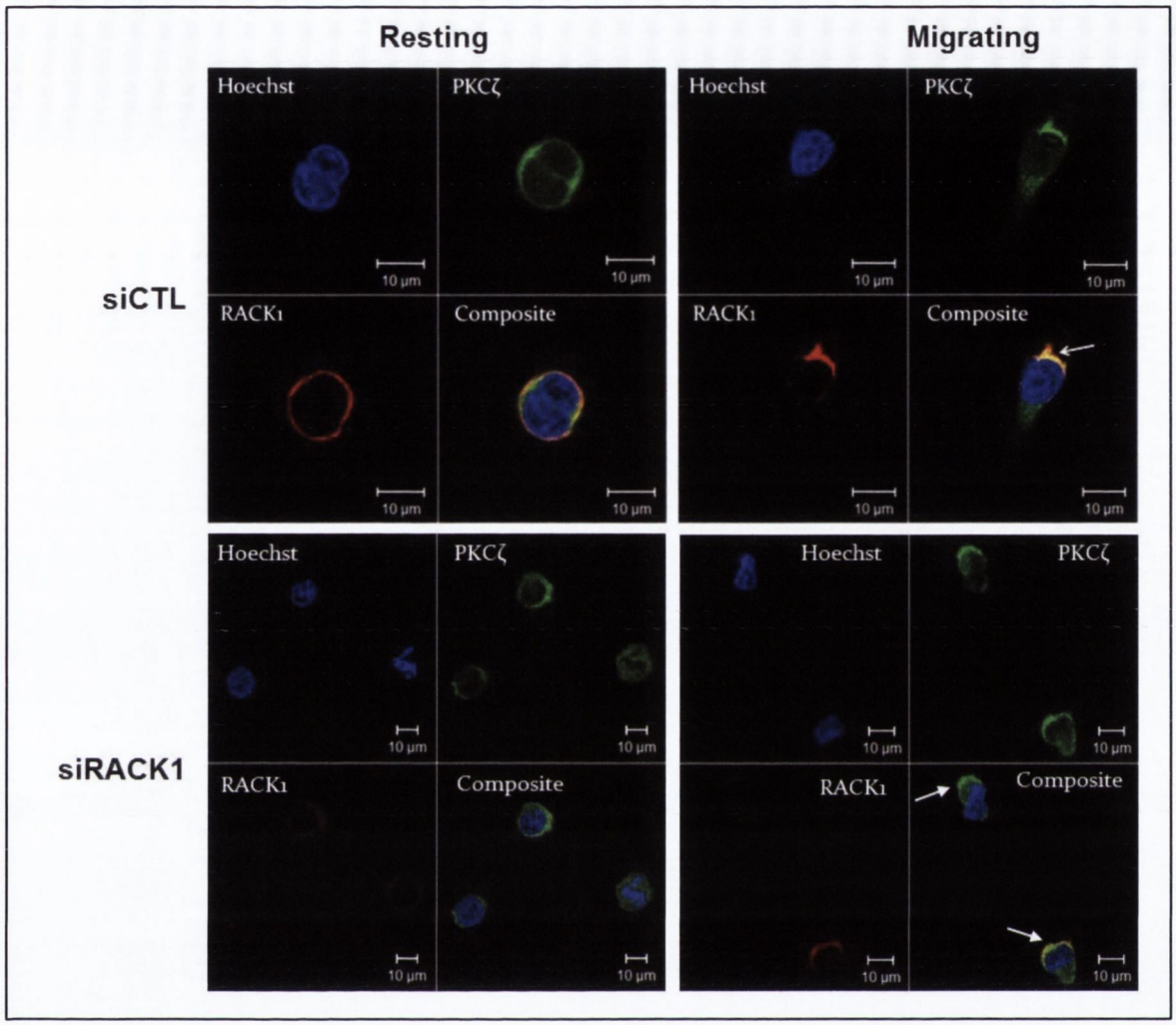

Figure 3.9: KD of RACK1 is Associated with a Decreased Variation in PKC ζ Subcellular Distribution.

HuT78 T cells were transfected with RACK1-specific siRNA (siRACK1) or non-targeting siRNA (siCTL). After 72 hours, cells were harvested and incubated with rhICAM-1 and divalent cations to induce integrin activation or unstimulated. Cells were fixed, permeabilised, and stained with Hoechst nuclear stain and immunofluorescent dyes conjugated to antibodies specific for RACK1 and PKC ζ. All images were acquired by confocal microscopy with 63X objective. White arrows indicate the leading edge of migrating T cells.

3.4 Discussion

Here, an *in vitro* model of T cell migration described in section 2.8 was used to induce a polarised migratory phenotype in T cells following LFA-1 activation. This model allowed the investigation of protein subcellular localisation and any changes in distribution in response to LFA-1 activation in both the HuT78 T cell line and primary T cells. Induction of cell polarisation was also induced by SDF-1α stimulation. A high resolution laser scanning confocal microscopy was employed in conjunction with immunocytochemistry to determine the subcellular localisation of RACK1 in resting and polarised migrating T cells. This study characterised RACK1 expression and co-localisation with cytoskeletal components and intracellular signalling molecules in primary T cells and the Hut78 T cell lymphoma line.

Through the use of immunocytochemistry, RACK1 was demonstrated to translocate from a cytosolic and peripheral distribution in resting cells to the directional lamellipodium, concentrating at the leading edge in LFA-1 induced migrating T cells, which is in keeping with the role of RACK1 as a membrane-associated scaffold protein involved in cell migration (Adams et al. 2011; McCahill et al. 2002). Moreover, RACK1 staining was also present in the protruding uropod and localised to the periphery of the cell neck. The anterior/posterior distribution of RACK1 is also in accordance with recent theories that lipid raft components (e.g. membrane- associated receptors and signalling molecules) are recycled from the posterior compartment to replenish new protrusions and adhesions and sustain directional migration in leukocytes (Barreiro et al. 2007; Fabbri et al. 2005; Ridley et al. 2003). As a putative membrane-associated adaptor protein, RACK1 may regulate polarity by targeting proteins to an anterior and posterior distribution in polarised migrating T cells. Furthermore, the dynamic translocation of RACK1 both to the leading edge as well as the trailing uropod would suggest that it may be continuously recycled during directional migration. This theory would also fit observations that T cells can rapidly alter migration direction in response to extracellular stimuli because of the differential expression and affinity of LFA-1. The dynamic cycling of RACK1 may allow the cell to mediate internal polarity and rapidly change direction. Interestingly, RACK1 appeared to be completely excluded from the nuclear region and mid cell body, where the ER responsible for protein translation is localised. This was somewhat surprising as RACK1 is a ribosomal-associated protein, which recruits PKC to the 40s eukaryotic ribosome, thereby linking signal transduction to protein synthesis (Sengupta et al. 2004; Shor et al. 2003). The translocation of RACK1 to the leading edge of LFA-1 induced

migrating T-cells is a novel finding and supports its potential involvement in defining polarity in T cells. In addition, the induction of polarised distribution was verified through fixed and live cell analysis of cells expression EGFP-RACK1. The IF results in HuT78 cells were corroborated by analysis of expression patterns in primary T cells.

Moreover, RACK1 partially co-localises with the actin and MT cytoskeleton in LFA-1 activated as well as in SDF-1α-stimulated T cells. This asymmetric distribution is consistent with a previous report indicating RACK1 translocates to the leading edge of SDF-1α-stimulated Jurkat cells, a leukemic T cell line (Chen et al. 2008). While, RACK1 appears to be excluded from the actin-rich microvilli, RACK1 did translocate at the leading edge where actin undergoes active polymerisation in the formation of new protrusions in the migrating cell (Alon and Shulman 2011; Porter et al. 2002; Ridley 2011; Ridley et al. 2003; Samstag et al. 2003). RACK1 appeared to localise immediately behind the filamentous actin in the forward extending lamellipodia. Behind the highly dynamic lamellipodium is a more stable region, called the lamella, which contributes to cell migration by coupling the actin network to non-muscle myosin II-mediated contractility and substrate adhesion (Ponti et al. 2004). Therefore, RACK1 may support the assembly of filamentous actin by recruiting proteins to the leading edge in response to diverse stimuli.

RACK1 did appear to co-localise with the MT network in both resting and LFA-1-activated migrating T cells. Both RACK1 and alpha-tubulin have a membrane - associated peripheral distribution in resting cells, and RACK1 co-localises with a subset of tubulin at the leading edge in migrating cells. RACK1 and alpha tubulin associated at the base of extending filopodia, with RACK1 localised to the growing ends of polymerised MTs. Further evaluation of the expression pattern indicated RACK1 localised to the region where the actin and MT cytoskeleton interact at the leading edge. This suggests the scaffolding molecule may act as a cytoskeletal adaptor protein and facilitate actin and MT interaction. While the MT spindle extends the entire length of cell, it originates from the MTOC. RACK1 did not appear to localise to the MTOC or cytosolic mitotic spindle as RACK1 association with tubulin was limited to the plasma membrane.

Despite association with both the actin and MT cytoskeleton in migrating T cells, RACK1 did not appear to co-localise with strongly with the actin associated protein PDLIM2. PDLIM2 displayed an even distribution in both resting and integrin-activated polarised T cells and did not translocate to the leading edge of uropod. This was somewhat surprising considering the preponderance of evidence suggesting PDLIM2 as a

membrane-associated scaffolding protein. Moreover, PDLIM2 did not strongly associate with filamentous actin in the lamellipodia or extending filopodia in polarised migrating T cells (unpublished data). Interestingly, while this actin-associated scaffolding protein did not appear to be enriched at the plasma membrane in either resting or polarised migrating cells, PDLIM2 did localise strongly with the nuclear membrane. This is in accordance with recent studies which demonstrated the actin network is also present in the nucleus in addition to the cytoplasm. Moreover, Tanaka and colleagues (2007) demonstrated PDLIM2 as a nuclear ubiquitin E3 ligase that targets p65 to discrete intra-nuclear compartments where it is degraded by the proteasome in mouse embryonic fibroblasts. The authors observed that latrunculin A, an inhibitor of actin polymerisation, impaired PDLIM2 intra-nuclear trafficking of p65. A member of the NF-κB family, p65 induces the expression of many pro-inflammatory cytokines essential to primary immune defence. However, deregulated p65 activation, by suppression of PDLIM2, was shown to cause irreversible damage to host tissues and result in human inflammatory diseases, such as asthma and arthritis (Tak and Firestein 2001; Tanaka et al. 2007). Using knock out Murine experiments, it was determined that the LIM domain of PDLIM2 is responsible for interacting with p65, while the PDZ domain is required for intra-nuclear trafficking. Proteins containing PDZ domains have been implicated in transporting proteins in diverse cell signalling pathways via protein-protein interactions (Harris and Lim 2001). Therefore, PDLIM2 may interact with the actin cytoskeleton of the nuclear membrane through its PDZ domain to engage activated transcription factors via its LIM domain, allowing it to target transcription factors to the nucleus in response to receptor-mediated stimuli.

Despite its putative role as a membrane-associated actin-binding protein, β Spectrin displayed a relatively even cytosolic distribution in resting cells and was not enriched at the plasma membrane. Preliminary evidence suggests RACK1 associates with β spectrin at the leading edge of polarised migrating T cells. However, despite a number of fixation techniques, suboptimal IF staining with the β Spectrin precluded further analysis. Induced translocation in association with RACK1 in polarised migrating cells is novel and should be pursued in future experiments.

Both polarity proteins Par 3 and PKC ζ were previously shown to translocate to the leading edge of chemokine-induced polarised T cells were they associated with the chemokine receptor CXCR4 (Gérard et al. 2007). The experiment was performed using the same commercially available antibody for Par 3 as was used in that study. However, the authors employed a different T lymphoma cell line (BW5147) and induced

polarisation by SDF-1α. Furthermore, our data suggests the immunofluorescence staining is non-specific as Par 3 was co-immunoprecipitated with RACK1 in T cells and, thus, should co-localise with RACK1 in lymphocytes. Nevertheless, examination of Par 3 subcellular localisation in association with RACK1 should be repeated using a different available antibody in chemokine-induced PBTLs.

Due to its abundance at the leading edge, RACK1 does not co-localise with PKC β1 or the MTOC in migrating T cells. In accordance with previous published data (Volkov et al. 2001), integrin activation induced a subset of PKC β1 to translocate to the MTOC and associate with the MT network. Moreover, PKC β1 did not translocate to the leading edge, and thus did not associate with RACK1 in polarised T cells. This finding suggests that PKC β1 subcellular localisation may not be directed by RACK1, as RACK proteins are thought to be isozyme specific (Adams et al. 2011).

RACK1 was found to associate with PKC ζ at the leading edge of LFA-1-activated migrating T cells. This association in integrin-activated cells is in accordance with RACK1's role in targeting activated PKC to appropriate subcellular locations, such as the plasma membrane (Adams et al. 2011; Csukai and Mochly-Rosen 1999; McCahill et al. 2002). This finding suggests RACK1 may transport PKC ζ to the leading edge in a stimulus-dependent manner. Once activated PKC ζ is targeted to its subcellular destination, it can phosphorylate target substrates. PKC ζ has previously been shown to translocate from cytosolic to membrane fractions in integrin-activated cells (Trucy et al. 2006). However, demonstration of PKC ζ translocation to the leading edge in LFA-1-mediated migrating T cells by immunocytochemistry is novel.

PKC ζ has long been implicated in cellular polarity through its well-defined interactions with members of the Par3/Par6 polarity complex that is conserved from worms and flies to vertebrates (Suzuki and Ohno 2006). Silencing RACK1 by siRNA inhibited PKC ζ translocation to the leading edge in LFA-1-induced migrating cells suggesting RACK1 targets PKC ζ to the leading edge, which was confirmed by analysis of high resolution images of cell exhibiting different levels of RACK1. However, reduction in PKC ζ activity by treating cells with a PKC ζ-specific pseudosubstrate inhibitor had no effect on the expression or subcellular distribution of RACK1 in resting or migrating T cells. This finding suggests activation of PKC does not determine RACK1 subcellular localisation, and RACK1 translocation to the leading edge in integrin-activated cells is independent of PKC activity. This is consistent with RACK1's role in targeting activated PKC to distinct subcellular locations (Adams et al. 2011; McCahill et al. 2002; Ron et al. 1999).

Furthermore, as RACK1 was previously shown to associate with both PKC and β Spectrin in activated lymphocytes (Di et al. 1997), successful immunofluorescence staining of β spectrin is pertinent in order to determine if depletion of RACK1 also inhibits β Spectrin enrichment at the leading edge of polarised cells. The polarised distribution of RACK1 in association with cytoskeletal elements and the polarity protein PKC ζ in LFA-1-mediated migrating T cells suggests RACK1 may have a role in mediating the polarity and motility of T cells. In addition, our studies have implicated RACK1 in directing the localisation of the atypical PKC ζ isoform, a well-established regulator of cell polarity (Gérard et al. 2009; Gérard et al. 2007; Real et al. 2007), to the leading edge of polarised migrating T cells.

3.4.1 Conclusion

Altogether these data suggest a role for RACK1 in mediating cell polarisation in integrin-activated and chemokine-induced polarised T cells. Further evaluation of the effects of altered levels of RACK1 expression on T cell polarisation and migration is detailed in Chapter 4.

CHAPTER FOUR

Functional Analysis of RACK1 in Integrin-Mediated T cell Migration

4 Functional Analysis of RACK1 in Integrin-Mediated T cell Migration

4.1 Introduction

A fundamental question in cell biology concerns how cells respond to their environment by polarising after sensing directional cues. As discussed in section 1.10.6, cellular interactions with the ECM and with adjacent cells profoundly influence a variety of signalling events including those involved in activation, survival, and differentiation. These signalling events dictate cellular actions during an immune response and induce the differential localisation of protein complexes in cells. Deregulation of immune cell signalling pathways can lead to devastating effects, including auto-immunity and cancer. Therefore, it is important to identify and understand how these complexes function. Understanding the contribution of individual components of immune cell signalling pathways that lead to a fully functional T lymphocyte could potentially generate more promising and specific immunomodulation therapies. Recent advances have provided insights into mechanisms underlying the ability of other cell adhesion molecules, such as integrins, to induce signal transduction cascades. These mechanisms often involve the ability of the cytoplasmic domains of these transmembrane receptors to initiate the formation of organised structures or scaffolds that permit appropriate protein interactions and, thus, the efficient flow of information in signalling pathways (Juliano 2002; Shaw and Filbert 2009). By behaving as molecular hubs, scaffolding proteins allow the formation of preassembled or signal-dependent multi-protein complexes that contribute to the accuracy of the spatiotemporal processing and transmission of a signal. In addition, an appropriate transmission of an intracellular signal can be achieved by the subcellular compartmentalisation of signalling proteins that typically requires post-translational modification and/or the association with scaffolding proteins (Kholodenko et al. 2010; Pawson and Scott 1997; Scott and Pawson 2009; Shaw and Filbert 2009).

Owing to its role in membrane recruitment of signalling proteins, RACK1 has been implicated in the regulation of diverse biological functions including cell growth, motility, and polarity (Adams et al. 2011; Battaini and Pascale 2005; Buensuceso et al. 2001; Cox et al. 2003; Kiely et al. 2008; Kiely et al. 2006; McCahill et al. 2002; Serrels et al. 2010; Wang et al. 2011). Due to their crucial role in mediating intracellular signalling related to cell proliferation and development, recent studies have highlighted the relevance of scaffold proteins in cell migration and indicated that interfering with their expression

and/or their ability to bind effector proteins can have dramatic effects on cell adhesion and migration.

Many biological functions have been ascribed to RACK1, but a recurring theme is its involvement in cell polarisation and migration. The role of RACK1 in cell motility has been investigated in diverse cell types, and there is mounting evidence implicating a role for RACK1 in integrin-mediated cell adhesion and migration. The preponderance of evidence indicates RACK1 may be essential for the regulation of migration in all cells types where it is expressed as the protein binds to many components of the cell migration machinery, including kinases, phosphatases, and the cytoplasmic domains of cell surface receptors (McCahill et al. 2002; Sklan et al. 2006). For example, RACK1 was found to interact with the membrane proximal region of the cytoplasmic tail of β-integrins (β_1, β_2, β_3, and β_5) in various cell types, which implicated a role in integrin-mediated adhesion (Liliental and Chang 1998). In addition, RACK1 has been shown to interact with and direct localisation of PKC isozymes in order to mediate cell migration through β-integrin outside-in signalling (Besson et al. 2002; Buensuceso et al. 2005; Buensuceso et al. 2001). The authors observed overexpression or activation of PKC by phorbol esters enhanced integrin-mediated cell adhesion. RACK1 targeted PKC to the β_2 integrin and allowed it to regulate the interaction between the LFA-1 integrin and the actin cytoskeleton (Besson et al. 2002). Once anchored to the integrin by RACK1, PKC has been shown to phosphorylate several residues of the β2 subunit, which allows it to bind the scaffolding molecule 14-3-3 resulting in subsequent sequestration of diverse signalling molecules. Antisense depletion of RACK1 or over-expression of a truncated form of RACK1 that lacks part of the integrin-binding region (WD repeats 6 and 7 and part of WD repeat 5) disrupted PKC ε translocation to integrin receptors and abrogated adhesion and migration (Besson et al. 2002).

In addition to PKC, RACK1 is also involved in coordinating the interaction and activity of key signalling molecules, including the tyrosine kinases Src and Jnk kinase during cell migration (Chang et al. 2002; Doan and Huttenlocher 2007; Kiely et al. 2005). This implicates a role in mediating signal transduction pathways required for cell locomotion. As previously discussed, integrin activation triggers a number of signalling pathways, including the Src/ MAPK pathway, which mediate cytoskeletal remodelling and formation of focal adhesion complexes (Brunton et al. 2004; Zhao and Guan 2011). Overexpression of RACK1 has been reported to enhance cell spreading, which was associated with an increased number of actin stress fibers and focal contacts and enhanced tyrosine phosphorylation of both focal adhesion kinase (FAK) and the focal

adhesion associated protein paxillin, while inhibiting overall cell migration (Buensuceso et al. 2001; Hermanto et al. 2002). Conversely, reduction of RACK1 expression in fibroblasts by antisense depletion blocked cell spreading and inhibited growth factor-stimulated cell proliferation (Hermanto et al. 2002). In addition, the ability of RACK1 to interact with and link multiple binding partners was reported to be essential for the regulation of cell polarity in fibroblasts. By serving as a molecular scaffold, RACK1 was able to bind FAK, which enabled the recruitment of specific components of the cAMP second-messenger system, including PDE4D5, to nascent integrin adhesions and to the leading edge of polarised cells (Serrels et al. 2011; Serrels et al. 2010). Therefore, RACK1 may serve as a scaffold for the sequestration of key signalling proteins to focal adhesion complexes in association with activated integrin. RACK1's role in integrin-mediated signalling is twofold as it targets signal transducers, such as PKC, to activated integrin and serves as an adaptor protein for integrin-mediated initiation of signalling pathways.

Although RACK1 has been implicated in cell migration in a number of cell types, the role of RACK1 in lymphocyte migration has been widely overlooked. Despite its association with increased cell spreading and migration, RACK1 has recently been implicated as a negative regulator of directed cell migration in T cells. Down-regulation of RACK1 was reported to significantly enhance chemotaxis of the Jurkat leukemic T cell line. Whereas, overexpression of RACK1 was shown to inhibit SDF-1α-stimulated cell migration by interfering with the Gβγ-dependent activation of key effectors critical for chemotaxis (Chen et al. 2008).

There has also been extensive research on the role of RACK1 in cancer progression, specifically in tumour cell growth, polarity, and migration (Adams et al. 2011; Cao et al. 2011; Kiely et al. 2008; Kiely et al. 2006; Serrels et al. 2010; Wang et al. 2011). RACK1 is significantly up-regulated during angiogenically active tissues and in carcinomas (Berns et al. 2000). In addition, a recent study demonstrated downregulation of RACK1 expression by RNAi in tumour cells markedly suppressed the proliferation and invasion of these cells *in vitro* and progression of tumour development *in vivo* via suppression of constitutive phosphorylation of the Akt and MAPK pathways (Wang et al. 2011). Moreover, RACK1 has also been shown to promote breast carcinoma proliferation and invasion/metastasis *in vitro* and *in vivo* by activation of the RhoA/Rho kinase pathway. Conversely, knockdown of RACK1 by siRNA inhibited proliferation, migration, and invasion (Cao et al. 2011; Cao et al. 2010). Because of its role in breast cancer invasion and metastasis, RACK1 has been identified as an independent prognostic indicator for

poor clinical outcome in breast carcinoma (Cao et al. 2010). PKC signalling is known to play an important role in angiogenesis and tumour growth. Therefore, the level of RACK1 expression may be relevant to the activity of downstream signalling of PKC in angiogenically active tissues.

4.2 Objectives

The scaffolding protein RACK1 has been implicated in regulating integrin-mediated adhesion and migration by interacting with numerous signalling proteins involved in cytoskeletal remodelling. While research has indicated RACK1's involvement in mediating cell migration through interaction with β-integrins and key signalling molecules in various cell types, the molecular mechanisms underlying the role of RACK1 in lymphocyte migration have been widely overlooked. Therefore, by manipulating expression levels, we sought to investigate the role of RACK1 in lymphocyte motility, specifically in LFA-1-mediated T cell polarisation, adhesion to ICAM-1, and SDF-1α-stimulated chemotaxis. By employing a HCA platform, we investigated the potential downstream events following targeted manipulation of RACK1 in primary T cells and the HuT78 T lymphoma cell line. An experimental flow-chart is shown in Figure 4.1.

In this study, we aimed to:

1.) Examine the effect of suppression of RACK1 on LFA-1-induced migration in the HuT78 T cell lymphoma line and in primary T cells.
2.) Determine the effect of RACK1 depletion on adhesion to ICAM-1 in the HuT78 T cell lymphoma line and in primary T cells.
3.) Examine the effect of knockdown and overexpression of RACK1 on chemotatic migration in a transwell system in the HuT78 T cell lymphoma line and in primary T cells.
4.) Determine the effect of suppression of RACK1 on the speed and persistence of chemokinetic migration in primary T cells.

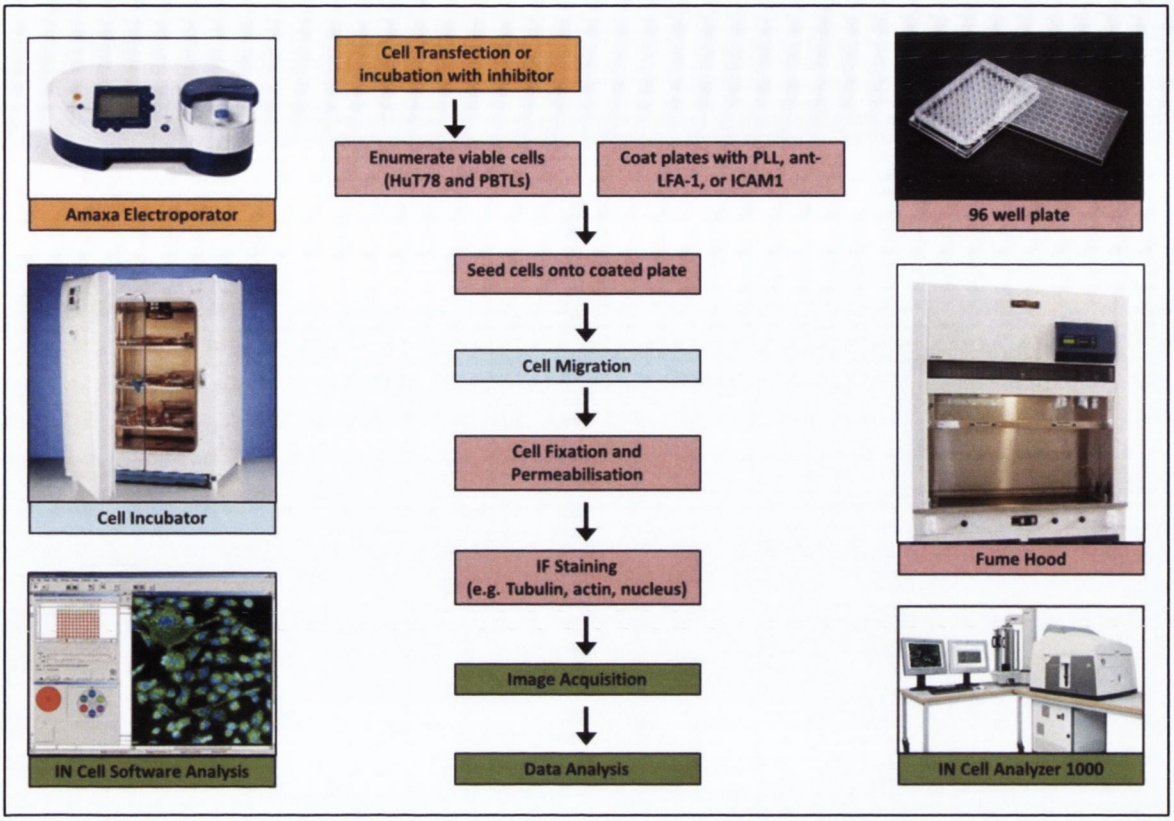

Figure 4.1: Experimental flow-chart for analysis of T cell migration using IN Cell HCA platform.

Schematic diagram detailing the steps required for high content analysis of morphology changes in migrating T cells following cell transfection or treatment with an inhibitor.

4.3 Results

4.3.1 KD of RACK1 Decreases T Cell Polarisation HuT78 T cell Line

The use of automated microscopic analysis has been previously employed by our group to determine the effect of known pharmacological inhibitors on LFA-1-mediated T lymphocyte morphology, and key sets of parameters used to quantitatively assess effects on lymphocyte morphology were identified (Freeley et al. 2010). The multi-parametric analysis of lymphocyte morphology was employed in this study to characterise RACK1 function in integrin-mediated T cell migration. Selective knockdown of RACK1 protein expression by siRNA was carried out in HuT78s followed by image-based high-content analysis (section 2.7). A transfection technique was optimised for the T lymphoma cell line (section 2.5.1). Knockdown of RACK1 expression was confirmed by western blot analysis (Figure 4.2B). A transfection efficiency of approximately 90% knockdown of endogenous RACK1 expression as measured by densitometry was consistently achieved. The phenotypic effect of RACK1 knockdown on LFA-1-induced migration was then assessed. The *in vitro* migration assay was carried out in HuT78 cells and performed in triplicate. Morphological analysis was based on fluorescent staining of the F-actin and alpha tubulin cytoskeleton. The 1/(form factor) morphology parameter was first used to quantify LFA -1-stimulated polarisation. The 1/(form factor) is a cell roundness index, with values ranging from 1 to infinity, where 1 is a perfect circle. The 1/(form factor) increases as the cells adopt a migratory phenotype and is thus a good measure of shape change. A significant increase in 1/(form factor) was observed when cells were stimulated with anti-LFA-1 compared to cells incubated on poly L-lysine (PLL) when morphological analysis was based on alpha tubulin staining (PLL = 1.23 ± 0.002, anti-LFA-1 = 1.78 ± 0.001, $p < 0.00005$). The measurement of 1/(form factor) was slightly different when the morphological analysis was based on F-actin staining (PLL = 1.37 ± 0.007, anti-LFA -1 = 2.127 ± 0.004, $p < 0.0001$). While both the activating antibody to LFA-1 and the native ligand ICAM-1 were used to stimulate a polarised morphology, cells stimulated with rhICAM-1 exhibited a less polarised morphology (1.38 ± 0.01 and 1.55 ± 0.009 for alpha tubulin and F-actin staining, respectively; $p < 0.005$ for both). This less pronounced phenotype is possibly due to differences in the affinities of these ligands for the LFA -1 receptor or to the fact that these ligands bind to distinct sites on the receptor. The 1/(form factor) values were slightly higher when analysis was based on F-actin staining compared to alpha tubulin staining. This likely reflects the fact that the F-actin cytoskeleton is distributed more peripherally in the cell and into extending

lamellipodia and filopodia, resulting in a more complex shape for analysis. Therefore, subsequent morphological analysis was quantified using cells incubated on anti-LFA-1 and based on F-actin staining.

A number of other morphological parameters were used to quantify the effects of KD of RACK1 on anti-LFA -1-mediated shape and polarisation of the cells as previously described (Freeley et al. 2010). These cell shape measurement included cell area, cell gyration radius (a measure of the spread of the cell), and nuclear displacement (the position of the nucleus relative to the centre of the cell body). For example, the relatively large nucleus that is typical of lymphocytes is usually positioned in the cell body centre in non-polarised cells and, therefore, has a low nuclear displacement value. In polarised lymphocytes, however, the nucleus is usually positioned toward the leading edge of the cell and away from the cell body centre, thereby resulting in an increase in nuclear displacement. Parameter definitions are listed in Appendix 3 Table 8. All four parameters significantly increased in HuT78 T cells following LFA-1 cross-linking compared to resting cells when morphological analysis was based on either F-actin or alpha tubulin staining (Freeley et al. 2010).

Viable cells 72 hours after transfection were enumerated and stimulated with anti-LFA-1 for three hours. Cells pre-treated with 5 μM of the cytoskeletal inhibitor Nocodazole for forty minutes prior to stimulation with anti-LFA-1 were included in the assay as a negative control. Nocodazole, a MT depolymerising agent, has previously been shown by our group to reduce cell polarisation in cells stimulated with anti-LFA-1 or ICAM-1 as measured using the selected morphology parameters (Freeley et al. 2010). Treatment with Nocodazole has been shown to prevent morphological polarisation and formation of a stable uropod structure (Takesono et al. 2010). Similarly, the measurements of morphology parameters were significantly reduced (Figure 4.2A), and the inhibitor-treated cells exhibited a stunted uropod phenotype (data not shown). Despite reducing cell polarisation, cells treated with MT depolymerising agents, such as Nocodazole and Colchicine, have been reported to migrate at a speed comparable to T cells (Niggli 2003; Takesono et al. 2010). Microscopic images of cells fixed and stained for the actin cytoskeleton demonstrated an observable phenotypic effect of suppression of RACK1 (Figure 4.2C). There were substantially less actin-based processes observed in the RACK1-deficient T cells. In addition, similar to cells treated with Nocodazole, suppression of RACK1 prevented cell polarisation and formation of stable uropod structures. In neutrophils, by contrast, an intact microtubule network does not appear to be required for migration.

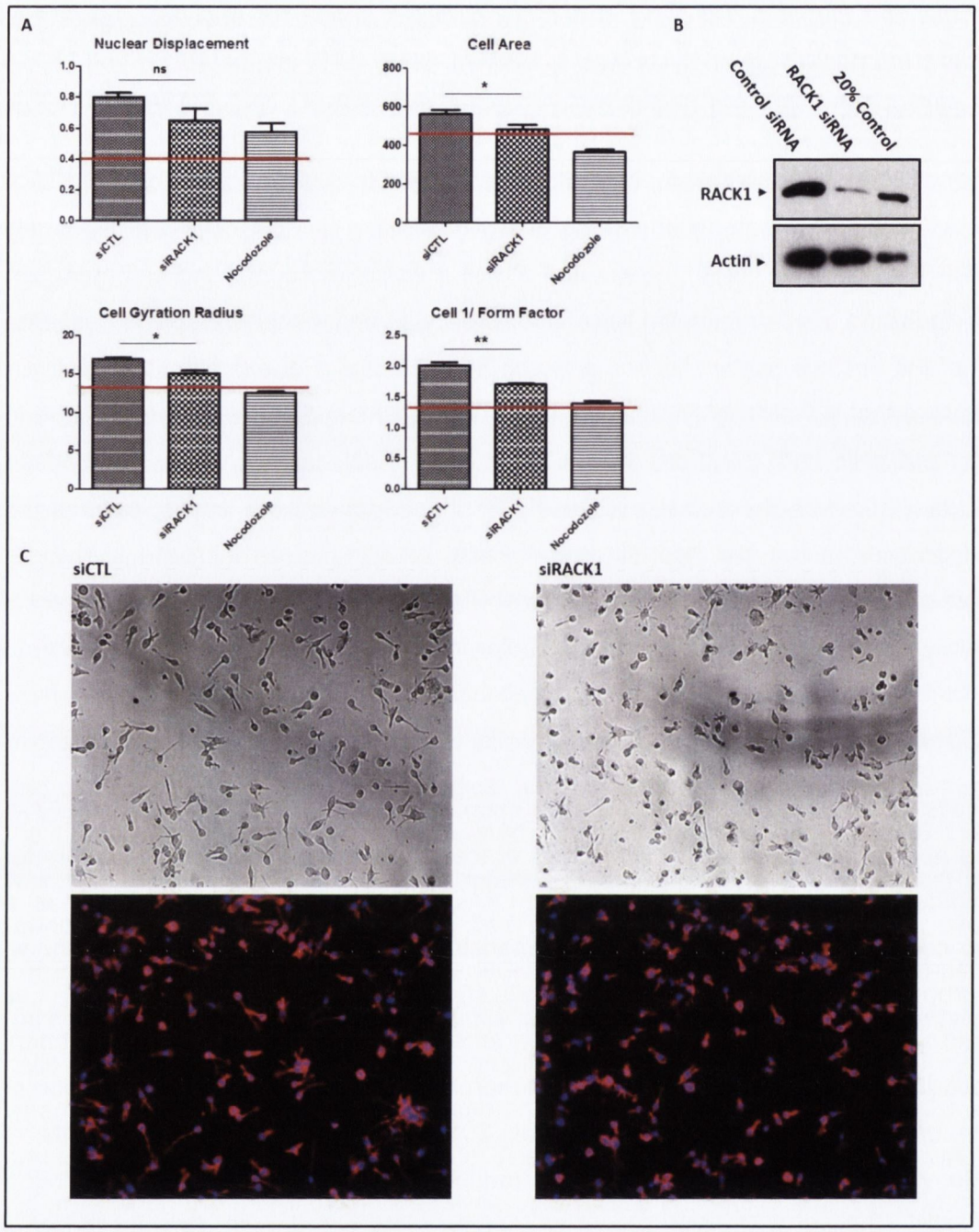

Figure 4.2: Suppression of RACK1 results in reduced LFA-1-mediated cell polarisation in HuT78 T cells.

(A) The measurement of morphology parameters cell area, cell1/form factor, cell gyration radius, and nuclear displacement in RACK1-deficient (siRACK1) and transfection control (siCTL) HuT78 T cells stimulated with anti-LFA-1. The red line depicts the resting cell measurement. The mean and SEM of N=4 performed in triplicate is shown. * denotes $p< 0.05$, ** $p<0.01$. (B) Immunoblot shown illustrates protein knockdown in HuT78 T cells transfected with siRNA. (C) Brightfield and fluorescent Images of siCTL and siRACK1 transfected HuT78 T cells. Image acquired with 10X objective on IN Cell Analyzer. Nucleus in blue and actin in red.

The selected morphology parameters for RACK1-deficient T cells (siRACK1) were consistently lower than in cells treated with control siRNA (siCTL) and untreated cells suggesting an overall decrease in T cell polarisation (Figure 4.2A). The cell measurements for cell 1/form factor, cell area, and cell gyration radius were significantly reduced in RACK1 depleted cells as compared to control cells. There was an observable downward trend in the displacement of the nucleus in RACK1-deficient cells. Furthermore, cells transfected with control siRNA yielded similar phenotypes and morphology parameter measurements to cells not electroporated, indicating minimal off-target effects by the chemically modified siRNA and the electroporation technique. Moreover, the cell area, cell gyration radius, and nuclear displacement data displayed the same trend as the 1/(form factor) parameter, irrespective of whether morphological analysis was based on F-actin or alpha tubulin staining. The morphology parameter measurements based on F-actin staining for transfected cells are displayed in Table 4.1

Table 4.1: Morphology parameter measurements based on F-actin staining for transfected HuT78 T cells (N=4).

	PLL	Anti-LFA-1		
	siCTL Mean ± SEM	siCTL Mean ± SEM	siRACK1 Mean ± SEM	P value
Cell 1/(form factor)	1.452 ± 0.005	2.018 ± 0.04	1.710 ± 0.0112	0.0035
Cell Area	435.2 ± 10.70	564.3 ± 18.15	483.3 ± 21.43	0.0448
Cell Gyration Radius	13.37 ± 0.1266	16.93 ± 0.2798	15.07 ± 0.3833	0.0170
Nuclear Displacement	0.4053 ± 0.0272	0.8015 ± 0.0277	0.6490 ± 0.0761	0.1330 (ns)

4.3.2 Investigation of KD of RACK1 on ICAM-1 Adhesion Assay in the HuT78 T cell Line

The next objective was to determine the role of RACK1 in T cell adhesion to ICAM-1, the native ligand of the integrin receptor LFA-1. The plate-based ICAM1 adhesion assay is described in section 2.10. The assay was first optimised for the adhesive properties of HuT78 cells. Therefore, cells were seeded on tissue culture plates coated with the goat anti- rhICAM-1 coating antibody (GαH), immobilised rhICAM-1 at 1 and 5 µg/ml, PLL, and anti-LFA-1 or left uncoated (plastic). The cells were stimulated with divalent cations, which induce the active conformation of LFA-1 on the surface of T cells, or unstimulated. Cation displacement induces conformational change of LFA-1, allowing it bind ICAM-1. When cations are not present, the LFA-1 remains in the inactive conformation and does not bind to the ICAM-1, and the cells are consequently washed away. The cells were incubated for 30min at 37°C and then washed three times with cation-free sterile PBS. The cells were then fixed and incubated with cell-permeable Hoechst nuclear stain. The plates were then imaged on the IN Cell Analyzer, and the cells were counted using the Analyzer software.

As expected, the cells had negligible adhesion to plastic or GαH regardless of the addition of divalent cations. In addition, the cell adhered strongly to both PLL and anti-LFA-1. This was expected as cells adhere strongly to both PLL-coated tissue culture plates as it introduces a positive charge and increases cell adherency (Vancha et al. 2004) and to anti-LFA-1 (clone SPV-L7), which recognises the alpha chain of LFA-1 (Keizer et al. 1985). Moreover, there was no discernable difference with the addition of cations. The HuT78 T cells exhibited strong adhesion to ICAM-1, which was dependent on the presence of divalent cations for activation of LFA-1 (Figure 4.3A). There was no significant different between the two concentrations of ICAM-1 used, as both generated a cell adhesion count with approximately an 18-fold difference for the presence of divalent cations as compared to control and was used in subsequent assays.

Next, we assessed the effect of pre-treatment with cytoskeletal inhibitors on adhesion to ICAM-1. Cytochalasin D, a potent inhibitor of actin polymerisation, and the MT depolymerising agent Nocodazole have previously been shown to abrogate T cells polarisation (Freeley et al. 2010). The cells were treated with either Nocodazole or Cytochalasin D at concentrations previously described (Freeley et al. 2010) for forty minutes prior to the assay. ICAM-1 adhesion was significantly decreased in inhibitor treated cells regardless of the addition of divalent cations compared to the untreated

control (Figure 4.3B). As expected, there was no significant difference to adhesion to PLL in inhibitor treated cells compared to untreated control. The cytoskeletal inhibitor Cytochalasin D was used as a negative control in subsequent experiments.

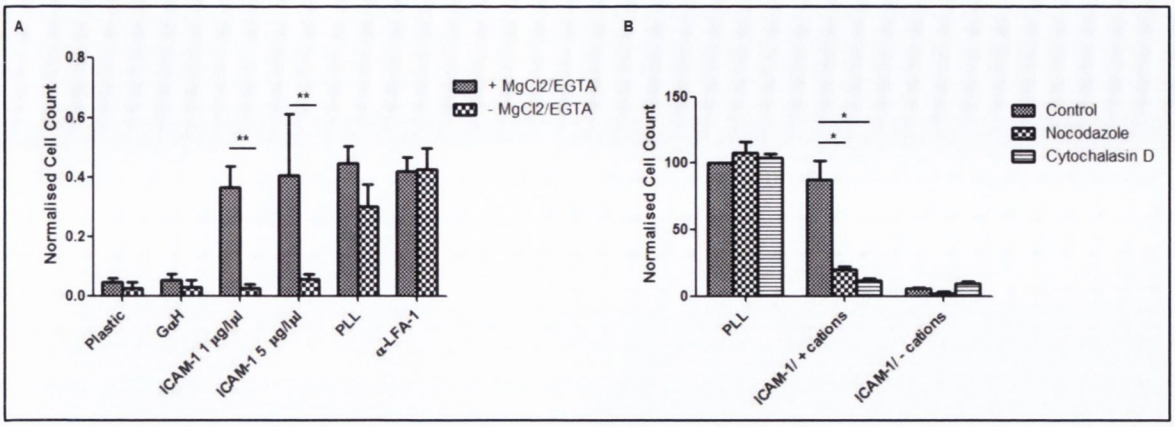

Figure 4.3: Optimisation of ICAM-1 Adhesion Assay in T cells.

(A) Quantification of HuT78 T cells seeded on plates coated with plastic, goat anti-human coating antibody (GαH), ICAM-1, PLL, and anti-LFA-1 stimulated with divalent cations or unstimulated. The mean and SEM of N=5 performed in triplicate is shown. ** denotes $p<0.01$ (B) Quantification of cells seeded on plates coated with ICAM-1 pre-treated with cytoskeletal inhibitors, Cytochalasin D and Nocodazole or unstimulated. The mean and SEM of N=3 performed in triplicate is shown. * denotes $p<0.05$

The effect of KD of RACK1 on adhesion to ICAM-1 was next assessed. While, transfected cells exhibited a decreased adhesion to ICAM-1 compared to untransfected cells, there was no significant difference between RACK1-deficient cells compared to the transfection control. This was possibly due to the incubation with divalent cations, which constitutively induce the active conformation of LFA-1, and may have superseded any effect suppression of RACK1 may have had on adhesion to ICAM-1. Therefore, the assay was altered by replacing divalent cations with the chemokine SDF-1α for induction of integrin activation. Chemokines, such as SDF-1α, also contribute to lymphocyte migration by activating intracellular signalling pathways that result in conformational changes in integrins including LFA-1 that permits cell adhesion to vascular barriers via interactions with its corresponding ligand ICAM-1 (Alon and Shulman 2011; Hogg et al. 2011). Optimisation of the assay was carried out using a range of concentrations of SDF-1α (1, 10, 100, 1000 ng/ ml). However, Hut78 T cells stimulated with SDF-1α did not adhere to ICAM-1 at the same rate as cells stimulated with divalent cations. The divalent cations induce the high affinity conformation of LFA-1, while SDF-1α triggers the intermediate affinity of the integrin to ICAM-1. In addition, the response to SDF-1α may diminish rapidly as *in vivo* the cell responds to a chemoattractant gradient. Due to the transient stimulation of the integrin in the *in vitro* adhesion assay, the ICAM-1-bound cells may have detached during the washing steps even in the presence of the chemokine. However, the results could also suggest that there is a redundant pathway leading to the activation of LFA-1 or that RACK1 may be involved in downstream pathways involved in T cell polarisation. Unfortunately, the effect of KD of RACK1 on ICAM-1 adhesion could not be ascertained in HuT78 T cells. However, the adhesion assay was optimised and repeated in primary T cells detailed in section 4.3.7.

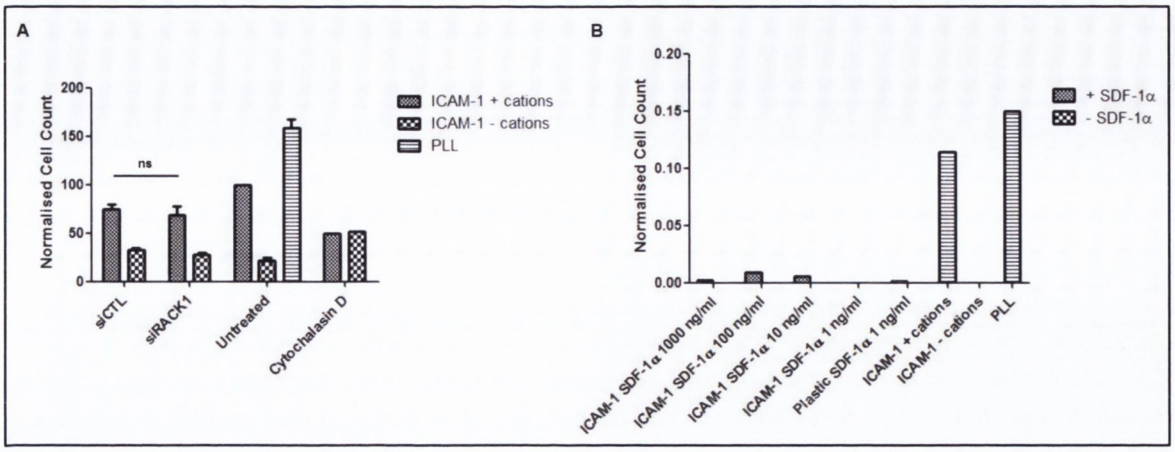

Figure 4.4: KD of RACK1 did not affect adhesion to ICAM-1 in T cells.

(A) Quantification of HuT78 T cells transfected with RACK1-specific or control siRNA and cells pre-treated with Cytochalasin D or left untreated, seeded on rhICAM-1 or PLL, and stimulated with divalent cations or unstimulated. The mean and SEM of N=3 performed in triplicate is shown. Cells pre-treated with Cytochalasin D were used as a negative control. (B) SDF-1α titration experiment using a range of concentrations of SDF-1α (1, 10, 100, 1000 ng/ ml). The cell counts were normalized to the input. Data shown is representative of one experiment performed in triplicate.

4.3.3 Inhibition of RACK1 Expression Enhances SDF-1α-stimulated Chemotaxis in HuT78 T cell Line

We also sought to ascertain the effect of depletion of RACK1 on SDF-1α-stimulated migration in HuT78 cells, which endogenously express CXCR4. The Transwell Chemotaxis Assay described in section 2.11 is an *in vitro* system which incorporates the three important T cell functions necessary for transendothelial migration. The transwell assay quantitatively assessed the ability of cells to bind, polarise, and migrate through an ICAM-1-bound filter toward a chemoattractant. The assay involved adding 1 $x10^5$ cells to the upper chamber and chemokine to the lower chamber, which are separated by an ICAM-1-coated porous membrane. The cells that successfully transmigrated to the lower chamber were counted and normalised to the input. It should be noted that unlike other chemotaxis methods, which include cells bound to the bottom of the filter in the final cell count (Curnock et al. 2003), only cells which successfully migrated into the lower chamber and detached from the membrane were counted. Experimental design was necessary to accurately assess the impact of ICAM-1 and presence of chemokine on the transwell system. Optimisation of the protocol involved comparing chemokines known to be involved in transendothelial migration, including MIP1α, MIP-1β, RANTES, and SDF-1α in combination with a rhICAM1-coated filter. In addition, optimisation experiments consisted of chemokine titrations to determine the optimal chemotatic concentration. The range of chemokine concentrations tested was based on relevant publications (Curnock et al. 2003). The impact of an ICAM-1-coated filter and the presence of chemokine had on the transwell system were determined by calculating the fold difference compared to the absence of ligand or chemokine as shown in Figure 4.5A. The results of the experimental design process indicated SDF-1α induced the greatest number of cells to migrate across the ICAM1-bound filter, which is in accordance with previous reports on chemotaxis assays (Curnock et al. 2003). In addition, chemokine titrations determined 50 ng/ml concentration of SDF-1α present in the lower chamber stimulated greatest transwell migration (data not shown). We observed the optimal chemotactic response of T cells required the combination of the ligand-bound membrane and the chemoattractant. While the presence of ICAM-1 was required for optimal chemotaxis in our study, previous reports have indicated filters coated with the ECM proteins fibronectin or collagen does not significantly increase chemotaxis of Jurkat T cells compared to chemokine alone (Chen et al. 2008). In all the experiments, the background migration was almost absent (<0.01% of the loaded cells did migrate in the absence of an ICAM-1-bound filter or chemokines).

The next objective was to determine if pre-treatment with cytoskeletal inhibitors known to inhibit T cell polarisation and migration could also disrupt chemotatic migration for use as a negative control in the transwell system. Similar to the *in vitro* LFA-1-mediated T cell migration and ICAM-1 adhesion assay, the cells were pre-treated with the cytoskeletal inhibitors Cytochalasin D and Nocodazole for forty minutes prior to the assay. As expected, pre-treated with Cytochalasin D disrupted chemotatic migration; however, cells pre-treated with Nocodazole significantly increased chemotaxis compared to untreated cells (Figure 4.5B). Therefore, cells pre-treated with Cytochalasin D served as a negative control, while pre-treatment with Nocodazole served as a positive control for subsequent transwell experiments. While disruption of the MT spindle disrupts migration of most cell types, drug-induced disassembly of MTs by Nocodazole has been reported to induce chemokinetic migration in neutrophils, a type of leukocyte (Keller et al. 1984; Niggli 2003), which may explain its enhancement of chemotatic migration of T cells in this study. In contrast, another study reported Nocodazole-treated differentiated HL-60 cells, a neutrophil cell line, exhibited impaired directional migration (Xu et al. 2005). Therefore, treatment with Nocodazole appears to enhance chemokinetic migration, but reduce chemotaxis toward a stationary chemoattractant.

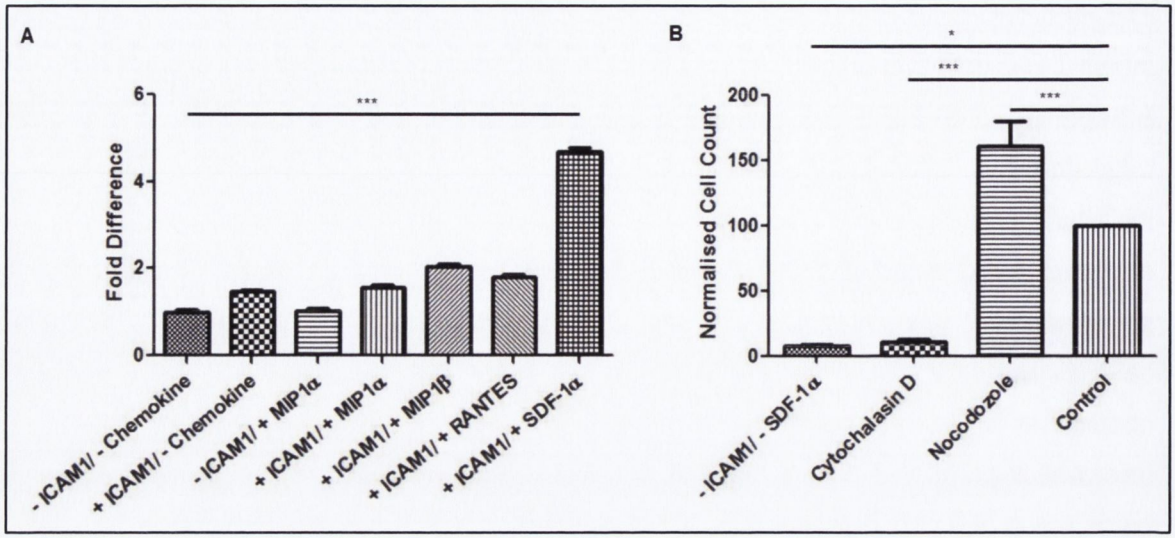

Figure 4.5: Optimisation of Transwell Chemotaxis Assay in T cells.

(A) Assessment of the impact of the ICAM1-bound filter and the type of chemokine on the transwell system using HuT78 T cells. The mean and SEM of N=3 performed in triplicate is shown. *** denotes $p<0.0001$ (B) Cells were pre-treated with Cytochalasin D or Nocodazole or untreated before addition to the transwell. Transwell contained ICAM1-coated membrane and SDF-1α unless otherwise noted. The mean and SEM of N=4 performed in duplicate is shown. * denotes $p< 0.05$ and *** $p<0.0005$

We next investigated the effect of RACK1 depletion on chemotatic migration. Cells transfected with non-targeting control siRNA (siCTL) and RACK1-specific siRNA (siRACK1) were enumerated and added to the transwell. In addition, untransfected cells pre-treated with Cytochalasin D or Nocodazole or untreated were enumerated and added to the transwell. As shown in Figure 4.6A, KD of RACK1 in resulted in approximately a 4-fold increase in chemokinetic migration compared to the transfection control cells. The migratory ability of cells transfected with non-targeting control siRNA was comparable to untransfected cells. Interestingly, while suppression of RACK1 decreased morphology parameters associated with polarisation, both RACK1-deficient T cells and Nocodazole-treated cells exhibited an increase in chemotatic migration. Nocodazole- treated cells exhibited approximately a 4-fold increase, while Cytochalasin D-treated cells exhibited a 3.5-fold decrease in chemotatic migration as compared to the control cells.

Notably, down-regulation of RACK1 significantly enhanced SDF-1α-stimulated cell migration, but had no effect on general motility of cells, as the transwell migration of cells in the absence of SDF-1α gradient is not significantly altered by decreased RACK1 expression (Figure 4.6B). These findings indicate that RACK1 negatively regulates chemotaxis but not random migration of HuT78 T cells. Moreover, addition of chemokine alone did not significantly increase migration in RACK1-deficient cells compared to the siCTL cells. The ICAM-1-coated filter alone was able to augment migration in both the KD and control cells. The combination of the ICAM-1-coated filter and addition of chemokine induced the greatest increase in chemotatic migration for both the transfected cell populations.

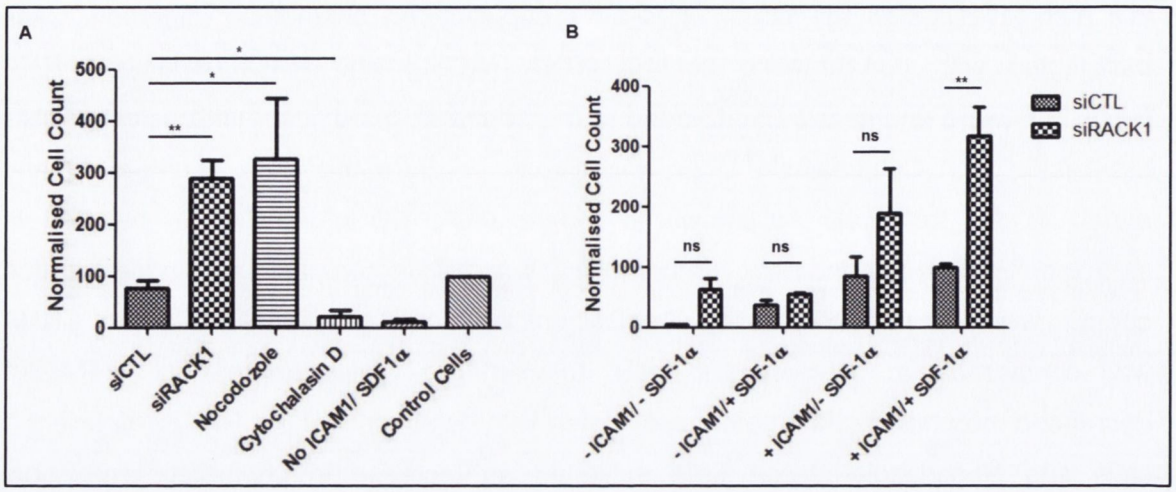

Figure 4.6: Suppression of RACK1 Enhances Chemotatic Migration, but not random migration in T cells.

(A) Quantification of HuT78 T cells that underwent transwell migration in response to ICAM-1-coated filter plus SDF-1α unless otherwise noted. Cell count was normalised relative to untreated control cells. The mean and SEM of N=4 performed in duplicate is shown. * denotes $p<0.05$ and ** $p<0.005$ with respect to siCTL cells. (B) The relative contribution of the ICAM-1-coated filter and SDF1α on the increased migratory ability of RACK1-deficient HuT78 T cells was assessed. The cell count was normalised to the mean of the siCTL with ICAM-1/ SDF-1α. The mean and SEM of N=3 performed in duplicate is shown. ** denotes $p<0.01$

4.3.4 Optimisation of siRNA Transfection of Primary T Cells

The results from the transwell assays implicate RACK1 in the regulation of LFA-1-induced T cell migration. Nevertheless, while SDF-1α stimulation induces migration in the HuT78 T cell line, the cell surface receptor CD26 may confound assays dependent on SDF-1α stimulation. Therefore, it was pertinent to design an electroporation technique with high transfection efficiency and cell viability and repeat all three assays in primary T cells.

Peripheral blood T lymphocytes were isolated from human blood and expanded with PHA and IL-2 as described in section 2.4. Primary suspension cells are generally regarded as difficult to transfect as electroporation with siRNA significantly reduces cell viability , which is the reason transformed adherent cell transfection models are widely employed (Elbashir et al. 2001; Paul et al. 2002). Primary T cells are particularly difficult to transfect as they exhibit the ability to degrade the machinery used to process siRNA (Yin et al. 2006). Optimisation of transfection with siRNA was carried out first experimenting with a number of time and voltage parameters with the BTX Electroporator. Unfortunately, the electroporation method significantly reduced cell viability. Amaxa Nucleofector® technology (electroporator with Nucleofector® solution for primary T cells) was next tested for transfection efficiency. Sufficient knockdown was achieved; however, the amount of protein knockdown was inconsistent and the electroporation process reduced cell viability. Finally, our group optimised a highly efficient and consistent transfection method with minimal cell death for PHA/IL-2-expanded PBTLs as described in section 2.5.1. The '2-hit' transfection method utilised the Amaxa technology (programme T-07) in combination with Ingenio® Electroporation Solution from Mirus Bio LLC, which silenced target RNA expression by more than 90% (Freeley et al., manuscript in preparation). This technique made feasible the transfection of primary T lymphocytes for the functional analysis of RACK1 in T cell polarity and motility.

4.3.5 KD of RACK1 Reduces Cell Polarisation in Primary T Cells

Expanded PBTLs were transfected with RACK1-targeting siRNA and scrambled control siRNA, and knockdown of protein was verified by Western blot (Figure 4.7B). The cells starved for 2 h in serum-free RPMI and then stimulated with the LFA-1 ligand ICAM-1 and divalent cations to induce cell polarisation and migration. All four morphology parameters measured a significant reduction in cell polarisation in RACK1-deficient cells

as compared to the control (Figure 4.7A). The RACK1-deficient cells exhibited a stunted polarity and rounded cell phenotype (Figure 4.7C). These results were consistent with the effects exhibited in the T cell line HuT78s and confirmed the defect in cell polarisation due to a depletion of RACK1. In addition, cells transfected with control siRNA yielded similar phenotypes and morphology parameter measurements to cells not electroporated, indicating minimal off-target effects by the primary T cell transfection technique (data not shown). As observed in HuT78 T cells, the morphology parameter data for PBTLs displayed the same trend irrespective of whether morphological analysis was based on F-actin or alpha tubulin staining. Moreover, the experimental data obtained from primary T cells validated the use of the HuT78 T cell line as a representative model for PBTLs in cell polarisation assays. The morphology parameter measurements based on F-actin staining for transfected cells incubated on PLL and ICAM-1are displayed in Table 4.2.

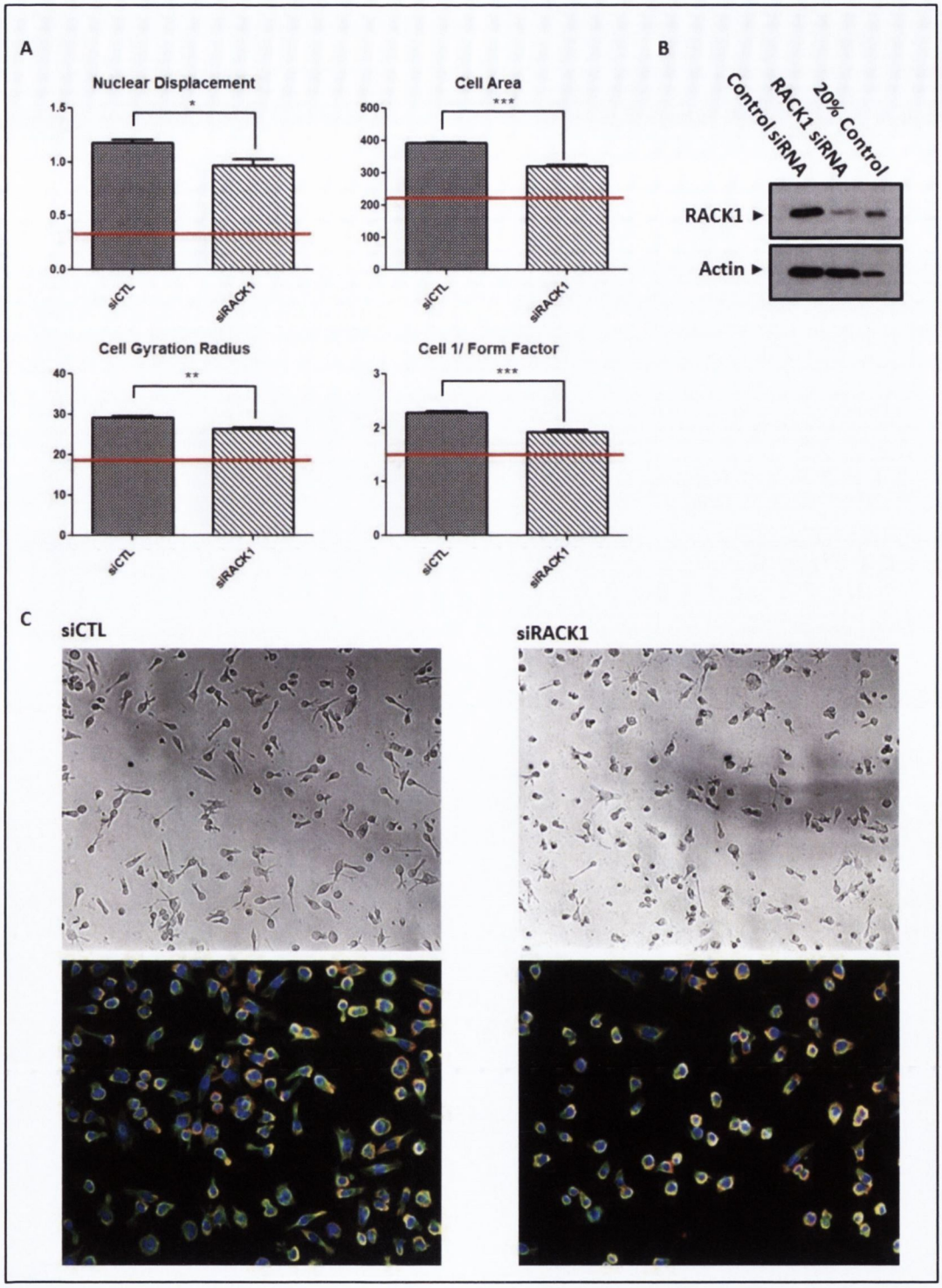

Figure 4.7: Polarisation Assay in PBTLs.

(A) Morphology parameter measurements based on F-actin staining for transfected PBTLs. The red line depicts the resting cell measurement. The mean and SEM of N=3 performed in triplicate is shown. * denotes $p < 0.05$, ** $p<0.01$, *** $p<0.001$ (B) Immunoblot shown illustrates protein knockdown in PBTLs. (C) Brightfield and IF staining of resting and LFA-1-induced migrating PBTLs. Nucleus in blue, actin in red, and alpha tubulin in green.

Table 4.2: Morphology parameter measurements based on F-actin staining for transfected PBTLs (N=3).

	PLL	ICAM-1		
	siCTL Mean ± SEM	siCTL Mean ± SEM	siRACK1 Mean ± SEM	P value
Cell 1/(form factor)	1.379 ± 0.0113	2.290 ± 0.0191	1.926 ± 0.0354	0.0008
Cell Area	213.4 ± 0.6953	391.8 ± 4.265	319.4 ± 6.140	0.0006
Cell Gyration Radius	18.82 ± 0.0428	29.30 ± 0.2853	26.51 ± 0.4081	0.0050
Nuclear Displacement	0.3676 ± 0.0029	1.181 ± 0.0274	0.9720 ± 0.0541	0.0262

4.3.6 KD of RACK1 Decreases Speed and Persistence of Migration in Primary T Cells

In order to further evaluate the consequence of depletion of RACK1 on T cell migration, we investigated measured the speed and persistence of cells stimulated with LFA-1 integrin and a uniform distribution of chemokine SDF-1α. The chemokinetic migration assay and cell tracking method are described in sections 2.8.2 and 2.8.3, respectively. Briefly, transfected PBTLs were enumerated and starved for 2 hours in serum-free RPMI. The cells were then incubated with immobilised ICAM-1 and SDF-1α, which induces random migration (Lefort and Kim 2010). Brightfield images of live cell migration were acquired every 30 seconds for 1 hour immediately after the cells were seeded with the 20X objective by the automated microscope IN Cell Analyzer 1000. The images were then processed in Image J using the plugin MtrackJ.

The results from four separate donor T cell populations demonstrated RACK1-deficient cells exhibited a reduced speed and persistence of LFA-1-mediated chemokinetic migration as compared to the control transfected cells (Figure 4.8A). Control transfected PBTLs exhibited a migratory velocity of approximately 20 μm/min, while cells with depleted levels of RACK1 migrated approximately 12 μm/min. This rate of migration is accordance with previous reports indicated PHA/IL-2-stimulated PBTLs exhibited a migratory velocity of approximately 15μm/min (Lefort and Kim 2010) indicating sufficient cell viability of the cultured PBTLs. Analysis of time-lapse microscopy indicated depletion of RACK1 prevented cell polarisation with a concomitant decrease in border complexity and number of cell processes characteristic of normal migrating T cells. However, many of the cells with depleted levels of RACK1 displayed a loss in polarity and exhibited multiple lamellipodia, which may explain the overall reduced speed and persistence. Further evaluation of migrating cells indicated siCTL cells exhibited a single broad lamellipodia, while RACK1-deficient cells displayed either a resting, non-responsive phenotype or multiple lamellipodia, both indicating a defect in polarity (Figure 4.8B). In addition, the RACK1-deficient cells frequently changed direction displaying a circuitous path profile, which likely contributes to the reduction in speed and persistence of migration. Certainly, the lack in polarity or formation of multiple leading edges in RACK1-deficient cells explains the reduction in measurements of cell morphology parameters. Analysis of time lapse microscopy of live cell migration of siCTL and siRACK1 PBTLs revealed the lamellipodia in control cells were highly dynamic and in many cells the lamellipodia underwent rapid changes in direction. The lamellipodia also often retracted

back into the cell, which was followed by the formation of a new lamellipodia in a different direction. In contrast, T lymphocytes with depleted levels of RACK1 made attempts at polarising but generated poorly-formed and less pronounced lamellipodia as well formation of multiple leading edges (supplementary videos).

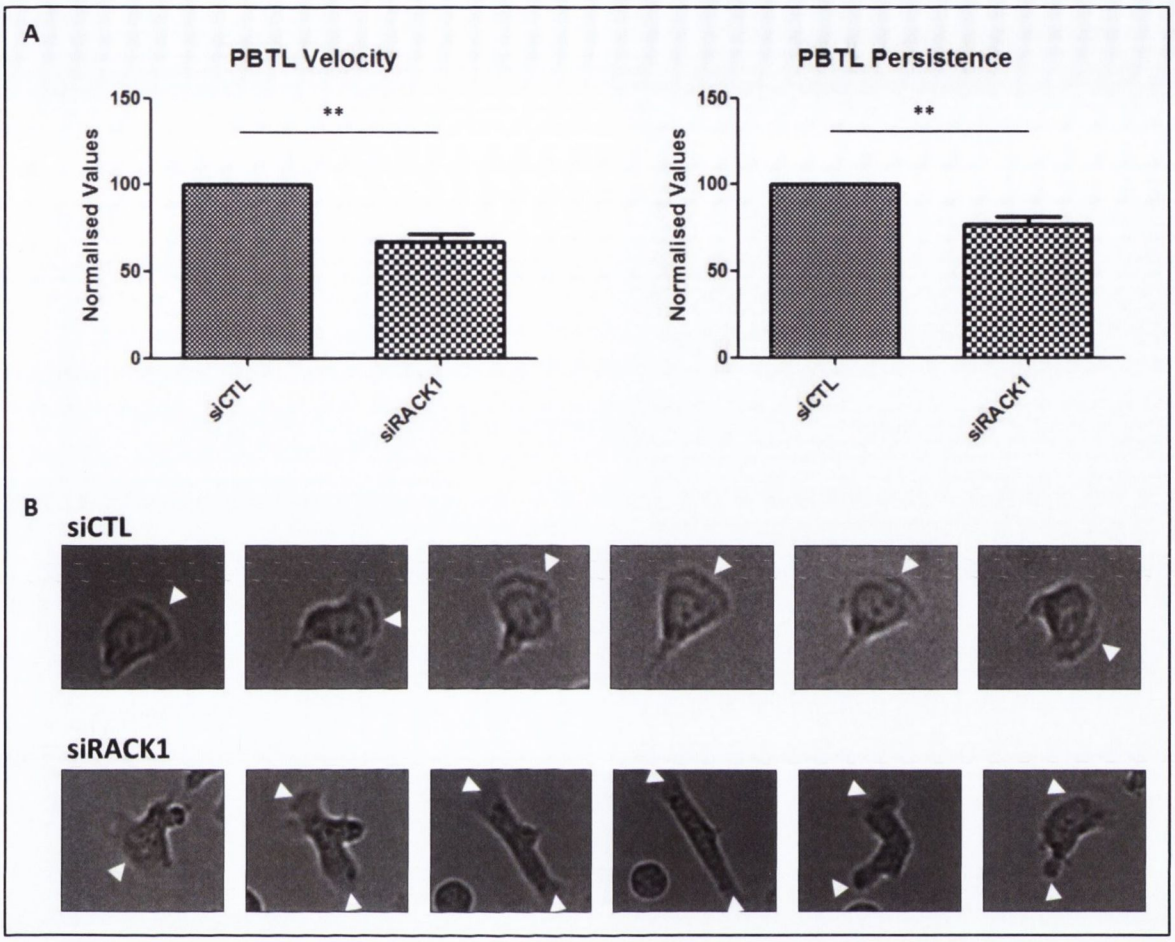

Figure 4.8: Depletion of RACK1 reduced speed and persistence of T cell chemokinetic migration.

(A) Speed and persistence measurement data of experimental means normalised to siCTL. The mean and SEM of N=4 performed in duplicate is shown. ** denotes $p< 0.01$ (B) Microscopic images at 20X of representative siCTL and siRACK1 migrating T cells. Each panel displays images of the same cell migrating on immobilised rhICAM1-/SDF-1α captured every 30sec over a three minute period. Arrowheads indicate leading edge of cell.

4.3.7 Depletion of RACK1 Does Not Affect Adhesion to ICAM1 in Primary T Cells

In order to ascertain whether or not RACK1 was involved in integrin LFA-1 avidity and affinity and subsequent adhesion to ICAM-1, the ICAM-1 adhesion assay was performed with primary T cells. The method optimised for PBTLs was modified slightly from the adhesion assay for HuT78 T cells by replacing the washing steps with reverse centrifugation as described in section 2.10. This ensured cells detachment was due to weak adherency and not from harsh washing steps, which may have been disrupting ligand/receptor adhesion.

Transfected PBTLs were serum starved for 2 h and then incubated on rhICAM-1 or PLL (positive control) and stimulated with the chemokine SDF-1α or divalent cations or unstimulated. The results from the adhesion assay with primary T cells indicated depletion of RACK did not significantly increase or decrease SDF-1α-stimulated T cell adhesion to ICAM-1 (Figure 4.9). The experiment was carried out in four separate donor T cell populations and there was significant variation between each cell population. This is expected due to the natural variation in the responsiveness of T cell populations from different individuals.

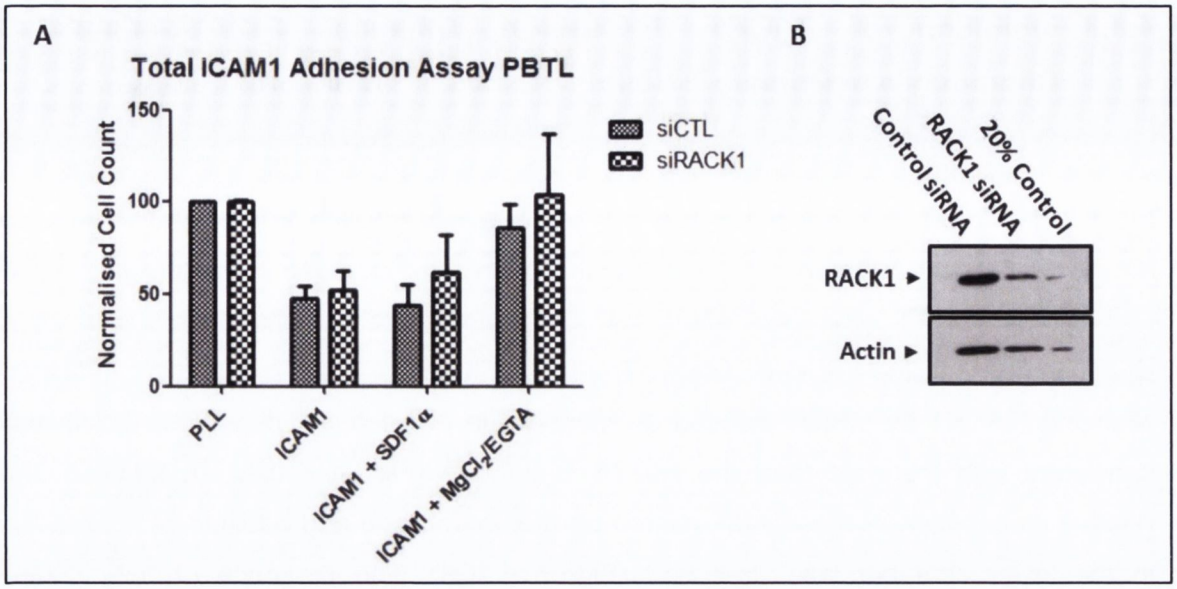

Figure 4.9: KD of RACK1 does not affect SDF1 stimulated T cell adhesion to ICAM1.

(A) Quantification of PBTLs transfected with RACK1-specific or control siRNA. The cells were harvested 72 hours after transfection and seeded on rhICAM-1 or PLL and stimulated with SDF1α, divalent cations, or left unstimulated. The mean ± SEM of N=4 performed in triplicate is shown. The cell counts were normalised to the input. (B) Immunoblot indicating level of protein knockdown 72 hours after transfection for primary T cells.

4.3.8 Inhibition of RACK1 Expression Enhances SDF-1α-stimulated Chemotaxis in Primary T Cells

In order to confirm the increased migratory ability due to depletion of RACK1 exhibited in the HuT78 T cell line, we performed the transwell assay with transfected PBTLs. In addition, because treatment with Nocodazole induced an increase in migratory ability in HuT78s, primary T cells pre-treated with the cytoskeletal inhibitor were used as a positive control in the transwell assay. The results from the PBTL experiment indicated silencing RACK1 by siRNA induced an increase in chemotactic migration, which was consistent with the data from the HuT78 T cell line (Figure 4.10A). In addition, the relative contribution of the ICAM1-coated porous membrane and addition of chemokine in the lower chamber was assessed (Figure 4.10B). The presence of both stimuli induced the greatest difference with RACK1-depleted cells having approximately a 2-fold increase in migratory ability over siCTL cells.

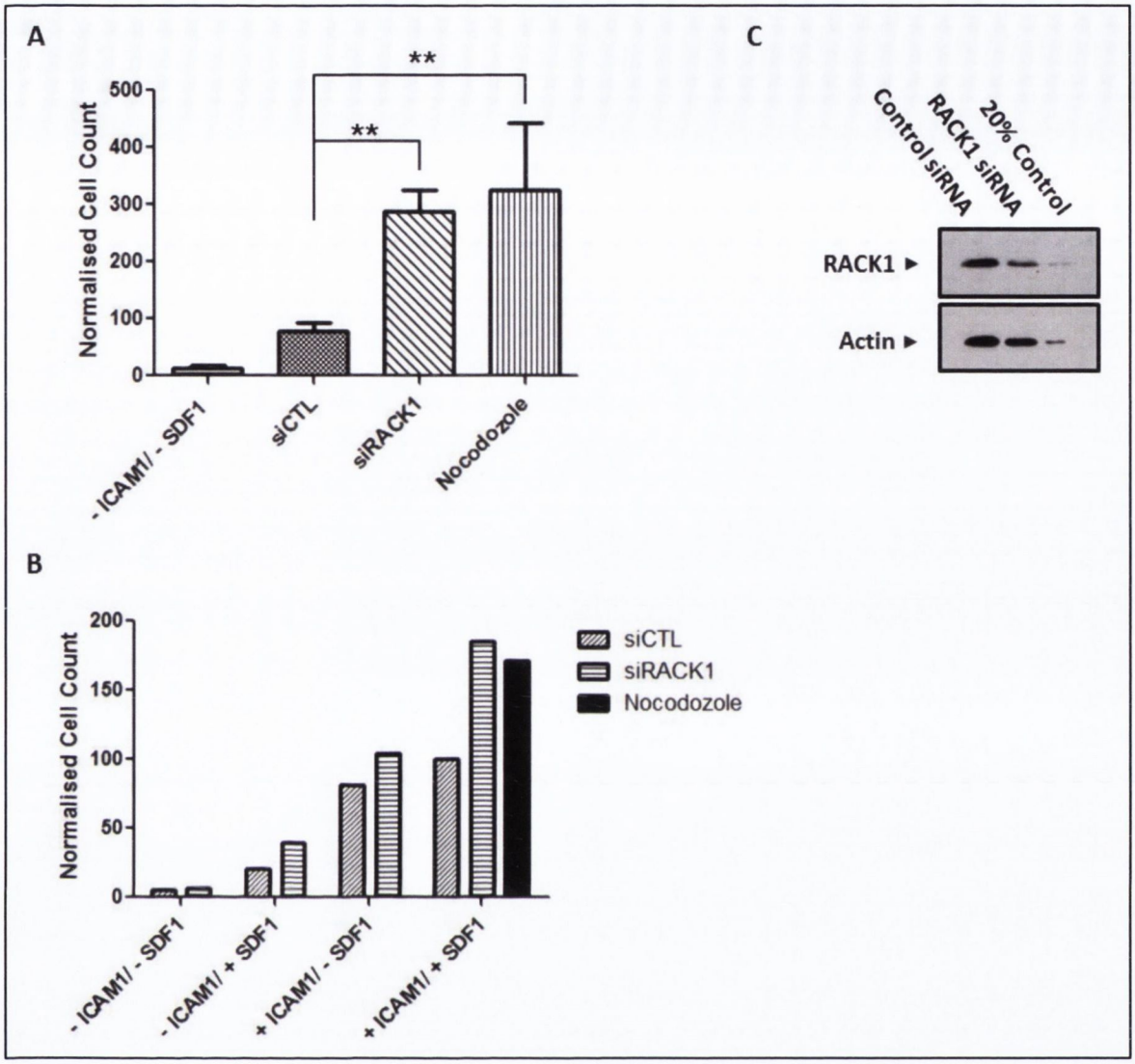

Figure 4.10: Suppression of RACK1 Enhances Chemotatic Migration, but not random migration in primary T cells.

(A) Quantification of PBTLs that underwent transwell migration in response to ICAM-1-coated filter and uniform distribution of SDF-1α. T cells were transfected with RACK1-specific or non-targeting control siRNA or pre-treated with Nocodazole (positive control). Cells were harvested 72 hours after transfection and seeded on rhICAM-1 or PLL and stimulated with SDF1α or left unstimulated. The cell count normalised to siCTL cells. The mean and SEM of N=3 performed in duplicate is shown. ** denotes $p< 0.005$. (B) Assessment of the relative contribution of the ICAM1-coated filter and addition of SDF-1α on the transwell system. The graph shown is representative of a single experiment performed in duplicate. Transwell contained ICAM1-coated membrane and SDF-1α unless otherwise noted. (C) Immunoblot indicating level of protein knockdown 72 hours after transfection for primary T cells.

4.3.9 Overexpression of RACK1 Inhibits SDF-1α-Stimulated Chemotaxis in Primary T Cells

We previously demonstrated depletion of RACK1 by siRNA enhanced chemotatic migration. Therefore, we sought to assess the effect of overexpression of RACK1 on both integrin-activated and chemokine-induced T cell migration. Nocodazole-treated cells also exhibited increased chemotatic migration. Thus, we hypothesised that overexpression of RACK1 would inhibit chemotatic migration and as well as attenuate the enhanced migration induced by Nocodazole. PBTLs were transfected with an EGFP-RACK1 or EGFP-control construct by Amaxa technology. Serum-starved PBTLs were then enumerated and loaded on to the transwell. As expected, RACK1 overexpression significantly decreased SDF-1α-stimulated chemotaxis and attenuated the enhanced chemotatic migration induced by Nocodazole (Figure 4.11). Moreover, cells overexpressing RACK1 and exposed to Nocodazole exhibited similar migratory ability to untreated cells. It is important to note that only cells expressing GFP were included in the cell count so as to compare the chemotaxis of cells expressing the EGFP-control construct to cells expressing the EGFP-RACK1 construct. Otherwise, the difference between cells expressing and not expressing high levels of GFP may have confounded the data.

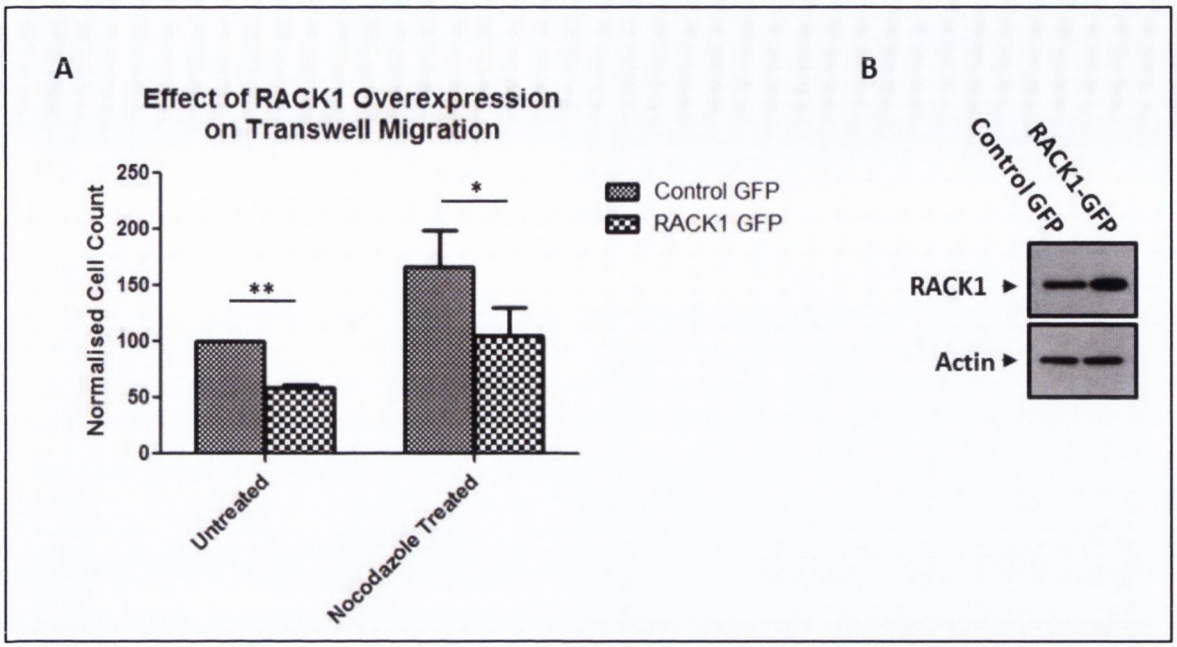

Figure 4.11: Overexpression of RACK1 inhibits SDF-1α-stimulated chemotaxis in primary T cells.

(A) Quantification of PBTLs that underwent transwell migration in response to ICAM-1-coated filter and uniform distribution of SDF-1α. T cells were transfected with RACK1-specific or non-targeting control siRNA or pre-treated with Nocodazole (positive control). Cells were harvested 72 hours after transfection and seeded on rhICAM-1 or PLL and stimulated with SDF1α. The cell count was normalised to the input. The mean and SEM of N=3 performed in duplicate. * denotes $p< 0.05$ and ** $p<0.01$. (B) Immunoblot indicating level of RACK1 protein expression 24 hours after control GFP or RACK1-GFP vector transfection in primary T cells.

4.4 Discussion

The role of RACK1 as a scaffold/adaptor protein involved in diverse cellular processes is well documented but widely varied. A number of published reports have implicated RACK1 in cell adhesion and migration, partially through its interaction with the a wide range of signalling kinases, including PKC β, PKC ε, Src, and FAK as well as with the cytosolic domain of membrane-bound receptors, such as beta integrins thereby integrating signals from various transduction pathways (Buensuceso et al. 2005; Buensuceso et al. 2001; Chang et al. 2001; Doan and Huttenlocher 2007; Liliental and Chang 1998; McCahill et al. 2002; Serrels et al. 2010). However, conflicting reports of RACK1 in either promoting or inhibiting cell migration are found in the literature, probably reflecting the context-dependent functions of RACK1. Certainly, RACK1 has been reported to facilitate cell migration and spreading in several adherent cell lines and tumour cells (Doan and Huttenlocher 2007; Kiely et al. 2008), while exhibiting a negative regulatory role in integrin-mediated migration in other cell types (Buensuceso et al. 2001; Chen et al. 2008).

The characterisation of RACK1 expression in T lymphocytes in the previous chapter indicated LFA-1 stimulation induces RACK1 translocation from a peripheral cytosolic localisation in the resting state to the leading edge and trailing uropod in polarised migrating cells. In addition, suppression of RACK1 by RNAi inhibited recruitment of PKC ζ to the leading edge of the cell. This anterior/posterior distribution in association with key polarity regulator PKC ζ implicates a role for RACK1 in the regulation of T cell polarity. In this chapter, the potential downstream events following targeted manipulation of RACK1 were explored in primary T cells and the T lymphoma HuT78 cell line. To further evaluate the role of RACK1 in integrin-mediated T cell migration, endogenous expression of RACK1 was attenuated by RNAi enabling the analysis of protein function. The effects of RACK1 depletion were quantitatively assessed by utilising an HCA-based platform previously described (Freeley et al., 2010). The use of automated microscopic analysis has been previously employed by our group to determine the effect of known pharmacological inhibitors on LFA-1-mediated T lymphocyte morphology. Key sets of parameters used to quantitatively assess effects on lymphocyte morphology were identified. The multi-parametric analysis of lymphocyte morphology was employed in this study to characterise RACK1 function in integrin-mediated and chemokine-induced T cell migration. Selected morphology parameters were significantly reduced in RACK1-deficient cells compared to control cells indicating a significant decrease in T cell

polarisation. The same effect was observed in both the T cell line HuT78 as well as in primary T cells. Moreover, depletion of RACK1 prevented formation of stable uropod structures, which could dictate the axis of migration. Similar to RACK1-deficient cells, cells treated with the MT depolymerising agent Nocodazole exhibited a reduction in morphological polarisation and a stunted uropod phenotype. This is in accordance with a previous study which reported Nocodazole-treated cells do not form a stable uropod structure, but rather small, uropod-like protrusions (Takesono et al. 2010).

RACK1-deficient PBTLs exhibited a significant reduction in the speed and persistence of LFA-1-mediated migration. Analysis of time-lapse microscopy indicated depletion of RACK1 prevented cell polarisation with a concomitant decrease in border complexity and number of cell processes characteristic of normal migrating T cells. This is in accordance with the reduced morphology parameter measurements exhibited by RACK1-deficient cells. However, many of the cells with depleted levels of RACK1 did not exhibit typical anterior/posterior polarisation, but rather a rounded, non-responsive phenotype or an elongated morphology due to formation of multiple lamellipodia. In addition, the RACK1-deficient cells frequently changed direction and presented a circuitous path profile, which would explain the reduction in persistence of migration. This type of migratory path profile with frequent turning has previously been reported in cells treated with Nocodazole (Takesono et al. 2010). The authors proposed the inhibitor-treated cells migrated by membrane blebbing rather than lamellipodia extension. Indeed, RACK1-deficient cells lacked a single extending lamellipodia, and migration was accompanied by multidirectional protrusions, which appeared to inhibit directional cell migration. This finding strongly suggests that RACK1 is involved in regulating polarity in T lymphocytes.

In order to further characterise RACK1 function in LFA-1-mediated T cell migration, we assessed the effects of depletion of RACK1 on LFA-1 avidity and affinity and subsequent adhesion to ICAM-1 in chemokine-induced cells. In our studies, we did not detect a role in adhesion to ICAM1 for RACK1 in primary T cells. This is in accordance with a previous observation that suppression of RACK1 did not effect adherency to ICAM-1 in the Jurkat leukemic T cell line (Chen et al. 2008). Therefore, RACK1 is required for SDF-1α-mediated lymphocyte migration on the integrin ligand ICAM-1 by influencing velocity and directionality but in a manner that is independent of LFA-1 integrin activation or adhesion.

Both RACK-1-deficient HuT78 and primary T cells exhibited an increased chemotatic migratory ability, whereas overexpression of full-length RACK1 inhibited SDF-1α-

stimulated chemotaxis. This is in accordance with another study which reported RACK1 negatively regulated cell migration in Jurkat T cells. The authors showed that down regulation of RACK1 enhanced chemotaxis, while overexpression of RACK1 inhibited chemotatic migration. In addition, the authors demonstrated RACK1 interacts with the heterotrimeric G protein Gβγ at the leading edge of cells and inhibits Gβγ-mediated P13Kγ activation and subsequent generation of Phosphatidylinositol (3,4,5)-triphosphate (PIP_3) (Chen et al. 2008), which is necessary to promote pseudopod formation and directed cell migration (Wang et al. 2002; Weiner et al. 2002). Moreover, the authors reported that overexpression of a RACK1 mutant lacking the PKC β and Src binding domain inhibited chemotaxis similar to full-length RACK1 suggesting that RACK1 is unlikely to modulate leukocyte migration through its effect on the activity of focal adhesions involving PKC β, Src, or integrins. As shown in Chapter 3 of this study, PKC β was not enriched at the leading edge in association with RACK1 suggesting they do not interact in LFA-1-stiumlated migrating T cells. Similarly, the authors did not detect an interaction of RACK1 with PKC β or Src in Jurkat T cells nor did inhibition of Src, PKCβ/ε, and MAPK by pharmacological inhibitors have an effect on SDF-1α-stimulated Jurkat cell transmigration. Another study also reported overexpression of full-length RACK1 inhibited chemotaxis, but not random migration (Cox et al. 2003). Similarly, in this study, we demonstrated suppression of RACK1 decreased migratory persistence suggesting RACK1 may be involved in regulating directional cell migration. Unlike Chen and colleagues, though, RACK1 was reported to localise to nascent focal adhesion complexes and negatively regulated integrin-mediated adhesion, protrusion, and chemotatic migration via its interaction with Src (Cox et al. 2003). This experiment, however, was carried out in Chinese hamster ovary (CHO)-K1 fibroblast-like cells as opposed to lymphocytes, which do not exhibit focal adhesion complexes characteristic of adherent cells.

Therefore, the role of RACK1 in integrin-mediated adhesion and migration appears to be cell-type and context dependent. For instance, in adherent cells, which form large focal adhesion complexes in association with beta integrin, RACK1 may recruit key signalling kinases to the plasma membrane, such as Src and FAK, to facilitate integrin-mediated cell spreading and migration. While overexpression of RACK1 is generally associated with increased cell spreading and tumour metastasis, elevated levels of RACK1 have also been shown to inhibit fibroblast cell migration via an excess formation of actin stress fibers and focal adhesions (Buensuceso et al. 2001). Alternatively, lymphocytes do not exhibit typical focal contact, which is thought to facilitate rapid migration. Therefore,

RACK1 may prevent the formation of stable focal adhesion contacts and facilitate a more transient integrin-mediated adhesion necessary for increased migratory speed. Furthermore, RACK1 overexpression did not effect PI3K pathway activation in fibroblast or epithelial cells (Chen et al. 2008; Hermanto et al. 2002); however, transfection with full length RACK1 did inhibit Gβγ-induced PI3K activity in the leukemic Jurkat T cell line. Therefore, chemokine receptor activation may induce immune cell-specific signalling pathways necessary for chemotaxis. These conflicting reports only further demonstrate the complex regulatory role of RACK1 in mediating migration according to different cells, tissues, and stimuli.

While our transwell chemotaxis assay was designed in accordance with other published methods using a modified Boyden chamber to measure chemotatic migration (Chen et al. 2008; Takesono et al. 2010; Vicente-manzanares et al. 2002), the concentration of chemokine gradually becomes distributed throughout the transwell, and thus may confound the data. In this method, the cells are exposed to a steep, yet transient chemoattractant gradient, which is thought to be a poor representation of gradients found in tissues (Lauffenburger et al. 1988). Ideally, chemotaxis should be measured by stimulating migration of cells toward a chemoattractant gradient. One particular assay, known as the under-agarose chemotaxis assay, involves filling a well with agarose, cutting two holes in either side of the well, and loading the cells in one and the chemoattractant in the other (Newton-Nash et al. 1990). The gradient that develops in the agarose is shallow and is thought to be an appropriate representation of naturally occurring gradients. Nevertheless, both the transwell and under-agarose chemotaxis assays are usually configured as end-point assays, only quantifying the number of cells which successfully undergo chemotaxis and not monitoring the type of migration (e.g. lamellipodial extension versus membrane blebbing). A recent study has demonstrated the use of video microscopy of to monitor chemotatic migrating cells in real time using electric currents (Pietrosimone et al. 2012). This technology has recently been patented and will be commercially available from Applied Biophysics, Inc. for future chemotaxis experiments. Another method recently developed involves measuring transendothelial migration under shear forces, which was designed to mimic the *in vivo* conditions of lymphocyte adhesion to the endothelium under blood flow (Shulman and Alon 2009). The assay enables *in vitro* live imaging microscopy tracking and dissection of leukocyte adhesion, motility, and crossing of endothelial barriers in real time and under physiologic flow conditions. This type of assay has been developed by our group in collaboration with Cellix Ltd. (Dublin, Ireland) to determine the effect of protein KD on TEM under

physiologic flow conditions (Freeley et. al., in press). Indeed, assessing the effects of altered levels of RACK1 on chemokine-induced TEM under shear flow would be an informative experiment and should be pursued in future research. Nevertheless, a search through the canonical literature indicates that the modified Boyden chamber is currently the primary method for chemotaxis assays, particularly for SDF-1α stimulation of T cell migration.

Interestingly, both depletion of RACK1 and pre-treatment with the MT depolymerising agent Nocodazole reduced cell polarisation but enhanced SDF-1α-stimulated chemotaxis of T cells. Nocodazole induces MT depolymerisation and subsequent release of the MT-associated Rho guanine exchange factor (GEF), GEF-H1 (Chang et al. 2006; Krendel et al. 2002). Free GEF-H1 activates RhoA and Rho coiled-coiled kinase (ROCK) phosphorylation of myosin light chain at serine19, which induces myosin contraction and the assembly of actin stress fibers and focal adhesions (Amano et al. 1997; Krendel et al. 2002). Both treatment with Nocodazole and overexpression of MT-binding deficient GEF-H1 have been shown to induce Rho-dependent actin stress fibre formation and contractile cell morphology in HeLa cells (Chang et al. 2008). Therefore, suppression of RACK1 may mimic the enhanced chemotatic ability exhibited by cells treated with Nocodazole by activating RhoA and actomyosin-based cell contractility. In our study, both depletion of RACK1 and drug-induced MT depolymerisation induced a contractile morphology in T cells with reduced cell polarity, which appeared to enhance chemotaxis in the HuT78 T cell lymphoma and primary T cells. Our data suggests RACK1 may mediate RhoA activity during directional cell migration. However, previous reports indicate RACK1 did not significantly affect RhoA activity, but did influence the activity of other signalling pathways downstream of SDF1/CXCR4, such as the PI3Kγ/Akt pathway, in the Jurkat T cell line (Chen et al. 2008). Nevertheless, the effect of RACK1 expression on SDF-1α-induced signalling pathways, including RhoA activation, should be examined in primary T cells.

A recent study reported exposure to Nocodazole increased the speed and distance of chemokinetic migration, in CCRF-CEM cells, a T lymphoblast-like cell (Takesono et al. 2010). However, the authors also reported a reduction in SDF-1α-stimulated chemotaxis, suggesting drug-induced MT depolymerisation enhances random migration. It is important to note that the data indicates only 5% of cells from the input successfully transmigrated in their system compared to 3% of Nocodazole-treated cells. This is contrast to our chemotaxis studies, where approximately 20% of control cells from the input successfully transmigrated. Moreover, as expected the data was more consistent in

experiments using the transformed T cell line than primary T cells, representing an increased variation between donor T cell populations. These conflicting data may also be explained by the concentration and time the Nocodazole was added to the cells. For instance, the authors indicated they added 20 μM Nocodazole to the growth medium in the transwell, while in our study cells were exposed to 5 μM Nocodazole for 30 min prior to the assay.

4.4.1 Conclusion

Through the use of HuT78 and primary T cells, our data unambiguously demonstrate that RACK1 has a regulatory role in T lymphocyte polarity and motility. Whereby, RACK1 is required for cell polarisation, but interfering with its expression can either enhance (suppression) or inhibit (overexpression) migration, suggesting the cellular balance of RACK1 is crucial for proper functioning. Therefore, we propose RACK1 is a negative regulator of directed cell migration in T lymphocytes.

CHAPTER FIVE

Identification of RACK1-associated Proteins by a Proteomic Approach

5 Identification of RACK1-associated Proteins by a Proteomic Approach

5.1 Introduction

As its name implies, RACK1 was first identified as a PKC-targeting protein. However, it is now well established that RACK1 interacts with a large number of proteins either directly or as part of a complex, implicating a role in cellular development, immune regulation, cytoskeletal remodelling, and protein synthesis (Adams et al. 2011; McCahill et al. 2002). As described in section 1.9, the structure of RACK1 facilitates protein binding and protein interactions with RACK1 have been shown to be either constitutive or stimulus-dependent. Adaptor proteins like RACK1 can assemble and compartmentalise multiple signalling and structural molecules, thereby providing a platform for their targeted positioning and efficient interactions (Adams et al. 2011; Pawson and Scott 1997). Because of its ability to coordinate the interaction of key signalling molecules, RACK1 is considered to play a central role in critical biological responses, including cell growth and homeostasis (Besson et al. 2002).

Due to its ubiquitous expression in almost all cell types and putative molecular scaffolding role, RACK1 has routinely been identified by proteomic profiling of diverse proteins/protein complexes. For instance, RACK1 has previously been identified in several mass spectrometric analyses of eukaryotic ribosome subunits and ribosomal-associated proteins (Jastrzebski et al. 2011; Link et al. 1999; Sengupta et al. 2004; Yu et al. 2005). Further studies have validated these associations and RACK1 has been shown to interact with the 40S subunit of the eukaryotic ribosome, where it has been shown to recruit kinases, including PKC, to stimulate phosphorylation-induced subunit assembly and initiation of translation of specific mRNAs (Sengupta et al. 2004; Shor et al. 2003).

In addition, RACK1 has been reported to be differentially expressed in a number of comparative proteomics studies of tumourigenesis and angiogenically active tissues. For example, RACK1 was shown to be differentially expressed in a CHO cell line that overexpressed the apoptosis inhibitor Bcl-X(L) gene. Moreover, RACK1 has been identified as a cancer biomarker in several studies. For instance, RACK1 was identified in a comparative proteomics approach used to identify differentially expressed proteins in oral squamous carcinoma cells (Wang et al. 2008). RACK1 is up-regulated in oral

squamous carcinoma, and was linked to clinical invasiveness and metastasis in carcinogenesis. The authors proposed RACK1 as a therapeutic target as RNAi specifically targeted to silence RACK1 could initiate apoptosis of oral squamous carcinoma cells. RACK1 has also been shown to promote breast carcinoma proliferation and invasion/metastasis *in vitro* and *in vivo* by activation of the RhoA/Rho kinase pathway. Because of its role in breast cancer invasion and metastasis, RACK1 has been identified as an independent prognostic indicator in poor clinical outcome in breast carcinoma (Cao et al. 2010). Therefore, these data suggest differential expression of RACK1 alters effector protein signalling pathways, which can have devastating effects on cell growth and development and is associated with tumourigenesis. As the main target of tumour-promoting phorbol esters, PKC signalling is known to play an important role in angiogenesis and tumour growth (Hofmann 2004; Lahn et al. 2006; Mischiati et al. 2008). Therefore, the level of RACK1 expression may be relevant to the activity of downstream signalling of PKC in angiogenically active tissues. These observations suggest that RACK1 may be a potential biomarker for early diagnosis and prognosis of several types of cancers as well as a novel target for anti-cancer therapies.

5.2 Objectives

Indeed, a number of binding partners have been identified for RACK1 in a variety of cell type-dependent contexts; however, there is a paucity of information regarding its precise function in these cells, particularly in human lymphocytes. Improved knowledge about the regulation of RACK1 and effector proteins is critical to understanding RACK1 involvement in lymphocyte migration required for an effective immune response and homeostasis. Yet, an in depth characterisation of proteins associated with RACK1 in lymphocytes has never been explored. Therefore, our aim was to identify proteins associated with RACK1 in T cells to further elucidate the regulatory role of RACK1 in T lymphocyte polarity and motility. We employed a targeted proteomics approach to identify putative binding partners for RACK1. Specifically, we were interested in identifying stimulus-dependent interactions resulting from LFA-1-induction of migration in T cells. Identifying differences in RACK1 protein associations in resting and LFA-1-stimulated migrating T cells will facilitate our understanding of the molecular mechanisms underlying RACK1 regulation of integrin-mediated migration. In order to isolate RACK1-associated proteins, resting and migrating T cells were lysed and immuno-affinity isolated using a RACK1-specific antibody (section 2.25). The RACK1 isolated proteins were then resolved by SDS-PAGE and subjected to mass spectrometric analysis and

bioinformatic analysis to identify putative binding partners for RACK1 (section 2.28). An experimental flow chart is displayed in Figure 5.1.

To achieve this aim, our specific objectives were to:

1.) Examine the RACK1-associated protein profile of resting and LFA-1-induced migrating T cells by immunoprecipitation.
2.) Identify RACK1-interacting proteins by mass spectrometry.
3.) Validate the mass spectrometry results by analysing a subsection of protein hits by co-immunoprecipitation and immunocytochemistry.
4.) Characterise the proteins identified to associate with RACK1 following LFA-1 stimulation by bioinformatic analysis.

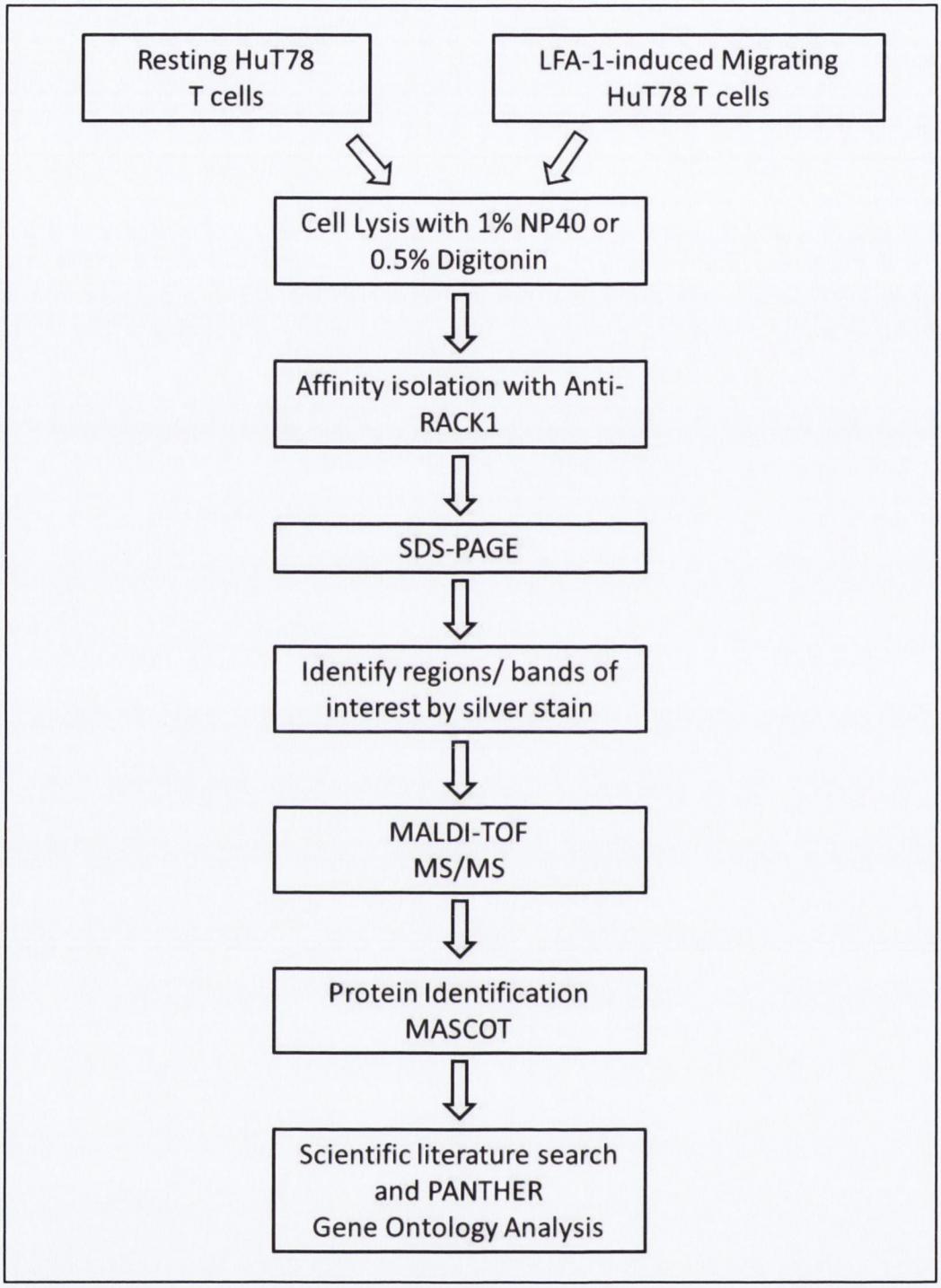

Figure 5.1: Experimental schema employed for identification of RACK1-associated proteins.

Resting or LFA-1-induced migrating T cells were lysed, immuno-affinity purified with RACK1-specfic antibody, and resolved by SDS-PAGE. The gel was then silver stained and regions/bands of interest were excised and subjected to mass spectrometric analysis for identification. The data was then mapped to the PANTHER database and categorised by Gene Ontology as well as known molecular functions according to the published scientific literature.

5.3 Results

5.3.1 Isolation of RACK1 Immunoprecipitates

Crosslinking of LFA-1 integrin receptor with monoclonal antibodies mimics multivalent interactions with natural ligands and has successfully been used as a model to study intracellular signalling processes (El Din El Homasany et al. 2005; Verma et al. 2009; Verma et al. 2008; Volkov et al. 2001). In the present study, we employed the *in vitro* LFA-1-mediated migration assay to stimulate polarisation and migration in HuT78 T cells. As previously shown in this study, LFA-1 stimulation with immobilised anti-LFA-1 induces a polarised cell morphology and activates signal transduction cascades necessary for T cell migration.

To investigate the effect of activation of LFA-1 on the repertoire of proteins associated with RACK1, we examined the cell lysates of resting and LFA-1-induced migrating T cells. The cells were lysed with two types of cell lysis buffers to compare the preservation of RACK1-associatied complexes by immunoprecipitation. RACK1 has previously been isolated using a cell lysis method containing 1% Nonidet P-40 or 0.5% Digitonin, which are utilised for their mild lytic properties and are known to preserve the cytoskeleton and associated elements (Kiely et al. 2006). The protein samples were immunoprecipitated with RACK1-specific antibody or non-specific IgM antibody (isotype control) and separated by SDS-PAGE. The gels were then stained with Coomassie Brilliant Blue stain or silver nitrate in order to visualise the proteome profile and compare RACK1-interacting proteins isolated in the resting and migrating states (Figure 5.2). Because it reversibly stains the protein present and is mass spectrometry compatible, Coomassie Blue stain method described in section 2.26 was employed first in order to distinguish banding patterns. While several bands were observed including the heavy and light chains of the antibodies utilised in the assay, the detail of the banding patterns was not sufficient for detecting differences in between resting and migrating T cells. Therefore, the experiment was repeated increasing the protein concentration, and the gel was stained with mass spectrometry-compatible silver nitrate stain method described in section 2.27. While this silver stain technique does not use formaldehyde in the staining process, which allows the gel to be subsequently analysed by mass spectrometry, the stain appears quickly and is irreversible. Nevertheless, silver stain techniques can allow protein detection in the very low nanogram range (even subnanogram), in that, they are 30–100 times more sensitive than colloidal Coomassie blue staining (Chevallet et al. 2006; Neuhoff et al. 1988) and enabled the visualisation of the differential banding patterns in resting and

migrating T cells. The results indicated RACK1 interacts with a different repertoire of proteins/protein complexes following LFA-1 activation. In addition, RACK1 appeared to interact with an increased number of proteins in polarised migrating T cells. Moreover, the banding patterns in the samples from both lysis buffers were similar indicating comparable preservation of RACK1 affinity purified proteins.

We identified segments exhibiting differential banding patterns following LFA-1 crosslinking. The segments of interest and equivalent IP controls were excised from the gel. These segments were subjected to mass spectrometry analysis as described in section 2.28. A total of 378 proteins were identified.

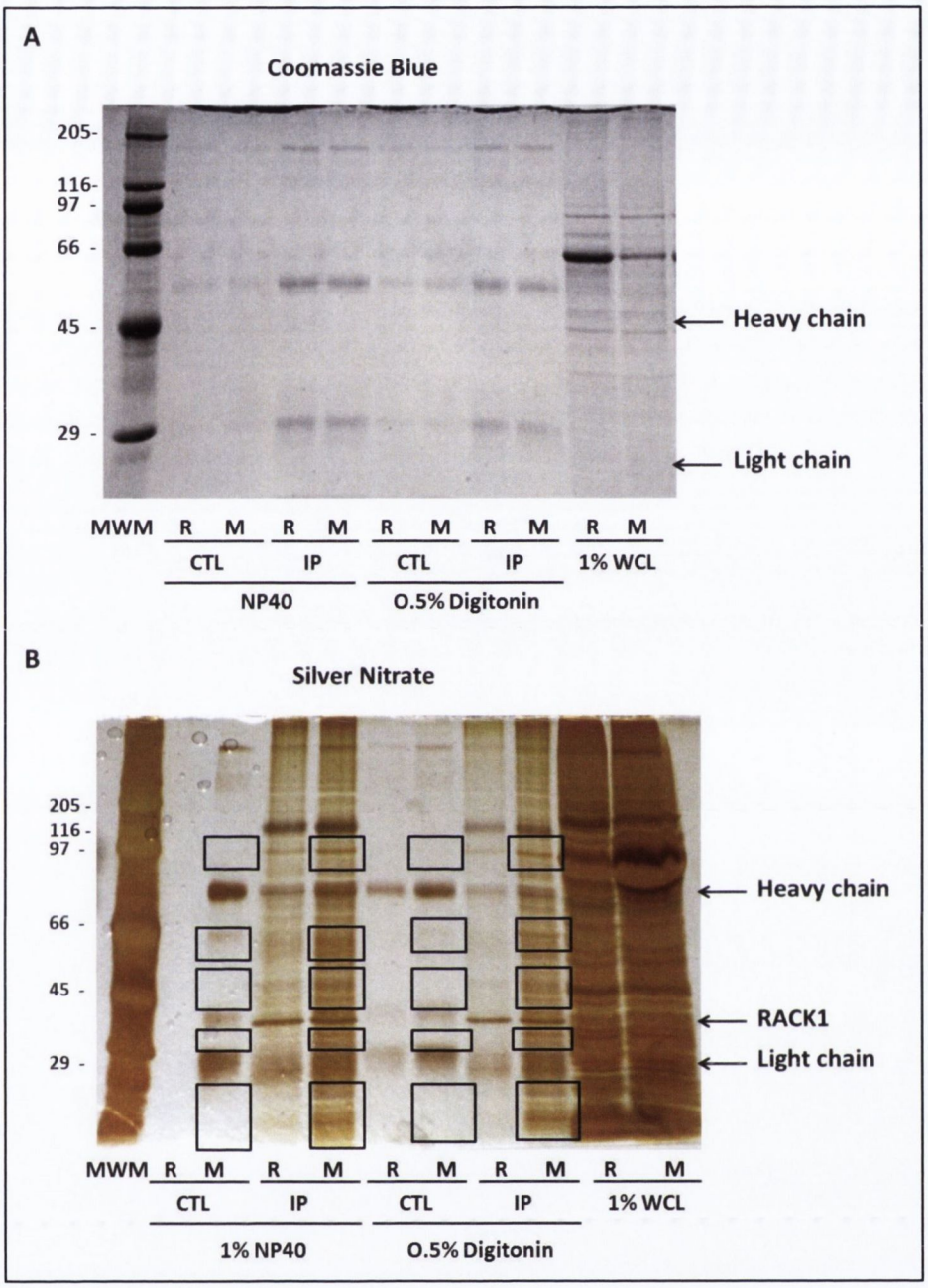

Figure 5.2: Coomassie Blue and silver nitrate staining of protein samples from resting and LFA-1-induced migrating T cells.

(A) Resting (R) and LFA-1-induced migrating (M) HuT78 T cells were lysed in cell lysis buffer containing 1% NP40 or 0.5% Digitonin, precipitated with anti-RACK1 antibody (IP) or control IgM antibody (CTL), and resolved on a 10% acrylamide gel by electrophoresis. The gel was stained with Coomassie Blue. (B) Same as A, but stained with mass spectrometry-compatible silver nitrate. Regions of interest excised from migrating T cell line and appropriate control IP lane and subjected to mass spectrometric analysis are indicated. 1% of the whole cell lysate (WCL) was included an input control. Arrows indicate antibody heavy and light chains at 50 and 25 kDa in size, respectively, as well as a probable RACK1 band visible in the 36kDa protein size range.

5.3.2 Categorisation of Proteins Identified by Mass Spectrometry

The results yielded high mascot scores and identified probable protein hits based on the frequency of peptides identified specific for a known protein by searching against the *Homo sapiens* NCBInr database. The results from the mass spectrometry analysis are arranged in order of decreasing mascot score in Appendix 1 Table 1. The protein hits were scrutinised through an extensive search through the scientific literature and are categorised by known function in Appendix 1 Table 2. In addition, we used PANTHER (Protein ANalysis Through Evolutionary Relationships, www.pantherdb.org) Gene Ontology to categorise all the proteins identified in the mass spectrometry analysis based on their molecular functions. The database was able to map 188 proteins from the analysis as some of the peptide hits had unique protein accession numbers but had not yet been documented in the search database (e.g. unknown protein). Appendix 1 Figure 1 depicts the observed versus the expected frequency of genes in any category for *H. sapiens*.

As expected, RACK1 (listed as GNB2L1: guanine nucleotide binding protein (G protein), beta polypeptide 2-like 1) had one of the highest Mascot scores. Notably, the RACK1 proteomic profile was in enriched in proteins involved in:

- Signal Transduction
- Cytoskeleton
- RNA maturation and protein biosynthesis
- Transcription Regulation
- Metabolic Enzymes
- Miscellaneous functions

Furthermore, a number of proteins identified in the mass spectrometry analysis have previously been reported to interact with RACK1 in various cell types and are discussed further in section 5.4.

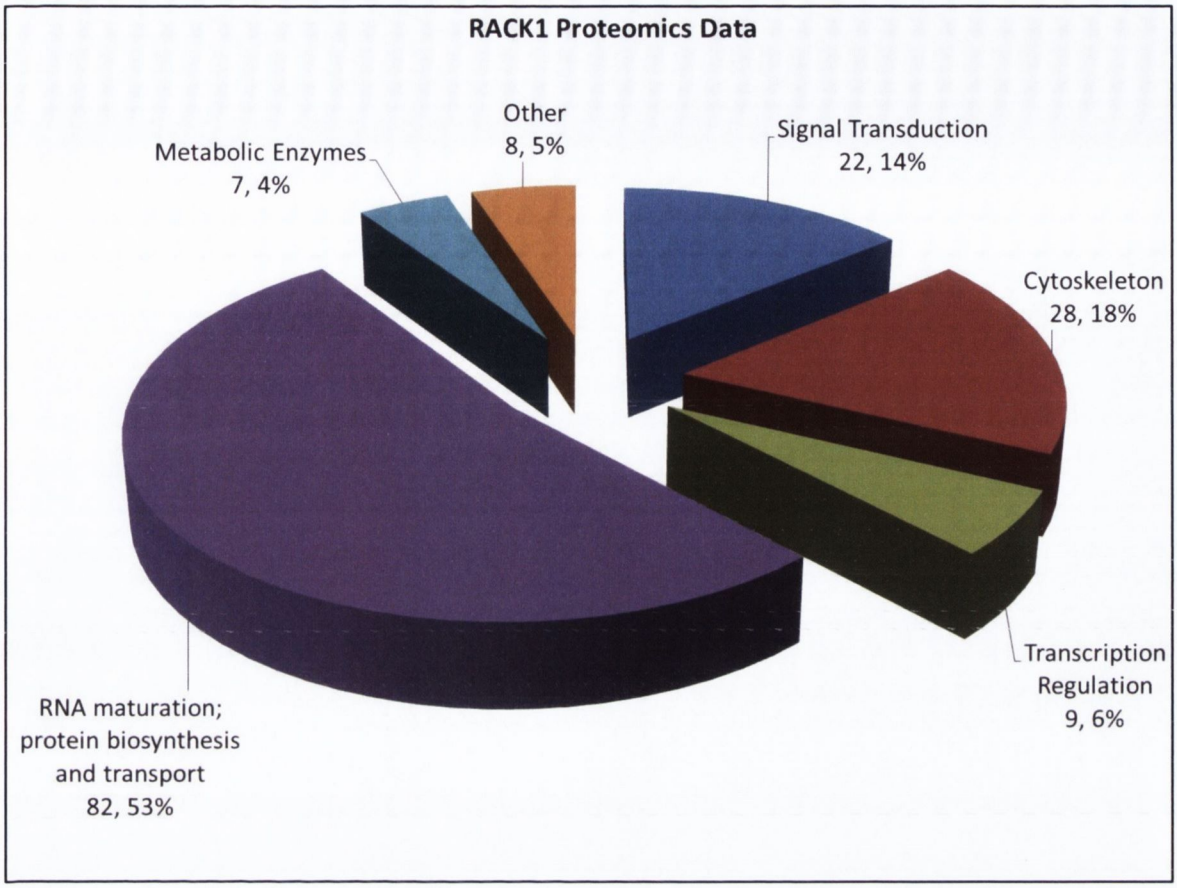

Figure 5.3: RACK1 Proteomics Data.

Proteins identified from anti-RACK1 affinity purification and mass spectrometric analysis were categorised based on known molecular function by searching NCBI database. Unknown proteins were excluded. The value and percentage of the total number of proteins is shown.

5.3.3 Validation of Mass Spectrometry by Immuno-assay Studies

In order to validate protein hits identified by mass spectrometry, the endogenous interaction between RACK1 and a number of candidate proteins was evaluated by immuno-assays. Resting and LFA-1-stimulated migrating T cells were lysed and immuno-affinity isolated with a RACK1-specific antibody or control anti-IgM. The protein samples were separated by SDS-PAGE, immunoblotted, and probed with an antibody specific for the protein of interest. Due to RACK1's putative role in cytoskeletal remodelling, the cytoskeletal components that were identified by mass spectrometry, including tubulin, vimentin, and myosin were used to validate the mass spectrometry data.

Due to differential preservation of proteins with the NP-40- and Digitonin-based lysis buffers, the cell lysis method was optimised by determining the cell lysis buffer which best preserved RACK1 in preparation for the immunoprecipitation studies. Therefore, resting and LFA-1-induced migrating T cells were lysed with either buffer and immunoprecipitated with RACK1-specific antibody or anti-IgM control antibody. The immunoprecipitates were separated by SDS-PAGE and immunoblotted with RACK1 antisera to compare the relative amount of RACK1 protein immunoprecipitated. As shown in Figure 5.4A, significantly more RACK1 protein was immuno-affinity purified in cells lysed with NP40 than Digitonin and was thus used in further immunoprecipitation experiments. In addition, 1% of the protein sample before and after immunoprecipitation was probed for RACK1, which indicated the efficiency of the IP reaction, or the amount of RACK1 protein isolated from the cell lysates (Figure 5.4B).

5.3.3.1 Vimentin

The endogenous interaction between RACK1 and Vimentin was investigated by co-immunoprecipitation. Vimentin, with a predicted molecular weight of 57 kDa, is the major structural component of intermediate filaments. Generally, intermediate filaments, along with the actin and MT cytoskeleton, are responsible for maintaining cellular shape and integrity. However, Vimentin exists as a dynamic structure and thus provides flexibility to the cytoskeleton (Goldman et al. 1996). Vimentin plays a significant role in supporting and anchoring the position of the organelles in the cytosol, including the nucleus, endoplasmic reticulum, and mitochondria (Katsumoto et al. 1990). Vimentin has also been implicated as a key regulator of diverse cell processes including adhesion, migration, and signalling (Ivaska et al. 2007). Phosphorylation is a key regulator of

intermediate filaments dynamics, modulating the organisation and subcellular distribution of intermediate filament proteins (Omary et al. 2006). In addition, the assembly/disassembly of intermediate filaments is dependent on numerous phosphorylation sites on exposed N' and C' terminal domains (Eriksson et al. 2004). A number of serine/threonine kinases have been implicated in the highly complex phosphorylation pattern of Vimentin, including PKCs, which are responsible for the regulation of integrin-mediated cell adhesion and the recycling of integrin receptors to facilitate directional cell migration (Ivaska et al. 2007). For instance, PKC ε-dependent phosphorylation of Vimentin has been shown to be essential for integrin recycling facilitating directional cell migration (Ivaska et al. 2005). Vimentin is the major intermediate filament protein present in leukocytes and has previously been implicated in lymphocyte adhesion and transmigration. For instance, the Vimentin network plays a crucial role both in the attachment of lymphocytes to the vascular endothelium and in the transcellular migration of lymphocytes through individual endothelial cells (Nieminen et al. 2006). In addition, lymphocytes from Vimentin-deficient mice had a reduced capacity to home to lymph nodes and a compromised ability to extravasate into inflamed tissues (Nieminen et al. 2006).

Co-immunoprecipitation (co-IP) confirmed that both hyperphosphorylated and hypophosphorylated Vimentin associated with RACK1 (Figure 5.4C). Hyperphosphorylated Vimentin was detected in both the resting and migrating RACK1 immunoprecipitates. However, hypophosphorylated Vimentin was only detected in the migrating protein samples. Indeed, both forms were detected in the whole cell lysate sample. Therefore, the data suggests that RACK1 interacts with hyperphosphorylated vimentin in both resting and LFA-1-induced migrating T cells, but only engages hypophosphorylated vimentin in migrating T cells. Intermediate filaments constitute at least 1% of total protein in the cell (Ivaska et al. 2007), which may explain why a protein band is present in one of the control IP lanes. The interaction between Vimentin and RACK1 in T cells is a novel observation and may implicate RACK1 in the regulation of lymphocyte morphology through PKC-dependent phosphorylation of Vimentin.

5.3.3.2 Non-muscle Myosin Heavy Chain- IIA (NMHC-IIA)

The next candidate protein was the heavy chain of non-muscle myosin IIA (MIIA). As described in section 1.11.4, MIIA is a bipolar, contractile protein composed of two myosin heavy chains (MHCs), two regulatory myosin light chains (MLCs), and two essential MLCs. MHC contains an N-terminal globular motor domain that moves actin as it

hydrolyses ATP and a C-terminal tail region that binds to the other MHC (Landsverk and Epstein 2005). MIIA associates with actin to form actomyosin complexes, which play key roles in cell structure, contractility, adhesion and migration (Geeves et al. 2005; Vicente-Manzanares et al. 2009b). Non-muscle myosin is different than cardiac and skeletal muscle, in that, MHC activity and localisation is regulated by MLC phosphorylation (Adelstein and Conti 1975; Vicente-Manzanares and Horwitz 2010).

Genomic analysis has identified at least three different non-muscle MHC type II isoforms in humans termed non-muscle MHC (NMHC)-IIA (MyH9), non-muscle MHC (NMHC)-IIB (MyH10), and non-muscle MHC (NMHC)-IIC (MyH14) (Berg et al. 2001). All three isoforms were identified in the mass spectrometry analysis. NMHC-IIA is preferentially expressed (Maupin et al. 1994) in immune cells and has previously been implicated in integrin-mediated lymphocyte motility (Morin et al. 2008; Vicente-Manzanares et al. 2009b) and was therefore selected for further evaluation. RACK1 was confirmed to associate with NMHC-IIA in T cells by co-IP (Figure 5.4D). While, NMHC-IIA appeared to associate with RACK1 in both resting and LFA-1-induced migrating cells, a reduced amount of NMHC-IIA associated in migrating cells. Equivalent bands at corresponding molecular weight were present in whole cell lysates.

5.3.3.3 Alpha Tubulin

Another major component of the cytoskeleton are microtubules, which consist of polymers of alpha and beta tubulin dimers, known as protofilaments, that bundle into hollow cylindrical filaments. Microtubules are nucleated and organised by the MTOC, which act as anchoring sites for proteins including gamma tubulin that in turn anchor microtubules. MTs serve as a structural support within cells and are involved in many cellular processes including mitosis, cytokinesis, and vesicular transport (Hawkins et al. 2010). All three forms of MTs: alpha, beta, gamma were identified in the mass spectrometry analysis. The tubulin subunit with the highest mascot score was alpha tubulin and was therefore chosen as a representative protein to analyse MT and RACK1 association. Co-IP data indicated alpha tubulin associated with RACK1 in both resting and LFA-1-induced migrating T cells (Figure 5.4E). Equivalent bands at corresponding molecular weight were present in 1% whole cell lysates.

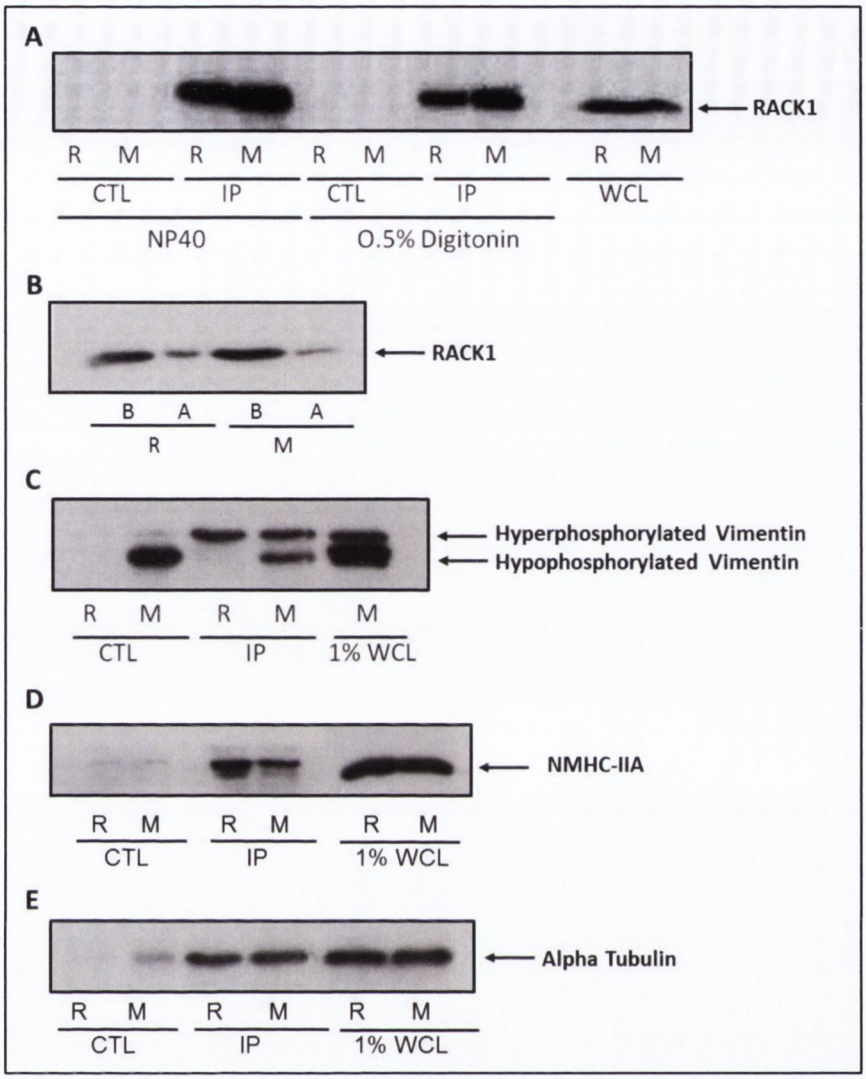

Figure 5.4: Validation of Mass Spectrometry Data for Candidate Protein by Immuno-assays.

(A) Resting (R) and LFA-1-stimulated migrating (M) HuT78 T cells were lysed in cell lysis buffer containing 1% NP40 and immuno-affinity precipitated with a RACK1-specific antibody or anti-IgM (isotype control). The protein samples were resolved on a 10% acrylamide gel by SDS-PAGE, immunoblotted, and probed for RACK1. (B) Efficiency of RACK1 IP reaction; protein samples from before (B) and after (A) immuno-purification. (C) Same as A, but probed with Vimentin-specific antibody. (D) Same as A, but probed with NMHC-IIA-specific antibody. (E) Same as A, but probed with alpha tubulin-specific antibody.

5.3.4 Investigation of Cytoskeletal Components and Associated Proteins in Resting and Migrating Lymphocytes

In migrating T cells, LFA-1 integrin connects the extracellular matrix with the cell interior both physically, through association with the cytoskeleton, and functionally as a bi-directional signal transducer (Volkov et al. 2001). LFA-1 conducts extracellular signals into the cell, activating a variety of signalling transducers, including PKC, involved in cytoskeletal rearrangement (Volkov et al. 2001). However, the exact sequence and regulation of signalling events resulting in the polarised distribution of cytoskeletal and signalling components are not fully understood.

Although the importance of the cytoskeleton in lymphocyte activation and migration has been long established, recent research advances have revealed direct mechanistic links between lymphocyte-specific components of signal transduction pathways and cytoskeletal remodelling (Rey et al. 2002; Takesono et al. 2010; Volkov et al. 2001). As described in section 1.11.2, MTs are essential components of the cytoskeleton and are involved in many cellular processes including cell division, growth, and migration (Hawkins et al. 2010; Watanabe et al. 2005). MTs are dynamic polymers of alpha/beta tubulin heterodimers arranged from head to tail forming hollow tubes. MTs form a well organised network with the growing or 'plus ends' leading into the cytoplasm, while the 'minus ends' are anchored at the MTOC. MTs play a key role in T cell migratory polarity, and MT retraction in the uropod is required for directional cell migration (Takesono et al. 2010; Vicente-manzanares et al. 2002; Volkov et al. 1998). Activation of LFA-1 induces reorganisation of the MT network, resulting in the collaborative assembly and disassembly of microtubules at the forward extending leading edge and trailing uropod (Takesono et al. 2010; Volkov et al. 2001; Watanabe et al. 2005). In addition, our group has previously demonstrated *in vitro* activation of LFA-1 induces MT polymerisation in T cells (Verma et al. 2008). In Chapter 4 of this study, we demonstrated suppression of RACK1 by siRNA phenocopies the enhanced chemotatic migration exhibited by cells treated with the MT depolymerising agent Nocodazole. Moreover, all three tubulin subunits were identified in the mass spectrometry analysis of RACK1 affinity isolated proteins, and the endogenous interaction of the MT cytoskeleton and the molecular scaffold was confirmed in both resting and LFA-1-stimulated migrating T cells by co-precipitation. The association between RACK1 and MTs has never been examined in the context of T cell migration. Therefore, we hypothesised RACK1 may have a role in regulating MT dynamics during directional cell migration by affecting MT stability through

association with proteins that mediate cross-talk between the MT and actin cytoskeleton or cytoskeletal components.

MTs are tightly regulated both spatially and temporally. This regulation involves nucleotides, MT-associated proteins (MAPs), kinases and phosphatases as well as coordinated interactions with other cytoskeletal components (Etienne-Manneville 2004; Gundersen and Cook 1999). A subset of MAPs accumulate specifically at the distal ends of growing microtubules and are known as plus-end binding proteins. These plus-end binding proteins include cytoplasmic linker proteins (CLIP)- 115 and -170 and CLIP-associated proteins (CLASPs), and are involved in MT stability and linking the cell cortex to the plus ends of MTs, both of which are necessary for cell migration (Galjart 2010; Watanabe et al. 2005). In addition, plus end-binding proteins can assemble at the distal end of polymerised MTs to couple the dynamic properties of MTs to the movement of cellular structures (Howard and Hyman 2003). *In vivo* studies have demonstrated CLIP-115 and -170 function as rescue factors, that is, they convert shrinking microtubules to growing ones and are considered positive regulators of MT growth and stability (Komarova et al. 2002). The CLIP binding proteins CLASP1 and CLASP2 are localised to subsets of stabilised MTs directed toward the leading edge and are implicated in cell migration (Akhmanova et al. 2001). In addition, CLASP proteins have been implicated in the regulation of kinetochore and spindle function during mitosis (Pereira et al. 2006). While the functions of plus end binding proteins appear to be largely redundant, CLIP and CLASP among other plus-end binding proteins act in concert to regulate MT polarity and stability. IQGAP1 is a scaffolding protein that binds to a diverse array of signalling and structural molecules that are often associated with cell polarisation and adhesion (Briggs and Sacks 2003). Originally identified to bind to actin IQGAP1 has been reported to associate with MTs through direct interaction with CLIP-170 *in vitro*. Through interaction with its target proteins, IQGAP1 participates in multiple cellular functions, including the regulation of the small GTPases Cdc42- and Rac1-dependent cytoskeletal changes (Gundersen 2002). Therefore, CLASPs bind CLIPs and MT, co-localise with the CLIPs at microtubule distal ends, and exert MT-stabilising effects.

In order to investigate the putative association of RACK1 with cytoskeletal proteins, we first sought to examine the detergent-solubility of these cytoskeletal associated proteins and whether they were enriched in the cytoskeletal fraction following activation of LFA-1. We then analysed the detergent extracts of resting and LFA-1-mediated migrating cells *in situ* by immunofluorescence microscopy in order to investigate possible co-localisation of these candidate cytoskeletal associated proteins with RACK1. Triton X-100 is a non-

ionic detergent commonly included in cell lysis buffers in addition to other detergents. Used separately at room temperature, TritonX-100 solubilises membrane and cytosolic proteins, while precipitating the cytoskeletal component (Foucault et al. 1984; Tanford and Reynolds 1976). This inherent difference in protein solubility allows the independent analysis of cytoskeletal enriched proteins both by western blot and immunofluorescence analysis.

Here, we use a method previously described (Ohanian et al. 2005) with minor modifications to investigate the detergent-solubility of cytoskeletal components by immunoblot. The detergent extraction assay with TritonX-100 is described in section 2.24. Briefly, resting and LFA-1-induced migrating T cells were exposed to the detergent Triton X-100 at room temperature for 5 min. The detergent-soluble fraction was carefully removed and the detergent-insoluble fraction was then resuspended in 2% SDS/ PBS buffer. The samples were separated by SDS-PAGE and transferred to an immunoblot.

First, we identified that alpha tubulin is preserved in the detergent-insoluble cytoskeletal fraction. We were then confident other cytoskeletal components, including MAPs, could also be examined by this technique. Therefore, we characterised the solubility of cytoskeletal associated proteins, including RACK1, CLIP-115 and -170, IQGAP1, L-plastin, vimentin, and NMHC-IIA; and signalling proteins, including PKC and Par 3, in detergent-extracted cells following activation of LFA-1. In this study, MAPK was included as positive control for the cytosolic fraction as this finding has previously been shown by our group (unpublished data). While we sought to examine CLASP1 and CLASP2, the antibodies yielded significant background on the immunoblot which precluded densitometric analysis of solubility. However, the CLASP1- and 2-specific antibodies were used in immunocytochemistry experiments described in section 5.3.5.

Detergent extraction revealed an increase in alpha tubulin in both the soluble (cytosolic) and insoluble (cytoskeletal) fractions following LFA-1 activation (Figure 5.5A). This is in accordance with previous observations that reported a net increase in polymerised MTs following LFA-1 activation in T cells (Verma et al. 2008). RACK1 was detected in both the cytosolic and cytoskeletal fraction in resting and migrating T cells. RACK1 was enriched in the cytoskeletal fraction in LFA-1-stimulated migrating cells; however, there was not a concomitant decrease detected in the triton-soluble (cytosolic) fraction. This would indicate a net increase in the amount of RACK1 protein present in the cell following LFA-1 activation. Moreover, an increase in both the triton-soluble and -insoluble fractions was detected for several proteins, including NMHC-IIA, PKC ε, PKC ζ, and

Vimentin, indicating a net increase in the amount of protein following LFA-1 activation. Vimentin was primarily detected in the triton-insoluble fraction, while MAPK was only detected in the cytosolic fractions. In addition, actin was observed in equal amounts in the soluble and insoluble fractions. In addition, an overall decrease in triton solubility following activation of LFA-1 was detected for Par 3 and L-plastin. Interestingly, a significant increase in triton solubility or enrichment in the cytosolic fraction in migrating cells was detected for the MT plus-end binding protein CLIP-115 and -170. While, there was no change detected for the solubility of IQGAP1 as a majority of the protein was cytosolic in both resting and migrating cells. As actin was detected in equivalent amounts in all four fractions, densitometric analysis was performed on the immunoblots and the data was normalised to actin (Figure 5.5B).

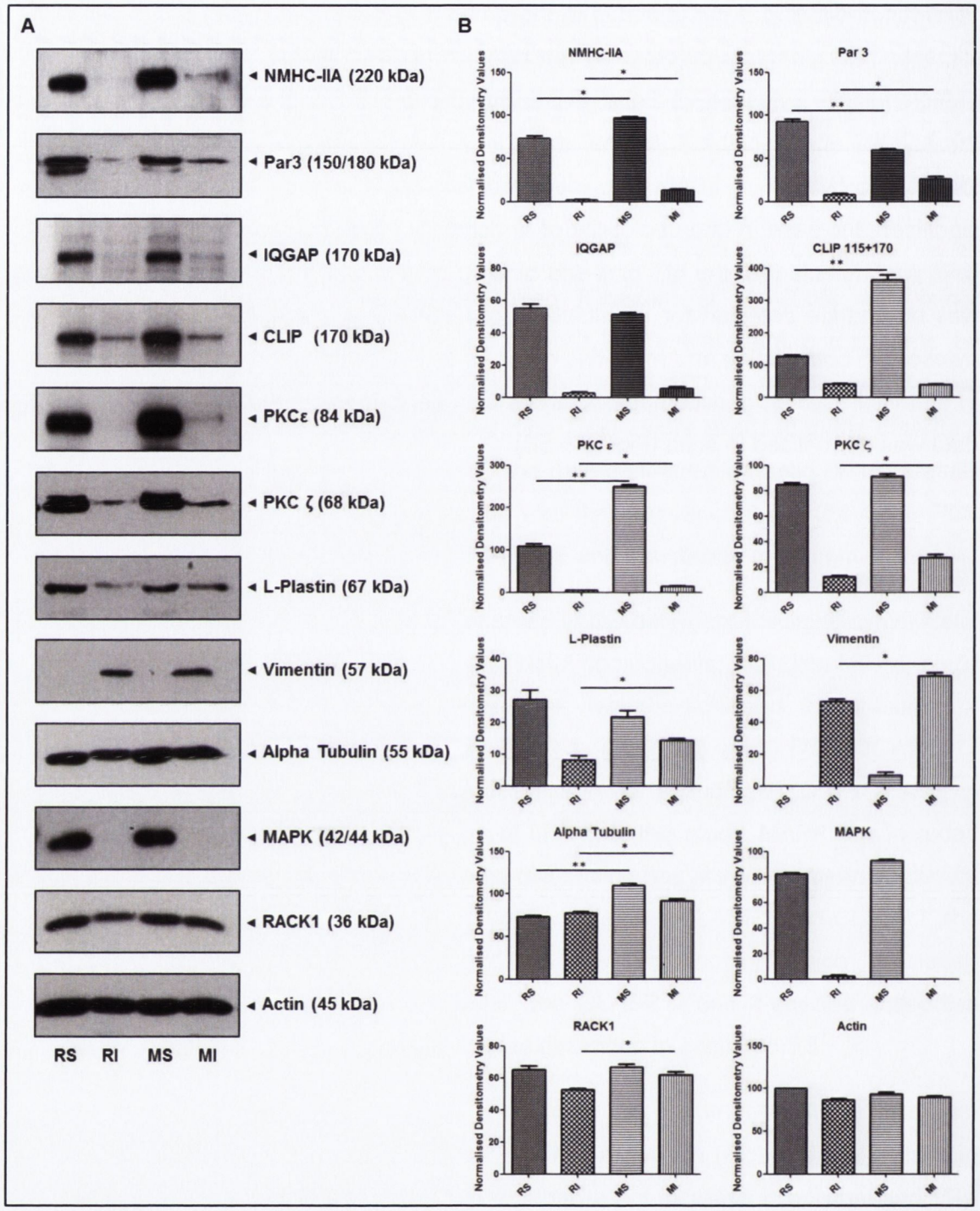

Figure 5.5: Analysis of TritonX-100 soluble and insoluble extracts of resting and LFA-1-induced migrating T cells.

(A) Immunoblot analysis of TritonX-100 soluble and insoluble extracts from resting and LFA-1-induced migrating HuT78 T cells probed with indicated antibodies. Actin was probed as the loading control. Detergent extraction fractions are as follows: Resting Soluble (RS), Migrating Soluble (MS), Resting Insoluble (RIS), and Migrating Insoluble (MIS). (B) Densitometry was performed on the blots and the mean and SEM of N=3 is shown. * denotes $p< 0.05$ and ** $p< 0.01$

5.3.5 RACK1 Associates with Polymerised MTs and MT Plus-end Binding Proteins in LFA-1-induced Migrating T cells

RACK1 was associated with MTs in resting and migrating T cells and was enriched in the cytoskeletal fraction following activation of LFA-1. In addition, RACK1-deficient cells exhibited a reduction in cell polarisation and concomitant increase in chemotatic migration similar to cells exposed to the MT-depolymerising agent Nocodazole. Therefore, we hypothesised RACK1 may have a role in regulating MT dynamics during directional cell migration by affecting MT stability. MT stability is regulated by the coordinated function of MAPs, specifically plus-end binding proteins. Therefore, we examined *in situ* the cytoskeletal fraction of RACK1 in association with alpha tubulin and the plus end binding proteins CLIP-115 and 170, IQGAP, and CLASP1 and 2 following detergent extraction of resting and LFA-1-induced migrating cells. In addition, we also examined the putative association of RACK1 and NMHC-IIA in PFA-fixed and detergent extracted T cells.

The detergent extraction technique for immunofluorescence staining is described in section 2.24. Briefly, resting and LFA-1-stimulated migrating HuT78 T cells were exposed to Triton X-100 at room temperature for 5 min. The triton-soluble fraction was carefully removed and the remaining insoluble fraction was labelled with Hoechst nuclear stain and immunofluorescent dyes conjugated to antibodies against the indicated proteins. The immunofluorescence staining of detergent extracts of resting and migrating cells was compared to the staining pattern of cells fixed with the standard PFA technique (section 2.23).

Immunofluorescence staining of the cytoskeletal fraction indicated RACK1, polymerised MTs and the MTOC, and the nucleus remained in the triton-insoluble fraction. As previously shown in Chapter 3, RACK1 has a cytosolic peripheral distribution in association with alpha tubulin in cells fixed with PFA. Examination of the triton-insoluble fraction revealed RACK1 specifically localised to the distal ends of MTs (Figure 5.6). Following LFA-1 activation, RACK1 was asymmetrically distributed to the leading edge and uropod, where it again associated with the plus-ends of polymerised MTs. In addition, the cytoskeletal-enriched fraction of RACK1 did not localise to the MTOC. Moreover, cytoskeletal-associated RACK1 was also excluded from the nucleus, but concentrated in a ring around the nucleus in both resting and migrating T cells. RACK1 has previously been reported to target PKC α and ζ from the cytosol to the perinuclear

membrane on activation (Disatnik et al. 1994; Yedovitzky et al. 1997). However, the functional implication of this subcellular localisation has not been investigated.

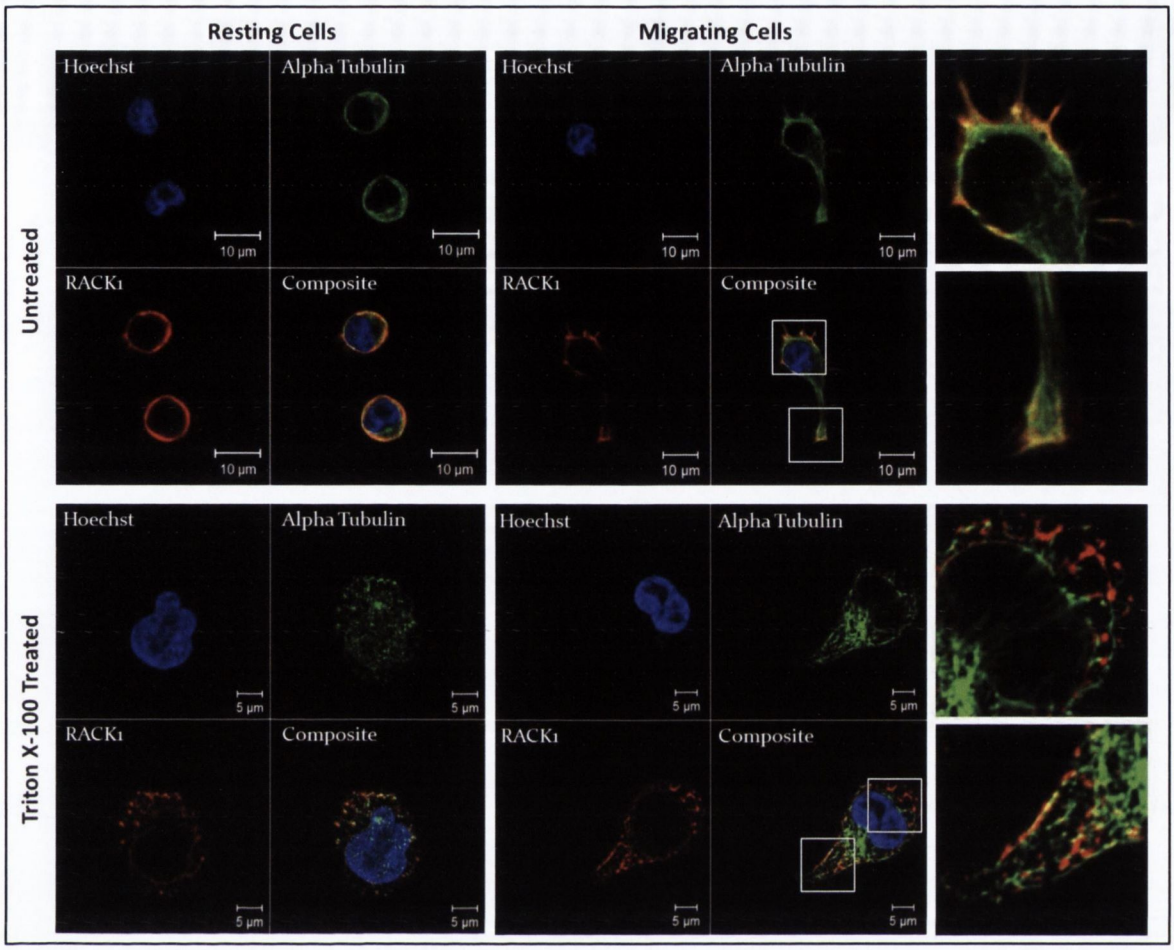

Figure 5.6: RACK1 Localises to the Plus-ends of MTs in T cells.

Resting and LFA-1-stimulated migrating T cells were fixed with PFA or exposed to TritonX- at room temperature for 5 min 100 and stained with RACK1- and alpha tubulin-specific fluorescently-conjugated antibodies. Final panel is a magnified view of the co-localisation. All images were acquired with a 63X objective.

In order to confirm RACK1 localisation at the distal ends of MTs, RACK1 was examined in association with plus-end binding proteins CLIP-115 and -170 and IQGAP. Confocal analysis indicates both CLIP-115 and -170 and IQGAP translocated from a cytosolic peripheral distribution in resting cells to the leading edge in association with RACK1 following LFA-1 activation (Figure 5.7 and Figure 5.8). Moreover, co-localisation analysis indicated that RACK1 and CLIP -115 and -170 displayed peak intensities in the same region at the leading edge (Appendix 1 Figure 2A). As expected, the actin-binding protein, IQGAP also extended in front of RACK1 in association with the actin-rich front and filopodia extensions. CLIP-115 and -170 exhibited a more even cytosolic distribution and localised in circular structures to the perinuclear region. Examination of detergent extracted cells indicated neither plus end binding protein was enriched in the cytoskeletal fraction, and were extracted in the cytosolic fraction. This is in accordance with the triton-solubility assay which indicated both proteins were enriched in the cytosolic fraction following detergent extraction. The detergent-solubility of CLIP-115 and-170 and IQGAP precluded the immunofluorescence analysis of their subcellular localisation following detergent extraction.

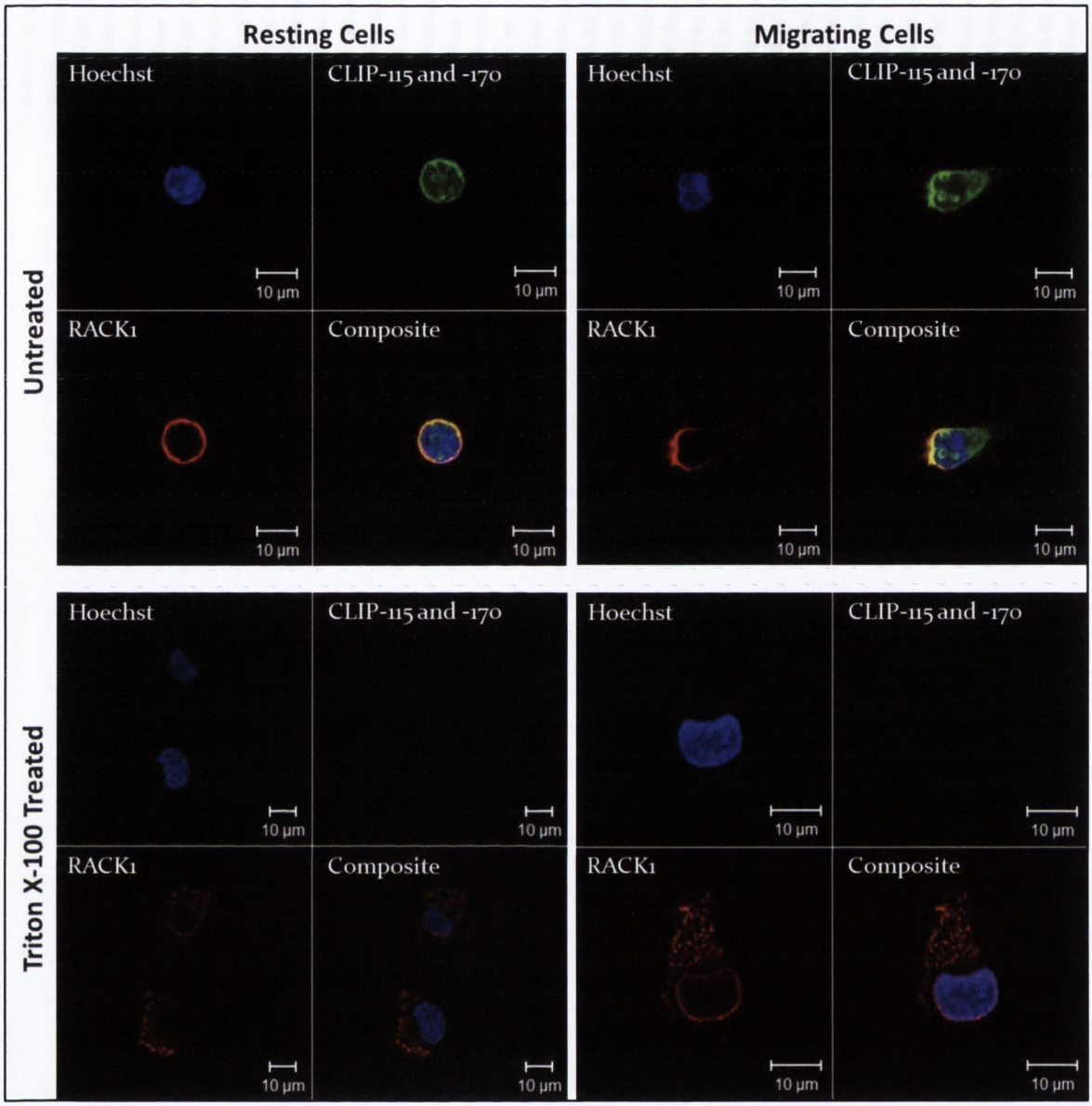

Figure 5.7: RACK1 Associates with CLIP -115 and -170 at the leading edge of LFA-1-stimulated migrating HuT78 T cells.

Resting and LFA-1-stimulated migrating T cells were fixed with PFA or exposed to TritonX-100 at room temperature for 5 min and stained with RACK1- and CLIP-specific fluorescently-conjugated antibodies. All images were acquired with a 63X objective.

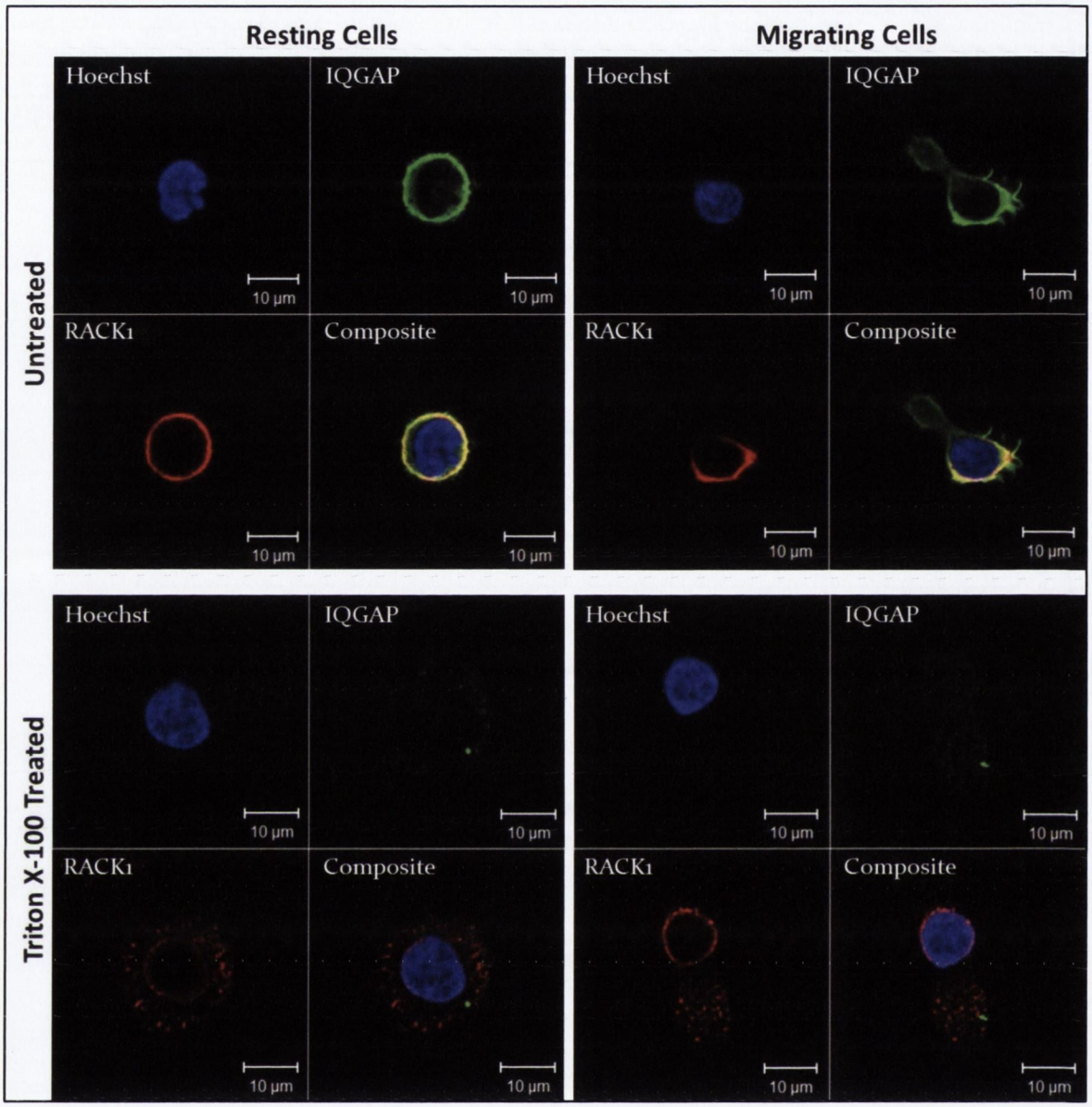

Figure 5.8: RACK1 Associates with IQGAP at the leading edge of LFA-1-stimulated migrating HuT78 T cells.

Resting and LFA-1-stimulated migrating T cells were fixed with PFA or exposed to TritonX-100 at room temperature for 5 min and stained with RACK1- and IQGAP-specific fluorescently-conjugated antibodies. All images were acquired with a 63X objective.

In order to confirm RACK1 localisation to the distal ends of MTs, RACK1 was examined in association with plus end tracking proteins CLASP1 and CLASP2. Confocal analysis of PFA-fixed cells indicated cytosolic CLASP1 and 2 translocated from a cytosolic peripheral distribution in resting cells to the leading edge and uropod in LFA-1-stimulated T cells (Figure 5.9 and Figure 5.10). Analysis of co-localisation histograms measured at the leading edge indicated that RACK1 and both CLASP1 and 2 displayed peak intensities in the same region (Appendix 1 Figure 2A). This anterior-posterior distribution was in association with RACK1 in polarised T cells. Examination of detergent extracted cells revealed both CLASP1 and CLASP2 remained in the cytoskeletal fraction and decorated the MT spindle, specifically at the distal ends of polymerised MTs. In addition, both proteins displayed an increased intensity at the MTOC. CLASP1 localised in discrete complexes in association with RACK1 at the leading edge. However, CLASP1 more strongly co-localised with RACK1 at the distal ends of MTs in the uropod. Cytoskeletal-associated CLASP2 decorated the MTs spindle, but was more concentrated at the MTOC. In addition, CLASP2 was not present at the leading edge but did partially co-localise with RACK1 at the perinuclear membrane and in the uropod. This was an unexpected observation as CLASP2 has previously been reported to localise to the leading edge of motile fibroblasts (Akhmanova et al. 2001). Therefore, CLASPs may have cell-type specific roles in MT stability. Nevertheless, the distinct subcellular localisation of these two structurally similar plus-end binding proteins supports their non-redundant functions in regulating MT dynamics (Akhmanova et al. 2001; Galjart 2005; Pereira et al. 2006).

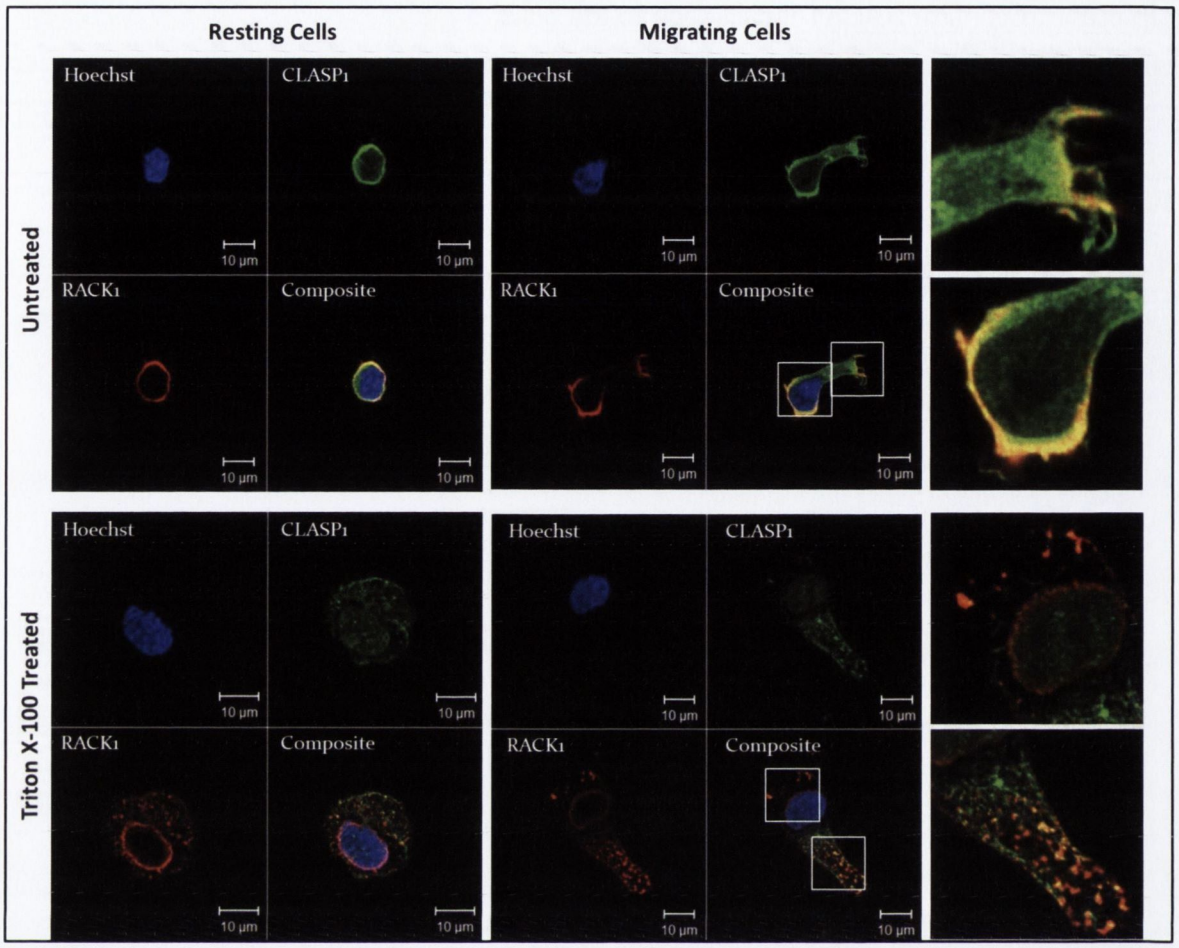

Figure 5.9: RACK1 associates with CLASP1 at the distal ends of polymerised MTs.

Resting and LFA-1-stimulated migrating HuT78 T cells were fixed with PFA or exposed to TritonX-100 at room temperature for 5 min and stained with RACK1- and CLASP1-specific fluorescently-conjugated antibodies. Final panel is a digitally- magnified view of the fluorescence co-localisation. All images were acquired with a 63X objective.

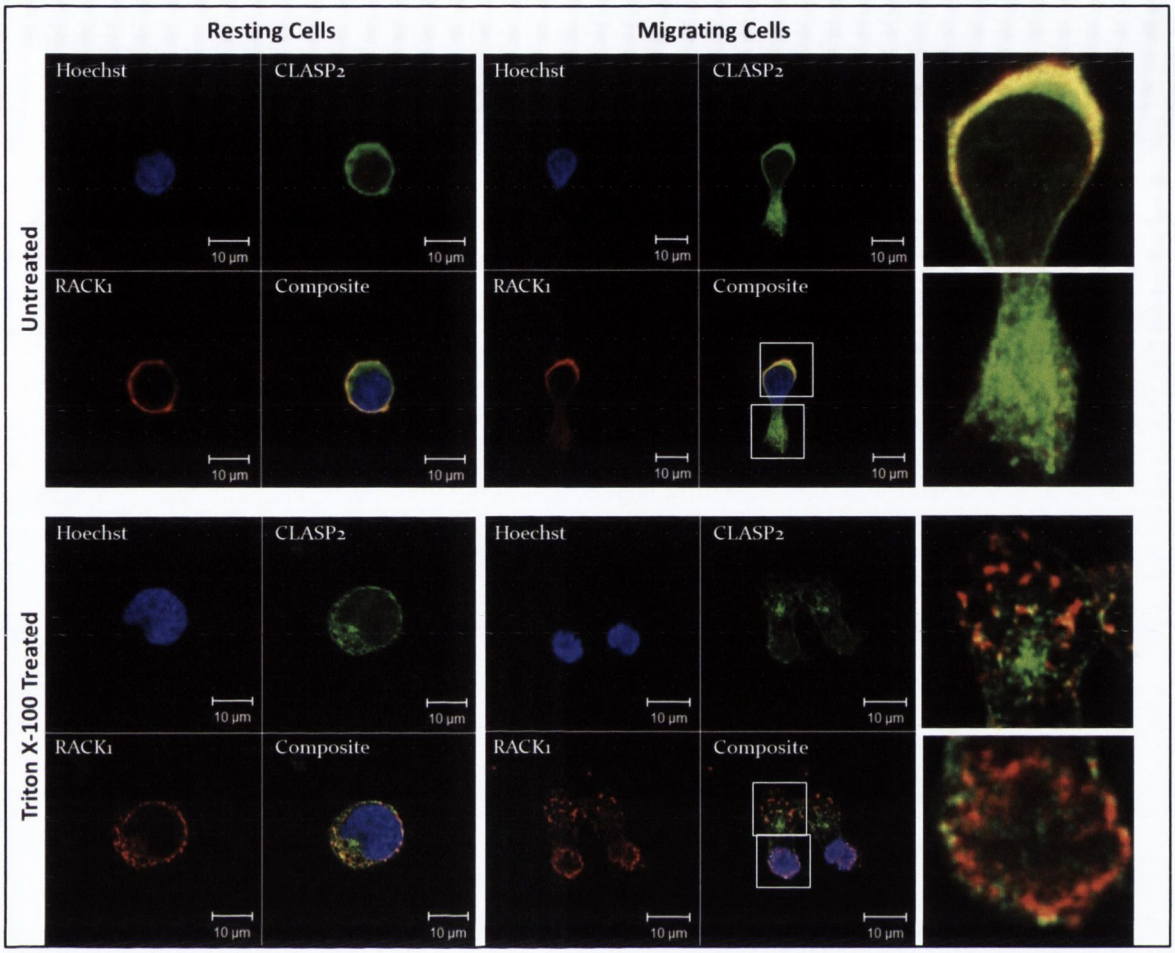

Figure 5.10: RACK1 does not associate with CLASP2 at the distal ends of polymerised MTs.

Resting and LFA-1-stimulated migrating HuT78 T cells were fixed with PFA or exposed to TritonX-100 at room temperature for 5 min and stained with RACK1- and CLASP2-specific fluorescently-conjugated antibodies. Final panel is a digitally- magnified view of the fluorescence co-localisation. All images were acquired with a 63X objective.

Confocal analysis of PFA-fixed cells indicated NMHC-IIA strongly co-localised with cytosolic RACK1 around the periphery of the resting cell (Figure 5.11). Following activation of LFA-1, NMHC-IIA translocated to the leading edge in association with RACK1. NMH-CIIA strongly co-localised with RACK1 in the forward extending lamellipodia as well as concentrated behind RACK1. While it is enriched at the leading edge in migrating cells, a subset of the myosin was localised behind the nucleus and in the trailing uropod. Confocal analysis of a z-stack indicated that, in fact, RACK1 and NMHC-IIA displayed peak intensities in the same region at the leading edge (Appendix 1 Figure 2A). Examination of detergent extracted cells indicated RACK1 associated with NMHC-IIA in discrete complexes both in the periphery of resting cells and at the leading edge and the uropod following LFA-1 induction of polarisation. Taken together, these data indicated RACK1 associated with NMCH-IIA in discrete complexes localised to the distal ends of polymerised MTs. This finding in conjunction with the fact RACK1 co-immunoprecipitated with alpha tubulin and NMHC-IIA suggests RACK1 may link actomyosin complexes to the MT network.

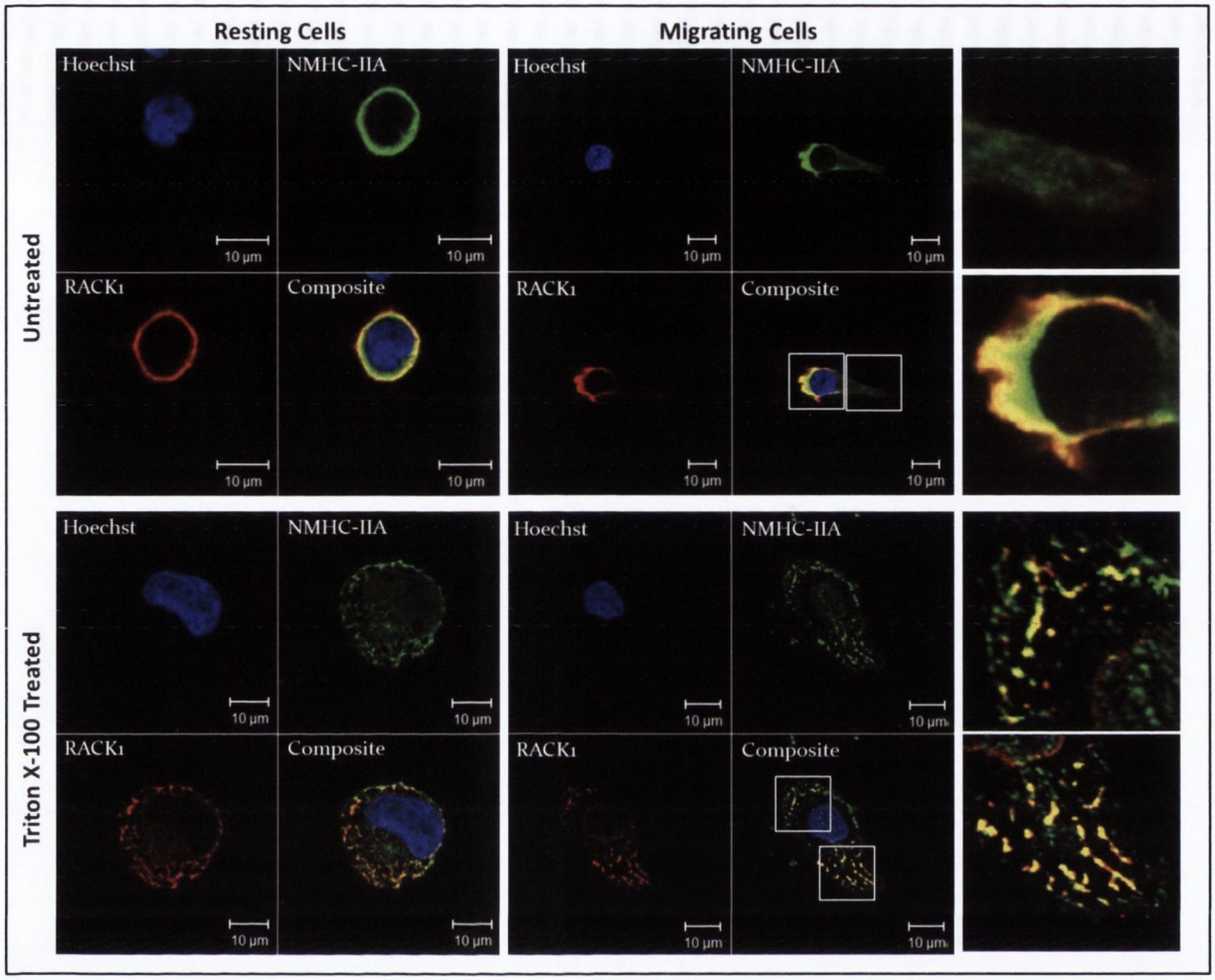

Figure 5.11: RACK1 Associates with NMHC-IIA at the Leading Edge and the Uropod of LFA-1-stimulated migrating T cells.

Resting and LFA-1-stimulated migrating T cells were fixed with PFA or exposed to TritonX-100 and stained with RACK1- and NMHC-IIA-specific antibody. Final panel is a digitally- magnified view of the fluorescence co-localisation. All images were acquired with a 63X objective.

5.4 Discussion

Integrin receptor engagement in T cells initiates signalling cascades consisting of various enzymes, their substrates, and scaffold/adaptor proteins. These signalling pathways induce the reorganisation of the cellular cytoskeleton and cell polarisation. The identification of effector proteins mediated by the molecular scaffold RACK1 is essential to understanding the molecular mechanism necessary for T cell polarity and motility. Rapid progress in mass spectrometric technology in the past few years has allowed comparative analysis and identification of protein complexes following activation. RACK1 has been reported to target a range of effector proteins in response to diverse stimuli. However, a proteomic profiling of RACK1 associated proteins in T lymphocytes had never been performed.

In this study, we employed a targeted proteomic approach to identify RACK1 stimulus-dependent interactions following LFA-1 activation in T lymphocytes. By immuno-affinity isolation coupled with mass spectrometry analysis, we identified proteins associated with RACK1 in LFA-1-stimulated T cells. Using the bioinformatics software PANTHER, the identified proteins were categorised by Gene Ontology. In addition, an extensive search of the canonical literature provided further evaluation of known molecular functions.

5.4.1 Cytoskeletal Proteins

Supporting the role of RACK1 in cell migration, several cytoskeletal proteins, including actin, tubulin, vimentin, myosin light and heavy chains were identified in the RACK1 proteomic profile. The ability of the actin cytoskeleton to rapidly respond to extracellular stimuli is in part due to a plethora of actin and MT binding proteins. These adaptor proteins are responsible for the dynamic cytoskeletal reorganisation, stabilisation, and degradation required for cell polarisation and migration (Samstag et al. 2003). Indeed, several adaptor proteins were also identified by mass spectrometry to associate with RACK1 in migrating T cells, including F-actin capping proteins, gelsolin, Arp2/3, coronin, RAB35, tropomodulin, and tropomyosin (Appendix 1 Table 2). Furthermore, the WD repeat protein WDR1 was also found to associate with RACK1. WDR1 has been reported to induce actin severing and disassembly through cooperation with the actin-severing protein cofilin (Fujibuchi et al. 2005). RACK1 has previously been shown to form heterodimers with other WD repeat-containing proteins, which is thought to facilitate multi-protein complexes (Chen et al. 2004a; Xu and Min 2011). To our knowledge, this is the first report of an interaction between RACK1 and the WD-repeat containing protein

WDR1. Altogether, these data suggest RACK1 may serve as a molecular scaffold and (in)directly associate with a number cytoskeletal components involved in cytoskeletal remodelling during directional cell migration.

5.4.2 Signal Transduction

We identified a range of cell signalling proteins, including GTP binding proteins, Ras-GTPase activating proteins (Ras-GAP), KHDRBS1, Prohibitin, WDR1, and several 14-3-3 isoforms (Appendix 1 Table 2). RACK1 has previously been reported to interact with Ras-GAP via its PH domain (Koehler and Moran 2001). In a recent report, RACK1 was also shown to interact with the scaffolding protein 14-3-3ζ (Neasta et al. 2012). Members of the 14-3-3 protein family are dimeric intracellular proteins that regulate cell cycle progression, apoptosis, and signal transduction by directing the subcellular localisation of target proteins (Bridges and Moorhead 2005) and therefore have a similar function to RACKs. Interaction with 14-3-3 is phosphorylation-dependent as the scaffolding protein only engages phosphoserine or phosphothreonine motifs (Bridges and Moorhead 2005; Morrison 2009). It was demonstrated that 14-3-3ζ shuttles RACK1 to the nucleus following activation of the cyclic AMP signalling pathway to initiate stimulus-dependent transcription (Neasta et al. 2012). In addition, 14-3-3 was also shown to interact with vimentin in a phosphorylation-dependent manner *in vivo* (Tzivion et al. 2000). As RACK1 was found in this study to associate with both 14-3-3 and vimentin, RACK1 could participate in the modulation of signalling processes requiring 14-3-3. This study has demonstrated an interaction between two multifunctional scaffolding proteins involved in signal transduction and may indicate a point of cross-talk between different signalling pathways.

Notably, the protein KH domain containing, RNA binding, signal transduction associated 1 (KHDRBS1) was also identified by mass spectrometry to interact with RACK1. KHDRBS1, also known as Sam68, is a member of the signal transduction and activation of RNA (STAR) family of proteins and is involved in both signal transduction and RNA maturation. Although ubiquitously expressed, Sam68 plays very specialized roles in different cellular environments. In most cells, Sam68 resides in the nucleus and is involved in several steps of mRNA processing, from transcription, to alternative splicing, to nuclear export as well as cell cycle regulation. In addition, Sam68 translocates to the cytoplasm upon cell stimulation. For instance, Sam68 is tyrosine phosphorylated upon TCR stimulation and functions as an adapter protein in signal transduction cascades by binding to SH2 and SH3 domain-containing proteins, such as src. RACK1 binding to src

inhibits its kinase activity and disruption of the RACK1-src complex prevents phosphorylation of Sam68 (Miller et al. 2004). In addition, it associates with the mRNA translation machinery and acts as a putative regulator of mRNA stability and/or translation rates. Interestingly, Sam68 and RACK1 are both regulated by tyrosine phosphorylation and have both been implicated in coordinating signal transduction cascades and regulating protein synthesis (Lukong and Richard 2003; Najib et al. 2005). Furthermore, recent evidence has linked Sam68 function to the onset and progression of endocrine tumours, such as prostate and breast carcinomas (Bielli et al. 2011).

5.4.3 Transcription Regulation

Proteins involved in transcription regulation were also identified. These include transcription factors, DNA binding proteins, DNA Helicase II, and transcription factors (Appendix 1 Table 2). As previously stated, 14-3-3 has been shown to target RACK1 to the nucleus and to initiate stimulus-dependent transcription.

5.4.4 RNA maturation, protein biosynthesis

Proteins imperative to mRNA translation, and subsequent protein folding, transportation, and degradation were abundant in the RACK1 proteomics profile, including ribosomal proteins, hnRNP, polyadenylate binding proteins, *etc.* (Appendix 1 Table 2). This was expected as RACK1 has been shown to interact with the 40S subunit of the eukaryotic ribosome and has been implicated in stimulus-dependent protein synthesis. For instance, RACK1 recruits PKC to the 40s eukaryotic ribosome, thereby linking signal transduction to protein synthesis (Sengupta et al. 2004; Shor et al. 2003). Moreover, RACK1 has been shown to be involved in local translation of proteins required for neuronal outgrowths. Therefore, RACK1 may be involved in local translation and targeting of structural and regulatory proteins required for cytoskeletal reorganisation and T cell polarisation.

5.4.5 Metabolic Enzymes

A number of proteins involved in energy metabolism including mitochondrial enzymes were identified to associate with RACK1 in T cells (Appendix 1 Table 2). Although this study did not directly analyse activity of the observed enzymes, we speculated association with RACK1 may mediate alteration of intermediary metabolism induced by LFA-1 in migrating T cells. Moreover, RACK1 expression was previously reported to be induced in response to H_2O_2-induced injury, which is reduced by metabolic enzymes

(Polosukhina et al. 2003). Interestingly, the enzyme Lactate dehydrogenase (LDH) has striking structural similarities to RACK1 as it has been shown to associate with the plasma membrane via its seven-stranded antiparallel beta-sheet (Dym et al. 2000). The structural conservation of protein-protein binding domains may allow RACK1 and the enzyme to interact as RACK1 has previously been shown to associate with other structurally similar proteins (Adams et al. 2011; Chen et al. 2004b).

5.4.6 Molecular Chaperones

Finally, several heat shock proteins were identified to associate with RACK1 in T cells. In addition to their role in cellular stress response, heat shock response proteins have also been reported to function as molecular chaperones and, thus, play a critical role in protein folding, intracellular trafficking of proteins, and coping with proteins denatured by heat and other stresses. For example, HSP 70 kDa, which was identified in the mass spectrometry analysis, has been shown to have ATPase activity, bind nascent peptide chains, and play a key role in protein folding, transmembrane transportation, and degradation (Borges and Ramos 2005). In addition, a few other molecular chaperones, such as histone, co-immunoprecipitated with RACK1 in migrating T cells (Appendix 1 Table 2). The nuclear protein Histone H1 has been implicated in signalling pathways of CD4+ T cells (Hsu et al. 2008).

Notably, no PKC isozymes were identified in the RACK1 proteomic profile. However, only regions of the gel exhibiting differences in RACK1-associated proteins following LFA-1 activation were investigated by mass spectrometry. Once an overwhelming feat, recent developments in bioinformatic analysis software like PANTHER allow for fast, effective analysis of mass spectrometry data. Therefore, a complete comparative proteomics analysis of resting and migrating T cells is imperative for a better understanding of constitutive and stimulus-dependent RACK1 protein interactions.

5.4.7 Validation of Mass Spectrometry

The mass spectrometry results were validated by confirming the endogenous association between RACK1 and a number of candidate proteins including tubulin, vimentin, and NMHC-IIA by co-immunoprecipitation. This validation allowed further evaluation of the RACK1 proteomic profile in lymphocytes.

5.4.8 Analysis of Cytosolic and Cytoskeletal Fractions Following Detergent Extraction in T cells

We have previously shown in this study that RACK1 associates with MTs in resting and migrating T cells and was enriched in the cytoskeletal fraction following activation of LFA-1. In addition, RACK1-deficient cells exhibited a reduction in cell polarisation and concomitant increase in chemotatic migration similar to cells exposed to the MT-depolymerising agent Nocodazole. Therefore, we hypothesised RACK1 may have a role in regulating MT dynamics during directional cell migration by affecting MT stability. Activation of LFA-1 induces MT polymerisation (Verma et al. 2009) in migrating cells. Detergent extraction revealed MTs were enriched in the cytoskeletal fraction following LFA-1 activation. Therefore, we examined the association of RACK1 with polymerised MTs and a number of cytoskeletal associated proteins by detergent extraction.

Here, we demonstrated that a number of proteins had an increased enrichment in the detergent-insoluble cytoskeletal fraction in LFA-1 stimulated T cells. These include the MT cytoskeleton, cytoskeletal associated proteins, including RACK1, L-plastin, vimentin, and NMHC-IIA, and signalling proteins, including PKC ζ, PKC ε, and Par 3. A marked increase in alpha tubulin was detected in both the soluble (cytosolic) and insoluble (cytoskeletal) fractions of migrating compared to resting cells. This is in accordance with previous observations that reported a net increase in polymerised MTs following LFA-1 stimulation in T cells (Verma et al. 2009). In addition, RACK1 was enriched in the both the cytosolic and cytoskeletal fractions in LFA-1-stimulated migrating cells, indicating an increase in RACK1 expression in response to LFA-1 activation. An increase in protein expression following LFA-1 activation was also demonstrated by RACK1 immunoprecipitation of HuT78 cell lysates (Figure 5.4A). Given the fact that RACK1 has been shown to modulate cell migration via competitive inhibition of effector activation, such as Gβγ (Chen et al. 2008), it is conceivable that dynamic changes in the expression level of RACK1 during physiological and pathological processes of immune responses may contribute to fine tuning of leukocyte function. Moreover, an increase in both the detergent-soluble and -insoluble fractions was also detected for several other proteins, indicating increased expression following LFA-1 activation. Certain proteins were primarily detected in the detergent-insoluble fraction, notably Vimentin, while the signal transducer MAPK was only detected in the cytosolic fractions. This was expected as we routinely use MAPK as a cytosolic fraction control for this technique, which confirmed the detergent extraction was successful and there was no cross-contamination between the

extracts. Conversely, cytoskeletal enrichment following activation of LFA-1 was detected for the polarity protein Par 3 and actin-binding protein L-plastin. Interestingly, a significant increase in detergent solubility or enrichment in the cytosolic fraction in migrating cells was detected for the CLIP-115 and -170. This was not expected as the MAPs bind to and stabilise polymerised MTs, which would have suggested a decrease in detergent solubility or enrichment in the cytoskeletal fraction in association with polymerised MTs.

5.4.9 RACK1 Localises to the Distal Ends of Polymerised MTs in T cells

MT stability is regulated by the coordinated function of MAPs, specifically plus-end binding proteins. In Chapter 3 of this study, we demonstrated RACK1 redistributes asymmetrically in migrating T cells and associated with MTs at the leading edge and uropod of migrating T cells. In accordance with the immunoblot analysis of detergent extracts, confocal analysis of confirmed RACK1 is preserved in the cytoskeletal fraction and localises specifically to the distal ends of polymerised MTs in both resting cells and migrating T cells. The localisation of RACK1 at the distal ends of MTs was substantiated by analysis of RACK1 in association with plus-end binding proteins CLASP1 and 2. In resting cells, CLASP1 and 2 decorated the MT spindle and associated with RACK1 in discrete complexes at the distal ends of polymerised MTs near the cell periphery. In migrating cells, RACK1 strongly associated with CLASP1 at the distal ends of polymerised MTs at the leading edge and in the uropod, while CLASP2 was more concentrated at the centrosome. While CLASPs have been previously reported to relocalise to distal segments of MTs at the leading edge of motile fibroblasts in response to stimulation (Akhmanova et al. 2001), neither CLASP protein was strongly localised at the leading edge of LFA-1-induced migrating T cells. This suggests the regulation of MT dynamics is cell-type specific and differs in rapidly migrating lymphocytes. Certainly, the preponderance of evidence would suggest that the regulatory role of RACK1 in cell migration is context-dependent. Interestingly, despite prominent roles in MT stability, neither CLIP-115 and-170 or IQGAP were enriched in the cytoskeletal fraction, which was in accordance with the immunoblot analysis (Figure 5.5). Confocal analysis of PFA-fixed cells revealed both CLIP-115 and-170 or IQGAP are enriched at the leading edge in association with RACK1 following LFA-1 activation in T cells. The actin-binding protein IQGAP1 was localised to the lamellipodia and extending filopodia presumably in association with F-actin. IQGAP1 has previously been shown to co-localise with actin filaments at polarised leading edges in fibroblast cells, to which CLIP-170-bound MTs

are targeted. In addition, activated Rac1 and Cdc42, small GTPases which regulate actin dynamics, were shown to enhance the interaction of IQGAP1 with CLIP-170 at the leading edge (Fukata et al. 2003). Moreover, RACK1 was recently identified to associate with IQGAP1 by a mass spectrometric analysis and was reported to localise at the cell membrane in association with IQGAP1 and Rac2 (Meng et al. 2007). Nevertheless, these analyses have been largely restricted to cells of epithelial and fibroblast origin. Furthermore, it was recently proposed that because plus-end binding proteins assemble in a conformationally distinct manner, the growing ends of MTs act as platforms for interactions with selected proteins in order to link MTs with other cytoskeletal elements. A number of cytoskeletal proteins were identified in the RACK1 proteomic profile. Therefore, RACK1 may serve as a protein scaffold providing a platform for the coordinated interaction of cytoskeletal proteins.

In this study, we provided evidence for the association of RACK1 and MAPs implicated in MT stability. This putative role for RACK1 in MT dynamics may explain the reduction in polarisation and increase in chemotatic migration observed in both Nocodazole-treated and cells deficient in RACK1. Therefore, we propose RACK1 may associate with plus-end binding proteins in the local regulation of microtubule dynamics in T cells in response to positional cues.

5.4.10 Examination of NMHC-IIA Interaction with RACK1 in T cells

Finally, the motor protein NMHC-IIA was identified by mass spectrometry to associate with RACK1 in migrating T cells and the endogenous interaction was confirmed by immunoprecipitation and immunofluorescence analysis. Here, we demonstrated NMHC-IIA translocated to the leading edge in association with RACK1 in polarised migrating T cells. This observation is in accordance with previous data demonstrating NMHC-IIA was enriched at the leading edge in SDF-1α-induced polarised T cells (Rey et al. 2002). Furthermore, confocal analysis of detergent extracted cells revealed RACK1 associated with NMCH-IIA in discrete complexes in association with the distal ends of polymerised MTs at the leading edge and uropod. This finding in conjunction with the fact RACK1 co-immunoprecipitated with alpha tubulin and NMHC-IIA suggests RACK1 may link actomyosin complexes to the MT network. This novel association was further investigated in the study described in Chapter 6.

5.4.11 Conclusion

In conclusion, by mass spectrometric analysis of RACK1 immuno-isolated proteins, we were able to gain insights into RACK1-associated proteins/protein complexes in LFA-1-stimulated migrating T cells. Our findings support the notion that RACK1 is a scaffolding protein capable of interacting with a wide variety of proteins. We propose these proteins, including several known and several novel associations, expand the previously incomplete list of RACK1 effector proteins, specifically in lymphocytes. Our study identified RACK1 binding partners in T cells previously identified in other cell types as well as novel associations not reported in the literature. These novel interactions may provide new insights into RACK1 functions in all cell types expressed. Identification of proteins associated with RACK1 will further our understanding of the molecular mechanisms by which RACK1 regulates cell polarisation and migration. In addition, these findings emphasise the importance of scaffold/adaptor proteins like RACK1 in signal transduction pathways. Collectively, these findings implicate RACK1 in association with cytoskeletal reorganisation in resting and migrating T cells. While a number of interacting partners have been identified for RACK1, the functional implications of these interactions have not been fully explored. Further investigation of the functional implications of RACK1 and the proteins identified in this study will be required for a better understanding of the role of RACK1 in T cell polarity and motility.

CHAPTER SIX

RACK1 Associates with NMHC-IIA in T Cells

6 RACK1 Associates with NMHC-IIA in T Cells

6.1 Introduction

There has been extensive research into the identification of proteins involved in cytoskeleton dynamics (Etienne-Manneville 2004; Rikitake and Takai 2011), yet the challenge now is to determine how the function of these proteins is coordinated. We identified several cytoskeletal proteins and signal transduction proteins in our analysis of RACK1-associated protein complexes in T cells. As an adaptor protein, RACK1 may serve to link signalling proteins to the cytoskeleton to regulate cytoskeleton dynamics. A number of myosin proteins were identified in the RACK1 proteomics profile, including the non-muscle myosin heavy chain NMHC-IIA. Immunoprecipitation experiments revealed that this association also occurs between the endogenous molecules in T lymphocytes. Moreover, in the study in Chapter 5, we demonstrated NMHC-IIA translocated in association with RACK1 to the leading edge of polarised migrating T cells. Myosins are actin-dependent molecular motors that use the energy of ATP hydrolysis to move along actin filaments (Krendel and Mooseker 2005). Myosin II in non- muscle cells (NMII) has been extensively studied in the context of cell migration. NMII is an important regulator of diverse cellular processes including cell polarity, adhesion, and migration, and these processes involve the dynamic remodelling of the actin cytoskeleton in response to stimuli (Conti and Adelstein 2008; Conti et al. 2008; Even-Ram et al. 2007; Vicente-Manzanares et al. 2009b; Vicente-Manzanares et al. 2007).

Genomic analysis has identified at least three different mammalian NMII isoforms, including NMHC-IIA, NMHC-IIB, and NMHC-IIC, which are encoded by *MYH9*, *MYH10*, and *MYH14*, respectively. They share structural features and are targeted by a number of the same kinases (Berg et al. 2001; Saitoh et al. 2001; Vicente-Manzanares et al. 2007). NMII are heterohexamers composed of a pair of heavy chains and two pairs of light chains. To date, there is no evidence that heterodimers of the heavy chains exist. In addition, while there are several isoforms for each MLC, at present, it is not known whether there is any specificity between light chain and heavy chain sets (Golomb et al. 2004). Moreover, while the three isoforms are ubiquitously expressed and more than one isoform can be present in a single cell, they show distinct patterns of tissue distribution, intracellular localisation and biochemical properties (Kim et al. 2005; Kolega 1998; Maupin et al. 1994; Vicente-Manzanares et al. 2011; Vicente-Manzanares et al. 2007). While all three myosin heavy chain isoforms were identified in the mass spectrometry

analysis, NMHC-IIA is reported to be the only NMII isoform expressed in T cells (Jacobelli et al. 2004b). This is probably due to the amino acid conservation between the three isoforms (Golomb et al. 2004). Indeed, NMHC-IIA had one of the highest mascot scores in our mass spectrometry study.

Dynamic control of filament assembly and disassembly is a primary method of regulating the spatial distribution and activity of NMII. The cell's ability to regulate the transient formation of myosin filaments allows NMII to participate in a wide array of cellular processes such as cytokinesis, embryonic development, and cell migration (Conti and Adelstein 2008; Conti et al. 2008; Even-Ram et al. 2007; Lo et al. 2004; Vicente-Manzanares et al. 2011; Vicente-Manzanares et al. 2009b). Therefore, NMII must be able to alter its assembly levels in different regions of the cell in response to varying stimuli. The regulation of NMII activity and filament assembly is dependent on phosphorylation of both its light chains and heavy chains (Adelstein and Conti 1975; Takashima 2009; Vicente-Manzanares and Horwitz 2010). The most critical determinant of NMII activity is phosphorylation of the regulatory MLC, also known as MLC20, on Ser19, which is essential for ATP-dependent myosin activity, filament assembly, and *in vitro* motility. Additional phosphorylation on Thr18, which normally succeeds Ser19 phosphorylation, results in a further increase in myosin activity and filament assembly, but does not effect *in vitro* motility (Ikebe et al. 2001; Umemoto et al. 1989). MLC can be phosphorylated on Ser19 by a number of kinases inducing myosin activation. To date, the most studied pathways are the Ca^{2+}-calmodulin-dependent myosin light chain kinase (MLCK) and the Rho coiled-coiled kinase (ROCK) (Matsumura et al. 2011; Zhao and Manser 2005). Phosphorylation of MLC at the leading edge is primarily performed by MLCK and is essential for actomyosin contraction. In contrast, ROCK mediates MLC phosphorylation at the rear of the cell to facilitate uropod detachment. While a number of substrates have been identified for ROCK including the myosin-binding subunit of myosin phosphatase, MLCK appears to be specific for MLC (Kimura et al. 1996; Matsumura et al. 2011). Totsukawa and colleagues (2004) proposed MLCK may regulate membrane ruffling at the periphery, while ROCK mediates focal adhesions in the main cell body. In addition to the phosphorylation sites at Ser19/Thr18 on MLC, phosphorylation of Ser1, Ser2, and Thr9 by PKC has been shown to inhibit myosin kinetic activity by decreasing the affinity of both MLCK and actin for phosphorylated myosin (Beach et al. 2011; Ikebe and Reardon 1990). Although phosphorylation of the MLC has been shown to play a critical role in regulating the activity of NMII, the regulatory role of MHC phosphorylation is not fully understood. Phosphorylation of

Ser1917 and Ser1944 of the NMHC-IIA isoform are mediated by PKC βII and casein kinase II, respectively, and have been shown to inhibit filament assembly (Ludowyke et al. 2006). For instance, activation of the TCR after peptide-MHC or anti-CD3 stimulation induced a rise in intracellular calcium (Jacobelli et al. 2004b). This induced phosphorylation of the tail domain of NMHC-IIA by PKC resulting in myosin inactivation. Furthermore, the authors proposed this phosphorylation event inhibited myosin-mediated motility in response antigen recognition by T cells (Jacobelli et al. 2004b).

NMIHC-IIA has been implicated in adherent cell adhesion and migration (Vicente-Manzanares et al. 2009b; Vicente-Manzanares et al. 2007). For instance, NMHC-IIA has been shown to regulate protrusions by promoting actin retrograde flow and adhesion-generated signalling (Vicente-Manzanares et al. 2011; Vicente-Manzanares et al. 2007). In addition, NMHC-IIA activation promotes adhesion maturation through its actin bundling and contractile activities in adherent cells (Vicente-Manzanares et al. 2009b). NMHC-IIA has also been implicated in defining cell polarity by regulating protrusions at the front and retraction in the rear (Xu et al. 2003; Yam et al. 2007). Ablation of NMHC-IIA results in pronounced defects in cellular contractility, focal adhesions, actin stress fibre organisation, and tail retraction (Even-Ram et al. 2007). Interestingly, NMHC-IIA-deficient cells display increased cell migration and exaggerated membrane ruffling due to increased MT polymerisation near the membrane. Therefore, NMHC-IIA is considered a negative regulator of cell migration by maintaining a balance between the actomyosin and MT systems and regulating MT dynamics (Even-Ram et al. 2007). Nevertheless, despite recent advances in this field, further investigation is needed to understand how integrin activation and downstream signalling pathways regulate myosin activity in immune cells.

While the actomyosin network works in concert with integrin-mediated focal adhesion complexes in adherent cells, lymphocytes requires different regulatory mechanisms to achieve rapid cell migration. For instance, LFA-1-induced T cell migration depends on dynamic changes to the actomyosin cytoskeleton mediated by MLCK and ROCK phosphorylation of MLC (Smith et al. 2003). Phosphorylation of MLC at the leading edge is primarily performed by MLCK to control LFA-1-mediated T cell adhesion and lamellipodial extension, while ROCK mediates MLC phosphorylation at the rear of the cell to facilitate retraction of the uropod (Smith et al. 2003). NMHC-IIA has previously been shown to localise to the posterior of migrating leukocytes (Eddy et al. 2000). Moreover, NMHC-IIA was shown to associate with LFA-1 in the uropod of migrating T lymphocytes and inhibition of the association of NMHC-IIA with LFA-1 resulted in

extreme uropod elongation, defective tail detachment, and decreased lymphocyte migration on ICAM-1, without affecting SDF-1α-induced LFA-1 activation (Morin et al. 2008). This is in accordance with a previous study, which demonstrated NMHC-IIA localised to the rear in anti-CD3 or PMA/ionomycin activated T cells where it was required for uropod formation but dispensable for immunological synapse formation (Jacobelli et al. 2004b). Taken together, these findings suggest NMHC-IIA is critical for uropod establishment and generating sufficient pulling force to detach LFA-1 from ICAM-1 at the tail and to retract the uropod.

Moreover, NMHC-IIA has also been implicated in chemokine-induced migration. NMHC-IIA was reported to interact with the C-terminal domain of the chemokine receptor CXCR4 in association with MLC and F-actin at the leading edge of SDF-1α-stimulated polarised T cells (Rey et al. 2002). This was the first report of a biochemical association between chemokine receptors and motor proteins and provided insight into a 'mechanotransducing' complex that may have a key role in lymphocyte migration. The precise spatial and temporal regulation of cell adhesion and de-adhesion is critical for dynamic lymphocyte migration, and the specific function of NMHC-IIA in regulating adhesion in rapidly migrating cells remains controversial and far from defined.

6.2 Objectives

Due to its position downstream of convergent signalling pathways, NMII plays a central role in the regulation of cell migration and adhesion (Vicente-Manzanares et al. 2009b). In addition, RACK1 has been implicated in targeting proteins involved in overlapping signal transduction cascades that regulate actomyosin dynamics in response to extracellular stimuli (Adams et al. 2011; Besson et al. 2002; McCahill et al. 2002; Mochly-Rosen et al. 1995). The spatiotemporal regulation of NMII by subcellular localisation and activation of its regulating kinases in lymphocytes is still poorly understood and warrants further investigation. To our knowledge, an interaction between RACK1 and NMII, specifically with NMHC-IIA, has never been previously reported. Therefore, the putative association of NMHC-IIA with RACK1 was investigated by mapping the NMHC-IIA binding sites on RACK1 and exploring the functional implications of this interaction in lymphocyte migration.

In this study, our specific objectives were to:

1.) Identify the NMHC-IIA binding sites on RACK1 by generating a NMHC-IIA FLAG fusion protein to use in conjunction with a RACK1 peptide array.

2.) Design and generate NMHC-IIA truncation mutants to determine the RACK1 binding domain on NMHC-IIA.
3.) Investigate the functional implications of this interaction in integrin-mediated and chemokine-induced T cell polarisation and migration.

6.3 Results

6.3.1 RACK1 Associates with NMHC-IIA in Resting and LFA-1-induced Migrating T lymphocytes

As shown in Chapter 5, RACK1 associates with NMHC-IIA in T cells following co-immunoprecipitation (Figure 5.4D). We found that endogenous RACK1 associated with NMHC-IIA in LFA-1-induced migrating cells as well as in resting cells. This endogenous association was further confirmed by immunocytochemistry (Figure 5.11). We also performed the reciprocal reaction, by immunoprecipitating NMHC-IIA from HuT78 T cells and subsequently probing for RACK1, verifying that RACK1 associated with NMHC-IIA before and after LFA-1 activation (data not shown). NMHC-IIA exhibited a cytosolic, peripheral distribution and strongly co-localised with RACK1 in resting cells, while translocating to the leading edge in association with RACK1 following LFA-1 activation. In addition, a subset of NMHC-IIA was localised with RACK1 in discrete complexes in the uropod. A previous study reported NMHC-IIA displayed an anterior/posterior distribution and was enriched in the uropod of LFA-1-induced migrating T cells expressing NMHC-IIA GFP (Morin et al. 2008). However, the subcellular distribution of NMHC-IIA may be confounded by NMHC-IIA overexpression, as cells transfected with RACK1-GFP also expressed higher levels of RACK1 at the rear of the cell in our study. Furthermore, due to the frequent turning of SDF-1-stimulated T cells migrating on ICAM-1, the direction of cell migration can often be misinterpreted in analysis of fixed cells. Nevertheless, our studies indicated NMHC-IIA is asymmetrically distributed in association with RACK1 in polarised T cells. Taken together, these data indicated that the interaction between NMHC-IIA and RACK1 is specific and constitutive. Therefore, we next sought to test whether the interaction was direct and, if so, identify the NMHC-IIA binding domain on RACK1.

6.3.2 Generation of Full Length and NMHC-IIA-derived FLAG Fusion Proteins

In order to investigate the functional implications of the interaction of NMHC-IIA with RACK1, a NMHC-IIA FLAG fusion protein was generated to use in conjunction with a RACK1 peptide array to identify the binding domain for NMHC-IIA on RACK1. The full length mammalian *MYH9* gene contains 1960 amino acids (aa), consisting of five core domains: the motor head which binds filamentous actin, the IQ domain which interacts with myosin light chains, the unknown domain, the coiled-coil tail, which is responsible for the dimerisation and filament assembly, and the globular tail, which is necessary for filament assembly and involved in myosin subcellular localisation (Conti et al. 2008; Ikebe et al. 2001). A shuttle clone containing the *MYH9* gene, which encodes NMHC-IIA, was obtained from ImaGenes (Source BioScience Ltd., Nottingham, UK). The materials and methods for purifying, amplifying, and sequencing are detailed in section 2.30. Briefly, the shuttle clone containing the full length *MYH9* gene was recombined into a high level mammalian expression vector with a CMV promoter containing an Ampicillin resistance gene with an N-terminal FLAG epitope cloned in the multiple cloning site using Gateway Cloning Technology (Invitrogen, Carlsbad, CA). The full length plasmid was then sequenced by Source BioScience and aligned to the cDNA of *MYH9* using Vector NTI Align X software to confirm it was identical to the original clone sequence.

We also sought to determine the reciprocal binding domain on NMHC-IIA for RACK1. As NMHC-IIA is a large protein at approximately 220 kDa, we sought to identify a putative RACK1 binding domain and produce a peptide array for the associated NMHC-IIA fragment. Thus, in addition to the full length, NMHC-IIA truncation mutants were also designed and generated to identify the RACK1 binding domain on NMHC-IIA. To this end, three deletion mutants were generated: Delta C, Delta Motor, and Delta N. The design of the NMHC-IIA fragments was based on the known functions of its structural domains and on previously described myosin fragments (Ikebe et al. 2001; Uehara et al. 2010). The three NMHC-IIA derived fragments were generated by selectively deleting three of the four main components of the myosin heavy chain. The last 28-residue repeat at the C-terminal end of the coiled-coil region is critical for thick filament formation and, therefore, had to remain intact (Ikebe et al. 2001; Sohn et al. 1997). The Delta C mutant does not contain the C-terminal globular tail, which is necessary for myosin subcellular localisation, but is otherwise intact (1-1919 aa). The Delta Motor mutant lacks the motor head and IQ domain, which are responsibly for interacting with actin and the essential

and regulatory lights chains, respectively but retains the unknown domain and an intact coiled-coil domain and globular tail (796-1960 aa). The Delta N mutant contains only the coiled-coil tail and globular domain (838-1960 aa). The gene sizes are as follows: full length MHY9: 5.880 kb, Delta C: 5.757 kb, Delta Motor: 3.495 kb, and Delta N: 3.369 kb. Figure 6.1 illustrates the structure of the myosin hexamer and the structural domains of the full length and NMHC-IIA derived mutants.

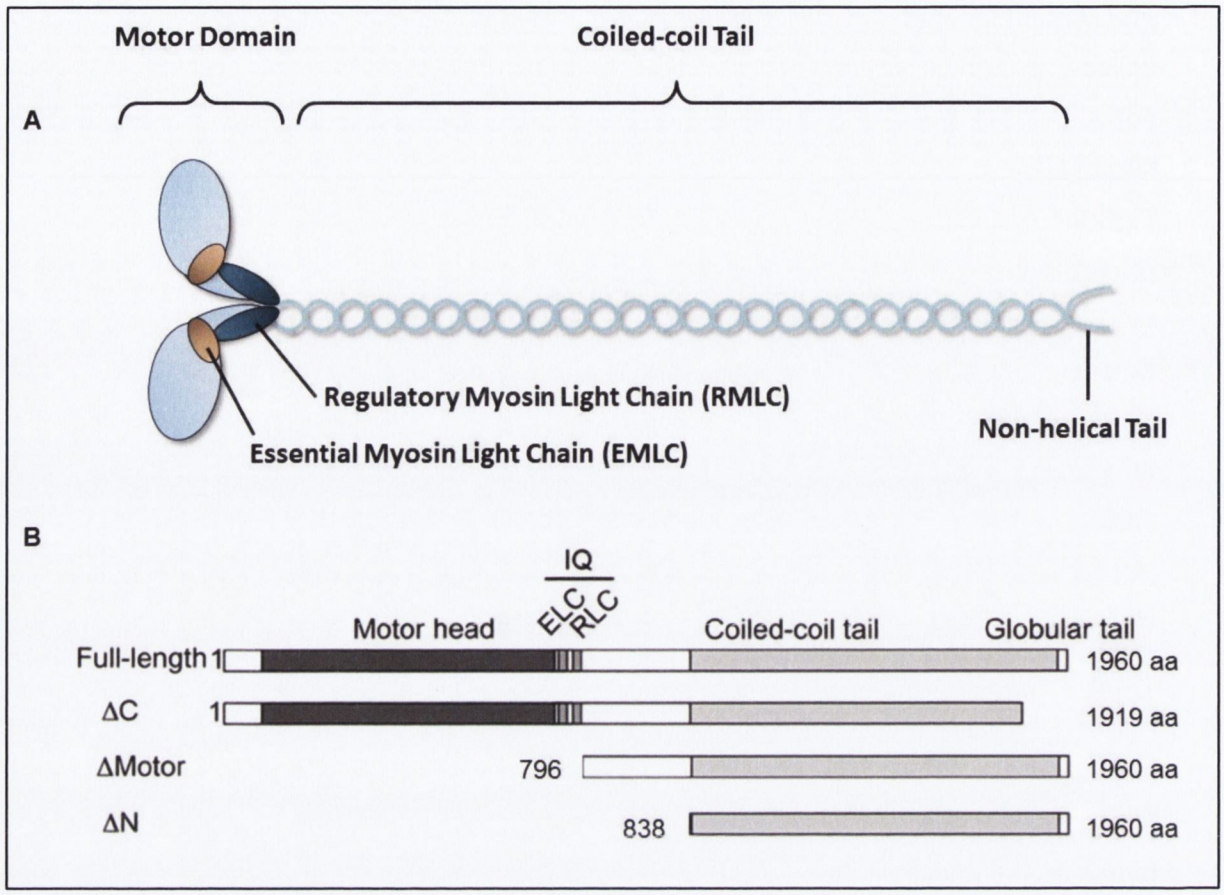

Figure 6.1: Non-muscle Myosin IIA

(A) Schematic diagram illustrating domains of Myosin hexamer consisting of two heavy chains in association with two regulatory and essential light chains. (B) Diagram of the deletion mutants generated from full length NMHC-IIA with respective fragment lengths.

Primers were designed and commercially produced (Sigma-Aldrich) for the selective amplification by PCR of the three NMHC-IIA-derived deletion mutants (sections 2.30.4 and 2.30.5). The PCR reaction was optimised using a number of forward and reverse primers and conditions (e.g. with or without DMSO). The amplicons were separated by size by gel electrophoresis in order to determine the optimal PCR conditions (Figure 6.2A). The size of full length *MYH9* gene is 5.880 kb, while the predicted fragments sizes of Delta C, Delta Motor, and Delta N are 5.757 kb, 3.495 kb, and 3.369 kb, respectively. Primers and PCR conditions that resulted in correctly sized fragments were identified, and these fragments were extracted and purified from the gel. The optimal PCR condition was repeated and the amplicons were separated by gel electrophoresis to ensure fragments were of predicted size. The first three lanes of the DNA gel in Figure 6.2B show the optimal conditions that yielded fragments of predicted size for all three deletion mutants. These fragments were extracted and purified from the gel for subsequent cloning experiments.

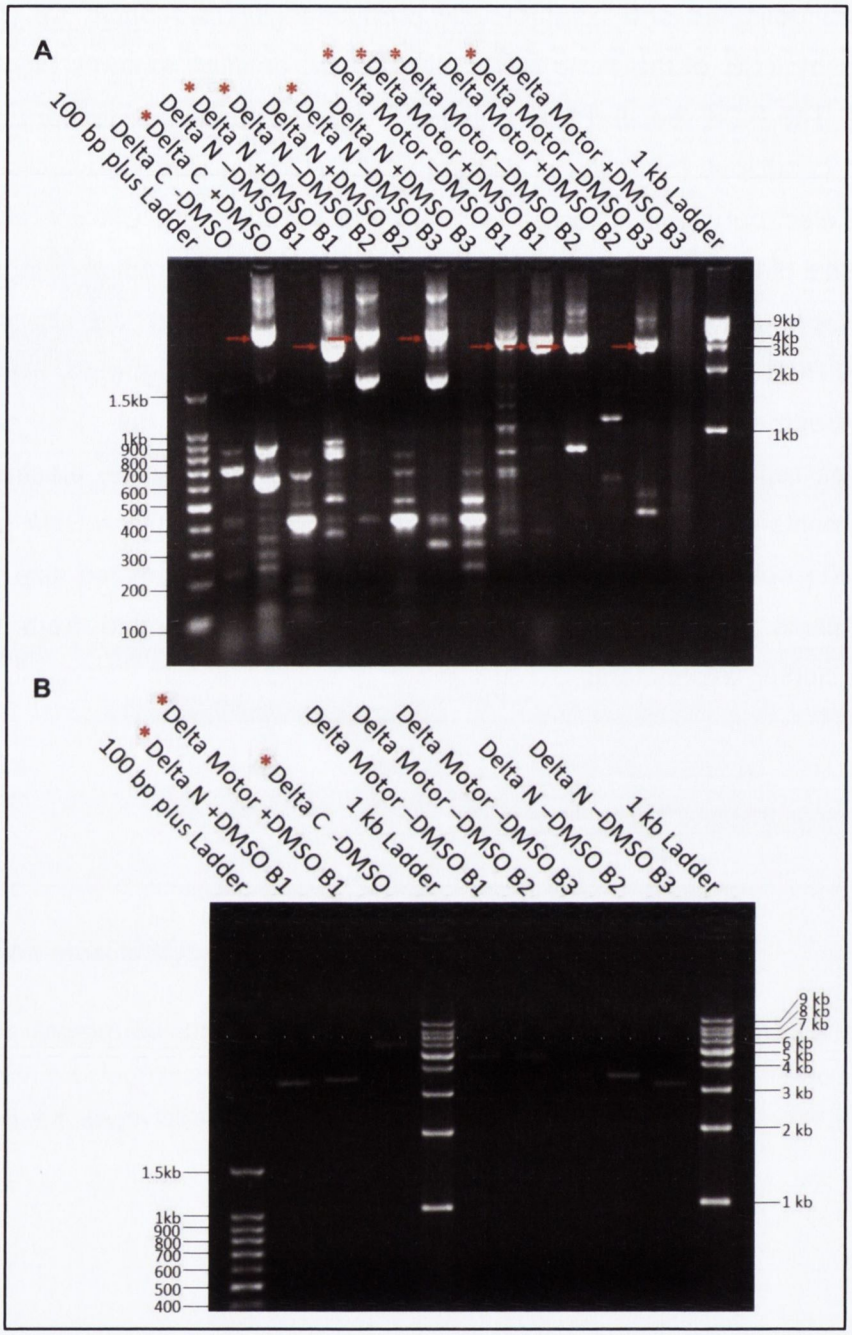

Figure 6.2: Generation of NMHC-IIA-derived Truncation Mutants.

(A) The PCR reaction was optimised using a number of forward and reverse primers and conditions (e.g. with or without DMSO). The amplicons of NMHC-IIA-derived fragments Delta C, Delta N, and Delta Motor were separated by size by gel electrophoresis. Red arrows and asterisks indicate bands from optimal PCR conditions. Bands of predicted fragment size were gel purified and selectively amplified again using the optimal PCR conditions. (B) The amplicons were again separated by size by gel electrophoresis to confirm predicted fragment size. Red asterisks indicate fragments selected for subsequent cloning experiments. Predicted fragments sizes of Delta C, Delta Motor, and Delta N are 5.757 kb, 3.495 kb, and 3.369 kb, respectively.

The plasmid DNA of the corresponding mutants were then cloned into entry vectors using topoisomerase cloning for amplification, which is described in detail in section 2.30.7. Briefly, the selected fragments were cloned into linearized entry vectors. The vectors were then transformed into competent *E. coli* for amplification. The plasmid DNA was then purified from the bacterial cells and plasmid then underwent a method known as restriction digest, an enzymatic technique used for cleaving DNA molecules at specific sites to ensure the vector contain the appropriate insert in the correct orientation. This process is described in detail in section 2.30.8. Six bacterial colonies from each of the three entry vectors were selected for plasmid purification to increase the probability of selecting the plasmid with an insert in the correct orientation. The plasmid DNA underwent a double digest with two restriction enzymes, which cut the vector backbone and asymmetrically cleaved the gene insert. The digested fragments were separated by gel electrophoresis, and the plasmid DNA containing the gene insert in the correct orientation was identified and used in subsequent experiments (Figure 6.3).

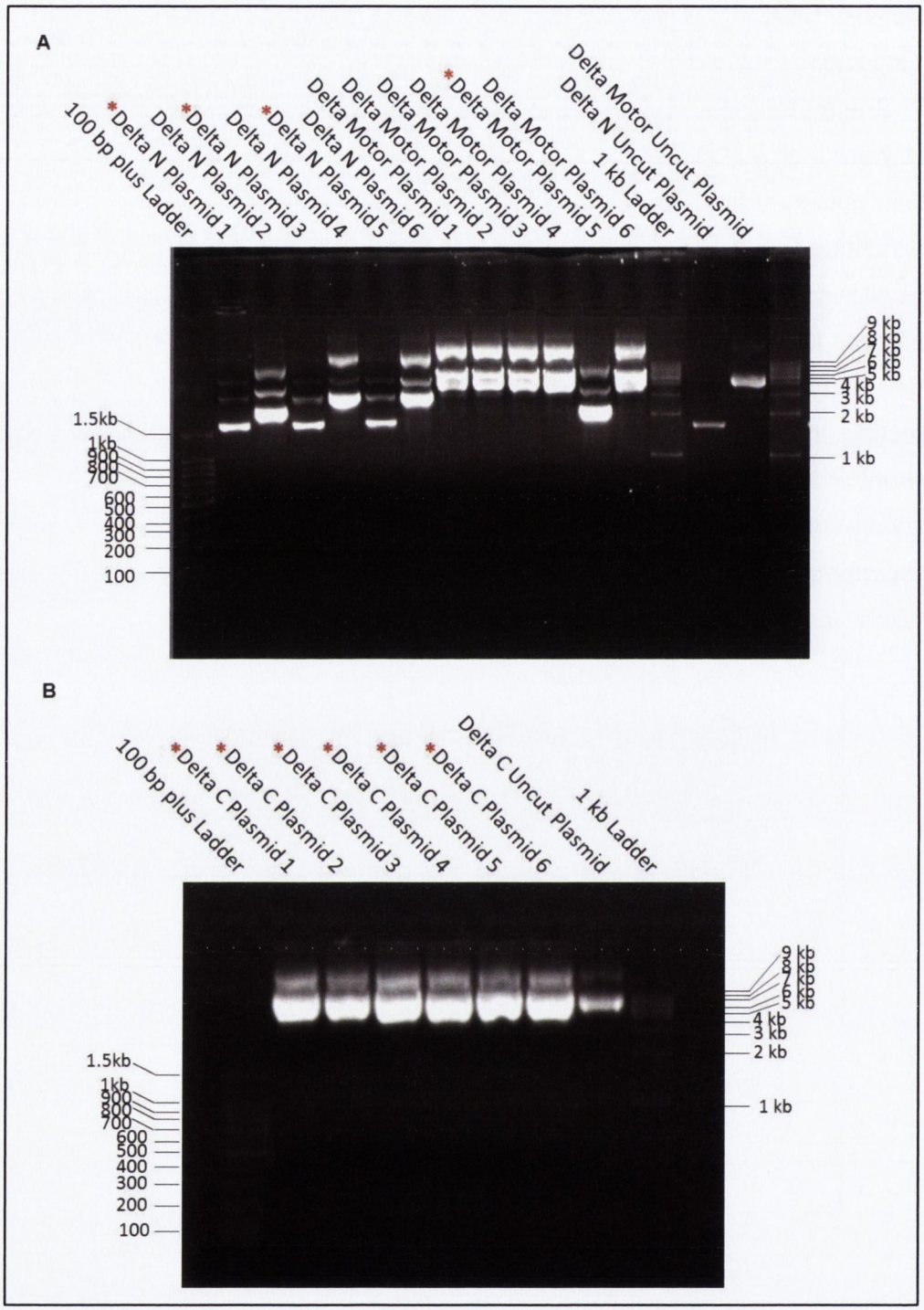

Figure 6.3: NMHC-IIA-derived FLAG Fusion Proteins.

(A) Six bacterial colonies from each of the three entry vectors were selected for plasmid purification and underwent a restriction digest in order to verify the orientation of the gene insert. Digested fragments of plasmid DNA containing the Delta N and Delta Motor inserts and uncut plasmid controls separated by gel electrophoresis. (B) Digested fragments of plasmid DNA containing the Delta C and uncut plasmid control. The red asterisks indicate plasmids containing the insert in the correct orientation and were suitable for subsequent experiments.

Gateway Technology was utilised to recombine the gene insert from the entry vector into a high level mammalian expression vector for functional analysis and protein expression. This technique and the Gateway system are described in detail in section 2.30.1. Notably, due to the size of the full length and NMHC-IIA-derived mutants, the plasmids were expressed in the mammalian cell model Human Embryonic Kidney (HEK) 293 cells using the FLAG expression system. The FLAG expression system utilizes a short, hydrophilic 8-amino acid peptide that is fused to the recombinant protein of interest. Because of its hydrophilic nature, the FLAG peptide is likely to be located on the surface of the fusion protein. As a result, the FLAG peptide is easily accessible for cleavage by Enterokinase and for detection with antibodies. In addition, because of the small size of the FLAG peptide tag, it is not likely to obscure other epitopes, domains, or alter function, secretion, or transport of the fusion protein. Therefore, these small hydrophilic tags facilitate superior detection and purification of recombinant fusion proteins when using the highly specific and sensitive anti-FLAG antibodies (Sigma-Aldrich). The correct orientation of the deletion mutant gene inserts in the expression vectors was confirmed by sequencing (Source BioScience).

The Calcium Phosphate transfection technique was optimised for HEK293s, a cell model robust to transfection methods, and is described in section 2.5.2. Expression vectors containing the FLAG-tagged NMHC-IIA full length and truncation mutants were then transfected into HEK293 cells for protein expression and functional analysis. The full length FLAG-NMHC-IIA fusion protein was successfully expressed in the HEK293 cells (Figure 6.4). The FLAG-NMHC-IIA was immunoprecipitated with M2 FLAG agarose beads (Sigma-Aldrich) using a range of cell lysate concentrations. The immunoprecipitates were separated by gel electrophoresis and subsequently blotted with FLAG antibody to ensure expression and purification of NMHC-IIA. The optimal concentration of cell lysate was determined and the immunoblot was probed for with RACK1-specific antibody to confirm association with endogenous RACK1. Ten 15cm plates of confluent HEK293 were transfected and the protein was harvested by immunoprecipitation to use in conjunction with a RACK1 peptide array, which is described in section 2.31.

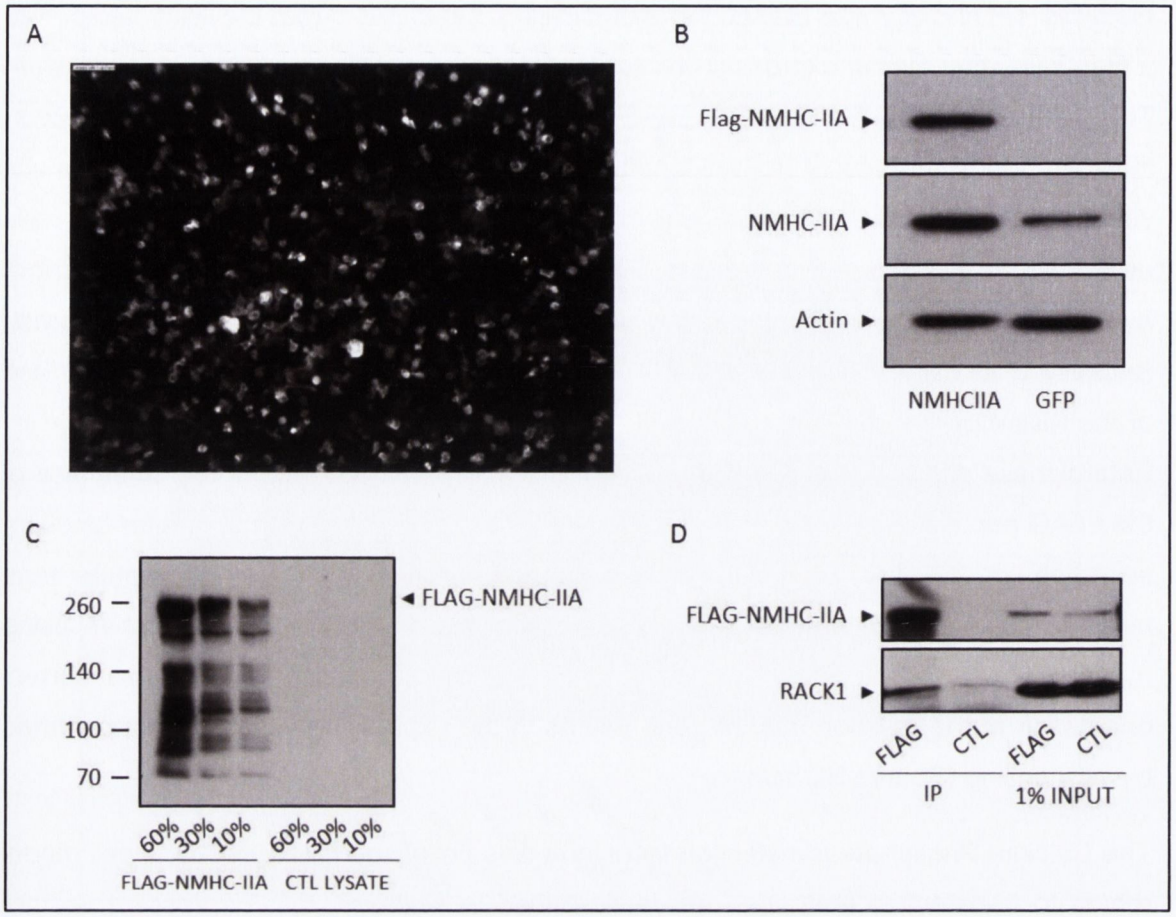

Figure 6.4: FLAG-NMHC-IIA Binds Endogenous RACK1.

(A) HEK293 cells were transfected with control EGFP to optimise calcium phosphate transfection. EGFP transfected cells were imaged by fluorescent microscopy at 10X to measure transfection efficiency. We obtained approximately 90% transfection efficiency. (B) HEK293 cells transfected with the expression vector containing FLAG-NMHC-IIA fusion protein or negative control EGFP. The cells were lysed in RIPA buffer and proteins separated by gel electrophoresis and blotted with antibody specific for FLAG, NMHC-IIA, or actin (loading control). (C) Same as B, but the cells were lysed in HS buffer and immunoprecipitated with anti-FLAG M2 agarose beads using a range of cell lysate concentrations, which are expressed as a percentage of total cell lysate. The immunoprecipitates from FLAG-NMHC-IIA transfected and control cell lysates were separated by gel electrophoresis and subsequently blotted with FLAG antibody. (D) The optimal concentration of FLAG-NMHC-IIA immunoprecipitate was identified and immunoblotted with RACK1-specific antibody to confirm association with endogenous RACK1.

Optimisation of deletion mutant expression in HEK293 cells was performed concurrently with the full length NMHC-IIA. Despite success with expression of the full length FLAG-NMHC-IIA, sufficient expression of the NMHC-IIA-derived mutants proved to be more difficult. The predicted molecular weights for the Delta C, Delta N, and Delta Motor NMHC-IIA-derived truncation mutants are 213kDa, 130kDa, and 125 kDa, respectively. Several non-specific bands due to immunoprecipitation with the anti-FLAG M2 antibody were detected in the vicinity of the deletion mutant band size. Thus, correct identification of deletion mutant bands was not possible and precluded further analysis. A total of six plasmids were selected for each of the deletion mutants and were confirmed by sequencing to all be in the correct orientation. It is pertinent the expression of the deletion mutants be optimised in order to identify the RACK1 binding domain on NMHC-IIA and for functional analysis in T lymphocytes. Therefore, transfection of HEK293 cells with the other plasmid DNA should be performed as different plasmids can have varying expression efficiencies. Moreover, the truncated mutants may also be less stable than the full length protein and, thus, targeted by proteasomal pathways. However, this is beyond the scope of the current project and will be continued in future studies.

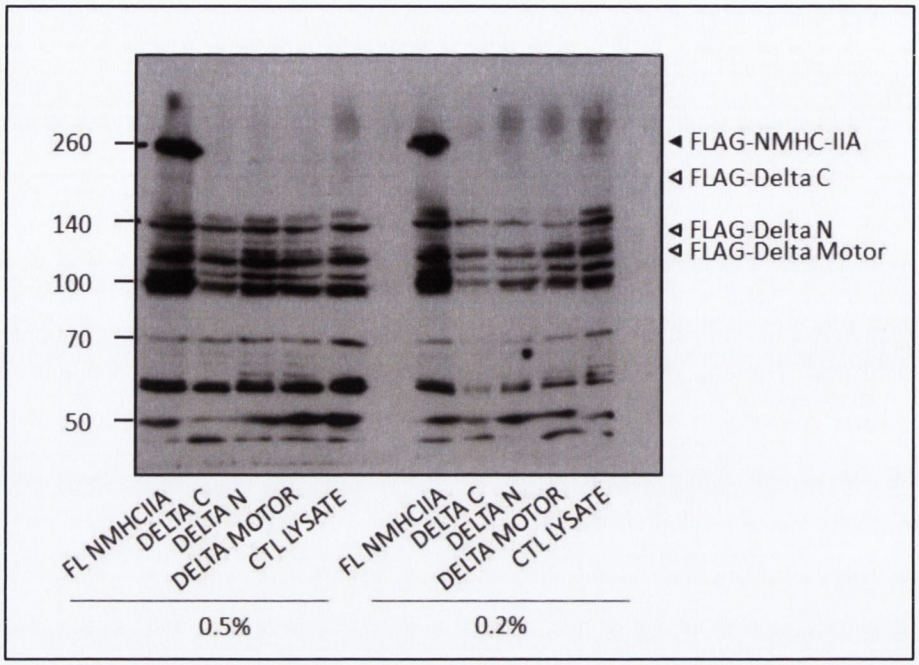

Figure 6.5: Expression of NMHCIIA-derived deletion mutants in HEK293 cells.

HEK293 cells were transfected with expression vector containing FLAG-NMHC-IIA, Delta C, Delta N, Delta Motor, or a no DNA control. The cells were lysed in RIPA buffer and the indicated percentage of M2 FLAG immunoprecipitate was separated by gel electrophoresis and transferred to an immunoblot, which was probed with FLAG-specific antibody. Filled arrowhead indicates full length FLAG-NMHC-IIA; unfilled arrowheads indicate predicted fragment sizes for NMHC-IIA-derived deletion mutants. The predicted molecular weights for the Delta C, Delta N, and Delta Motor NMHC-IIA-derived truncation mutants are 213kDa, 130kDa, and 125 kDa, respectively.

6.3.3 Evidence for the Direct Interaction between RACK1 and NMHC-IIA

This project was performed in collaboration with Dr. Patrick Kiely (University of Limerick, Limerick, Ireland) and Professor David Adams (Heriot-Watt University, Edinburgh, UK). The interaction between RACK1 and NMHC-IIA was investigated by overlaying the purified NMHC-IIA protein on a RACK1 peptide array as described in section 2.31. The RACK1 peptide array consisting of peptide libraries of overlapping 18-mer peptides, each shifted to the right by 4 amino acids, and encompassing the entire sequence of RACK1 was spot-synthesized on nitrocellulose membranes to generate RACK1 peptide arrays. Bound peptides were then overlaid with NMHC-IIA protein or anti-FLAG M2 control immunoprecipitate. The peptides that bound to NMHC-IIA protein were identified by probing the array with FLAG antibody (Figure 6.6). A table listing the positive binding region containing the peptide sequences, sequence location, and type of the interaction is shown in Appendix 1 Table 3.

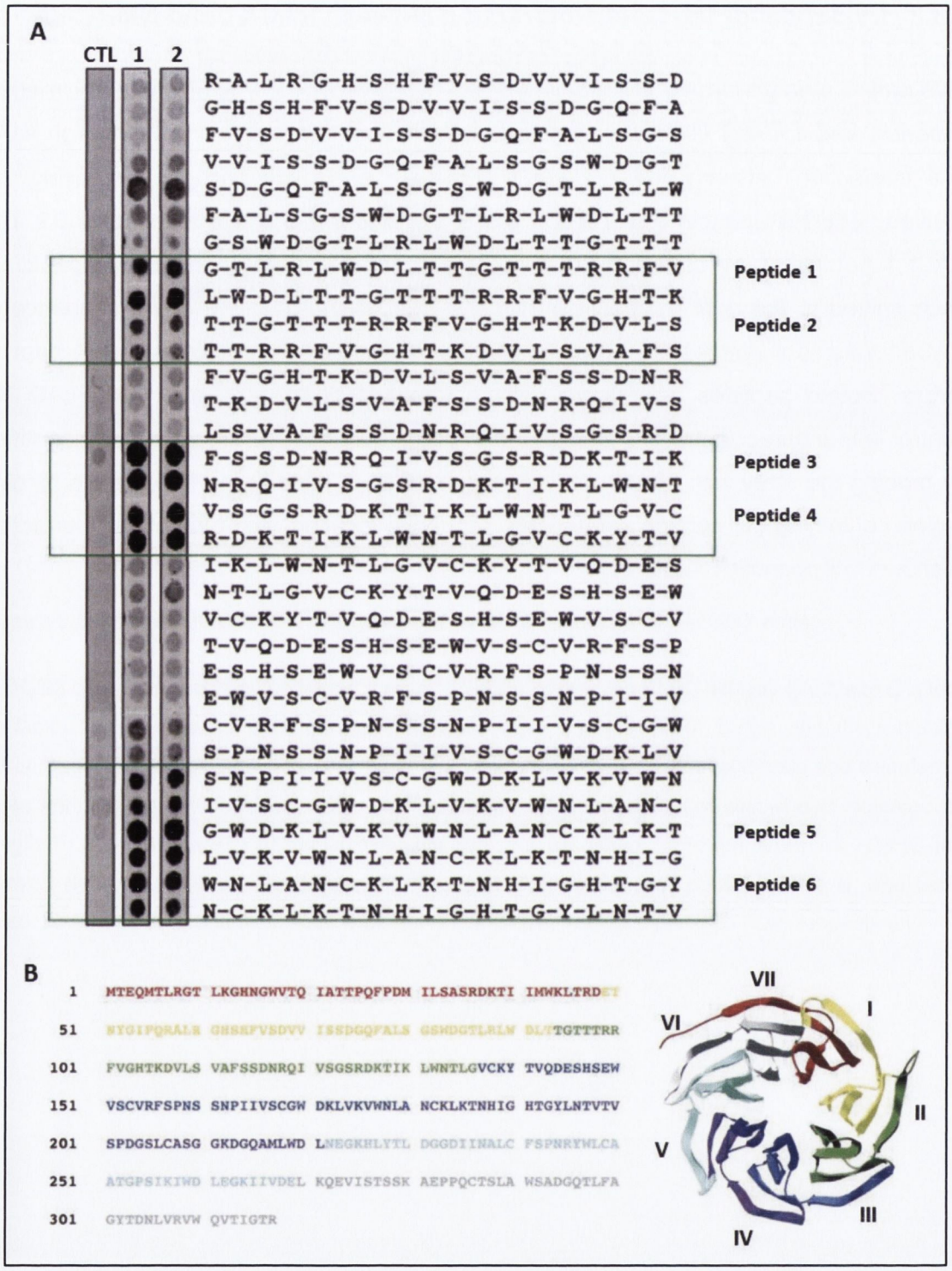

Figure 6.6: RACK1 Interacts with Full length NMHC-IIA.

(A) A RACK1 peptide array consisting of peptide libraries of overlapping 18-mer peptides covering the entire sequence of RACK1 was overlaid with NMHC-IIA protein or anti-FLAG M2 control immunoprecipitate (CTL). The overlay was performed in duplicate and the anti-FLAG IP control had no binding events. Peptides that bound to NMHC-IIA protein are indicated. (B) RACK1 amino acid sequence with colour-coded WD repeats.

Next, to identify the specific amino acids that are crucial for the interaction of RACK1 with NMHC-IIA, we used peptide-scanning substitution arrays derived from 'parent' peptides that bound NMHC-IIA using the same synthesis procedure as the full length RACK1 peptide array. Six parent peptides were sequentially substituted with an alanine along the entire sequence of the 18-mer parent peptide spot, and in cases where the parent amino acid was an alanine, it was substituted for aspartate. NMHC-IIA bound positively to Peptide 3, 4, 5 and 6 (Figure 6.7A). Despite initial strong binding to Peptides 1 and 2, the relative binding to those peptides appeared to be much lower but were included in the subsequent analysis.

Densitometry was performed on the immunoblots and the data was normalised to the control parent sequence. Using the progeny array derived from peptides, we found that individual alanine substitutions for specific residues decreased binding to NMHC-IIA (Figure 6.7B). Therefore, we determined the amino acids R^{125}, K^{127}/K^{130}, C^{138}, K^{172}/K^{175}, K^{183}/K^{185} were very important for binding NMHC-IIA. The amino acids K^{127}/K^{130} were present in both peptides 3 and 4, while K^{183}/K^{185} were present in both peptides 5 and 6. All four amino acids showed a consistent decrease in binding after alanine substitution in different peptides, which verified the results of the substation array. Further analysis of peptides 1 and 2 revealed residues R^{99}, R^{100}, and K^{106} also significantly decreased binding to NMHC-IIA when substituted. Together, these data led to the identification of three candidate regions within the RACK1 sequence that contribute to a NMHC-IIA binding interface, namely residues that span the propeller blades WD2, WD3, and WD4 of RACK1 mediate the interaction with NMHC-IIA (Figure 6.8).

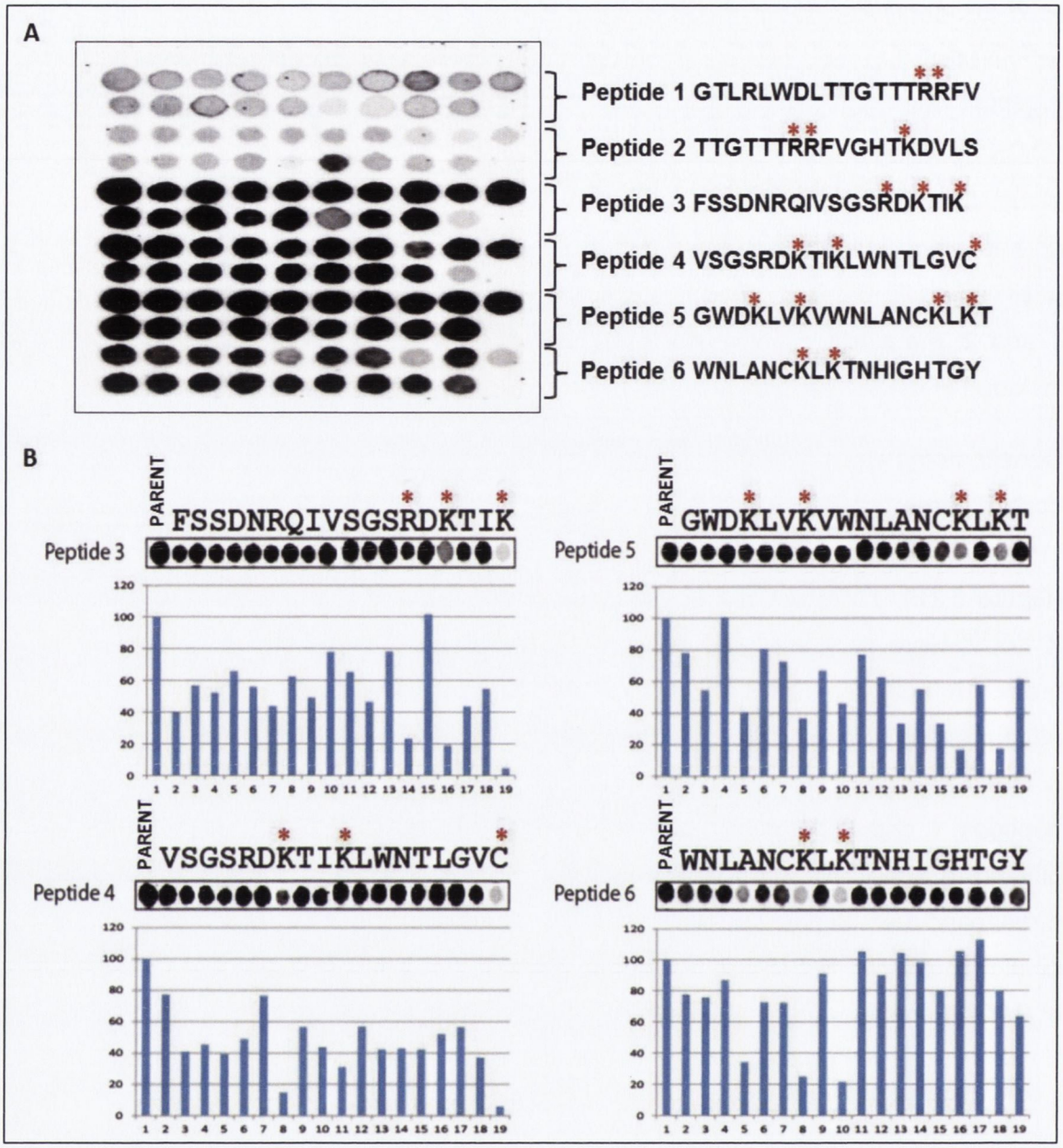

Figure 6.7: RACK1 Peptide Substitution Arrays.

(A) The peptides of RACK1 selected for positive binding with NMHC-IIA were sequentially substituted with alanine along the entire sequence of the 18-mer parent peptide spot. In cases where the parent amino acid was alanine, it was substituted for aspartate. The amino acid constitution for each peptide chosen for the alanine substitutions scans is also shown. NMHC-IIA was overlaid on the substitution array and probed with FLAG antibody. A minimum of a 60% decrease of the binding compared with the parent peptide was applied to identify amino acids critical for the interaction. Red asterisks indicate the residues, when substituted, decreased NMHC-IIA binding. (B) The binding of NMHC-IIA to each alanine substituted RACK1 peptide was quantified by densitometry and presented as a percentage of the control 'parent' sequence. The amino acids putatively involved in NMHC-IIA interaction are indicated with a red asterisk.

Several repetitive amino acid sequences in the peptides were identified which corresponded with amino acid residues that were identified to be crucial for NMHC-IIA binding in the peptide-substitution array. These included R^{99}/R^{100} in Peptides 1 and 2, $K^{127}/T^{128}/I^{129}/K^{130}$ in Peptides 3 and 4, and $K1^{72}/L^{173}/V^{174}/K^{175}$ and $K^{183}/L^{184}/K^{185}$ in Peptides 5 and 6. Furthermore, an additional peptide (Peptide 0.1) was included in subsequent analysis due to moderate binding to determine if an amino acid present in the sequence was critical for NMHC-IIA.

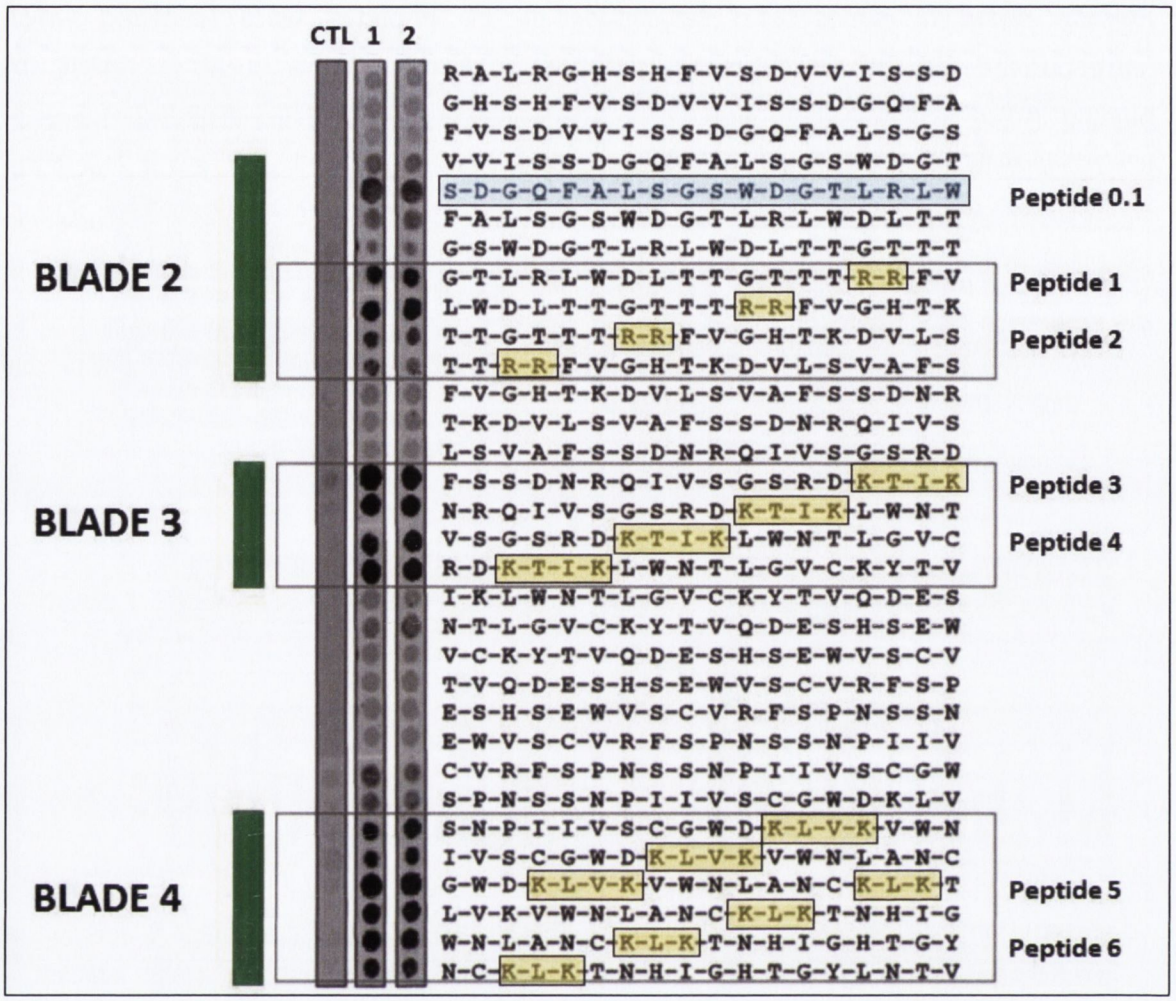

Figure 6.8: Repetitive Sequences Involved in Interaction with NMHC-IIA.

Several repetitive amino acid sequences in the peptides were identified that were crucial for the interaction with NMHC-IIA. These included R^{99}/R^{100} in Peptides 1 and 2, $K^{127}/T^{128}/I^{129}/K^{130}$ in Peptides 3 and 4, and $K1^{72}/L^{173}/V^{174}/K^{175}$ and $K^{183}/L^{184}/K^{185}$ in Peptides 5 and 6 that span the RACK1 blades 2, 3 and 4, which corresponded with amino acid residues that were identified to be crucial for NMHC-IIA binding in the peptide-substitution array.

If amino acids R^{99} /R^{100}, K^{106}, R^{125}, K^{127}/K^{130}, C^{138}, $K1^{72}$/K^{175}, and K^{183}/K^{185} within the RACK1 sequence contribute to the direct interaction with NMHC-IIA, they should be present on the outer surface of RACK1. At present, the x-ray crystal structure for human RACK1 has not been solved. However, inspection of the structure of the highly homologous Asc1 protein from *S. cerevisiae* (Link et al. 1999; Shor et al. 2003) allowed us to assess the likelihood of surface exposure of the candidate NMHC-IIA-interacting residues. We observed that the Asc1 sequence ^{99}QRFVGHKSD^{107} corresponding to RACK1 ^{99}RRFVGHTKD^{107}, which contains the residues R^{99} (Q^{99} in Asc1), R^{100}, and K^{106} (S^{106} in Asc1), is part of the outer edge of propeller blade WD2 and the loop of blade WD3, and all three amino acids are prominently exposed within this region (Figure 6.9). The sequence of Peptide 0.1 spans this region, and it was determined the peptide exhibited moderate binding on the peptide array due to its proximity rather than its amino acid composition. In addition, we observed that the cognate residues K^{127}, K^{130}, C^{138} (S^{130} in Asc1), and K^{139} (not shown in the current scanning substitution array) display prominent exposure on the outer edge of propeller blade WD3 (Figure 6.9). Moreover, we observed that the conserved residues K^{172} and K^{175} and cognate residues K^{183} and K^{185} (Q^{185} and E^{187} in Asc1) are also exposed on the outer β-strand of the propeller blade WD4 (Figure 6.9). Furthermore, the topological presentation of basic residues on blades WD3 (K^{127}, K^{130}, and K^{139}) and WD4 ($K1^{72}$, K^{175}, K^{183}, and K^{185}) is very similar (Figure 6.9C). Interestingly, the relative positions of R^{99}, R^{100}, and K^{106} and on blade 2 might partially mimic this presentation. Together, these results strongly suggest that these amino acids are important for the interaction of RACK1 and the motor protein.

The following figure contains the Asc1/ RACK1 protein structure with putative NMHC-IIA-binding residues, which was generating using PyMOL (W. L. DeLano, DeLano Scientific) by Professor David Adams as part of a collaborative effort in determining NMHC-IIA binding sites on RACK1.

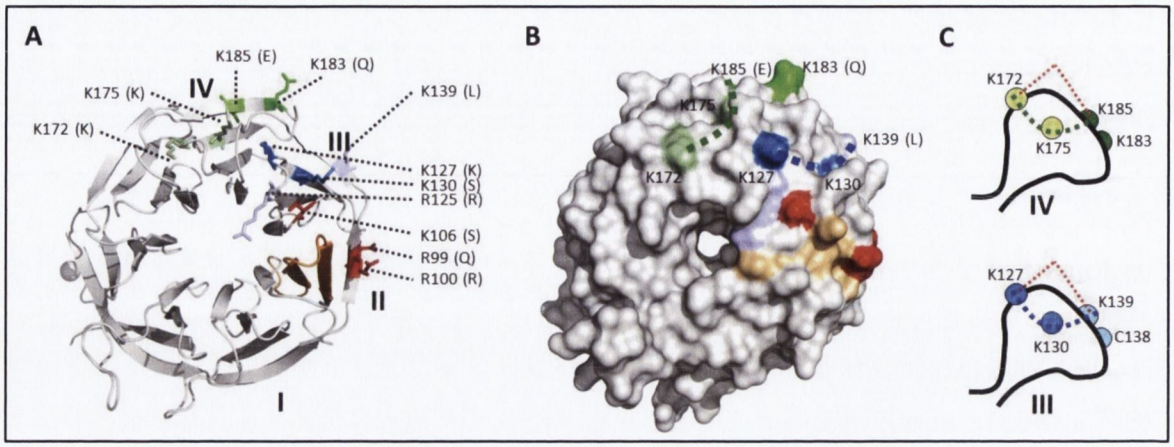

Figure 6.9: Putative NMHC-IIA Binding Sites on RACK1.

(A) Structure of RACK1 ortholog Asc1 protein from *S. cerevisiae* (Link et al. 1999; Shor et al. 2003) showing prominently surface-exposed side chains of basic residues R^{99}, R^{100}, K^{106} and (red) from peptide 2; K^{127}, K^{130}, and K^{139} (blue) from peptides 3 and 4; and K^{172}, K^{175}, K^{183} and K^{185} (green) from peptides 5/6. Cognate Asc1 residues are shown in parenthesis. (B) Same as in A, but with surface rendition, which reveals residues with prominent exposure on the edge of propeller blade WD3 and connecting loop to blade WD4. The region corresponding to peptide 0.1 is marked in orange. (C) Cartoon diagram of basic residues on blades WD3 and WD4 showing similar topological presentation (red dotted lines).

6.3.4 RACK1 Translocates to the Actin-rich cap in Association with NMHC-IIA and Chemokine Receptor CXCR4 in SDF-1α-Activated T cells

The binding of SDF-1α to chemokine receptor CXCR4 initiates rearrangement of the actin and MT cytoskeleton resulting in T cell polarisation and lymphocyte migration (Vicente-manzanares et al. 2002). We previously demonstrated RACK1 and NMHC-IIA co-localised at the leading edge LFA-1-mediated migrating T cells. In addition, we have shown RACK1 localises to the actin-rich cap of SDF-1α-stimulated polarised T cells. NMHC-IIA has previously been shown to associate with membrane-bound CXCR4 and filamentous actin at the leading edge of chemokine-induced polarised T cells and may provide a key mechanical link between signal transduction and myosin contractility (Rey et al. 2002). We hypothesised that RACK1 also associates with the motor protein and chemokine receptor at the leading edge of chemokine-induced polarised T cells.

To test this, we starved PBTLs in serum-free RPMI for at least 2 hours and stimulated PBTLs with soluble SDF-1α for 20min to induce cell polarisation. We then fixed and stained cells with immunofluorescent dyes conjugated to antibodies specific for RACK1, NMHC-IIA, and cell surface CXCR4 and to Phalloidin for visualisation of F-actin. Confocal analysis of immunofluorescent staining indicated that RACK1 translocates to the leading edge in association with NMHC-IIA, membrane-bound CXCR4, and F-actin in SDF-1α-induced polarised T cells (Figure 6.10). This is consistent with reports that NMHC-IIA and the chemokine receptor CXCR4 localise to the leading edge of chemokine-stimulated lymphocytes (Nieto et al. 1997; Rey et al. 2002), while NMHC-IIB localises to the uropod is association with ICAM-3 (Campanero et al. 1994; Rey et al. 2002). Therefore, the scaffolding protein RACK1 may serve as a scaffold between the chemokine receptor and myosin motor protein to recruit key signalling proteins necessary for induction of signal transduction pathways that regulate cytoskeletal remodelling and lymphocyte migration.

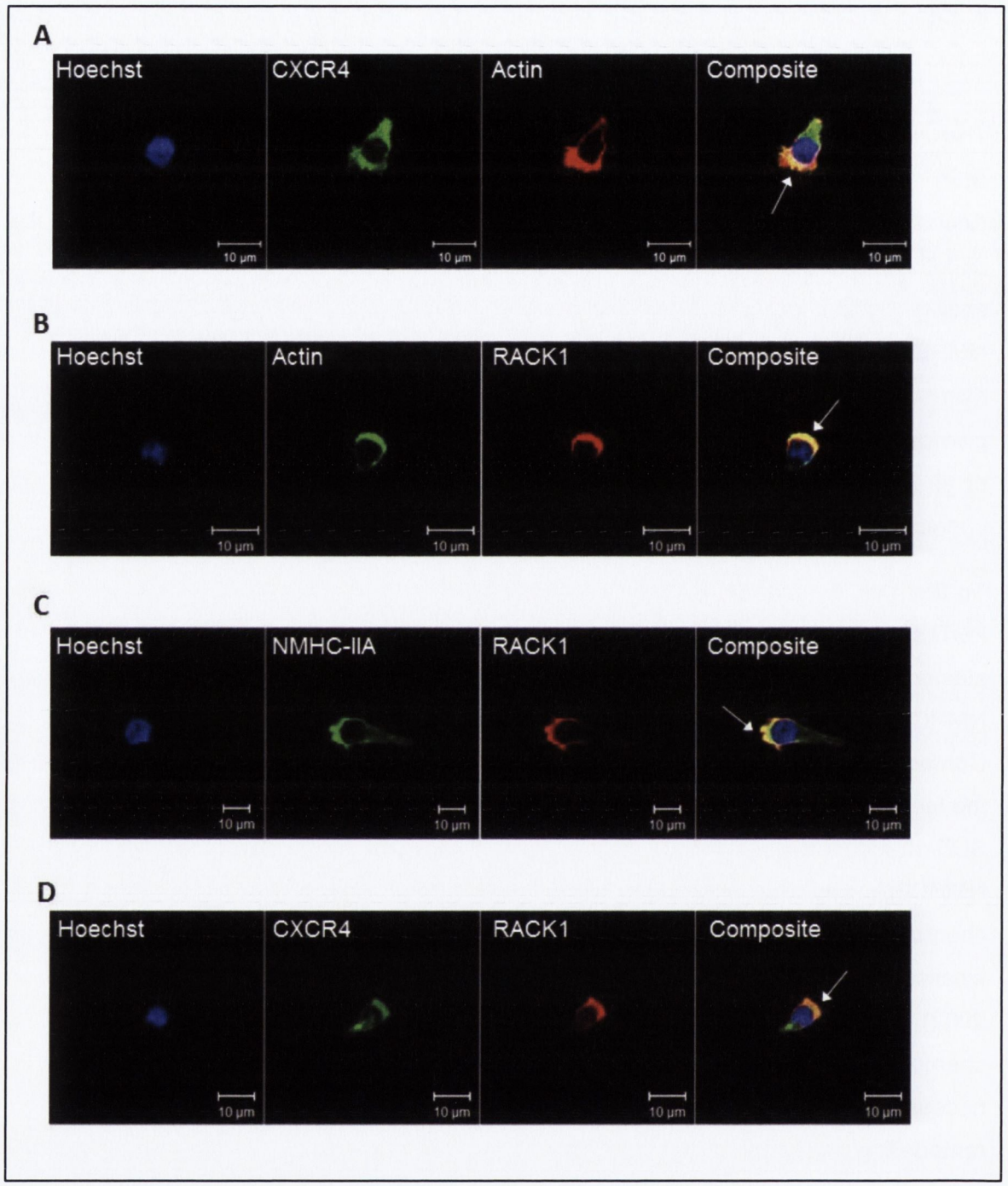

Figure 6.10: RACK1 Localises to Actin-rich Cap in Association with NMHCIIA and membrane-bound CXCR4 in SDF-1α-Activated Cells.

Serum starved PBTLs were stimulated with soluble SDF-1α for 20min to induce cell polarisation. Cells were fixed and stained cells with immunofluorescent dyes conjugated to antibodies specific for cell surface CXCR4 with Phalloidin (A) RACK1 with Phalloidin (B), RACK1 with NMHC-IIA (C), and RACK1 with cell surface CXCR 4 (D). Arrows indicate co-localisation at the leading edge.

6.3.5 The Effect of KD of RACK1 on CXCR4 Cell Surface Expression in SDF1α-1-stimulated Jurkat T cells

Stimulation of lymphocytes with SDF-1α induces an association between NMHC-IIA and the chemokine receptor CXCR4 (Rey et al. 2002). Activated CXCR4 is then internalised into the cell in order to modulate chemotactic responses of leukocytes (Vroon et al. 2006). We previously demonstrated KD of RACK1 enhanced SDF-1α-induced chemotatic migration, and hypothesised RACK1 interaction with NMHC-IIA may affect the cell surface expression/ internalisation of the chemokine receptor. Therefore, serum starved Jurkat T cells previously transfected with control siRNA or RACK1-specific siRNA were stimulated with SDF-1α for 20 min or 60 min or left unstimulated to assess the effect of depletion of RACK1 on CXCR4 internalisation. Membrane-bound CXCR4 was labelled with PE-tagged CXCR4 and the mean fluorescence intensity (MFI) was measured by flow cytometry. While KD of RACK1 expression slightly increased the surface levels of expression of CXCR4, the rate of internalisation of the CXCR4 receptor from the cell surface following SDF-1α stimulation was similar in control T cells. These data suggest RACK1 does not alter CXCR4 expression in response to SDF-1α stimulation in PBTLs.

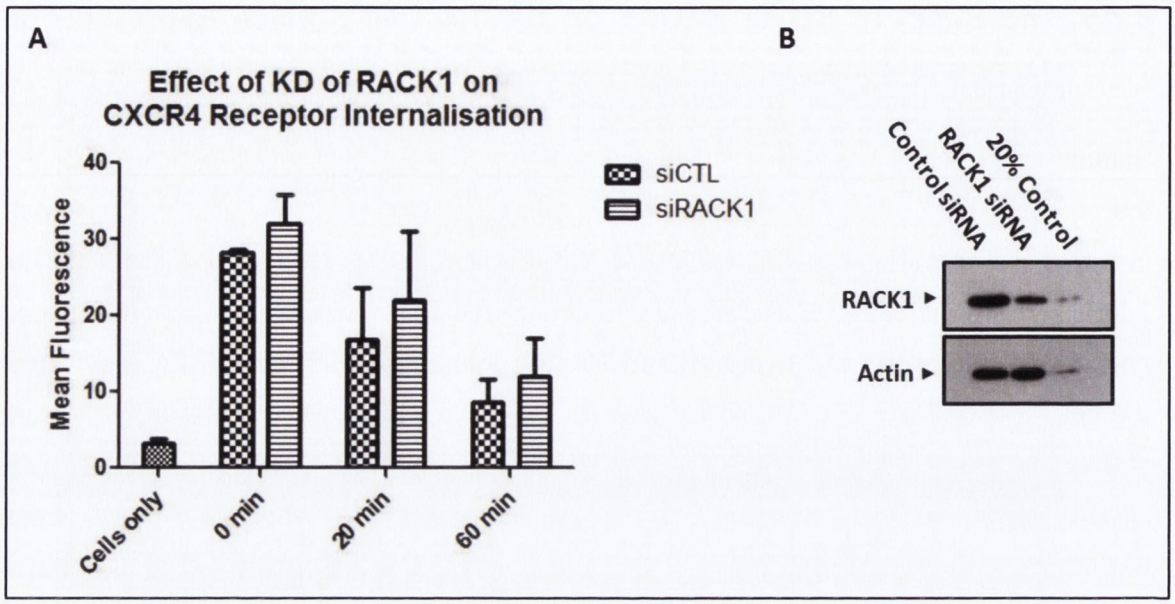

Figure 6.11: KD of RACK1 does not affect chemokine receptor CXCR4 internalisation in response to SDF-1α.

(A) Serum starved Jurkat T cells previously transfected with control siRNA or RACK1-specific siRNA were stimulated with SDF-1α for 20 min or 60 min or left unstimulated. Membrane-bound CXCR4 was labelled with PE-tagged CXCR4 and the mean fluorescence intensity was measured by flow cytometry. "Cells only" indicates cells not labelled with PE-tagged CXCR4. The mean ± SEM of N=4 in duplicate is shown. (B) Immunoblot indicating level of protein knockdown of RACK1 72 hours after transfection with siRNA in Jurkat T cells.

6.3.6 The Effect of KD of RACK1 on Localisation of NMHC-IIA, RMLC, and pMLC ser19 in SDF-1α-stimulated PBTLs

Stimulation of lymphocytes with SDF-1α induces activation of the RhoA/ROCK axis and phosphorylation of MLC at ser19. Phosphorylation of MLC at Ser19 mediates activity and localisation of NMII and thus NMHC-IIA (Vicente-manzanares et al. 2002). If RACK1 serves as a scaffold to recruit effector proteins to SDF-1α-bound CXCR4 and facilitate MLC phosphorylation, suppression of RACK1 should affect the phosphorylation and subsequent subcellular localisation of pMLC Ser19. To test this, we starved PBTLs in serum-free RPMI for at least 2 hours and stimulated PBTLs with soluble SDF-1α for 20min to induce cell polarisation. We then fixed and stained cells with immunofluorescent dyes conjugated to antibodies specific for RACK1, NMHC-IIA, and CXCR4 and to Phalloidin for visualisation of F-actin. High content analysis parameters measuring fluorescence intensity and Cell Intensity CV of F-actin, NMHC-IIA, and pMLC Ser19 were used to assess the effect of depletion of RACK1 on protein expression and subcellular localisation. We determined the Cell Intensity CV values for F-actin in unstimulated T lymphocytes was typically 0.4 – 0.6, while SDF-1α-stimulated polarised cells with F-actin distributed at the leading edge typically had Cell Intensity CV values in the range of 0.8 – 1.3. Preliminary data indicate a decrease in cell intensity CV of pMLC in RACK1-deficient cells as compared to control PBTLs (data not shown). This work is being further evaluated by high resolution confocal microscopy.

6.3.7 Investigation of the Effect of Suppression of RACK1 on Phosphorylation of Myosin Light Chain at Ser19

The GTPase RhoA signalling pathway is induced by SDF-1α stimulation, resulting in ROCK-dependent phosphorylation of MLC at Ser19. Moreover, inhibition of ROCK with the Y-27632 inhibitor has been reported to decrease phosphorylation of MLC at Ser19 and prevent SDF-1α-induced chemotaxis (Vicente-manzanares et al. 2002). In addition, MLCK inhibition with the inhibitor ML-7 prevents T cell polarisation and also impairs chemotaxis (Vicente-manzanares et al. 2002). First, we sought to replicate this data in primary T cells. Serum-starved PBTLs were pre-treated with Calyculin A (a serine/threonine phosphatase inhibitor which prevents MLC dephosphorylation), the MLCK inhibitor ML-7 (a highly specific inhibitor of myosin light chain kinase), and the ROCK inhibitor Y-27632 (activating myosin phosphatase) and then stimulated with SDF-1α (described in section 2.13). The experiment was repeated in three separate donor T cell populations. Calyculin A induced phosphorylation of MLC as previously reported

(Henson et al. 2003; MacKintosh and MacKintosh 1994). While ML-7 did not significantly inhibit MLC phosphorylation, the ROCK inhibitor did significantly prevent phosphorylation at Ser19.

We previously demonstrated RACK1-deficient cells exhibit enhanced chemotaxis similar to cells treated with MT depolymerising agent Nocodazole in response to SDF-1α. MT depolymerisation results in a release of Rho-GEF, which induces RhoA activity (Chang et al. 2006; Krendel et al. 2002). Therefore, we hypothesised RACK1 may be influencing MT stability, thereby altering RhoA activity. If RACK1 influences RhoA activity, RhoA/ROCK-dependent phosphorylation of MLC may also be altered. Therefore, we proposed RACK1 may affect the phosphorylation of Ser19 on MLC through its interaction with NMHC-IIA. To verify a specific role for the interaction of RACK1 and NMHC-IIA in the molecular mechanisms underlying SDF-1α-induced T lymphocyte polarisation and migration, serum starved PBTLs previously transfected with RACK1-specfic siRNA or control siRNA were incubated with SDF-1α for the indicated times. The phosphorylation of MLC at Ser19 was then analysed by Western Blot. The experiment was repeated in three separate donor T cell populations. In accordance with previous observations (Vicente-manzanares et al. 2002), stimulation with SDF-1α induced phosphorylation of MLC at Ser19 by 2min and the phosphorylation peaked at 20min. However, suppression of RACK1 did not significantly affect the amount or rate of phosphorylation. There did appear to be an increase in the basal level of MLC Ser19 phosphorylation; however, this was not consistent and may reflect variation between donor T cell populations. These findings suggest RACK1 does not negatively regulate chemotaxis by altering the phosphorylation of MLC Ser19. Nevertheless, as RACK1 is associated with myosin at the leading edge and in the uropod, it may be affecting myosin activity differently at the front and at the back as MLC Ser19 phosphorylation is regulated by different kinases (e.g. MLCK at the front and ROCK in the rear). Therefore, the activity of RhoA should be assessed in RACK1-depleted PBTLs in order to shed light on the molecular mechanisms by which RACK1 regulates lymphocyte migration.

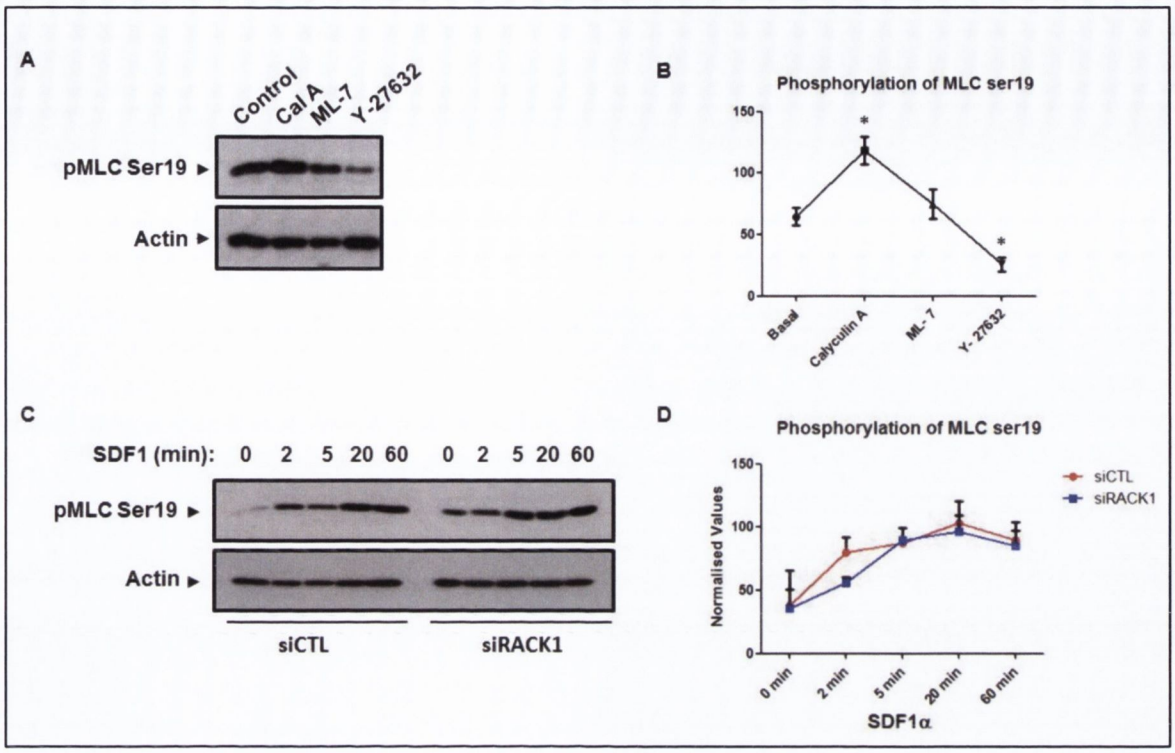

Figure 6.12: Effect of suppression of RACK1 on phosphorylation of MLC at serine 19 (pMLC ser19).

(A) Immunoblot analysis of the phosphorylation of ser19 of MLC in primary T cells pre-treated with 100nM Calyculin A (Cal A), 20μM MLCK inhibitor ML-7, and 20μM ROCK inhibitor Y-27632 compared to untreated PBTLs. (B) Densitometry was performed on the immunoblots and the mean ± SEM of N=3 is shown. (C) Immunoblot analysis of the phosphorylation of ser19 of MLC in response to SDF-1α activation in PBTLs 72 hours after transfection with RACK1-specific and control siRNA. (D) Densitometry was performed on the immunoblots and the mean and SEM of N=3 is shown.

6.4 Discussion

In the present study, we set out to identify the molecular mechanisms by which RACK1 mediates cell polarisation and negatively regulates integrin-mediated and chemokine-induced lymphocyte migration. We previously identified NMHC-IIA as a binding partner of RACK1 in T lymphocytes using a proteomics strategy. In addition, we provided evidence for the endogenous association between the scaffolding protein RACK1 and the motor protein NMHC-IIA, which appeared to be constitutive as activation of LFA-1 did not significantly alter the association. Moreover, we demonstrated RACK1 translocated to the leading edge in association with NMHC-IIA and F-actin in LFA-1-induced migrating T cells. Furthermore, we mapped the putative binding sites for NMHC-IIA on RACK1 through the use of a RACK1 peptide array and identified three candidate regions within the RACK1 sequence that contribute to a NMHC-IIA binding interface, namely residues that span the propeller blades WD2, WD3, and WD4 of RACK1. We then determined the amino acids on RACK1 involved in NMHC-IIA interaction by peptide-substitution arrays and *in silico* modelling on Asc1, the yeast homolog of RACK1. The fact that we identified three binding regions for NMHC-IIA on the RACK1 sequence is not surprising because RACK1 has been shown to make multiple contacts with its various binding partners (Adams et al. 2011; Chen et al. 2004b). A peptide-substitution array used to identify amino acids within the RACK1 sequence that mediate the interaction between RACK1 and NMHC-IIA implicated three sets of residues: Arg^{99}, Arg^{100}, and Lys^{106} on RACK1 blade WD2; K^{127}, K^{130}, C^{138}, and K^{139} on blade WD3; and K^{172}, K^{175}, K^{183}, and K^{185} on blade WD4. Each sequence is exposed on the outer β-strand of the propeller blades and available for protein-protein interactions. Furthermore, the relative position of the basic residues on blades WD3 and WD4 is very similar. Interestingly, the topological presentation of the basic residues on blade WD2 might partially mimic this presentation. Therefore, these data suggest NMHC-IIA interacts with RACK1 on three highly conserved and homologous sites. Together, these findings strongly suggest that these amino acids are important for the interaction of RACK1 and the motor protein NMHC-IIA.

The ^{93}TTGTTTRRFVGHTK^{106} region has previously been reported to mediate other RACK1 interactions such as with PKC βII (Grosso et al. 2008) and the scaffolding protein 14-3-3 (Neasta et al. 2012). The fact that PKC βII, 14-3-3, and NMHC-IIA share a binding region on RACK1 is of particular interest because multiple 14-3-3 isoforms have also been reported to directly interact with several PKC isoforms (Jones et al. 1995; Meller et al. 1996; Robinson et al. 1994). In addition, PKC is also responsible for the

phosphorylation of MLC at Ser1, Ser2, and Thr9 (Beach et al. 2011; Ikebe and Reardon 1990). Finally, 14-3-3 has been shown to interact directly with NMHC-IIA and MTs and act downstream of the small Rac GTPase RacE (Zhou et al. 2010), which triggers actin polymerisation and inhibits NMII activation unlike other small GTPases, such as RhoA, which promote myosin activation (Vicente-Manzanares et al. 2009a). The authors demonstrated 14-3-3 acts to stabilise MTs and to promote NMII bipolar thick filament remodelling to coordinate cell shape change (Zhou et al. 2010). Furthermore, whereas RACK1 binds activated PKC (Mochly-Rosen et al. 1995; Ron et al. 1994), 14-3-3 binding to PKC inhibits its activity (Bridges and Moorhead 2005; Meller et al. 1996; Robinson et al. 1994). Therefore, it is plausible that a competition between PKC and 14-3-3 for RACK1 binding might also regulate PKC signalling. The scaffolding molecules may also compete to sequester distinct 'pools' of PKC, active and inactive. For instance, as PKC-dependent phosphorylation of Ser1, Ser2, and Thr9 has been shown to inhibit myosin kinetic activity by decreasing the affinity of both MLCK and actin (Beach et al. 2011; Ikebe and Reardon 1990), RACK1 binding to 14-3-3 may prevent RACK1-mediated PKC phosphorylation of MLC, thereby enhancing myosin activity. Moreover, while NMHC-IIA was associated with RACK1 following LFA-1 activation, there did appear to be a decrease in migrating cells (Figure 5.4D). This suggests a subset of NMHC-IIA is not bound to RACK1 during migration supporting the negative regulatory role of RACK1 in lymphocyte migration. In this study, we also found suppression of RACK1 by siRNA did not significantly affect MLC phosphorylation at Ser19 or CXCR4 internalisation. Therefore, RACK1 may not regulate the RhoA/ROCK axis downstream of CXCR4, but rather mediate PKC-dependent MLC phosphorylation at Ser1, Ser2, and Thr9. Indeed in the study in Chapter 4, cells with depleted levels of RACK1 exhibited a reduction in cell polarisation possibly due to myosin hyperactivity and contractility and an associated increased chemotaxis. Whereas, overexpression of RACK1 may enhance myosin-mediated lamellipodia stabilisation and adhesion maturation (Vicente-Manzanares et al. 2009b), thereby preventing rapid cell migration.

It is also worthwhile to note that RACK1 can dimerise to increase its binding partners, and analysis of the homodimer of the RACK1 yeast homolog Asc1 indicates the ^{93}TTGTTTRRFVGHTK^{106} region and key residues implicated in the NMHC-IIA interaction are still exposed in the homodimer (Appendix 1 Figure 3). Indeed, immunoprecipitation of NMHC-IIA and subsequent immunoblotting with RACK1 indicates the putative RACK1 homodimer is also associated with NMHC-IIA in lymphocytes (data not shown). Therefore, RACK1 may interact with a combination of NMHC-IIA, 14-3-3, and PKC in a

context-dependent manner. In addition, as 14-3-3 is considered a genetic suppressor of Nocodazole due to its MT stabilising activity (Zhou et al. 2010), RACK1 interaction with 14-3-3 may explain why overexpression of RACK1 attenuates the Nocodazole-enhanced chemotaxis as demonstrated in Chapter 4. Indeed, several isoforms of 14-3-3 were identified in the RACK1 proteomic profile in migrating lymphocytes in Chapter 5; the interaction between RACK1 and 14-3-3 may constitute a protein scaffold for integrating signals from different cellular processes. The functional implications of the interaction between these two scaffolding proteins have not yet been studied in lymphocytes and may have profound implications in regulating signalling pathways contributing to lymphocyte migration. In addition, the effect of altered levels of RACK1 on MT stability by measuring MT polymerisation in resting and migrating T cells should be addressed in future work. Furthermore, this RACK1-mediated protein complex needs to be further evaluated to shed light on the regulatory mechanisms of cytoskeletal remodelling during directional cell migration.

Certainly, further work is necessary to reveal the functional implications of the RACK1 and NMHC-IIA interaction in lymphocyte migration. In addition to silencing RACK1 by siRNA, the interaction between RACK1 and NMHC-IIA can be further evaluated by preventing binding with RACK1-derived peptides specific for the NMHC-IIA binding site. RACK1-derived peptides have been previously used to investigate the interaction of RACK1 and its binding partners (Neasta et al. 2012). For instance, following identification of the 14-3-3 binding site on RACK1, a peptide derived from the RACK1 binding region was fused to the cell-penetrating peptide TAT, which enables intracellular transduction (Gump and Dowdy 2007). Pre-treatment with the TAT fusion protein blocked the interaction between the two scaffolding proteins (Neasta et al. 2012). Unlike RACK1 knockdown by siRNA, which suppresses the cellular level of RACK1 protein, RACK1-derived peptides can block interactions with selective proteins. This may prove crucial in identifying the functional implications of protein-specific interactions of scaffolding molecules, which have numerous binding partners. Therefore, this method should be employed in studying the RACK1-mediated complexes in lymphocyte migration.

While RACK1 did not appear to have an effect on SDF-1α-activated RhoA/ROCK-dependent myosin phosphorylation, RACK1 has been reported to bind the heterotrimeric protein Gβγ, which associates with CXCR4 (Chen et al. 2008). Thus, RACK1 may regulate a subset of signalling pathways downstream of the CXCR4 receptor in response to SDF-1α stimulation in human T lymphocytes, but does not regulate CXCR4

internalisation. If RACK1 indeed does not have an effect on CXCR4 surface expression, it is unlike other regulatory proteins such as arrestins and G protein Regulatory Kinases (GRKs), which negatively modulate chemotactic responses of leukocytes by down-regulating functions of chemokine receptors through phosphorylation and internalisation of GPCRs (Vroon et al. 2006). In addition, Regulator of G protein Signalling (RGS) proteins inhibit chemotaxis by shortening the lifetime of the active Gα-GTP subunit (Kehrl 2006).

Cellular polarisation and the formation of the leading edge/lamellipodia in response to chemokine stimulation is driven by activation of GTPases such as Rac1 (Gómez-Moutón and Mañes; Ridley 2011; Tybulewicz and Henderson 2009), while the PI3K/Akt and ERK pathways are also activated downstream of SDF-1α/CXCR4 signalling in human T lymphocytes (Patrussi and Baldari 2008; Tilton et al. 2000). Interestingly, suppression of RACK1 was reported to significantly increase both basal and SDF-1α-induced Akt phosphorylation by PI3Kγ as well as enhance the activation of PLCβ and PKC ζ in Jurkat T cells, whereas overexpression of RACK1 inhibited both the basal and SDF-1α-induced PI3Kγ-dependent Akt phosphorylation (Chen et al. 2008). In contrast to its effects on PLCβ, PI3Kγ, and PKC ζ activities, silencing RACK1 did not affect either basal or SDF-1α-stimulated ERK activity (Chen et al. 2008). Therefore, the findings from this study in conjunction with other RACK1 studies suggest that RACK1 regulates a subset of signalling pathways downstream of the CXCR4 receptor in response to SDF-1α stimulation in human T lymphocytes, including PLCβ and PI3Kγ/Akt, while other signalling pathways such as ERK activation and CXCR4 internalisation are unaffected. Further evaluation is necessary to define the role of RACK1 in selectively regulating the activation of downstream signalling pathways in response to SDF-1α stimulation.

6.4.1 Conclusion

In summary, we have provided evidence for the direct interaction between RACK1 and the motor protein NMHC-IIA in T lymphocytes. Future work is necessary to elucidate the functional implications of this interaction and other RACK1-mediated protein complexes to further define the role of RACK1 in regulating directional cell migration.

CHAPTER SEVEN

Discussion and Conclusion

7 Discussion and Conclusion

7.1 Contribution of this Study to the Understanding of T lymphocyte Migration

Understanding T cell migration presents a formidable challenge because it results from the coordinated activity of several individual intra- and extracellular component processes. These processes include several signalling pathways, and require significant and well-orchestrated cross-talk between cell surface receptors, signal transducers, adaptor proteins, and elements of the cell cytoskeleton. Moreover, it is becoming increasingly clear that coordinated redistribution of signalling and cytoskeletal components contribute to functional lymphocyte migration. Several distinct, but integrated, biochemical pathways regulate changes in cell morphology necessary for T cell migration. Due to the multifaceted and overlapping nature of these pathways, research on cell migration requires multidisciplinary approaches and concepts.

In recent years, there have been progressive and seminal advances in the understanding of the molecular basis of lymphocyte migration. Several signalling, adaptor, and regulatory molecules have been identified and the mechanisms of their involvement in immune cell migration are gradually being elucidated. Researchers now recognise that lymphocytes require internal structural flexibility and dynamic migratory behaviour to fulfil their role as immune cells and that cell surface receptors, such as integrins, have a key function in mediating these activities. However, despite vast amount of research in the field, scientists do not fully understand how the coordinated functions of downstream signalling pathways of integrins are regulated. Moreover, we have yet to discover the full signalling potential of integrins expressed on T cells and the information they uniquely contribute when cooperating with other immune cell receptors, such as the TCR. Furthermore, unlike many other studied cell types, T cells do not exhibit easily identifiable integrin-mediated focal adhesions or associated complexes. Therefore, the current challenge is to elucidate the mechanisms of integrin-mediated signalling that enable rapid lymphocyte migration.

Lymphocyte polarisation and migration is the product of dramatic changes in cell morphology and cyto-architecture. While the importance of cytoskeletal structures in lymphocyte activation has long been established, only recently have experimental advances revealed direct mechanistic links between the activation of lymphocyte-specific

components of signal transduction pathways and the downstream machinery affecting cytoskeletal reorganisation. Our research group and others have previously demonstrated and established that the T cell integrin LFA-1 has the ability to transduce a variety of signals, including activation of PKC, resulting in rearrangement of the cytoskeleton (Evans et al. 2009; Hogg et al. 2004; Serrador et al. 1999; Smith et al. 2005; Smith et al. 2003; Stanley et al. 2008; Stewart et al. 1998; Volkov et al. 2001). These signalling events dictate cellular actions during an immune response and induce the differential localisation of protein complexes in cells. Deregulation of immune cell signalling pathways can lead to devastating effects, including auto-immunity and cancer. Therefore, it is important to identify and understand how these complexes function. Understanding the contribution of individual components of immune cell signalling pathways that lead to a fully functional T lymphocyte could potentially generate more promising and specific immunomodulation therapies. Recent advances have provided insights into mechanisms underlying the ability of cell adhesion molecules, such as integrins, to induce signal transduction cascades. Integrin receptor engagement in T cells initiates the activation of signalling pathways by recruiting scaffolding proteins that, in turn, contribute to the assembly of a 'signalsome', a multi-protein complex comprised of various enzymes, their substrates, and adaptor proteins that permit appropriate protein interactions and, thus, the efficient flow of information in signalling pathways (Juliano 2002; Shaw and Filbert 2009). By behaving as molecular hubs, scaffolding proteins allow the formation of these preassembled or signal-dependent multi-protein complexes that contribute to the accuracy of the spatiotemporal processing and transmission of a signal. In addition, an appropriate transmission of an intracellular signal can be achieved by the subcellular compartmentalisation of signalling proteins that typically requires post-translational modification and/or the association with scaffolding proteins (Kholodenko et al. 2010; Pawson and Scott 1997; Scott and Pawson 2009; Shaw and Filbert 2009). However, it is still unclear how integrins coordinate the redistribution of signalling and cytoskeletal components necessary for T cell motility.

Inspired by the recent advances in the field of cell migration and newly available technologies, we realised the importance of identifying the components of T cell signalling pathways and elucidating the regulatory mechanisms employed by lymphocytes. The role of the molecular scaffold RACK1 in cell motility has been investigated in diverse cell types, and there is mounting evidence implicating a role for RACK1 in integrin-mediated cell adhesion and migration. Yet, many of the findings have been descriptive rather than providing mechanistic links. The preponderance of evidence

indicates RACK1 may be essential for regulation of migration in all cells types where it is expressed. However, the role of RACK1 in lymphocyte migration has been widely overlooked. Therefore, the overall aim of this Ph.D. project was to investigate the molecular interactions of RACK1 during lymphocyte directional cell migration and to examine in detail the functional implications of the associations of this scaffolding protein in T cells.

7.2 Importance of RACK1 in Lymphocyte Polarisation and Migration

Due to their crucial role in mediating intracellular signalling related to cell proliferation and development, recent studies have highlighted the relevance of scaffold proteins in cell migration and indicated that interfering with their expression and/or their ability to bind effector proteins can have dramatic effects on cell adhesion and migration. The molecular scaffold RACK1 is essential for cell polarisation and migration, and the protein binds to many components of the cell migration machinery including kinases, phosphatases, and the cytoplasmic domains of cell surface receptors (Adams et al. 2011; McCahill et al. 2002). RACK1 was originally identified as a receptor for activated protein kinase C and has been implicated in the reorganisation of the actin framework in response to different stimuli (Adams et al. 2011; McCahill et al. 2002). Overall the hypothesis proposed in this thesis is that RACK1 is involved in regulating T lymphocyte polarity and motility. As RACK1 is known to interact with members of the PKC family and several polarity complex proteins, including PKC ζ, have been implicated in T cell migration and translocate to the leading edge upon integrin activation (Gérard et al. 2007; Real et al. 2007), we hypothesised that induction of LFA-1 would also induce RACK1 translocation. Recent advances in imaging technology have begun to uncover when and how the cytoskeleton, signalling molecules, and adhesion molecules are asymmetrically distributed during migration. The *in vitro* model of LFA-1-mediated T cell polarisation and migration employed in this study allows the investigation of protein subcellular localisation and any changes in distribution in response to LFA-1 activation. In addition, the comparative analysis of cell populations with the use of high content imaging technology enables the identification of proteins involved in cell migration.

In the study in Chapter 3, we demonstrated that following activation of LFA-1, RACK1 displays an asymmetrical distribution and translocates from a peripheral, cytosolic distribution in resting cells to the leading edge and trailing uropod of polarised migrating T cells. Live cell imaging further corroborated this dynamic polarised redistribution in migrating T cells. In addition, we found RACK1 localises to the forward extending

lamellipodia behind filamentous actin and co-localises with the MT network. As a putative membrane-associated adaptor protein, RACK1 may regulate the polarity axis by targeting proteins to an anterior/posterior distribution in polarised migrating T cells. Stimulation with the chemokine SDF-1α triggers cytoskeletal remodelling and a polarised morphology, which we demonstrated induces RACK1 translocation to the actin-rich front and trailing uropod of polarised T cells. This asymmetric distribution is consistent with a previous report indicating RACK1 translocates to the leading edge of SDF-1α-stimulated Jurkat cells, a leukemic T cell line (Chen et al. 2008). Furthermore, the dynamic translocation of RACK1 both to the leading edge as well as to the trailing uropod would suggest that it may be continuously recycled during directional migration, which is in accordance with recent theories that lipid raft components, such as membrane-associated receptors and signalling molecules, are recycled from the posterior compartment to replenish new protrusions and adhesions and sustain directional migration in leukocytes (Barreiro et al. 2007; Fabbri et al. 2005; Ridley et al. 2003). This theory would also fit observations that T cells can rapidly alter migration direction in response to extracellular stimuli because of the differential expression and affinity of LFA-1 (Smith et al. 2007a; Smith et al. 2005).

The dynamic cycling of the molecular scaffold may allow the cell to redistribute a host of signalling molecules to mediate internal polarity and rapidly change direction. Indeed, we demonstrated RACK1 co-localised with the polarity protein atypical PKC ζ at the leading edge of polarised migrating T cells. Furthermore, silencing RACK1 by siRNA inhibited recruitment of PKC ζ to the forward extending lamellipodia, which has previously been shown to be required for regulating T cell polarity (Gérard et al. 2007; Real et al. 2007). This finding reflects the role of RACK1 as a mediator of signal transduction by targeting PKC isoforms to discrete subcellular locations, where it phosphorylates effector proteins (Adams et al. 2011; Csukai and Mochly-Rosen 1999; McCahill et al. 2002). LFA-1-stimulated T lymphocyte migration involves the rearrangement and polarisation of the cellular cytoskeleton, a process which is dependent on the translocation of PKC isozymes (Volkov et al. 2001; Volkov et al. 1998). The translocation of RACK1 to leading edge of LFA-1 induced migrating T cells in association with cytoskeletal elements and the atypical PKC ζ, a well-established regulator of cell polarity (Gérard et al. 2009; Gérard et al. 2007; Real et al. 2007) at the leading edge of the cell supports its involvement in defining polarity and regulating motility in T cells.

Therefore, in the following study in Chapter 4, we sought to investigate the functional effects of altered levels of RACK1 expression on T cell polarisation and migration. The

role of RACK1 as a scaffold/adaptor protein involved in diverse cellular processes is well documented but widely varied. A number of published reports have implicated RACK1 in cell adhesion and migration, partially through its interaction with the a wide range of signalling kinases, including PKC β, PKC ε, Src, and FAK as well as with the cytosolic domain of membrane-bound receptors, such as beta integrins, thereby integrating signals from various transduction pathways (Buensuceso et al. 2005; Buensuceso et al. 2001; Chang et al. 2001; Doan and Huttenlocher 2007; Liliental and Chang 1998; McCahill et al. 2002; Serrels et al. 2010). However, conflicting reports of RACK1 in either promoting or inhibiting cell migration are found in the literature, probably reflecting the context-dependent functions of RACK1. Certainly, RACK1 has been reported to facilitate cell migration and spreading in several adherent cell lines and tumour cells (Doan and Huttenlocher 2007; Kiely et al. 2008), while exhibiting a negative regulatory role in integrin-mediated migration in other cell types (Buensuceso et al. 2001; Chen et al. 2008).

The multi-parametric analysis of lymphocyte morphology was employed in this study to characterise RACK1 function in integrin-mediated and chemokine-induced T cell migration. Selected morphology parameters were significantly reduced in RACK1-deficient cells compared to control cells indicating a significant decrease in T cell polarisation in both the T cell line HuT78 as well as in primary T cells. Moreover, depletion of RACK1 prevented formation of stable uropod structures, which could dictate the axis of migration. Similar to RACK1-deficient cells, cells treated with the MT depolymerising agent Nocodazole exhibited a reduction in morphological polarisation and a stunted uropod phenotype, in accordance with a previous study that reported Nocodazole-treated cells do not form a stable uropod structure, but rather small, uropod-like protrusions (Takesono et al. 2010). In addition, RACK1-deficient PBTLs exhibited a significant reduction in the speed and persistence of LFA-1-mediated migration. Time-lapse microscopy analysis of migrating cells also indicated RACK1-deficient cells lacked a single extending lamellipodia, and migration was accompanied by multi-directional protrusions, which appeared to inhibit directional cell migration. This finding strongly suggests that RACK1 is involved in regulating polarity in T lymphocytes. In accordance with a previous observation that suppression of RACK1 did not effect adherency to ICAM-1 in the Jurkat leukemic T cell line (Chen et al. 2008), we did not detect a role in adhesion to ICAM1 for RACK1 in primary T cells. Therefore, RACK1 is required for SDF-1α-mediated lymphocyte migration on the integrin ligand ICAM-1 by influencing velocity and directionality but in a manner that is independent of LFA-1 integrin activation or

adhesion. Both RACK-1-deficient HuT78 and primary T cells exhibited an increased chemotatic migratory ability, whereas overexpression of full-length RACK1 inhibited SDF-1α-stimulated chemotaxis. This is in accordance with another study which reported RACK1 negatively regulated cell migration in Jurkat T cells, which demonstrated that down-regulation of RACK1 enhanced chemotaxis, while overexpression of RACK1 inhibited chemotatic migration. Interestingly, both depletion of RACK1 and pre-treatment with the MT depolymerising agent Nocodazole reduced cell polarisation but enhanced SDF-1α-stimulated chemotaxis of T cells. Therefore, suppression of RACK1 may mimic the enhanced chemotatic ability exhibited by cells treated with Nocodazole by interfering with MT stability, resulting in the release of Rho-GEF, thereby activating RhoA and actomyosin-based cell contractility. In our study, both depletion of RACK1 and drug-induced MT depolymerisation induced a contractile morphology in T cells with reduced cell polarity, which appeared to enhance chemotaxis in the HuT78 T cell lymphoma and primary T cells.

While most studies have indicated RACK1 expression is associated with increased cell spreading and migration, the results from this study clearly implicate a negative regulatory role for RACK1 in immune cell migration. Therefore, the role of RACK1 in integrin-mediated migration and chemotaxis appears to be cell-type and context dependent. These conflicting reports only further demonstrate the complex regulatory role of RACK1 in mediating migration according to different cells, tissues, and stimuli. As lymphocytes do not exhibit typical focal contacts, which is thought to facilitate rapid migration (Smith et al. 2005), RACK1 may prevent the formation of stable focal adhesion contacts and facilitate a more transient integrin-mediated adhesion necessary for increased migratory speed. Nevertheless, the results from this study and several others indicate the cellular balance of RACK1 is crucial for controlled cell migration. Moreover, these findings clearly demonstrate a regulatory role for RACK1 in T lymphocyte polarity and motility. These results were added to a current simplified model of T cell signalling and chemotaxis in response to SDF1α (Figure 7.1). However, further work is necessary to elucidate the molecular mechanisms, including its effects on immune cell signalling pathways, by which RACK1 mediates lymphocyte migration.

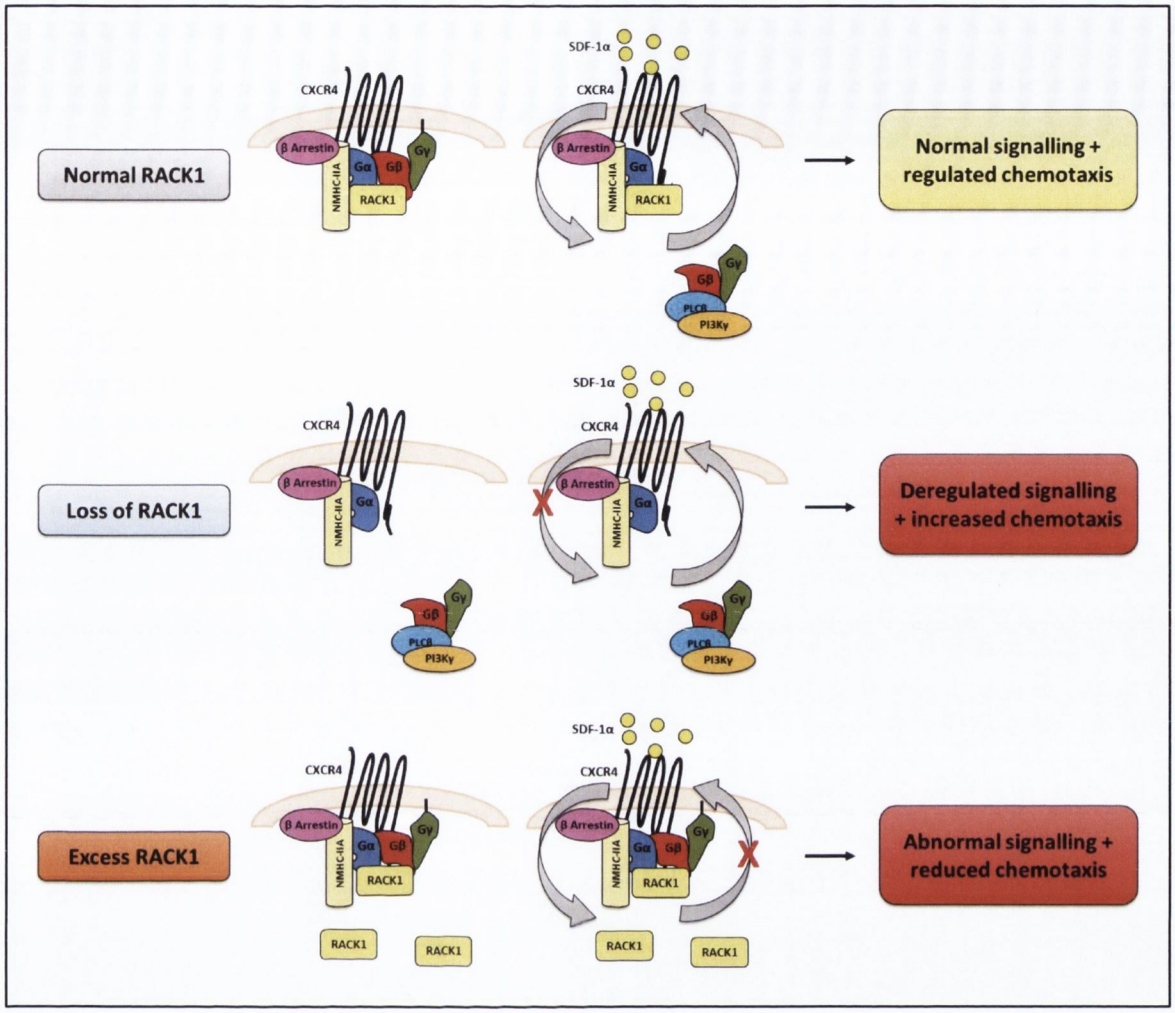

Figure 7.1: Controlled T cell migration requires a regulated cellular expression of RACK1.

Schematic diagram summarising the results of this study demonstrating the impact of normal, diminished, and elevated levels of RACK1 on T cell signalling and chemotaxis in response to SDF1α. Regulated RACK1 expression results in Gβγ dissociation from the scaffolding protein and association with effector proteins (e.g. PLCβ and PI3Kγ). The chemokine receptor CXCR4 is endocytosed to ensure cells are continually responsive to a chemokine gradient. Down-regulation of RACK1 results in unregulated dissociation of Gβγ from CXCR4 and constitutive association with effector proteins resulting in deregulation of signalling and increased chemotaxis. Moreover, loss of RACK1 may also inhibit CXCR4 internalisation in response to SDF1α also resulting in an enhanced chemotatic ability. Up-regulation of RACK1 results in sequestering of Gβγ and prevention of association with effector proteins and reduced chemotaxis. Excess RACK1 may also prevent recycling of CXCR4 to the cell surface, thereby diminishing the chemotatic response to SDF1α.

7.3 The Contribution of High Content Analysis to the Study of Lymphocyte Biology

The role of RACK1 in T cell polarisation and migration was largely investigated with the use of a HCA platform approach, which permits large-scale screening and comparative analysis of cell populations. In recent years, advances in the field of HCA have provided researchers with powerful new tools to observe cellular phenotypes and functions on the basis of multiple experimental parameters. HCA combines automated fluorescence microscopic imaging and image analysis and has become an invaluable tool in cell biology and drug discovery. The advantage of HCA is that it enables the large-scale and simultaneous quantification and correlation of multiple biological phenotypic response and physiological reactions using sophisticated software solutions that permit assay-specific image analysis. High throughput screening of complex biological phenotypes reveals the cellular impact(s) and facilitates reaching definitive conclusions at an early stage. Our group is currently employing HCA technology in conjunction with a siRNA library screen to identify novel proteins affecting specific facets of cell polarisation and migration. In addition, our group has recently published a study using the HCA platform approach for a large-scale screen of chemical libraries to identify the effect of pharmacological inhibitors on lymphocyte polarisation and migration (Freeley et al. 2010). Key sets of parameters that quantitatively assess effects on lymphocyte morphology were identified and the multi-parametric toolbox was employed in the study in Chapter 4 to characterise RACK1 function in integrin-mediated T cell migration. The HCA siRNA screen will identify novel proteins involved in lymphocyte polarisation and migration. Subsequent functional analysis of these protein hits may generate promising new therapeutic targets for the treatment of immune disorders. Furthermore, HCA of the effect of pharmacological inhibitors on T cell migration may prove crucial for the development of novel immuno-suppressants.

7.4 Identification of RACK1-associated Proteins in Lymphocytes

It is now well established that RACK1 interacts with a large number of proteins either directly or as part of a complex, implicating a role in diverse cellular processes, such as cell growth and development, immune regulation, cytoskeletal remodelling, and protein synthesis (Adams et al. 2011; Besson et al. 2002; McCahill et al. 2002). Adaptor proteins like RACK1 can assemble and compartmentalise multiple signalling and structural molecules, thereby providing a platform for their targeted positioning and

efficient interactions (Adams et al. 2011; Pawson and Scott 1997). Because of its ability to coordinate the interaction of key signalling molecules, RACK1 may serve as a molecular hub to integrate diverse signalling pathways required for lymphocyte activation. Furthermore, through its multiple protein binding domains, RACK1 has been implicated in assembling competent signalling complexes by recruiting various enzymes and substrates. For instance, RACK1 serves as a scaffold for the sequestration of key signalling proteins to focal adhesion complexes in association with activated integrin (Serrels et al. 2010). These proteins transduce a number of downstream signalling cascades required for cell activation and migration. Thus, RACK1-associated proteins represent a rich source of potential targets of therapeutic intervention in the treatment and prevention of diseases and as potential markers for early detection of disease states. Indeed, RACK1 is implicated in tumourigenesis (Kiely et al. 2008; Serrels et al. 2010) and has been identified as a cancer biomarker for oral squamous and breast carcinoma as its up-regulation is associated with poor clinical outcome (Cao et al. 2010; Wang et al. 2008). It is therefore of pivotal importance to identify both constitutive and stimulus-dependent protein associations with RACK1.

In the study in Chapter 5, a proteomic approach was employed to determine proteins associated with RACK1 in lymphocytes following LFA-1 activation. Several protein hits ware identified by mass spectrometric analysis and several candidate proteins, namely cytoskeletal elements, were used to confirm endogenous interaction with RACK1 by immunoassays. In addition to cytoskeletal proteins, we identified numerous RACK1-associated proteins involved in signal transduction, transcription regulation, RNA maturation and protein synthesis, and metabolism. The identification of the RACK1 proteomic profile, at least in part, should prove relevant to human lymphocyte biology. Of the putative RACK1-interacting proteins, many are concordant with previously reported observations. For example, RACK1 has recently been reported to interact with the scaffolding molecule 14-3-3 (Neasta et al. 2012). Several 14-3-3 isoforms were identified in our analysis and, similar to RACK1, 14-3-3 proteins can dimerise to interact with numerous signalling proteins and direct the subcellular localisation of target proteins (Aitken 2006; Bridges and Moorhead 2005; Jones et al. 1995). In addition, 14-3-3 was also shown to interact with vimentin in a phosphorylation-dependent manner *in vivo* (Tzivion et al. 2000). As RACK1 was found in this study to associate with both 14-3-3 and vimentin, RACK1 could participate in the modulation of signalling processes requiring 14-3-3 proteins. For instance, the heavy and light chains of NMII were also identified to associate with RACK1. NMII has been reported to interact with PKC ε, and

PKC ε-dependent phosphorylation of vimentin has been implicated in integrin recycling and motility (Ivaska et al. 2005). This implicates RACK1 in mediating PKC signalling and integrin-dependent migration. We have provided evidence for an interaction between two multifunctional scaffolding proteins involved in signal transduction, which may serve as a point of integration for convergent signalling cascades or cross-talk between divergent pathways. This finding only further supports the essential role of adaptor proteins like RACK1 in regulating receptor mediated signal transduction.

We also evaluated the putative association between RACK1 and alpha tubulin and its role in MT stability. In Chapter 4, we demonstrated RACK1-deficient cells exhibit enhanced chemotaxis similar to cells treated with the MT depolymerising agent Nocodazole in response to SDF-1α. Detergent extraction of cells with TritonX-100 allows the independent analysis of cytosolic and cytoskeletal enriched proteins. MT polymerisation is induced following LFA-1 activation and the MT spindle and associated proteins are highly enriched in the cytoskeletal fraction (Verma et al. 2009; Volkov et al. 1998). Therefore, we analysed changes in detergent solubility of candidate proteins following LFA-1 activation by western blotting and immunocytochemistry. We demonstrated RACK1 is enriched in both the cytosolic and cytoskeletal fractions following LFA-1 activation suggesting an increase in RACK1 expression during cell migration. Analysis of RACK1 by immunoprecipitation also indicated an increase in the level of RACK1 protein in migrating cells. Furthermore, we provided evidence for the association between RACK1 and the distal ends of MTs in association with MT stabilising plus-end binding proteins, implicating a role in MT stability during cell migration. This putative role for RACK1 in MT dynamics may explain the reduction in polarisation and increase in chemotatic migration observed in both Nocodazole-treated and cells deficient in RACK1. Therefore, we propose RACK1 may associate with plus-end binding proteins in the local regulation of MT dynamics in T cells in response to positional cues.

The findings from this study support the notion that RACK1 is a scaffolding protein capable of interacting with a wide variety of proteins. These proteins, including several known and several novel associations, have the potential to expand the knowledge database of RACK1-associated complexes and to promote the understanding of the molecular mechanisms of RACK1 signal integration at the systems level. While a number of interacting partners have been identified for RACK1, future studies should incorporate the functional analysis of the identified proteins in order to fully elucidate the implication of RACK1 interactions with individual proteins or as a complex. Certainly,

these studies will broaden the view on protein-protein interaction, signal transduction, and cytoskeletal regulation, all of which are required for functional lymphocyte migration.

7.5 Importance of Mapping Protein Binding Domains on RACK1 for the Study of RACK1-interacting Proteins and Associated Complexes

As an adaptor protein, RACK1 may serve to link signalling proteins to the cytoskeleton to regulate cytoskeleton dynamics. A number of myosin proteins were identified in the RACK1 proteomics profile, including the non-muscle myosin heavy chain NMHC-IIA. We provided evidence for the endogenous association between the scaffolding protein RACK1 and the motor protein NMHC-IIA in both resting and LFA-1-induced migrating T cells. Moreover, while NMHC-IIA was associated with RACK1 following LFA-1 activation, there did appear to be a decreased interaction in migrating cells, suggesting a subset of NMHC-IIA is not bound to RACK1 during migration. This supports a negative regulatory role of RACK1 in lymphocyte migration. Furthermore, we demonstrated RACK1 translocated to the leading edge in association with NMHC-IIA and F-actin in LFA-1-induced migrating T cells. We then mapped the putative binding sites for NMHC-IIA on RACK1 through the use of a RACK1 peptide array and identified that NMHC-IIA interacts with a number of residues exposed on the outer β-strand of the propeller blades WD2, WD3, and WD4 of RACK1. The is in accordance with other studies which have indicated that RACK1 has multiple contact sites with its various binding partners (Adams et al. 2011; Chen et al. 2004b). Furthermore, a peptide-substitution array was used to identify three sets of residues: Arg^{99}, Arg^{100}, and Lys^{106} on RACK1 blade WD2; K^{127}, K^{130}, and C^{138} on blade WD3; and K^{172}, K^{175}, K^{183} on blade WD4 critical for NMCH-IIA binding. Analysis by *in silico* interaction modelling indicated the relative positions of the basic residues on each of the three blades produce a similar 3D arrangement. Even more intriguing, the NMHC-IIA binding sequence on RACK1 overlaps with binding regions for other RACK1 interacting proteins, including 14-3-3 (Neasta et al. 2012) and PKC βII (Grosso et al. 2008). Thus, competitive binding between PKC and 14-3-3 for RACK1 might also regulate PKC signalling. Therefore, identification of binding sites on RACK1 is pertinent to understanding the ability of RACK1 to form multi-protein complexes and may shed light on the integration and regulation of diverse signalling pathways.

Certainly, the association between RACK1 and 14-3-3 by Neasta and colleagues was an intriguing discovery, and one which may have important relevance in immune cell

signalling as we also identified several 14-3-3 isoforms in our lymphocyte RACK1 proteomic analysis. Like RACKs, 14-3-3 proteins are a family of ubiquitously expressed proteins with an astonishingly large number of binding partners. Consequently, 14-3-3 proteins modulate an enormous and diverse group of cellular processes including the cell cycle, metabolism, and signal transduction (Aitken 2006; Bridges and Moorhead 2005; Fu et al. 2000), and have recently gained interest in many fields of biology. This stems from the notion that they are central components of numerous regulatory mechanisms. As adaptor proteins, the number of interacting proteins has estimated to be in the range of several hundred (Bridges and Moorhead 2005; Fu et al. 2000). Although scaffolding molecules like 14-3-3 and RACK1 may therefore be considered too pleiotropic to represent relevant targets for therapeutic intervention, it has been reported that inactivation of select 14-3-3 proteins greatly sensitized cancer cells to stress-induced apoptosis (Niemantsverdriet et al. 2008). While the data is largely circumstantial, members of the 14-3-3 family are reported to be either tumour-promoting or tumour-suppressing (Tzivion et al. 2006), suggesting the cellular balance of 14-3-3 isoforms is crucial for the proper functioning of cells. The ability of 14-3-3 to undergo Ser/Thr phosphorylation and interact with MTs (Zhou et al. 2010), Rho GTPases, such as Cdc42 and Rac1 (Bialkowska et al. 2003), and signalling proteins, including PKC (Gannon-Murakami and Murakami 2002; Meller et al. 1996; Robinson et al. 1994), indicates its relevance in lymphocyte biology and integrin-mediated signalling. While we have only demonstrated the putative association between RACK1 and 14-3-3 in T lymphocytes by mass spectrometry, evidence as binding partners in other cell types supports their direct interaction in lymphocytes. If future experiments elucidate the functional implications of RACK1 association with 14-3-3 in lymphocyte signalling and migration, this interaction could be exploited as a useful molecular target in various pathological conditions involving immune and inflammatory responses. For instance, RACK1 and 14-3-3 may interact with a discrete profile of proteins during a pathological state. Thus, the interaction of the scaffolding molecules with specific moieties may be individually blocked using protein-derived blocking peptides.

7.6 Future Directions

Much of the current understanding about the signalling mechanisms implicated in T cell migration is based on studies performed on a small fraction of known cell surface receptors, such as in the integrin LFA-1. The coordination of diverse signalling pathways regulating cytoskeletal dynamics is still not well defined and constitutes a major

challenge for future studies. In particular, the signalling pathways that regulate MT dynamics in response to integrin activation are yet to be fully elucidated. MT-associated proteins like RACK1 are likely to play a key role in MT stability and reorganisation and defining the axis of polarity in response to directional cues.

We are only beginning to understand how the signalling mechanisms for individual receptors involved in homeostatic and inflammatory trafficking differ in the *in vitro* setting. A complete understanding of the mechanisms guiding lymphocyte migration will be essential in providing new avenues for potential therapeutics in inflammatory and autoimmune diseases states.

The project in this thesis has generated substantial data and formed a foundation from which subsequent studies can be pursued. We have identified a number of RACK1-associated proteins in lymphocytes; however, we are still uncovering the functional implications of these interactions in the context of T cell migration. Furthermore, our RACK1 proteomic profile represents only a subset of RACK1-associated proteins, and a complete and comparative analysis of the RACK1 proteomic profile in resting and migrating cells is necessary to fully elucidate its role in lymphocyte migration. Moreover, we provided evidence for the direct interaction of RACK1 and NMHC-IIA in lymphocytes. However, we have only begun to uncover the functional implications of this interaction in regulating T cell polarisation and migration. Further work is necessary to dissect the mechanisms by which RACK1 influences myosin activity during directional cell migration.

In addition, the role of RACK1 in cell signalling and migration can be further explored through the use of RACK1-derived peptides, which selectively block protein interactions. This may prove crucial in identifying the functional implications of protein-specific interactions of scaffolding molecules, which have numerous binding partners. Furthermore, the impact of RACK1 depletion on NMII activity can be further explored by assessing the phosphorylation status of the heavy chain as well as the regulatory light chain. Unfortunately, there are not commercially available phospho-specific antibodies to all known phosphorylation sites on NMHC-IIA. Therefore, identifying differences in the global and site-specific phosphorylation status of NMHC-IIA could be analysed by a specialised form of mass spectrometric technology and implementing a post-translational modification algorithm previously described (Olsen et al. 2006).

Finally, although the findings from this study contribute to our understanding of RACK1 function in integrin-mediated lymphocyte migration, it is still unclear how these mechanisms relate to *in vivo* processes. Therefore, *in vivo* studies, including the use of a

mouse model should be considered. In addition, stimulated mouse T cells migrating on ICAM-1 have been reported to behave similarly to their human counterparts (Smith et al. 2007a) and therefore may use the same mechanisms to migrate. In order to understand the biophysical effects of RACK1 on myosin activity during directional cell movement, experiments with RACK1-knockout mice, which, have yet to be generated, will be required to determine what influence RACK1's association with NMHC-IIA has on myosin activity *in vivo*. While RACK1 null mouse models would most likely be embryonically lethal, conditional knockout mice for RACK1 would be useful in revealing the functional importance of RACK1 in the maintenance of the immune system and specifically lymphocyte trafficking.

7.7 Importance of this Study in the Societal Context

Uncontrolled inflammation, a trademark of asthma and allergies, and auto immune disorders, such as rheumatoid arthritis, are considered a major health problem in western society. As T lymphocytes play a central role in the inflammation response, advances in this scientific field may enhance our understanding of the molecular mechanisms associated with disease progression and potentially identify early intervention strategies or develop more efficient and new cost effective therapeutic targets.

Since migration is central to physiological processes, it is not surprising that the dysregulation of cell adhesion and motility can lead to pathological events such as invasion and metastasis of cancer cells. Elucidating the mechanisms underlying T lymphocyte polarisation and migration in normal and aberrant immune responses is essential to understanding and developing novel treatments for uncontrolled inflammation, T cell lymphomas, and auto immune disorders. Studies on T cell migration are yielding promising targets for new anti-inflammatory therapies, as the development of antagonists for integrin receptors, adhesion molecules, and cytoskeletal dynamics is among the most actively pursued areas in pharmaceutical research. However, the lack of studies that effectively elucidate the regulation of signalling cascades in T cell migration highlights the need of further experiments to decipher the exact role of regulatory mechanisms in T cell migration.

Indeed, it has been shown that adhesive associations between cells are important for transmitting spatial and temporal information that is critical for immune system function, including activation, recruitment, and transmigration of lymphocytes. Integrins are

adhesion receptors important for haematopoiesis, leukocyte trafficking, and formation of immunological synapses; hence, they may provide targets for therapeutic intervention in leukocyte-driven pathologies. Blocking integrin-ligand binding is one strategy for inhibiting integrins; however, a complete loss of integrin function can lead to mechanism-based toxicities. This has led to the design of novel therapeutic agents targeting integrin-associated proteins that may prove effective in treating immune disorders (Cantor et al. 2008; Lunsford et al. 2011; Zimmerman and Blanco 2008). Interference with signalling molecules involved in the leukocyte recruitment cascade has been a popular strategy for therapeutic intervention in inflammatory disorders. With a few exceptions, the outcome of clinical trials with adhesion molecule blockers has been variable and largely disappointing. However, as many inflammatory diseases are inadequately responsive to current medications and the incidence of some inflammatory diseases, such as Asthma and type 1 diabetes, is on the rise, there is an urgent need for new anti-inflammatory drugs (Mackay 2008).

The results of many on-going clinical trials and recent development of several new drugs should further validate the impact this new class of drugs will have on human health and may revolutionise anti-inflammatory therapies. For instance, the first migration inhibitory drug to be approved, natalizumab (Tysabri), an integrin monoclonal antibody (mAb) which binds α4 integrin, has shown proven efficacy in the treatment of multiple sclerosis and Crohn's disease by limiting T cell migration to an inflamed tissue (Gold et al. 2007). A second major recent development has been the discovery of various cell migration molecules required for diverse inflammatory responses. Targeting these molecules in animal models has proven a highly effective way to ameliorate inflammation (Lee et al. 2006; Mackay 2008; Mihara et al. 2005). Finally, the pharmaceutical industry has begun to develop effective and selective small molecule inhibitors for many important cell migration molecules, including the chemokine receptors. While adhesion molecules, such as the integrins, have generally been targeted by blocking antibodies, chemokine receptors involved in immune cell chemotaxis bind endogenous chemical ligands and can be targeted by organic small molecule drugs.

A complete understanding of the signal transduction and biochemical mechanisms that contribute to a fully functional T cells will lead to better treatment options for a range of diseases. Altogether, this study will add to our current understanding of the mechanisms that control immune cell migration, which has direct relevance to the treatment of multiple human diseases, including autoimmune disorders and cancer.

7.8 Translational Benefits

Despite the fact that this work did not involve any *in vivo* or clinical material, it has the potential to narrow the gap between fundamental research and clinical benefits to patients in several ways. For example, High Content Analysis together with computational screening is a new method for discovering novel proteins involved in cell migration as well as drug compounds in the industry not yet studied in T cell migration. In an era of increased demand for primary drug screening, the HCA platform will give pharmaceutical and life sciences researchers a robust, stable, and advanced toolbox of multi-parameter analysis. This method should accelerate pharmaceutical research and drug discovery processes by easily identifying suitable drugs affecting T cell migration. Overall, the discoveries made in this thesis have the potential to be translated to a clinical benefit, particularly in the understanding of complexes disease phenotypes associated with immunological processes in autoimmune reactions, such as those involved in rheumatoid arthritis, lupus, and multiple sclerosis, as well as in conditions aggravated by excessive inflammation like atherosclerosis, asthma, and transplant rejection, and finally, for understanding mechanisms underlying lymphocyte homing in responses against tumours, viruses, and other pathogens.

7.9 Conclusion

In conclusion, we demonstrated that RACK1 plays a crucial regulatory role in T cell polarisation and migration. By identifying RACK1-associated proteins and characterising the binding domains on RACK1 for the motor protein NMHC-IIA, we can determine the functional implications of these interactions during directional cell migration. This study supports the putative role of RACK1 in the reorganisation of the cytoskeleton in response to extracellular stimuli and warrants further research to fully elucidate the function of RACK1 in integrin-mediated immune cell migration.

8 References

Abram CL, Lowell CA (2009) The ins and outs of leukocyte integrin signaling. Annual review of immunology 27:339–62. doi: 10.1146/annurev.immunol.021908.132554

Adair BD, Yeager M (2002) Three-dimensional model of the human platelet integrin alpha IIbbeta 3 based on electron cryomicroscopy and x-ray crystallography. Proceedings of the National Academy of Sciences of the United States of America 99:14059–64. doi: 10.1073/pnas.212498199

Adams DR, Ron D, Kiely PA (2011) RACK1, A Multifaceted Scaffolding Protein: Structure and Function. Cell communication and signaling : CCS 9:22. doi: 10.1186/1478-811X-9-22

Adelstein RS, Conti MA (1975) Phosphorylation of platelet myosin increases actin-activated myosin ATPase activity. Nature 256:597–8.

Aifantis I, Feinberg J, Fehling HJ, et al. (1999) Early T cell receptor beta gene expression is regulated by the pre-T cell receptor-CD3 complex. The Journal of experimental medicine 190:141–4.

Aitken A (2006) 14-3-3 proteins: a historic overview. Seminars in cancer biology 16:162–72. doi: 10.1016/j.semcancer.2006.03.005

Akhmanova a, Hoogenraad CC, Drabek K, et al. (2001) Clasps are CLIP-115 and -170 associating proteins involved in the regional regulation of microtubule dynamics in motile fibroblasts. Cell 104:923–35.

Alon R, Dustin ML (2007) Force as a facilitator of integrin conformational changes during leukocyte arrest on blood vessels and antigen-presenting cells. Immunity 26:17–27. doi: 10.1016/j.immuni.2007.01.002

Alon R, Feigelson S (2002) From rolling to arrest on blood vessels: leukocyte tap dancing on endothelial integrin ligands and chemokines at sub-second contacts. Seminars in immunology 14:93–104. doi: 10.1006/smim.2001.0346

Alon R, Shulman Z (2011) Chemokine triggered integrin activation and actin remodeling events guiding lymphocyte migration across vascular barriers. Experimental cell research 317:632–41. doi: 10.1016/j.yexcr.2010.12.007

Altman A, Villalba M (2003) Protein kinase C-theta (PKCtheta): it's all about location, location, location. Immunological reviews 192:53–63.

Amano M, Chihara K, Kimura K, et al. (1997) Formation of actin stress fibers and focal adhesions enhanced by Rho-kinase. Science (New York, NY) 275:1308–11.

von Andrian UH, Mackay CR (2000) T-cell function and migration. Two sides of the same coin. The New England journal of medicine 343:1020–34. doi: 10.1056/NEJM200010053431407

Aoudjit F, Vuori K (2000) Engagement of the alpha2beta1 integrin inhibits Fas ligand expression and activation-induced cell death in T cells in a focal adhesion kinase-dependent manner. Blood 95:2044–51.

Appelbaum FR (2001) Haematopoietic cell transplantation as immunotherapy. Nature 411:385–9. doi: 10.1038/35077251

Ardouin L, Bracke M, Mathiot A, et al. (2003) Vav1 transduces TCR signals required for LFA-1 function and cell polarization at the immunological synapse. European journal of immunology 33:790–7. doi: 10.1002/eji.200323858

Armulik A, Nilsson I, von Heijne G, Johansson S (1999) Determination of the border between the transmembrane and cytoplasmic domains of human integrin subunits. The Journal of biological chemistry 274:37030–4.

Arnaout MA, Mahalingam B, Xiong J-P (2005) Integrin structure, allostery, and bidirectional signaling. Annual review of cell and developmental biology 21:381–410. doi: 10.1146/annurev.cellbio.21.090704.151217

Auerbach M, Liedtke CM (2007) Role of the scaffold protein RACK1 in apical expression of CFTR. American journal of physiology Cell physiology 293:C294–304. doi: 10.1152/ajpcell.00413.2006

Bach I (2000) The LIM domain: regulation by association. Mechanisms of development 91:5–17.

Baier G (2007) PKC isotype functions in T lymphocytes. Ernst Schering Foundation symposium proceedings 29–41.

Baier G (2003) The PKC gene module: molecular biosystematics to resolve its T cell functions. Immunological reviews 192:64–79.

Barreiro O, de la Fuente H, Mittelbrunn M, Sánchez-Madrid F (2007) Functional insights on the polarized redistribution of leukocyte integrins and their ligands during leukocyte migration and immune interactions. Immunological reviews 218:147–64. doi: 10.1111/j.1600-065X.2007.00529.x

Battaini F, Pascale A (2005) Protein kinase C signal transduction regulation in physiological and pathological aging. Annals of the New York Academy of Sciences 1057:177–92. doi: 10.1196/annals.1356.011

Beach JR, Licate LS, Crish JF, Egelhoff TT (2011) Analysis of the role of Ser1/Ser2/Thr9 phosphorylation on myosin II assembly and function in live cells. BMC cell biology 12:52. doi: 10.1186/1471-2121-12-52

Bella J, Kolatkar PR, Marlor CW, et al. (1998) The structure of the two amino-terminal domains of human ICAM-1 suggests how it functions as a rhinovirus receptor and as an LFA-1 integrin ligand. Proceedings of the National Academy of Sciences of the United States of America 95:4140–5.

Bennett V, Gilligan DM (1993) The spectrin-based membrane skeleton and micron-scale organization of the plasma membrane. Annual review of cell biology 9:27–66. doi: 10.1146/annurev.cb.09.110193.000331

Berg JS, Powell BC, Cheney RE (2001) A millennial myosin census. Molecular biology of the cell 12:780–94.

Berns H, Humar R, Hengerer B, et al. (2000) RACK1 is up-regulated in angiogenesis and human carcinomas. FASEB journal : official publication of the Federation of American Societies for Experimental Biology 14:2549–58. doi: 10.1096/fj.99-1038com

Bertram A, Ley K (2011) Protein kinase C isoforms in neutrophil adhesion and activation. Archivum immunologiae et therapiae experimentalis 59:79–87. doi: 10.1007/s00005-011-0112-7

Besson A, Wilson TL, Yong VW (2002) The anchoring protein RACK1 links protein kinase Cepsilon to integrin beta chains. Requirements for adhesion and motility. The Journal of biological chemistry 277:22073–84. doi: 10.1074/jbc.M111644200

Betschinger J, Mechtler K, Knoblich JA (2003) The Par complex directs asymmetric cell division by phosphorylating the cytoskeletal protein Lgl. Nature 422:326–30. doi: 10.1038/nature01486

Bialkowska K, Zaffran Y, Meyer SC, Fox JEB (2003) 14-3-3 zeta mediates integrin-induced activation of Cdc42 and Rac. Platelet glycoprotein Ib-IX regulates integrin-induced signaling by sequestering 14-3-3 zeta. The Journal of biological chemistry 278:33342–50. doi: 10.1074/jbc.M301217200

Bielli P, Busà R, Paronetto MP, Sette C (2011) The RNA-binding protein Sam68 is a multifunctional player in human cancer. Endocrine-related cancer 18:R91–R102. doi: 10.1530/ERC-11-0041

Billadeau DD, Nolz JC, Gomez TS (2007) Regulation of T-cell activation by the cytoskeleton. Nature reviews Immunology 7:131–43. doi: 10.1038/nri2021

Bini L, Heid H, Liberatori S, et al. Two-dimensional gel electrophoresis of Caenorhabditis elegans homogenates and identification of protein spots by microsequencing. Electrophoresis 18:557–62. doi: 10.1002/elps.1150180337

Bleul CC, Fuhlbrigge RC, Casasnovas JM, et al. (1996) A highly efficacious lymphocyte chemoattractant, stromal cell-derived factor 1 (SDF-1). The Journal of experimental medicine 184:1101–9.

von Boehmer H, Fehling HJ (1997) Structure and function of the pre-T cell receptor. Annual review of immunology 15:433–52. doi: 10.1146/annurev.immunol.15.1.433

Boguth CA, Singh P, Huang C, Tesmer JJG (2010) Molecular basis for activation of G protein-coupled receptor kinases. The EMBO journal 29:3249–59. doi: 10.1038/emboj.2010.206

Bolomini-Vittori M, Montresor A, Giagulli C, et al. (2009) Regulation of conformer-specific activation of the integrin LFA-1 by a chemokine-triggered Rho signaling module. Nature immunology 10:185–94. doi: 10.1038/ni.1691

van den Boorn JG, Le Poole IC, Luiten RM (2006) T-cell avidity and tuning: the flexible connection between tolerance and autoimmunity. International reviews of immunology 25:235–58. doi: 10.1080/08830180600743081

Borges JC, Ramos CHI (2005) Protein folding assisted by chaperones. Protein and peptide letters 12:257–61.

Boyden S (1962) The chemotactic effect of mixtures of antibody and antigen on polymorphonuclear leucocytes. The Journal of experimental medicine 115:453–66.

Bradley LM (2003) Migration and T-lymphocyte effector function. Current Opinion in Immunology 15:343–348. doi: 10.1016/S0952-7915(03)00043-8

Braun MU, Mochly-Rosen D (2003) Opposing effects of delta- and zeta-protein kinase C isozymes on cardiac fibroblast proliferation: use of isozyme-selective inhibitors. Journal of molecular and cellular cardiology 35:895–903.

Bridges D, Moorhead GBG (2005) 14-3-3 proteins: a number of functions for a numbered protein. Science's STKE : signal transduction knowledge environment 2005:re10. doi: 10.1126/stke.2962005re10

Briggs MW, Sacks DB (2003) IQGAP proteins are integral components of cytoskeletal regulation. EMBO reports 4:571–4. doi: 10.1038/sj.embor.embor867

Broderick MJF, Winder SJ (2005) Spectrin, alpha-actinin, and dystrophin. Advances in protein chemistry 70:203–46. doi: 10.1016/S0065-3233(05)70007-3

Brown MJ, Hallam J a, Colucci-Guyon E, Shaw S (2001) Rigidity of circulating lymphocytes is primarily conferred by vimentin intermediate filaments. Journal of immunology (Baltimore, Md : 1950) 166:6640–6.

Brunton VG, MacPherson IRJ, Frame MC (2004) Cell adhesion receptors, tyrosine kinases and actin modulators: a complex three-way circuitry. Biochimica et biophysica acta 1692:121–44. doi: 10.1016/j.bbamcr.2004.04.010

Buensuceso CS, Obergfell A, Soriani A, et al. (2005) Regulation of outside-in signaling in platelets by integrin-associated protein kinase C beta. The Journal of biological chemistry 280:644–53. doi: 10.1074/jbc.M410229200

Buensuceso CS, Woodside D, Huff JL, et al. (2001) The WD protein Rack1 mediates protein kinase C and integrin-dependent cell migration. Journal of cell science 114:1691–8.

Burkhardt JK, Carrizosa E, Shaffer MH (2008) The actin cytoskeleton in T cell activation. Annual review of immunology 26:233–59. doi: 10.1146/annurev.immunol.26.021607.090347

Burns S, Cory GO, Vainchenker W, Thrasher AJ (2004) Mechanisms of WASp-mediated hematologic and immunologic disease. Blood 104:3454–62. doi: 10.1182/blood-2004-04-1678

Cabañas C, Sánchez-Madrid F (1999) CD11a (leukocyte integrin LFA-1 alpha subunit). Journal of biological regulators and homeostatic agents 13:126–9.

Cai Y, Fleming C, Yan J (2012) New insights of T cells in the pathogenesis of psoriasis. Cellular & molecular immunology 9:302–9. doi: 10.1038/cmi.2012.15

Cameron AJM, Parker PJ (2010) Protein kinase C - a family of protein kinases, allosteric effectors or both? Advances in enzyme regulation 50:169–77. doi: 10.1016/j.advenzreg.2009.10.004

Campanero MR, Sánchez-Mateos P, del Pozo M a, Sánchez-Madrid F (1994) ICAM-3 regulates lymphocyte morphology and integrin-mediated T cell interaction with endothelial cell and extracellular matrix ligands. The Journal of cell biology 127:867–78.

Campbell JJ, Butcher EC (2000) Chemokines in tissue-specific and microenvironment-specific lymphocyte homing. Current opinion in immunology 12:336–41.

Candotti F, Facchetti F, Blanzuoli L, et al. (1999) Retrovirus-mediated WASP gene transfer corrects defective actin polymerization in B cell lines from Wiskott-Aldrich syndrome patients carrying "null" mutations. Gene therapy 6:1170–4. doi: 10.1038/sj.gt.3300926

Cantor JM, Ginsberg MH, Rose DM (2008) Integrin-associated proteins as potential therapeutic targets. Immunological reviews 223:236–51. doi: 10.1111/j.1600-065X.2008.00640.x

Cao X-X, Xu J-D, Xu J-W, et al. (2011) RACK1 promotes breast carcinoma migration/metastasis via activation of the RhoA/Rho kinase pathway. Breast cancer research and treatment 126:555–63. doi: 10.1007/s10549-010-0955-3

Cao X-X, Xu J-WJ-D, Liu X-LX-P, et al. (2010) RACK1 promotes breast carcinoma proliferation and invasion/metastasis in vitro and in vivo. Breast cancer research and treatment 123:375–86. doi: 10.1007/s10549-009-0657-x

Carman CV, Springer T a (2004) A transmigratory cup in leukocyte diapedesis both through individual vascular endothelial cells and between them. The Journal of cell biology 167:377–88. doi: 10.1083/jcb.200404129

Cather JC, Cather JC, Menter A (2003) Modulating T cell responses for the treatment of psoriasis: a focus on efalizumab. Expert opinion on biological therapy 3:361–70. doi: 10.1517/14712598.3.2.361

Chan JR, Hyduk SJ, Cybulsky MI (2000) Alpha 4 beta 1 integrin/VCAM-1 interaction activates alpha L beta 2 integrin-mediated adhesion to ICAM-1 in human T cells. Journal of immunology (Baltimore, Md : 1950) 164:746–53.

Chang BY, Chiang M, Cartwright C a (2001) The interaction of Src and RACK1 is enhanced by activation of protein kinase C and tyrosine phosphorylation of RACK1. The Journal of biological chemistry 276:20346–56. doi: 10.1074/jbc.M101375200

Chang BY, Harte R a, Cartwright C a (2002) RACK1: a novel substrate for the Src protein-tyrosine kinase. Oncogene 21:7619–29. doi: 10.1038/sj.onc.1206002

Chang Y, Nalbant P, Chang Z, Bokoch GM (2008) GEF-H1 Couples Nocodazole-induced Microtubule Disassembly to Cell Contractility via RhoA. Molecular Biology of the Cell 19:2147–2153. doi: 10.1091/mbc.E07

Chang Y-C, Lee H-H, Chen Y-J, et al. (2006) Contribution of guanine exchange factor H1 in phorbol ester-induced apoptosis. Cell death and differentiation 13:2023–32. doi: 10.1038/sj.cdd.4401901

Charest PG, Firtel RA (2007) Big roles for small GTPases in the control of directed cell movement. The Biochemical journal 401:377–90. doi: 10.1042/BJ20061432

Chen S, Dell EJ, Lin F, et al. (2004a) RACK1 regulates specific functions of Gbetagamma. The Journal of biological chemistry 279:17861–8. doi: 10.1074/jbc.M313727200

Chen S, Lin F, Hamm HE (2005) RACK1 binds to a signal transfer region of G betagamma and inhibits phospholipase C beta2 activation. The Journal of biological chemistry 280:33445–52. doi: 10.1074/jbc.M505422200

Chen S, Lin F, Shin ME, et al. (2008) RACK1 regulates directional cell migration by acting on G betagamma at the interface with its effectors PLC beta and PI3K gamma. Molecular biology of the cell 19:3909–22. doi: 10.1091/mbc.E08-04-0433

Chen S, Spiegelberg BD, Lin F, et al. (2004b) Interaction of Gbetagamma with RACK1 and other WD40 repeat proteins. Journal of molecular and cellular cardiology 37:399–406. doi: 10.1016/j.yjmcc.2004.04.019

Chevallet M, Luche S, Rabilloud T (2006) Silver staining of proteins in polyacrylamide gels. Nature protocols 1:1852–8. doi: 10.1038/nprot.2006.288

Chou YC, Chou CC, Chen YK, et al. (1999) Structure and genomic organization of porcine RACK1 gene. Biochimica et biophysica acta 1489:315–22.

Christen U, von Herrath MG (2005) Infections and autoimmunity--good or bad? Journal of immunology (Baltimore, Md : 1950) 174:7481–6.

Conti M a., Adelstein RS (2008) Nonmuscle myosin II moves in new directions. Journal of Cell Science 121:404–404. doi: 10.1242/jcs.03496

Conti MA, Kawamoto S, Adelstein RS (2008) Myosins: A Superfamily of Molecular Motors. In: Coluccio LM (ed) Amino Acids. Springer, pp 223–264

Cooles FAH, Isaacs JD (2011) Pathophysiology of rheumatoid arthritis. Current opinion in rheumatology 23:233–40. doi: 10.1097/BOR.0b013e32834518a3

Cooper JA (1987) Effects of cytochalasin and phalloidin on actin. The Journal of cell biology 105:1473–8.

Cose S (2007) T-cell migration: a naive paradigm? Immunology 120:1–7. doi: 10.1111/j.1365-2567.2006.02511.x

Cose S, Brammer C, Khanna KM, et al. (2006) Evidence that a significant number of naive T cells enter non-lymphoid organs as part of a normal migratory pathway. European journal of immunology 36:1423–33. doi: 10.1002/eji.200535539

Cox EA, Bennin D, Doan AT, et al. (2003) Protrusion , and Chemotactic Cell Migration via Its Src- binding Site □. Molecular Biology of the Cell 14:658 – 669. doi: 10.1091/mbc.E02

Critchley DR (2009) Biochemical and structural properties of the integrin-associated cytoskeletal protein talin. Annual review of biophysics 38:235–54. doi: 10.1146/annurev.biophys.050708.133744

Csukai M, Mochly-Rosen D (1999) Pharmacologic modulation of protein kinase C isozymes: the role of RACKs and subcellular localisation. Pharmacological research : the official journal of the Italian Pharmacological Society 39:253–9. doi: 10.1006/phrs.1998.0418

Curnock AP, Sotsios Y, Wright KL, Ward SG (2003) Optimal chemotactic responses of leukemic T cells to stromal cell-derived factor-1 requires the activation of both class IA and IB phosphoinositide 3-kinases. Journal of immunology (Baltimore, Md : 1950) 170:4021–30.

Dawid IB, Toyama R, Taira M (1995) LIM domain proteins. Comptes rendus de l'Académie des sciences Série III, Sciences de la vie 318:295–306.

Debes GF, Dahl ME, Mahiny AJ, et al. (2006) Chemotactic responses of IL-4-, IL-10-, and IFN-gamma-producing CD4+ T cells depend on tissue origin and microbial stimulus. Journal of immunology (Baltimore, Md : 1950) 176:557–66.

Delahunty M, Zennadi R, Telen MJ (2006) LW protein: a promiscuous integrin receptor activated by adrenergic signaling. Transfusion clinique et biologique : journal de la Société française de transfusion sanguine 13:44–9. doi: 10.1016/j.tracli.2006.02.022

Dempsey EC, Newton AC, Mochly-Rosen D, et al. (2000) Protein kinase C isozymes and the regulation of diverse cell responses. American journal of physiology Lung cellular and molecular physiology 279:L429–38.

Denucci CC, Mitchell JS, Shimizu Y (2009) Integrin function in T-cell homing to lymphoid and nonlymphoid sites: getting there and staying there. Critical reviews in immunology 29:87–109.

Di YP, Repasky EA, Subjeck JR (1997) Distribution of HSP70, protein kinase C, and spectrin is altered in lymphocytes during a fever-like hyperthermia exposure. Journal of cellular physiology 172:44–54. doi: 10.1002/(SICI)1097-4652(199707)172:1<44::AID-JCP5>3.0.CO;2-D

Disatnik MH, Buraggi G, Mochly-Rosen D (1994) Localization of protein kinase C isozymes in cardiac myocytes. Experimental cell research 210:287–97. doi: 10.1006/excr.1994.1041

Disatnik MH, Rando TA (1999) Integrin-mediated muscle cell spreading. The role of protein kinase c in outside-in and inside-out signaling and evidence of integrin cross-talk. The Journal of biological chemistry 274:32486–92.

Djinovic-Carugo K, Gautel M, Ylänne J, Young P (2002) The spectrin repeat: a structural platform for cytoskeletal protein assemblies. FEBS letters 513:119–23.

Doan AT, Huttenlocher A (2007) RACK1 regulates Src activity and modulates paxillin dynamics during cell migration. Experimental cell research 313:2667–79. doi: 10.1016/j.yexcr.2007.05.013

Dransfield I, Cabañas C, Craig A, Hogg N (1992) Divalent cation regulation of the function of the leukocyte integrin LFA-1. The Journal of cell biology 116:219–26.

Dunn GA (1983) Characterising a kinesis response: time averaged measures of cell speed and directional persistence. Agents and actions Supplements 12:14–33.

Dupré L, Trifari S, Follenzi A, et al. (2004) Lentiviral vector-mediated gene transfer in T cells from Wiskott-Aldrich syndrome patients leads to functional correction. Molecular therapy : the journal of the American Society of Gene Therapy 10:903–15. doi: 10.1016/j.ymthe.2004.08.008

Dustin ML, Chan AC (2000) Signaling takes shape in the immune system. Cell 103:283–94.

Dustin ML, Rothlein R, Bhan AK, et al. (1986) Induction by IL 1 and interferon-gamma: tissue distribution, biochemistry, and function of a natural adherence molecule (ICAM-1). Journal of immunology (Baltimore, Md : 1950) 137:245–54.

Dustin ML, Springer TA (1989) T-cell receptor cross-linking transiently stimulates adhesiveness through LFA-1. Nature 341:619–24. doi: 10.1038/341619a0

Dym O, Pratt EA, Ho C, Eisenberg D (2000) The crystal structure of D-lactate dehydrogenase, a peripheral membrane respiratory enzyme. Proceedings of the National Academy of Sciences of the United States of America 97:9413–8.

D'Souza-Schorey C, Boettner B, Van Aelst L (1998) Rac regulates integrin-mediated spreading and increased adhesion of T lymphocytes. Molecular and cellular biology 18:3936–46.

Ebert LM, Schaerli P, Moser B (2005) Chemokine-mediated control of T cell traffic in lymphoid and peripheral tissues. Molecular immunology 42:799–809. doi: 10.1016/j.molimm.2004.06.040

Eddy RJ, Pierini LM, Matsumura F, Maxfield FR (2000) Ca2+-dependent myosin II activation is required for uropod retraction during neutrophil migration. Journal of cell science 113 (Pt 7:1287–98.

El Din El Homasany BS, Volkov Y, Takahashi M, et al. (2005) The scaffolding protein CG-NAP/AKAP450 is a critical integrating component of the LFA-1-induced signaling complex in migratory T cells. Journal of immunology (Baltimore, Md : 1950) 175:7811–8.

Elbashir SM, Harborth J, Lendeckel W, et al. (2001) Duplexes of 21-nucleotide RNAs mediate RNA interference in cultured mammalian cells. Nature 411:494–8. doi: 10.1038/35078107

Engelhardt B, Wolburg H (2004) Mini-review: Transendothelial migration of leukocytes: through the front door or around the side of the house? European journal of immunology 34:2955–63. doi: 10.1002/eji.200425327

Eriksson JE, Dechat T, Grin B, et al. (2009) Introducing intermediate filaments: from discovery to disease. The Journal of clinical investigation 119:1763–71. doi: 10.1172/JCI38339

Eriksson JE, He T, Trejo-Skalli AV, et al. (2004) Specific in vivo phosphorylation sites determine the assembly dynamics of vimentin intermediate filaments. Journal of cell science 117:919–32. doi: 10.1242/jcs.00906

Etienne-Manneville S (2004) Actin and microtubules in cell motility: which one is in control? Traffic (Copenhagen, Denmark) 5:470–7. doi: 10.1111/j.1600-0854.2004.00196.x

Etienne-Manneville S, Hall A (2002) Rho GTPases in cell biology. Nature 420:629–35. doi: 10.1038/nature01148

Etienne-Manneville S, Manneville J-B, Nicholls S, et al. (2005) Cdc42 and Par6-PKCzeta regulate the spatially localized association of Dlg1 and APC to control cell polarization. The Journal of cell biology 170:895–901. doi: 10.1083/jcb.200412172

Evans R, Lellouch AC, Svensson L, et al. (2011) The integrin LFA-1 signals through ZAP-70 to regulate expression of high-affinity LFA-1 on T lymphocytes. Blood 117:3331–42. doi: 10.1182/blood-2010-06-289140

Evans R, Patzak I, Svensson L, et al. (2009) Integrins in immunity. Journal of cell science 122:215–25. doi: 10.1242/jcs.019117

Even-Ram S, Doyle AD, Conti MA, et al. (2007) Myosin IIA regulates cell motility and actomyosin-microtubule crosstalk. Nature cell biology 9:299–309. doi: 10.1038/ncb1540

Fabbri M, Di Meglio S, Gagliani MC, et al. (2005) Dynamic partitioning into lipid rafts controls the endo-exocytic cycle of the alphaL/beta2 integrin, LFA-1, during leukocyte chemotaxis. Molecular biology of the cell 16:5793–803. doi: 10.1091/mbc.E05-05-0413

Fanning AS, Anderson JM (1999) PDZ domains: fundamental building blocks in the organization of protein complexes at the plasma membrane. The Journal of clinical investigation 103:767–72. doi: 10.1172/JCI6509

Feigelson SW, Pasvolsky R, Cemerski S, et al. (2010) Occupancy of lymphocyte LFA-1 by surface-immobilized ICAM-1 is critical for TCR- but not for chemokine-triggered LFA-1 conversion to an open headpiece high-affinity state. Journal of immunology (Baltimore, Md : 1950) 185:7394–404. doi: 10.4049/jimmunol.1002246

Feng D, Nagy J a, Pyne K, et al. (1998) Neutrophils emigrate from venules by a transendothelial cell pathway in response to FMLP. The Journal of experimental medicine 187:903–15.

Fire A, Xu S, Montgomery MK, et al. (1998) Potent and specific genetic interference by double-strandedRNAin Caenorhabditis elegans. Nature 391:806–811.

Foucault G, Raymond MN, Coffe G, Pudles J (1984) [Study of a lysis medium stabilizing microfilaments and microtubules in vitro and in vivo]. Biology of the cell / under the auspices of the European Cell Biology Organization 52:53–9.

Frank R (2002) High-density synthetic peptide microarrays: emerging tools for functional genomics and proteomics. Combinatorial chemistry & high throughput screening 5:429–40.

Frank R, Overwin H (1996) SPOT synthesis. Epitope analysis with arrays of synthetic peptides prepared on cellulose membranes. Methods in molecular biology (Clifton, NJ) 66:149–69. doi: 10.1385/0-89603-375-9:149

Freeley M, Bakos G, Davies A, et al. (2010) A high-content analysis toolbox permits dissection of diverse signaling pathways for T lymphocyte polarization. Journal of biomolecular screening 15:541–55. doi: 10.1177/1087057110369703

Friedl P, Bröcker EB (2000) The biology of cell locomotion within three-dimensional extracellular matrix. Cellular and molecular life sciences : CMLS 57:41–64.

Friedman RS, Jacobelli J, Krummel MF (2006) Surface-bound chemokines capture and prime T cells for synapse formation. Nature immunology 7:1101–8. doi: 10.1038/ni1384

Fu H, Subramanian RR, Masters SC (2000) 14-3-3 proteins: structure, function, and regulation. Annual review of pharmacology and toxicology 40:617–47. doi: 10.1146/annurev.pharmtox.40.1.617

Fujibuchi T, Abe Y, Takeuchi T, et al. (2005) AIP1/WDR1 supports mitotic cell rounding. Biochemical and biophysical research communications 327:268–75. doi: 10.1016/j.bbrc.2004.11.156

Fukata M, Nakagawa M, Kaibuchi K (2003) Roles of Rho-family GTPases in cell polarisation and directional migration. Current opinion in cell biology 15:590–7.

Gahmberg CG, Tian L, Ning L, Nyman-Huttunen H (2008) ICAM-5--a novel two-facetted adhesion molecule in the mammalian brain. Immunology letters 117:131–5. doi: 10.1016/j.imlet.2008.02.004

Gahmberg CG, Tolvanen M, Kotovuori P (1997) Leukocyte adhesion--structure and function of human leukocyte beta2-integrins and their cellular ligands. European journal of biochemistry / FEBS 245:215–32.

Gahmberg CG, Valmu L, Tian L, et al. (1999) Leukocyte adhesion--a fundamental process in leukocyte physiology. Brazilian journal of medical and biological research = Revista brasileira de pesquisas médicas e biológicas / Sociedade Brasileira de Biofísica . [et al] 32:511–7.

Galjart N (2005) CLIPs and CLASPs and cellular dynamics. Nature reviews Molecular cell biology 6:487–98. doi: 10.1038/nrm1664

Galjart N (2010) Plus-end-tracking proteins and their interactions at microtubule ends. Current biology : CB 20:R528–37. doi: 10.1016/j.cub.2010.05.022

Gallego MD, de la Fuente MA, Anton IM, et al. (2006) WIP and WASP play complementary roles in T cell homing and chemotaxis to SDF-1alpha. International immunology 18:221–32. doi: 10.1093/intimm/dxh310

Ganju RK (1998) The alpha -Chemokine, Stromal Cell-derived Factor-1alpha , Binds to the Transmembrane G-protein-coupled CXCR-4 Receptor and Activates Multiple Signal Transduction Pathways. Journal of Biological Chemistry 273:23169–23175. doi: 10.1074/jbc.273.36.23169

Gannon-Murakami L, Murakami K (2002) Selective association of protein kinase C with 14-3-3 zeta in neuronally differentiated PC12 Cells. Stimulatory and inhibitory effect of 14-3-3 zeta in vivo. The Journal of biological chemistry 277:23116–22. doi: 10.1074/jbc.M201478200

Garnotel R, Monboisse JC, Randoux A, et al. (1995) The binding of type I collagen to lymphocyte function-associated antigen (LFA) 1 integrin triggers the respiratory burst of human polymorphonuclear neutrophils. Role of calcium signaling and tyrosine phosphorylation of LFA 1. The Journal of biological chemistry 270:27495–503.

Geeves MA, Fedorov R, Manstein DJ (2005) Molecular mechanism of actomyosin-based motility. Cellular and molecular life sciences : CMLS 62:1462–77. doi: 10.1007/s00018-005-5015-5

Germain RN (2002) T-cell development and the CD4-CD8 lineage decision. Nature reviews Immunology 2:309–22. doi: 10.1038/nri798

Giagulli C, Scarpini E, Ottoboni L, et al. (2004) RhoA and zeta PKC control distinct modalities of LFA-1 activation by chemokines: critical role of LFA-1 affinity triggering in lymphocyte in vivo homing. Immunity 20:25–35.

Giancotti FG, Ruoslahti E (1999) Integrin signaling. Science (New York, NY) 285:1028–32.

Giannoni E, Chiarugi P, Cozzi G, et al. (2003) Lymphocyte function-associated antigen-1-mediated T cell adhesion is impaired by low molecular weight phosphotyrosine phosphatase-dependent inhibition of FAK activity. The Journal of biological chemistry 278:36763–76. doi: 10.1074/jbc.M302686200

Gold R, Jawad A, Miller DH, et al. (2007) Expert opinion: guidelines for the use of natalizumab in multiple sclerosis patients previously treated with immunomodulating therapies. Journal of neuroimmunology 187:156–8. doi: 10.1016/j.jneuroim.2007.04.006

Goldman RD, Khuon S, Chou YH, et al. (1996) The function of intermediate filaments in cell shape and cytoskeletal integrity. The Journal of cell biology 134:971–83.

Goldman YE (1998) Wag the tail: structural dynamics of actomyosin. Cell 93:1–4.

Golomb E, Ma X, Jana SS, et al. (2004) Identification and characterization of nonmuscle myosin II-C, a new member of the myosin II family. The Journal of biological chemistry 279:2800–8. doi: 10.1074/jbc.M309981200

Gomes ER, Jani S, Gundersen GG (2005) Nuclear movement regulated by Cdc42, MRCK, myosin, and actin flow establishes MTOC polarization in migrating cells. Cell 121:451–63. doi: 10.1016/j.cell.2005.02.022

Gomez TS, Billadeau DD (2008) T cell activation and the cytoskeleton: you can't have one without the other. Advances in immunology 97:1–64. doi: 10.1016/S0065-2776(08)00001-1

Gottlieb AB (2005) Psoriasis: emerging therapeutic strategies. Nature reviews Drug discovery 4:19–34. doi: 10.1038/nrd1607

Gottlieb AB, Krueger JG, Wittkowski K, et al. (2002) Psoriasis as a model for T-cell-mediated disease: immunobiologic and clinical effects of treatment with multiple doses of efalizumab, an anti-CD11a antibody. Archives of dermatology 138:591–600.

Gottschalk KE, Adams PD, Brunger AT, Kessler H (2002) Transmembrane signal transduction of the alpha(IIb)beta(3) integrin. Protein science : a publication of the Protein Society 11:1800–12. doi: 10.1110/ps.4120102

Griner EM, Kazanietz MG (2007) Protein kinase C and other diacylglycerol effectors in cancer. Nature reviews Cancer 7:281–94. doi: 10.1038/nrc2110

Groskreutz D, Schenborn ET (1997) Reporter systems. Methods in molecular biology (Clifton, NJ) 63:11–30. doi: 10.1385/0-89603-481-X:11

Grosso S, Volta V, Sala LA, et al. (2008) PKCbetaII modulates translation independently from mTOR and through RACK1. The Biochemical journal 415:77–85. doi: 10.1042/BJ20080463

Gump JM, Dowdy SF (2007) TAT transduction: the molecular mechanism and therapeutic prospects. Trends in molecular medicine 13:443–8. doi: 10.1016/j.molmed.2007.08.002

Gundersen GG (2002) Microtubule Capture : IQGAP and CLIP-170 Expand the Repertoire Rho GTPases regulate microtubule capture near the. Science 12:645–647.

Gundersen GG, Cook TA (1999) Microtubules and signal transduction. Current opinion in cell biology 11:81–94.

Gérard A, van der Kammen RA, Janssen H, et al. (2009) The Rac activator Tiam1 controls efficient T-cell trafficking and route of transendothelial migration. Blood 113:6138–47. doi: 10.1182/blood-2008-07-167668

Gérard A, Mertens AEE, van der Kammen R a, Collard JG (2007) The Par polarity complex regulates Rap1- and chemokine-induced T cell polarization. The Journal of cell biology 176:863–75. doi: 10.1083/jcb.200608161

Gómez-Moutón C, Mañes S Establishment and maintenance of cell polarity during leukocyte chemotaxis. Cell adhesion & migration 1:69–76.

Gómez-Móuton C, Abad JL, Mira E, et al. (2001) Segregation of leading-edge and uropod components into specific lipid rafts during T cell polarization. Proceedings of the National Academy of Sciences of the United States of America 98:9642–7. doi: 10.1073/pnas.171160298

Haan C, Behrmann I (2007) A cost effective non-commercial ECL-solution for Western blot detections yielding strong signals and low background. Journal of immunological methods 318:11–9. doi: 10.1016/j.jim.2006.07.027

Harper MT, Poole AW (2007) Isoform-specific functions of protein kinase C: the platelet paradigm. Biochemical Society transactions 35:1005–8. doi: 10.1042/BST0351005

Harris BZ, Lim WA (2001) Mechanism and role of PDZ domains in signaling complex assembly. Journal of cell science 114:3219–31.

Hawkins T, Mirigian M, Selcuk Yasar M, Ross JL (2010) Mechanics of microtubules. Journal of biomechanics 43:23–30. doi: 10.1016/j.jbiomech.2009.09.005

Hayflick JS, Kilgannon P, Gallatin WM (1998) The intercellular adhesion molecule (ICAM) family of proteins. New members and novel functions. Immunologic research 17:313–27. doi: 10.1007/BF02786454

He D-Y, Neasta J, Ron D (2010) Epigenetic regulation of BDNF expression via the scaffolding protein RACK1. The Journal of biological chemistry 285:19043–50. doi: 10.1074/jbc.M110.100693

He D-Y, Vagts AJ, Yaka R, Ron D (2002) Ethanol induces gene expression via nuclear compartmentalization of receptor for activated C kinase 1. Molecular pharmacology 62:272–80.

Heasman SJ, Carlin LM, Cox S, et al. (2010) Coordinated RhoA signaling at the leading edge and uropod is required for T cell transendothelial migration. The Journal of cell biology 190:553–63. doi: 10.1083/jcb.201002067

Henson JH, Kolnik SE, Fried CA, et al. (2003) Actin-based centripetal flow: phosphatase inhibition by calyculin-A alters flow pattern, actin organization, and actomyosin distribution. Cell motility and the cytoskeleton 56:252–66. doi: 10.1002/cm.10149

Hermanto U, Zong CS, Li W, Wang L (2002) RACK1 , an Insulin-Like Growth Factor I (IGF-I) Receptor-Interacting Protein , Modulates IGF-I-Dependent Integrin Signaling and Promotes Cell Spreading and Contact with Extracellular Matrix. Society 22:2345–2365. doi: 10.1128/MCB.22.7.2345

Herrmann H, Bär H, Kreplak L, et al. (2007) Intermediate filaments: from cell architecture to nanomechanics. Nature reviews Molecular cell biology 8:562–73. doi: 10.1038/nrm2197

Herrmann H, Strelkov SV, Burkhard P, Aebi U (2009) Intermediate filaments: primary determinants of cell architecture and plasticity. The Journal of clinical investigation 119:1772–83. doi: 10.1172/JCI38214

Hofmann J (2004) Protein kinase C isozymes as potential targets for anticancer therapy. Current cancer drug targets 4:125–46.

Hogg N, Laschinger M, Giles K, McDowall A (2003) T-cell integrins: more than just sticking points. Journal of cell science 116:4695–705. doi: 10.1242/jcs.00876

Hogg N, Patzak I, Willenbrock F (2011) The insider's guide to leukocyte integrin signalling and function. Nature reviews Immunology 11:416–26. doi: 10.1038/nri2986

Hogg N, Smith A, McDowall A, et al. (2004) How T cells use LFA-1 to attach and migrate. Immunology letters 92:51–4. doi: 10.1016/j.imlet.2003.10.014

Howard J, Hyman AA (2003) Dynamics and mechanics of the microtubule plus end. Nature 422:753–8. doi: 10.1038/nature01600

Hsu LW, Chen CL, Nakano T, et al. (2008) The role of a nuclear protein, histone H1, on signalling pathways for the maturation of dendritic cells. Clinical and experimental immunology 152:576–84. doi: 10.1111/j.1365-2249.2008.03652.x

Hu C-T, Wu J-R, Cheng C-C, et al. (2011) Reactive oxygen species-mediated PKC and integrin signaling promotes tumor progression of human hepatoma HepG2. Clinical & experimental metastasis 28:851–63. doi: 10.1007/s10585-011-9416-6

Hung AY, Sheng M (2002) PDZ domains: structural modules for protein complex assembly. The Journal of biological chemistry 277:5699–702. doi: 10.1074/jbc.R100065200

Ikebe M, Komatsu S, Woodhead JL, et al. (2001) The tip of the coiled-coil rod determines the filament formation of smooth muscle and nonmuscle myosin. The Journal of biological chemistry 276:30293–300. doi: 10.1074/jbc.M101969200

Ikebe M, Reardon S (1990) Phosphorylation of smooth muscle caldesmon by calmodulin-dependent protein kinase II. Identification of the phosphorylation sites. The Journal of biological chemistry 265:17607–12.

Ivaska J, Kermorgant S, Whelan R, et al. (2003) Integrin-protein kinase C relationships. Biochemical Society transactions 31:90–3. doi: 10.1042/

Ivaska J, Pallari H-M, Nevo J, Eriksson JE (2007) Novel functions of vimentin in cell adhesion, migration, and signaling. Experimental cell research 313:2050–62. doi: 10.1016/j.yexcr.2007.03.040

Ivaska J, Vuoriluoto K, Huovinen T, et al. (2005) PKCepsilon-mediated phosphorylation of vimentin controls integrin recycling and motility. The EMBO journal 24:3834–45. doi: 10.1038/sj.emboj.7600847

Jacobelli J, Andres PG, Boisvert J, Krummel MF (2004a) New views of the immunological synapse: variations in assembly and function. Current opinion in immunology 16:345–52. doi: 10.1016/j.coi.2004.03.008

Jacobelli J, Chmura S a, Buxton DB, et al. (2004b) A single class II myosin modulates T cell motility and stopping, but not synapse formation. Nature immunology 5:531–8. doi: 10.1038/ni1065

Janeway, Jr CA, Travers P, Walport M, Shlomchik MJ (2001) Immunobiology, 5th Editio. New York: Garland Science Publishing

Jastrzebski K, Hannan KM, House CM, et al. (2011) A phospho-proteomic screen identifies novel S6K1 and mTORC1 substrates revealing additional complexity in the signaling network regulating cell growth. Cellular signalling 23:1338–47. doi: 10.1016/j.cellsig.2011.03.016

Jin M The Jin Lab, Biomedical Engineering, Cornell University. http://jin-lab.org/wiki/research/index?rev=1176949999. Accessed 28 Sep 2011

Jin T, Xu X, Hereld D (2008) Chemotaxis, chemokine receptors and human disease. Cytokine 44:1–8. doi: 10.1016/j.cyto.2008.06.017

Johnston B, Butcher EC (2002) Chemokines in rapid leukocyte adhesion triggering and migration. Seminars in immunology 14:83–92. doi: 10.1006/smim.2001.0345

Jones DH, Martin H, Madrazo J, et al. (1995) Expression and structural analysis of 14-3-3 proteins. Journal of molecular biology 245:375–84. doi: 10.1006/jmbi.1994.0031

Juliano RL (2002) Signal transduction by cell adhesion receptors and the cytoskeleton: functions of integrins, cadherins, selectins, and immunoglobulin-superfamily members. Annual review of pharmacology and toxicology 42:283–323. doi: 10.1146/annurev.pharmtox.42.090401.151133

Kadrmas JL, Beckerle MC (2004) The LIM domain: from the cytoskeleton to the nucleus. Nature reviews Molecular cell biology 5:920–31. doi: 10.1038/nrm1499

Kane LP, Lin J, Weiss A (2000) Signal transduction by the TCR for antigen. Current opinion in immunology 12:242–9.

Kanner SB, Grosmaire LS, Ledbetter JA, Damle NK (1993) Beta 2-integrin LFA-1 signaling through phospholipase C-gamma 1 activation. Proceedings of the National Academy of Sciences of the United States of America 90:7099–103.

Katsumoto T, Mitsushima A, Kurimura T (1990) The role of the vimentin intermediate filaments in rat 3Y1 cells elucidated by immunoelectron microscopy and computer-graphic reconstruction. Biology of the cell / under the auspices of the European Cell Biology Organization 68:139–46.

Kehrl JH (2006) Chemoattractant receptor signaling and the control of lymphocyte migration. Immunologic research 34:211–27. doi: 10.1385/IR:34:3:211

Keizer GD, Borst J, Figdor CG, et al. (1985) Biochemical and functional characteristics of the human leukocyte membrane antigen family LFA-1, Mo-1 and p150,95. European journal of immunology 15:1142–8. doi: 10.1002/eji.1830151114

Keller HU, Naef A, Zimmermann A (1984) Effects of colchicine, vinblastine and nocodazole on polarity, motility, chemotaxis and cAMP levels of human polymorphonuclear leukocytes. Experimental cell research 153:173–85.

Khaitlina SY (2001) Functional specificity of actin isoforms. International review of cytology 202:35–98.

Kholodenko BN, Hancock JF, Kolch W (2010) Signalling ballet in space and time. Nature reviews Molecular cell biology 11:414–26. doi: 10.1038/nrm2901

Khurana T, Khurana B, Noegel AA (2002) LIM proteins: association with the actin cytoskeleton. Protoplasma 219:1–12.

Kiely P a, Baillie GS, Barrett R, et al. (2009) Phosphorylation of RACK1 on tyrosine 52 by c-Abl is required for insulin-like growth factor I-mediated regulation of focal adhesion kinase. The Journal of biological chemistry 284:20263–74. doi: 10.1074/jbc.M109.017640

Kiely P a, Baillie GS, Lynch MJ, et al. (2008) Tyrosine 302 in RACK1 is essential for insulin-like growth factor-I-mediated competitive binding of PP2A and beta1 integrin and for tumor cell proliferation and migration. The Journal of biological chemistry 283:22952–61. doi: 10.1074/jbc.M800802200

Kiely P a, Leahy M, O'Gorman D, O'Connor R (2005) RACK1-mediated integration of adhesion and insulin-like growth factor I (IGF-I) signaling and cell migration are defective in cells expressing an IGF-I receptor mutated at tyrosines 1250 and 1251. The Journal of biological chemistry 280:7624–33. doi: 10.1074/jbc.M412889200

Kiely P a, O'Gorman D, Luong K, et al. (2006) Insulin-like growth factor I controls a mutually exclusive association of RACK1 with protein phosphatase 2A and beta1 integrin to promote cell migration. Molecular and cellular biology 26:4041–51. doi: 10.1128/MCB.01868-05

Kiely P a, Sant A, O'Connor R (2002) RACK1 is an insulin-like growth factor 1 (IGF-1) receptor-interacting protein that can regulate IGF-1-mediated Akt activation and protection from cell death. The Journal of biological chemistry 277:22581–9. doi: 10.1074/jbc.M201758200

Kim K-Y, Kovács M, Kawamoto S, et al. (2005) Disease-associated mutations and alternative splicing alter the enzymatic and motile activity of nonmuscle myosins II-B and II-C. The Journal of biological chemistry 280:22769–75. doi: 10.1074/jbc.M503488200

Kim M, Carman CV, Springer TA (2003) Bidirectional transmembrane signaling by cytoplasmic domain separation in integrins. Science (New York, NY) 301:1720–5. doi: 10.1126/science.1084174

Kimura K, Ito M, Amano M, et al. (1996) Regulation of myosin phosphatase by Rho and Rho-associated kinase (Rho-kinase). Science (New York, NY) 273:245–8.

Koehler J a, Moran MF (2001) RACK1, a protein kinase C scaffolding protein, interacts with the PH domain of p120GAP. Biochemical and biophysical research communications 283:888–95. doi: 10.1006/bbrc.2001.4889

Kolega J (1998) Cytoplasmic dynamics of myosin IIA and IIB: spatial "sorting" of isoforms in locomoting cells. Journal of cell science 111 (Pt 1:2085–95.

Komarova YA, Akhmanova AS, Kojima S-I, et al. (2002) Cytoplasmic linker proteins promote microtubule rescue in vivo. The Journal of cell biology 159:589–99. doi: 10.1083/jcb.200208058

Konstandin MH, Sester U, Klemke M, et al. (2006) A novel flow-cytometry-based assay for quantification of affinity and avidity changes of integrins. Journal of immunological methods 310:67–77. doi: 10.1016/j.jim.2005.12.005

van Kooyk Y, Figdor CG (2000) Avidity regulation of integrins : the driving force in leukocyte adhesion. Current Opinion in Cell Biology 12:542–547.

van Kooyk Y, van de Wiel-van Kemenade P, Weder P, et al. (1989) Enhancement of LFA-1-mediated cell adhesion by triggering through CD2 or CD3 on T lymphocytes. Nature 342:811–3. doi: 10.1038/342811a0

Kotovuori A, Pessa-Morikawa T, Kotovuori P, et al. (1999) ICAM-2 and a peptide from its binding domain are efficient activators of leukocyte adhesion and integrin affinity. Journal of immunology (Baltimore, Md : 1950) 162:6613–20.

Kotovuori P, Tontti E, Pigott R, et al. (1993) The vascular E-selectin binds to the leukocyte integrins CD11/CD18. Glycobiology 3:131–6.

Kramer A, Schneider-Mergener J (1998) Synthesis and screening of peptide libraries on continuous cellulose membrane supports. Methods in molecular biology (Clifton, NJ) 87:25–39.

Krendel M, Mooseker MS (2005) Myosins: tails (and heads) of functional diversity. Physiology (Bethesda, Md) 20:239–51. doi: 10.1152/physiol.00014.2005

Krendel M, Zenke FT, Bokoch GM (2002) Nucleotide exchange factor GEF-H1 mediates cross-talk between microtubules and the actin cytoskeleton. Nature cell biology 4:294–301. doi: 10.1038/ncb773

Krummel MF, Macara I (2006) Maintenance and modulation of T cell polarity. Nature immunology 7:1143–9. doi: 10.1038/ni1404

Kucia M, Jankowski K, Reca R, et al. (2004) CXCR4-SDF-1 signalling, locomotion, chemotaxis and adhesion. Journal of molecular histology 35:233–45.

Kucik DF, Dustin ML, Miller JM, Brown EJ (1996) Adhesion-activating phorbol ester increases the mobility of leukocyte integrin LFA-1 in cultured lymphocytes. The Journal of clinical investigation 97:2139–44. doi: 10.1172/JCI118651

Kwak JM, Kim SA, Lee SK, et al. (1997) Insulin-induced maturation of Xenopus oocytes is inhibited by microinjection of a Brassica napus cDNA clone with high similarity to a mammalian receptor for activated protein kinase C. Planta 201:245–51.

De La Luz Sierra M, Yang F, Narazaki M, et al. (2004) Differential processing of stromal-derived factor-1alpha and stromal-derived factor-1beta explains functional diversity. Blood 103:2452–9. doi: 10.1182/blood-2003-08-2857

Lahn M, Sundell K, Köhler G (2006) The role of protein kinase C-alpha in hematologic malignancies. Acta haematologica 115:1–8. doi: 10.1159/000089458

Landsverk ML, Epstein HF (2005) Genetic analysis of myosin II assembly and organization in model organisms. Cellular and molecular life sciences : CMLS 62:2270–82. doi: 10.1007/s00018-005-5176-2

Langner M, Repasky EA, Hui SW (1992) Relationship between membrane lipid mobility and spectrin distribution in lymphocytes. FEBS letters 305:197–202.

Laudanna C, Campbell JJ, Butcher EC (1996) Role of Rho in chemoattractant-activated leukocyte adhesion through integrins. Science (New York, NY) 271:981–3.

Laudanna C, Mochly-Rosen D, Liron T, et al. (1998) Evidence of zeta protein kinase C involvement in polymorphonuclear neutrophil integrin-dependent adhesion and chemotaxis. The Journal of biological chemistry 273:30306–15.

Lauffenburger DA, Tranquillo RT, Zigmond SH (1988) Concentration gradients of chemotactic factors in chemotaxis assays. Methods in enzymology 162:85–101.

Lebwohl M (2003) Psoriasis. Lancet 361:1197–204. doi: 10.1016/S0140-6736(03)12954-6

Lebwohl M, Tyring SK, Hamilton TK, et al. (2003) A novel targeted T-cell modulator, efalizumab, for plaque psoriasis. The New England journal of medicine 349:2004–13. doi: 10.1056/NEJMoa030002

Lee H, Zahra D, Vogelzang A, et al. (2006) Human C5aR knock-in mice facilitate the production and assessment of anti-inflammatory monoclonal antibodies. Nature biotechnology 24:1279–84. doi: 10.1038/nbt1248

Lee H-S, Millward-Sadler SJ, Wright MO, et al. (2002) Activation of Integrin-RACK1/PKCalpha signalling in human articular chondrocyte mechanotransduction. Osteoarthritis and cartilage / OARS, Osteoarthritis Research Society 10:890–7.

Leeuwen FN, Kain HE, Kammen RA, et al. (1997) The guanine nucleotide exchange factor Tiam1 affects neuronal morphology; opposing roles for the small GTPases Rac and Rho. The Journal of cell biology 139:797–807.

Lefort CT, Kim M (2010) Human T lymphocyte isolation, culture and analysis of migration in vitro. Journal of visualized experiments : JoVE. doi: 10.3791/2017

Leitinger B, Hogg N (2002) The involvement of lipid rafts in the regulation of integrin function. Journal of cell science 115:963–72.

Lemmon MA, Ferguson KM, Abrams CS (2002) Pleckstrin homology domains and the cytoskeleton. FEBS letters 513:71–6.

Leonardi C, Menter A, Hamilton T, et al. (2008) Efalizumab: results of a 3-year continuous dosing study for the long-term control of psoriasis. The British journal of dermatology 158:1107–16. doi: 10.1111/j.1365-2133.2008.08548.x

Lewis JM, Cheresh DA, Schwartz MA (1996) Protein kinase C regulates alpha v beta 5-dependent cytoskeletal associations and focal adhesion kinase phosphorylation. The Journal of cell biology 134:1323–32.

Lewis TL, Brundage KM, Brundage RA, Barnett JB (2008) 3,4-Dichloropropionanilide (DCPA) inhibits T-cell activation by altering the intracellular calcium concentration following store depletion. Toxicological sciences : an official journal of the Society of Toxicology 103:97–107. doi: 10.1093/toxsci/kfn031

Ley K, Laudanna C, Cybulsky MI, Nourshargh S (2007) Getting to the site of inflammation: the leukocyte adhesion cascade updated. Nature reviews Immunology 7:678–89. doi: 10.1038/nri2156

Liliental J, Chang DD (1998) Rack1, a receptor for activated protein kinase C, interacts with integrin beta subunit. The Journal of biological chemistry 273:2379–83.

Link AJ, Eng J, Schieltz DM, et al. (1999) Direct analysis of protein complexes using mass spectrometry. Nature biotechnology 17:676–82. doi: 10.1038/10890

Lo C-M, Buxton DB, Chua GCH, et al. (2004) Nonmuscle myosin IIb is involved in the guidance of fibroblast migration. Molecular biology of the cell 15:982–9. doi: 10.1091/mbc.E03-06-0359

Long EO (2011) ICAM-1: getting a grip on leukocyte adhesion. Journal of immunology (Baltimore, Md : 1950) 186:5021–3. doi: 10.4049/jimmunol.1100646

Loughran G, Healy NC, Kiely PA, et al. (2005) Mystique is a new insulin-like growth factor-I-regulated PDZ-LIM domain protein that promotes cell attachment and migration and suppresses Anchorage-independent growth. Molecular biology of the cell 16:1811–22. doi: 10.1091/mbc.E04-12-1052

Lub M, van Kooyk Y, Figdor CG (1995) Ins and outs of LFA-1. Immunology today 16:479–83.

Lub M, van Kooyk Y, van Vliet SJ, Figdor CG (1997) Dual role of the actin cytoskeleton in regulating cell adhesion mediated by the integrin lymphocyte function-associated molecule-1. Molecular biology of the cell 8:341–51.

Ludford-Menting MJ, Oliaro J, Sacirbegovic F, et al. (2005) A network of PDZ-containing proteins regulates T cell polarity and morphology during migration and immunological synapse formation. Immunity 22:737–48. doi: 10.1016/j.immuni.2005.04.009

Ludowyke RI, Elgundi Z, Kranenburg T, et al. (2006) Phosphorylation of nonmuscle myosin heavy chain IIA on Ser1917 is mediated by protein kinase C beta II and coincides with the onset of stimulated degranulation of RBL-2H3 mast cells. Journal of immunology (Baltimore, Md : 1950) 177:1492–9.

Ludwig A, Otto GP, Riento K, et al. (2010) Flotillin microdomains interact with the cortical cytoskeleton to control uropod formation and neutrophil recruitment. The Journal of cell biology 191:771–81. doi: 10.1083/jcb.201005140

Lukong KE, Richard S (2003) Sam68, the KH domain-containing superSTAR. Biochimica et biophysica acta 1653:73–86.

Lunsford KE, Barbas AS, Brennan TV (2011) Recent advances in immunosuppressive therapy for prevention of renal allograft rejection. Current opinion in organ transplantation 16:390–7. doi: 10.1097/MOT.0b013e328348b420

Luo B-H, Carman CV, Springer TA (2007) Structural basis of integrin regulation and signaling. Annual review of immunology 25:619–47. doi: 10.1146/annurev.immunol.25.022106.141618

Luo B-H, Springer TA, Takagi J (2004) A specific interface between integrin transmembrane helices and affinity for ligand. PLoS biology 2:e153. doi: 10.1371/journal.pbio.0020153

MacKintosh C, MacKintosh RW (1994) Inhibitors of protein kinases and phosphatases. Trends in biochemical sciences 19:444–8.

Mackay CR (2008) Moving targets: cell migration inhibitors as new anti-inflammatory therapies. Nature immunology 9:988–98. doi: 10.1038/ni.f.210

Major EO (2010) Progressive multifocal leukoencephalopathy in patients on immunomodulatory therapies. Annual review of medicine 61:35–47. doi: 10.1146/annurev.med.080708.082655

Matsumura F, Yamakita Y, Yamashiro S (2011) Myosin light chain kinases and phosphatase in mitosis and cytokinesis. Archives of biochemistry and biophysics 510:76–82. doi: 10.1016/j.abb.2011.03.002

Maupin P, Phillips CL, Adelstein RS, Pollard TD (1994) Differential localization of myosin-II isozymes in human cultured cells and blood cells. Journal of cell science 107 (Pt 1:3077–90.

Mañes S, Lacalle R a, Gómez-Moutón C, et al. (2001) Membrane raft microdomains in chemokine receptor function. Seminars in immunology 13:147–57. doi: 10.1006/smim.2000.0306

McCahill A, Warwicker J, Bolger GB, et al. (2002) The RACK1 scaffold protein: a dynamic cog in cell response mechanisms. Molecular pharmacology 62:1261–73.

Meller N, Liu YC, Collins TL, et al. (1996) Direct interaction between protein kinase C theta (PKC theta) and 14-3-3 tau in T cells: 14-3-3 overexpression results in inhibition of PKC theta translocation and function. Molecular and cellular biology 16:5782–91.

Mellor H, Parker PJ (1998) The extended protein kinase C superfamily. The Biochemical journal 332 (Pt 2:281–92.

Mempel TR, Henrickson SE, Von Andrian UH (2004) T-cell priming by dendritic cells in lymph nodes occurs in three distinct phases. Nature 427:154–9. doi: 10.1038/nature02238

Meng X, Krokhin O, Cheng K, et al. (2007) Characterization of IQGAP1-containing complexes in NK-like cells: evidence for Rac 2 and RACK1 association during homotypic adhesion. Journal of proteome research 6:744–50. doi: 10.1021/pr060382t

Mihara K, Smit M-J, Krajnc-Franken M, et al. (2005) Human CXCR2 (hCXCR2) takes over functionalities of its murine homolog in hCXCR2 knockin mice. European journal of immunology 35:2573–82. doi: 10.1002/eji.200526021

Miletic AV, Swat M, Fujikawa K, Swat W (2003) Cytoskeletal remodeling in lymphocyte activation. Current Opinion in Immunology 15:261–268. doi: 10.1016/S0952-7915(03)00054-2

Miller LD, Lee KC, Mochly-Rosen D, Cartwright CA (2004) RACK1 regulates Src-mediated Sam68 and p190RhoGAP signaling. Oncogene 23:5682–6. doi: 10.1038/sj.onc.1207735

Miller LJ (2008) G protein-coupled receptor structures, molecular associations, and modes of regulation. Annals of the New York Academy of Sciences 1144:1–5. doi: 10.1196/annals.1418.000

Miller MJ, Wei SH, Cahalan MD, Parker I (2003) Autonomous T cell trafficking examined in vivo with intravital two-photon microscopy. Proceedings of the National Academy of Sciences of the United States of America 100:2604–9. doi: 10.1073/pnas.2628040100

Millán J, Montoya MC, Sancho D, et al. (2002) Lipid rafts mediate biosynthetic transport to the T lymphocyte uropod subdomain and are necessary for uropod integrity and function. Blood 99:978–84.

Mischiati C, Melloni E, Corallini F, et al. (2008) Potential role of PKC inhibitors in the treatment of hematological malignancies. Current pharmaceutical design 14:2075–84.

Mochly-Rosen D, Gordon AS (1998) Anchoring proteins for protein kinase C: a means for isozyme selectivity. FASEB journal : official publication of the Federation of American Societies for Experimental Biology 12:35–42.

Mochly-Rosen D, Smith BL, Chen CH, et al. (1995) Interaction of protein kinase C with RACK1, a receptor for activated C-kinase: a role in beta protein kinase C mediated signal transduction. Biochemical Society transactions 23:596–600.

Moissoglu K, Schwartz MA (2006) Integrin signalling in directed cell migration. Biology of the cell / under the auspices of the European Cell Biology Organization 98:547–55. doi: 10.1042/BC20060025

Mora JR, Von Andrian UH (2006) Specificity and plasticity of memory lymphocyte migration. Current topics in microbiology and immunology 308:83–116.

Morin N a, Oakes PW, Hyun Y-M, et al. (2008) Nonmuscle myosin heavy chain IIA mediates integrin LFA-1 de-adhesion during T lymphocyte migration. The Journal of experimental medicine 205:195–205. doi: 10.1084/jem.20071543

Morrison DK (2009) The 14-3-3 proteins: integrators of diverse signaling cues that impact cell fate and cancer development. Trends in cell biology 19:16–23. doi: 10.1016/j.tcb.2008.10.003

Moser B, Loetscher P (2001) Lymphocyte traffic control by chemokines. Nature immunology 2:123–8. doi: 10.1038/84219

Munn DH, Mellor AL (2006) The tumor-draining lymph node as an immune-privileged site. Immunological reviews 213:146–58. doi: 10.1111/j.1600-065X.2006.00444.x

Munn DH, Mellor AL (2003) Macrophages and the regulation of self-reactive T cells. Current pharmaceutical design 9:257–64.

Nadeau K, McDonald-Hyman C, Noth EM, et al. (2010) Ambient air pollution impairs regulatory T-cell function in asthma. The Journal of allergy and clinical immunology 126:845–852.e10. doi: 10.1016/j.jaci.2010.08.008

Najib S, Martín-Romero C, González-Yanes C, Sánchez-Margalet V (2005) Role of Sam68 as an adaptor protein in signal transduction. Cellular and molecular life sciences : CMLS 62:36–43. doi: 10.1007/s00018-004-4309-3

Narducci MG, Scala E, Bresin A, et al. (2006) Skin homing of Sézary cells involves SDF-1-CXCR4 signaling and down-regulation of CD26/dipeptidylpeptidase IV. Blood 107:1108–15. doi: 10.1182/blood-2005-04-1492

Neasta J, Kiely PA, He D-Y, et al. (2012) Direct interaction between scaffolding proteins RACK1 and 14-3-3ζ regulates brain-derived neurotrophic factor (BDNF) transcription. The Journal of biological chemistry 287:322–36. doi: 10.1074/jbc.M111.272195

Nellen W, Lichtenstein C (1993) What makes an mRNA anti-sense-itive? Trends in biochemical sciences 18:419–23.

Neuhoff V, Arold N, Taube D, Ehrhardt W (1988) Improved staining of proteins in polyacrylamide gels including isoelectric focusing gels with clear background at nanogram sensitivity using Coomassie Brilliant Blue G-250 and R-250. Electrophoresis 9:255–62. doi: 10.1002/elps.1150090603

Neves SR, Ram PT, Iyengar R (2002) G protein pathways. Science (New York, NY) 296:1636–9. doi: 10.1126/science.1071550

Newton-Nash DK, Tonellato P, Swiersz M, Abramoff P (1990) Assessment of chemokinetic behavior of inflammatory lung macrophages in a linear under-agarose assay. Journal of leukocyte biology 48:297–305.

Ng T, Shima D, Squire A, et al. (1999) PKCalpha regulates beta1 integrin-dependent cell motility through association and control of integrin traffic. The EMBO journal 18:3909–23. doi: 10.1093/emboj/18.14.3909

Niemantsverdriet M, Wagner K, Visser M, Backendorf C (2008) Cellular functions of 14-3-3 zeta in apoptosis and cell adhesion emphasize its oncogenic character. Oncogene 27:1315–9. doi: 10.1038/sj.onc.1210742

Nieminen M, Henttinen T, Merinen M, et al. (2006) Vimentin function in lymphocyte adhesion and transcellular migration. Nature cell biology 8:156–62. doi: 10.1038/ncb1355

Nieto M, Frade JM, Sancho D, et al. (1997) Polarization of chemokine receptors to the leading edge during lymphocyte chemotaxis. The Journal of experimental medicine 186:153–8.

Niggli V (2003) Microtubule-disruption-induced and chemotactic-peptide-induced migration of human neutrophils: implications for differential sets of signalling pathways. Journal of cell science 116:813–22.

Nijhara R, van Hennik PB, Gignac ML, et al. (2004) Rac1 mediates collapse of microvilli on chemokine-activated T lymphocytes. Journal of immunology (Baltimore, Md : 1950) 173:4985–93.

Nilsson J, Sengupta J, Frank J, Nissen P (2004) Regulation of eukaryotic translation by the RACK1 protein: a platform for signalling molecules on the ribosome. EMBO reports 5:1137–41. doi: 10.1038/sj.embor.7400291

Nishida N, Xie C, Shimaoka M, et al. (2006) Activation of leukocyte beta2 integrins by conversion from bent to extended conformations. Immunity 25:583–94. doi: 10.1016/j.immuni.2006.07.016

Nobes CD, Hall a (1999) Rho GTPases control polarity, protrusion, and adhesion during cell movement. The Journal of cell biology 144:1235–44.

Ochs HD, Thrasher AJ (2006) The Wiskott-Aldrich syndrome. The Journal of allergy and clinical immunology 117:725–38; quiz 739. doi: 10.1016/j.jaci.2006.02.005

Ohanian V, Gatfield K, Ohanian J (2005) Role of the actin cytoskeleton in G-protein-coupled receptor activation of PYK2 and paxillin in vascular smooth muscle. Hypertension 46:93–9. doi: 10.1161/01.HYP.0000167990.82235.3c

Oldham WM, Hamm HE (2008) Heterotrimeric G protein activation by G-protein-coupled receptors. Nature reviews Molecular cell biology 9:60–71. doi: 10.1038/nrm2299

Olsen JV, Blagoev B, Gnad F, et al. (2006) Global, in vivo, and site-specific phosphorylation dynamics in signaling networks. Cell 127:635–48. doi: 10.1016/j.cell.2006.09.026

Omary MB, Ku N-O, Tao G-Z, et al. (2006) "Heads and tails" of intermediate filament phosphorylation: multiple sites and functional insights. Trends in biochemical sciences 31:383–94. doi: 10.1016/j.tibs.2006.05.008

Ostermann G, Weber KSC, Zernecke A, et al. (2002) JAM-1 is a ligand of the beta(2) integrin LFA-1 involved in transendothelial migration of leukocytes. Nature immunology 3:151–8. doi: 10.1038/ni755

Palazzo AF, Cook TA, Alberts AS, Gundersen GG (2001) mDia mediates Rho-regulated formation and orientation of stable microtubules. Nature cell biology 3:723–9. doi: 10.1038/35087035

Parker PJ, Murray-Rust J (2004) PKC at a glance. Journal of cell science 117:131–2. doi: 10.1242/jcs.00982

Partridge AW, Liu S, Kim S, et al. (2005) Transmembrane domain helix packing stabilizes integrin alphaIIbbeta3 in the low affinity state. The Journal of biological chemistry 280:7294–300. doi: 10.1074/jbc.M412701200

Pasvolsky R, Grabovsky V, Giagulli C, et al. (2008) RhoA is involved in LFA-1 extension triggered by CXCL12 but not in a novel outside-in LFA-1 activation facilitated by CXCL9. Journal of immunology (Baltimore, Md : 1950) 180:2815–23.

Patrussi L, Baldari CT (2008) Intracellular mediators of CXCR4-dependent signaling in T cells. Immunology letters 115:75–82. doi: 10.1016/j.imlet.2007.10.012

Paul CP, Good PD, Winer I, Engelke DR (2002) Effective expression of small interfering RNA in human cells. Nature biotechnology 20:505–8. doi: 10.1038/nbt0502-505

Pawson T, Scott JD (1997) Signaling through scaffold, anchoring, and adaptor proteins. Science (New York, NY) 278:2075–80.

Pereira AL, Pereira AJ, Maia ARR, et al. (2006) Mammalian CLASP1 and CLASP2 cooperate to ensure mitotic fidelity by regulating spindle and kinetochore function. Molecular biology of the cell 17:4526–42. doi: 10.1091/mbc.E06-07-0579

Perez OD, Mitchell D, Jager GC, et al. (2003) Leukocyte functional antigen 1 lowers T cell activation thresholds and signaling through cytohesin-1 and Jun-activating binding protein 1. Nature immunology 4:1083–92. doi: 10.1038/ni984

Pietrosimone KM, Yin X, Knecht DA, Lynes MA (2012) Measurement of Cellular Chemotaxis with ECIS/Taxis. Journal of visualized experiments : JoVE. doi: 10.3791/3840

Pitcher JA, Freedman NJ, Lefkowitz RJ (1998) G protein-coupled receptor kinases. Annual review of biochemistry 67:653–92. doi: 10.1146/annurev.biochem.67.1.653

Pitcher JA, Inglese J, Higgins JB, et al. (1992) Role of beta gamma subunits of G proteins in targeting the beta-adrenergic receptor kinase to membrane-bound receptors. Science (New York, NY) 257:1264–7.

Polosukhina D, Singaravelu K, Padanilam BJ (2003) Activation of protein kinase C isozymes protects LLCPK1 cells from H2O2 induced necrotic cell death. American journal of nephrology 23:380–9. doi: 10.1159/000073984

Pomies P, Pashmforoush M, Vegezzi C, et al. (2007) The Cytoskeleton-associated PDZ-LIM Protein, ALP, Acts on Serum Response Factor Activity to Regulate Muscle Differentiation. Molecular Biology of the Cell 18:1723–1733. doi: 10.1091/mbc.E06-09-0815

Ponti A, Machacek M, Gupton SL, et al. (2004) Two distinct actin networks drive the protrusion of migrating cells. Science (New York, NY) 305:1782–6. doi: 10.1126/science.1100533

Porter JC, Bracke M, Smith A, et al. (2002) Signaling through integrin LFA-1 leads to filamentous actin polymerization and remodeling, resulting in enhanced T cell adhesion. Journal of immunology (Baltimore, Md : 1950) 168:6330–5.

del Pozo MA, Nieto M, Serrador JM, et al. (1998) The two poles of the lymphocyte: specialized cell compartments for migration and recruitment. Cell adhesion and communication 6:125–33.

del Pozo MA, Sánchez-Mateos P, Nieto M, Sánchez-Madrid F (1995) Chemokines regulate cellular polarization and adhesion receptor redistribution during lymphocyte interaction with endothelium and extracellular matrix. Involvement of cAMP signaling pathway. The Journal of cell biology 131:495–508.

del Pozo MA, Vicente-Manzanares M, Tejedor R, et al. (1999) Rho GTPases control migration and polarization of adhesion molecules and cytoskeletal ERM components in T lymphocytes. European journal of immunology 29:3609–20. doi: 10.1002/(SICI)1521-4141(199911)29:11<3609::AID-IMMU3609>3.0.CO;2-S

Pribila JT, Shimizu Y (2003) Signal transduction events regulating integrin function and T cell migration: new functions and complexity. Immunologic research 27:107–28.

Qiu Y, Mao T, Zhang Y, et al. (2010) A crucial role for RACK1 in the regulation of glucose-stimulated IRE1alpha activation in pancreatic beta cells. Science signaling 3:ra7. doi: 10.1126/scisignal.2000514

Rabinovitz I, Toker A, Mercurio AM (1999) Protein kinase C-dependent mobilization of the alpha6beta4 integrin from hemidesmosomes and its association with actin-rich cell protrusions drive the chemotactic migration of carcinoma cells. The Journal of cell biology 146:1147–60.

Ratner S, Sherrod WS, Lichlyter D (1997) Microtubule retraction into the uropod and its role in T cell polarization and motility. Journal of immunology (Baltimore, Md : 1950) 159:1063–7.

Real E, Faure S, Donnadieu E, Delon J (2007) Cutting edge: Atypical PKCs regulate T lymphocyte polarity and scanning behavior. Journal of immunology (Baltimore, Md : 1950) 179:5649–52.

dos Remedios CG, Chhabra D, Kekic M, et al. (2003) Actin binding proteins: regulation of cytoskeletal microfilaments. Physiological reviews 83:433–73. doi: 10.1152/physrev.00026.2002

Ren XD, Kiosses WB, Schwartz MA (1999) Regulation of the small GTP-binding protein Rho by cell adhesion and the cytoskeleton. The EMBO journal 18:578–85. doi: 10.1093/emboj/18.3.578

Renkonen R, Paavonen T, Nortamo P, Gahmberg CG (1992) Expression of endothelial adhesion molecules in vivo. Increased endothelial ICAM-2 expression in lymphoid malignancies. The American journal of pathology 140:763–7.

Revenu C, Athman R, Robine S, Louvard D (2004) The co-workers of actin filaments: from cell structures to signals. Nature reviews Molecular cell biology 5:635–46. doi: 10.1038/nrm1437

Rey M, Vicente-manzanares M, Yáñez-mó M, et al. (2002) Cutting Edge: Association of the Motor Protein Nonmuscle Myosin Heavy Chain-IIA with the C Terminus of the Chemokine Receptor CXCR4 in T Lymphocytes. The Journal of Immunology

Rickert P, Weiner OD, Wang F, et al. (2000) Leukocytes navigate by compass: roles of PI3Kgamma and its lipid products. Trends in cell biology 10:466–73.

Ridley AJ (1999) Rho family proteins and regulation of the actin cytoskeleton. Progress in molecular and subcellular biology 22:1–22.

Ridley AJ (2011) Life at the leading edge. Cell 145:1012–22. doi: 10.1016/j.cell.2011.06.010

Ridley AJ, Schwartz M a, Burridge K, et al. (2003) Cell migration: integrating signals from front to back. Science (New York, NY) 302:1704–9. doi: 10.1126/science.1092053

Rikitake Y, Takai Y (2011) Directional cell migration regulation by small G proteins, nectin-like molecule-5, and afadin. International review of cell and molecular biology 287:97–143. doi: 10.1016/B978-0-12-386043-9.00003-7

Robey E, Fowlkes BJ (1994) Selective events in T cell development. Annual review of immunology 12:675–705. doi: 10.1146/annurev.iy.12.040194.003331

Robinson DS (2010) The role of the T cell in asthma. The Journal of allergy and clinical immunology 126:1081–91; quiz 1092–3. doi: 10.1016/j.jaci.2010.06.025

Robinson K, Jones D, Patel Y, et al. (1994) Mechanism of inhibition of protein kinase C by 14-3-3 isoforms. 14-3-3 isoforms do not have phospholipase A2 activity. The Biochemical journal 299 (Pt 3:853–61.

Robles MS, Boyault C, Knutti D, et al. (2010) Identification of RACK1 and protein kinase Calpha as integral components of the mammalian circadian clock. Science (New York, NY) 327:463–6. doi: 10.1126/science.1180067

Rochman Y, Spolski R, Leonard WJ (2009) New insights into the regulation of T cells by gamma(c) family cytokines. Nature reviews Immunology 9:480–90. doi: 10.1038/nri2580

Rodriguez MM, Ron D, Touhara K, et al. (1999) RACK1, a Protein Kinase C Anchoring Protein, Coordinates the Binding of Activated Protein Kinase C and Select Pleckstrin Homology Domains in Vitro †. Biochemistry 38:13787–13794. doi: 10.1021/bi991055k

Rodríguez-Fernández JL (1999) Why do so many stimuli induce tyrosine phosphorylation of FAK? BioEssays : news and reviews in molecular, cellular and developmental biology 21:1069–75. doi: 10.1002/(SICI)1521-1878(199912)22:1<1069::AID-BIES13>3.0.CO;2-C

Rodríguez-Fernández JL, Sánchez-Martín L, Rey M, et al. (2001) Rho and Rho-associated kinase modulate the tyrosine kinase PYK2 in T-cells through regulation of the activity of the integrin LFA-1. The Journal of biological chemistry 276:40518–27. doi: 10.1074/jbc.M102896200

Ron D, Chen CH, Caldwell J, et al. (1994) Cloning of an intracellular receptor for protein kinase C: a homolog of the beta subunit of G proteins. Proceedings of the National Academy of Sciences of the United States of America 91:839–43.

Ron D, Jiang Z, Yao L, et al. (1999) Coordinated movement of RACK1 with activated betaIIPKC. The Journal of biological chemistry 274:27039–46.

Rose DM, Grabovsky V, Alon R, Ginsberg MH (2001) The affinity of integrin alpha(4)beta(1) governs lymphocyte migration. Journal of immunology (Baltimore, Md : 1950) 167:2824–30.

Rose DM, Liu S, Woodside DG, et al. (2003) Paxillin binding to the alpha 4 integrin subunit stimulates LFA-1 (integrin alpha L beta 2)-dependent T cell migration by augmenting the activation of focal adhesion kinase/proline-rich tyrosine kinase-2. Journal of immunology (Baltimore, Md : 1950) 170:5912–8.

Russell S (2008) How polarity shapes the destiny of T cells. Journal of cell science 121:131–6. doi: 10.1242/jcs.021253

Russell S, Oliaro J (2006) Compartmentalization in T-cell signalling: membrane microdomains and polarity orchestrate signalling and morphology. Immunology and cell biology 84:107–13. doi: 10.1111/j.1440-1711.2005.01415.x

Saiki RK, Gelfand DH, Stoffel S, et al. (1988) Primer-directed enzymatic amplification of DNA with a thermostable DNA polymerase. Science (New York, NY) 239:487–91.

Saiki RK, Scharf S, Faloona F, et al. (1985) Enzymatic amplification of beta-globin genomic sequences and restriction site analysis for diagnosis of sickle cell anemia. Science (New York, NY) 230:1350–4.

Saitoh T, Takemura S, Ueda K, et al. (2001) Differential localization of non-muscle myosin II isoforms and phosphorylated regulatory light chains in human MRC-5 fibroblasts. FEBS letters 509:365–9.

Samstag Y, Eibert SM, Klemke M, Wabnitz GH (2003) Actin cytoskeletal dynamics in T lymphocyte activation and migration. Journal of leukocyte biology 73:30–48. doi: 10.1189/jlb.0602272.http

Sasse J, Gallagher SR (2004) Staining proteins in gels. Current protocols in immunology / edited by John E Coligan . [et al] Chapter 8:Unit 8.9. doi: 10.1002/0471142735.im0809s58

Schechtman D, Mochly-Rosen D (2001) Adaptor proteins in protein kinase C-mediated signal transduction. Oncogene 20:6339–47. doi: 10.1038/sj.onc.1204778

Scherer LJ, Rossi JJ (2003) Approaches for the sequence-specific knockdown of mRNA. Nature biotechnology 21:1457–65. doi: 10.1038/nbt915

Schwarz BA, Bhandoola A (2006) Trafficking from the bone marrow to the thymus: a prerequisite for thymopoiesis. Immunological reviews 209:47–57. doi: 10.1111/j.0105-2896.2006.00350.x

Schürpf T, Springer T a (2011) Regulation of integrin affinity on cell surfaces. The EMBO journal 1–16. doi: 10.1038/emboj.2011.333

Scott JD, Pawson T (2009) Cell signaling in space and time: where proteins come together and when they're apart. Science (New York, NY) 326:1220–4. doi: 10.1126/science.1175668

Sellers JR (2000) Myosins: a diverse superfamily. Biochimica et biophysica acta 1496:3–22.

Sengupta J, Nilsson J, Gursky R, et al. (2004) Identification of the versatile scaffold protein RACK1 on the eukaryotic ribosome by cryo-EM. Nature structural & molecular biology 11:957–62. doi: 10.1038/nsmb822

Serrador JM, Nieto M, Sánchez-Madrid F (1999) Cytoskeletal rearrangement during migration and activation of T lymphocytes. Trends in cell biology 9:228–33.

Serrels B, Sandilands E, Frame MC (2011) Signaling of the direction-sensing FAK/RACK1/PDE4D5 complex to the small GTPase Rap1. Small GTPases 2:54–61. doi: 10.4161/sgtp.2.1.15137

Serrels B, Sandilands E, Serrels A, et al. (2010) A complex between FAK, RACK1, and PDE4D5 controls spreading initiation and cancer cell polarity. Current biology : CB 20:1086–92. doi: 10.1016/j.cub.2010.04.042

Shamri R, Grabovsky V, Gauguet J-M, et al. (2005) Lymphocyte arrest requires instantaneous induction of an extended LFA-1 conformation mediated by endothelium-bound chemokines. Nature immunology 6:497–506. doi: 10.1038/ni1194

Sharp PA (2001) RNA interference--2001. Genes & development 15:485–90. doi: 10.1101/gad.880001

Shaw AS, Filbert EL (2009) Scaffold proteins and immune-cell signalling. Nature reviews Immunology 9:47–56. doi: 10.1038/nri2473

Shimaoka M, Takagi J, Springer TA (2002) Conformational regulation of integrin structure and function. Annual review of biophysics and biomolecular structure 31:485–516. doi: 10.1146/annurev.biophys.31.101101.140922

Shimizu Y (2003) LFA-1: more than just T cell Velcro. Nature immunology 4:1052–4. doi: 10.1038/ni1103-1052

Shor B, Calaycay J, Rushbrook J, McLeod M (2003) Cpc2/RACK1 is a ribosome-associated protein that promotes efficient translation in Schizosaccharomyces pombe. The Journal of biological chemistry 278:49119–28. doi: 10.1074/jbc.M303968200

Shulman Z, Alon R (2009) Chapter 14. Real-time in vitro assays for studying the role of chemokines in lymphocyte transendothelial migration under physiologic flow conditions. Methods in enzymology 461:311–32. doi: 10.1016/S0076-6879(09)05414-7

Shulman Z, Shinder V, Klein E, et al. (2009) Lymphocyte crawling and transendothelial migration require chemokine triggering of high-affinity LFA-1 integrin. Immunity 30:384–96. doi: 10.1016/j.immuni.2008.12.020

Siderovski DP, Willard FS (2005) The GAPs, GEFs, and GDIs of heterotrimeric G-protein alpha subunits. International journal of biological sciences 1:51–66.

Sklan EH, Podoly E, Soreq H (2006) RACK1 has the nerve to act: structure meets function in the nervous system. Progress in neurobiology 78:117–34. doi: 10.1016/j.pneurobio.2005.12.002

Skubitz APN (2002) Adhesion molecules. Cancer treatment and research 107:305–29.

Small JV, Kaverina I (2003) Microtubules meet substrate adhesions to arrange cell polarity. Current opinion in cell biology 15:40–7.

Small JV, Kaverina I, Krylyshkina O, Rottner K (1999) Cytoskeleton cross-talk during cell motility. FEBS letters 452:96–9.

Smith A, Bracke M, Leitinger B, et al. (2003) LFA-1-induced T cell migration on ICAM-1 involves regulation of MLCK-mediated attachment and ROCK-dependent detachment. Journal of cell science 116:3123–33. doi: 10.1242/jcs.00606

Smith A, Carrasco YR, Stanley P, et al. (2005) A talin-dependent LFA-1 focal zone is formed by rapidly migrating T lymphocytes. The Journal of cell biology 170:141–51. doi: 10.1083/jcb.200412032

Smith A, Stanley P, Jones K, et al. (2007a) The role of the integrin LFA-1 in T-lymphocyte migration. Immunological reviews 218:135–46. doi: 10.1111/j.1600-065X.2007.00537.x

Smith L, Webb A, Ward SG (2007b) T-lymphocyte navigation and migration: beyond the PI3K paradigm. Biochemical Society transactions 35:193–8. doi: 10.1042/BST0350193

Smith L a, Aranda-Espinoza H, Haun JB, et al. (2007c) Neutrophil traction stresses are concentrated in the uropod during migration. Biophysical journal 92:L58–60. doi: 10.1529/biophysj.106.102822

Smith-Garvin JE, Koretzky GA, Jordan MS (2009) T cell activation. Annual review of immunology 27:591–619. doi: 10.1146/annurev.immunol.021908.132706

Snapper SB, Rosen FS, Mizoguchi E, et al. (1998) Wiskott-Aldrich syndrome protein-deficient mice reveal a role for WASP in T but not B cell activation. Immunity 9:81–91.

Soede RD, Wijnands YM, Van Kouteren-Cobzaru I, Roos E (1998) ZAP-70 tyrosine kinase is required for LFA-1-dependent T cell migration. The Journal of cell biology 142:1371–9.

Sohn RL, Vikstrom KL, Strauss M, et al. (1997) A 29 residue region of the sarcomeric myosin rod is necessary for filament formation. Journal of molecular biology 266:317–30. doi: 10.1006/jmbi.1996.0790

Solomon GE (2010) T-cell agents in the treatment of rheumatoid arthritis. Bulletin of the NYU hospital for joint diseases 68:162–5.

Somersalo K, Carpén O, Saksela E, et al. (1995) Activation of natural killer cell migration by leukocyte integrin-binding peptide from intracellular adhesion molecule-2 (ICAM-2). The Journal of biological chemistry 270:8629–36.

Sondek J, Siderovski DP (2001) Ggamma-like (GGL) domains: new frontiers in G-protein signaling and beta-propeller scaffolding. Biochemical pharmacology 61:1329–37.

Soriani A, Moran B, de Virgilio M, et al. (2006) A role for PKCtheta in outside-in alpha(IIb)beta3 signaling. Journal of thrombosis and haemostasis : JTH 4:648–55. doi: 10.1111/j.1538-7836.2006.01806.x

Springer TA (1990a) Leucocyte adhesion to cells. Scandinavian journal of immunology 32:211–6.

Springer TA (1990b) Adhesion receptors of the immune system. Nature 346:425–34. doi: 10.1038/346425a0

Springer TA, Dustin ML, Kishimoto TK, Marlin SD (1987) The lymphocyte function-associated LFA-1, CD2, and LFA-3 molecules: cell adhesion receptors of the immune system. Annual review of immunology 5:223–52. doi: 10.1146/annurev.iy.05.040187.001255

Stanley P, Smith A, McDowall A, et al. (2008) Intermediate-affinity LFA-1 binds alpha-actinin-1 to control migration at the leading edge of the T cell. The EMBO journal 27:62–75. doi: 10.1038/sj.emboj.7601959

Staunton DE, Dustin ML, Erickson HP, Springer TA (1990) The arrangement of the immunoglobulin-like domains of ICAM-1 and the binding sites for LFA-1 and rhinovirus. Cell 61:243–54.

Stefansson A, Armulik A, Nilsson I, et al. (2004) Determination of N- and C-terminal borders of the transmembrane domain of integrin subunits. The Journal of biological chemistry 279:21200–5. doi: 10.1074/jbc.M400771200

Steindler C, Li Z, Algarté M, et al. (2004) Jamip1 (marlin-1) defines a family of proteins interacting with janus kinases and microtubules. The Journal of biological chemistry 279:43168–77. doi: 10.1074/jbc.M401915200

Stewart M, Hogg N (1996) Regulation of leukocyte integrin function: affinity vs. avidity. Journal of cellular biochemistry 61:554–61. doi: 10.1002/(SICI)1097-4644(19960616)61:4<554::AID-JCB8>3.0.CO;2-N

Stewart MP, Cabanas C, Hogg N (1996) T Cell Adhesion to ICAM-1 is Controlled by Cell Spreading and the Activation of Integrin LFA-1. The Journal of Immunology 1810–1817.

Stewart MP, McDowall A, Hogg N (1998) LFA-1-mediated adhesion is regulated by cytoskeletal restraint and by a Ca2+-dependent protease, calpain. The Journal of cell biology 140:699–707.

Stirnimann CU, Petsalaki E, Russell RB, Müller CW (2010) WD40 proteins propel cellular networks. Trends in biochemical sciences 35:565–74. doi: 10.1016/j.tibs.2010.04.003

Suzuki A, Ohno S (2006) The PAR-aPKC system: lessons in polarity. Journal of cell science 119:979–87. doi: 10.1242/jcs.02898

Syamaladevi DP, Spudich JA, Sowdhamini R (2012) Structural and functional insights on the Myosin superfamily. Bioinformatics and biology insights 6:11–21. doi: 10.4137/BBI.S8451

Sánchez-Madrid F, del Pozo MA (1999) Leukocyte polarization in cell migration and immune interactions. The EMBO journal 18:501–11. doi: 10.1093/emboj/18.3.501

Sánchez-Madrid F, Serrador JM (2009) Bringing up the rear: defining the roles of the uropod. Nature reviews Molecular cell biology 10:353–9. doi: 10.1038/nrm2680

Tak PP, Firestein GS (2001) NF-kappaB: a key role in inflammatory diseases. The Journal of clinical investigation 107:7–11. doi: 10.1172/JCI11830

Takagi J, Springer TA (2002) Integrin activation and structural rearrangement. Immunological reviews 186:141–63.

Takagi J, Strokovich K, Springer TA, Walz T (2003) Structure of integrin alpha5beta1 in complex with fibronectin. The EMBO journal 22:4607–15. doi: 10.1093/emboj/cdg445

Takai Y, Sasaki T, Matozaki T (2001) Small GTP-binding proteins. Physiological reviews 81:153–208.

Takashima S (2009) Phosphorylation of myosin regulatory light chain by myosin light chain kinase, and muscle contraction. Circulation journal : official journal of the Japanese Circulation Society 73:208–13.

Takesono A, Heasman SJ, Wojciak-Stothard B, et al. (2010) Microtubules regulate migratory polarity through Rho/ROCK signaling in T cells. PloS one 5:e8774. doi: 10.1371/journal.pone.0008774

Tan S-L, Parker PJ (2003) Emerging and diverse roles of protein kinase C in immune cell signalling. The Biochemical journal 376:545–52. doi: 10.1042/BJ20031406

Tanaka T, Grusby MJ, Kaisho T (2007) PDLIM2-mediated termination of transcription factor NF-kappaB activation by intranuclear sequestration and degradation of the p65 subunit. Nature immunology 8:584–91. doi: 10.1038/ni1464

Tanford C, Reynolds JA (1976) Characterization of membrane proteins in detergent solutions. Biochimica et biophysica acta 457:133–70.

Thelen M, Stein JV (2008) How chemokines invite leukocytes to dance. Nature immunology 9:953–9. doi: 10.1038/ni.f.207

Thomas PD, Kejariwal A, Campbell MJ, et al. (2003) PANTHER: a browsable database of gene products organized by biological function, using curated protein family and subfamily classification. Nucleic acids research 31:334–41.

Thornton C, Tang K-C, Phamluong K, et al. (2004) Spatial and temporal regulation of RACK1 function and N-methyl-D-aspartate receptor activity through WD40 motif-mediated dimerization. The Journal of biological chemistry 279:31357–64. doi: 10.1074/jbc.M402316200

Thrasher AJ (2002) WASp in immune-system organization and function. Nature reviews Immunology 2:635–46. doi: 10.1038/nri884

Tilton B, Ho L, Oberlin E, et al. (2000) Signal transduction by CXC chemokine receptor 4. Stromal cell-derived factor 1 stimulates prolonged protein kinase B and extracellular signal-regulated kinase 2 activation in T lymphocytes. The Journal of experimental medicine 192:313–24.

De Toni-Costes F, Despeaux M, Bertrand J, et al. (2010) A New alpha5beta1 integrin-dependent survival pathway through GSK3beta activation in leukemic cells. PloS one 5:e9807. doi: 10.1371/journal.pone.0009807

Torrado M (2004) Pdlim2, a Novel PDZ-LIM Domain Protein, Interacts with -Actinins and Filamin A. Investigative Ophthalmology & Visual Science 45:3955–3963. doi: 10.1167/iovs.04-0721

Totsukawa G, Wu Y, Sasaki Y, et al. (2004) Distinct roles of MLCK and ROCK in the regulation of membrane protrusions and focal adhesion dynamics during cell migration of fibroblasts. The Journal of cell biology 164:427–39. doi: 10.1083/jcb.200306172

Trucy M, Barbat C, Fischer A, Mazerolles F (2006) CD4 ligation induces activation of protein kinase C zeta and phosphoinositide-dependent-protein kinase-1, two kinases required for down-regulation of LFA-1-mediated adhesion. Cellular immunology 244:33–42. doi: 10.1016/j.cellimm.2007.02.002

Tybulewicz VLJ, Henderson RB (2009) Rho family GTPases and their regulators in lymphocytes. Nature reviews Immunology 9:630–44. doi: 10.1038/nri2606

Tzivion G, Gupta VS, Kaplun L, Balan V (2006) 14-3-3 proteins as potential oncogenes. Seminars in cancer biology 16:203–13. doi: 10.1016/j.semcancer.2006.03.004

Tzivion G, Luo ZJ, Avruch J (2000) Calyculin A-induced vimentin phosphorylation sequesters 14-3-3 and displaces other 14-3-3 partners in vivo. The Journal of biological chemistry 275:29772–8. doi: 10.1074/jbc.M001207200

Uehara R, Goshima G, Mabuchi I, et al. (2010) Determinants of myosin II cortical localization during cytokinesis. Current biology : CB 20:1080–5. doi: 10.1016/j.cub.2010.04.058

Ullah H, Scappini EL, Moon AF, et al. (2008) Structure of a signal transduction regulator, RACK1, from Arabidopsis thaliana. Protein science : a publication of the Protein Society 17:1771–80. doi: 10.1110/ps.035121.108

Umemoto S, Bengur AR, Sellers JR (1989) Effect of multiple phosphorylations of smooth muscle and cytoplasmic myosins on movement in an in vitro motility assay. The Journal of biological chemistry 264:1431–6.

Vancha AR, Govindaraju S, Parsa KVL, et al. (2004) Use of polyethyleneimine polymer in cell culture as attachment factor and lipofection enhancer. BMC biotechnology 4:23. doi: 10.1186/1472-6750-4-23

Vasiliev JM, Gelfand IM, Domnina LV, et al. (1970) Effect of colcemid on the locomotory behaviour of fibroblasts. Journal of embryology and experimental morphology 24:625–40.

Verma NK, Dempsey E, Conroy J, et al. (2008) A new microtubule-targeting compound PBOX-15 inhibits T-cell migration via post-translational modifications of tubulin. Journal of molecular medicine (Berlin, Germany) 86:457–69. doi: 10.1007/s00109-008-0312-8

Verma NK, Dourlat J, Davies AM, et al. (2009) STAT3-stathmin interactions control microtubule dynamics in migrating T-cells. The Journal of biological chemistry 284:12349–62. doi: 10.1074/jbc.M807761200

Vicente-Manzanares M, Choi CK, Horwitz a. R (2009a) Integrins in cell migration - the actin connection. Journal of Cell Science 122:1473–1473. doi: 10.1242/jcs.052894

Vicente-Manzanares M, Horwitz AR (2010) Myosin light chain mono- and di-phosphorylation differentially regulate adhesion and polarity in migrating cells. Biochemical and biophysical research communications 402:537–42. doi: 10.1016/j.bbrc.2010.10.071

Vicente-Manzanares M, Ma X, Adelstein RS, Horwitz AR (2009b) Non-muscle myosin II takes centre stage in cell adhesion and migration. Nature reviews Molecular cell biology 10:778–90. doi: 10.1038/nrm2786

Vicente-Manzanares M, Newell-Litwa K, Bachir AI, et al. (2011) Myosin IIA/IIB restrict adhesive and protrusive signaling to generate front-back polarity in migrating cells. The Journal of cell biology 193:381–96. doi: 10.1083/jcb.201012159

Vicente-Manzanares M, Sancho D, Yáñez-Mó M, Sánchez-Madrid F (2002) The leukocyte cytoskeleton in cell migration and immune interactions. International review of cytology 216:233–89.

Vicente-Manzanares M, Zareno J, Whitmore L, et al. (2007) Regulation of protrusion, adhesion dynamics, and polarity by myosins IIA and IIB in migrating cells. The Journal of cell biology 176:573–80. doi: 10.1083/jcb.200612043

Vicente-manzanares M, Cabrero JR, Rey M, et al. (2002) A Role for the Rho-p160 Rho Coiled-Coil Kinase Axis in the Chemokine Stromal Cell-Derived Factor-1-Induced Lymphocyte Actomyosin and Microtubular Organization and Chemotaxis.

Vila-Coro AJ, Rodríguez-Frade JM, Martín De Ana A, et al. (1999) The chemokine SDF-1alpha triggers CXCR4 receptor dimerization and activates the JAK/STAT pathway. The FASEB journal : official publication of the Federation of American Societies for Experimental Biology 13:1699–710.

Volkov Y, Long A, Kelleher D (1998) Inside the crawling T cell: leukocyte function-associated antigen-1 cross-linking is associated with microtubule-directed translocation of protein kinase C isoenzymes beta(I) and delta. Journal of immunology (Baltimore, Md : 1950) 161:6487–95.

Volkov Y, Long A, McGrath S, et al. (2001) Crucial importance of PKC-beta(I) in LFA-1-mediated locomotion of activated T cells. Nature immunology 2:508–14. doi: 10.1038/88700

Vomastek T, Iwanicki MP, Schaeffer H-J, et al. (2007) RACK1 targets the extracellular signal-regulated kinase/mitogen-activated protein kinase pathway to link integrin engagement with focal adhesion disassembly and cell motility. Molecular and cellular biology 27:8296–305. doi: 10.1128/MCB.00598-07

Vroon A, Heijnen CJ, Kavelaars A (2006) GRKs and arrestins: regulators of migration and inflammation. Journal of leukocyte biology 80:1214–21. doi: 10.1189/jlb.0606373

Wall MA, Coleman DE, Lee E, et al. (1995) The structure of the G protein heterotrimer Gi alpha 1 beta 1 gamma 2. Cell 83:1047–58.

Wang F, Herzmark P, Weiner OD, et al. (2002) Lipid products of PI(3)Ks maintain persistent cell polarity and directed motility in neutrophils. Nature cell biology 4:513–8. doi: 10.1038/ncb810

Wang F, Yamauchi M, Muramatsu M, et al. (2011) RACK1 regulates VEGF/Flt1-mediated cell migration via activation of a PI3K/Akt pathway. The Journal of biological chemistry 286:9097–106. doi: 10.1074/jbc.M110.165605

Wang N, Stamenovic D (2002) Mechanics of vimentin intermediate filaments. Journal of muscle research and cell motility 23:535–40.

Wang S, Chen J-Z, Zhang Z, et al. (2003) Cloning, expression and genomic structure of a novel human GNB2L1 gene, which encodes a receptor of activated protein kinase C (RACK). Molecular biology reports 30:53–60.

Wang Z, Jiang L, Huang C, et al. (2008) Comparative proteomics approach to screening of potential diagnostic and therapeutic targets for oral squamous cell carcinoma. Molecular & cellular proteomics : MCP 7:1639–50. doi: 10.1074/mcp.M700520-MCP200

Ward SG, Westwick J (1998) Chemokines: understanding their role in T-lymphocyte biology. The Biochemical journal 333 (Pt 3:457–70.

Watanabe T, Noritake J, Kaibuchi K (2005) Regulation of microtubules in cell migration. Trends in cell biology 15:76–83. doi: 10.1016/j.tcb.2004.12.006

Weiner OD, Neilsen PO, Prestwich GD, et al. (2002) A PtdInsP(3)- and Rho GTPase-mediated positive feedback loop regulates neutrophil polarity. Nature cell biology 4:509–13. doi: 10.1038/ncb811

Westermann J, Ehlers EM, Exton MS, et al. (2001) Migration of naive, effector and memory T cells: implications for the regulation of immune responses. Immunological reviews 184:20–37.

Westermann S, Weber K (2003) Post-translational modifications regulate microtubule function. Nature reviews Molecular cell biology 4:938–47. doi: 10.1038/nrm1260

Wieland T, Faulstich H (1978) Amatoxins, phallotoxins, phallolysin, and antamanide: the biologically active components of poisonous Amanita mushrooms. CRC critical reviews in biochemistry 5:185–260.

Wilkinson S, Paterson HF, Marshall CJ (2005) Cdc42-MRCK and Rho-ROCK signalling cooperate in myosin phosphorylation and cell invasion. Nature cell biology 7:255–61. doi: 10.1038/ncb1230

Williams RJ (2003) Restriction endonucleases: classification, properties, and applications. Molecular biotechnology 23:225–43.

Wilson CM (1983) Staining of proteins on gels: comparisons of dyes and procedures. Methods in enzymology 91:236–47.

Woodland DL, Kohlmeier JE (2009) Migration, maintenance and recall of memory T cells in peripheral tissues. Nature reviews Immunology 9:153–61. doi: 10.1038/nri2496

Woodside DG, Liu S, Ginsberg MH (2001) Integrin activation. Thrombosis and haemostasis 86:316–23.

Xiao J, Chen L-W, Chen J-X, et al. (2011) Construction of a recombinant eukaryotic expression plasmid containing human PDLIM2 gene and its biological activity. Plasmid 66:106–11. doi: 10.1016/j.plasmid.2011.06.005

Xiao T, Takagi J, Coller BS, et al. (2004) Structural basis for allostery in integrins and binding to fibrinogen-mimetic therapeutics. Nature 432:59–67. doi: 10.1038/nature02976

Xu C, Min J (2011) Structure and function of WD40 domain proteins. Protein & cell 2:202–14. doi: 10.1007/s13238-011-1018-1

Xu J, Wang F, Van Keymeulen A, et al. (2003) Divergent signals and cytoskeletal assemblies regulate self-organizing polarity in neutrophils. Cell 114:201–14.

Xu J, Wang F, Van Keymeulen A, et al. (2005) Neutrophil microtubules suppress polarity and enhance directional migration. Proceedings of the National Academy of Sciences of the United States of America 102:6884–9. doi: 10.1073/pnas.0502106102

Yaka R, Thornton C, Vagts AJ, et al. (2002) NMDA receptor function is regulated by the inhibitory scaffolding protein, RACK1. Proceedings of the National Academy of Sciences of the United States of America 99:5710–5. doi: 10.1073/pnas.062046299

Yam PT, Wilson CA, Ji L, et al. (2007) Actin-myosin network reorganization breaks symmetry at the cell rear to spontaneously initiate polarized cell motility. The Journal of cell biology 178:1207–21. doi: 10.1083/jcb.200706012

Yang H (2012) Structure, Expression, and Function of ICAM-5. Comparative and functional genomics 2012:368938. doi: 10.1155/2012/368938

Yarwood SJ, Steele MR, Scotland G, et al. (1999) The RACK1 signaling scaffold protein selectively interacts with the cAMP-specific phosphodiesterase PDE4D5 isoform. The Journal of biological chemistry 274:14909–17.

Yavin E, Yavin Z (1974) Attachment and culture of dissociated cells from rat embryo cerebral hemispheres on polylysine-coated surface. The Journal of cell biology 62:540–6.

Yedovitzky M, Mochly-Rosen D, Johnson JA, et al. (1997) Translocation inhibitors define specificity of protein kinase C isoenzymes in pancreatic beta-cells. The Journal of biological chemistry 272:1417–20.

Yin J, Ma Z, Selliah N, et al. (2006) Effective gene suppression using small interfering RNA in hard-to-transfect human T cells. Journal of immunological methods 312:1–11. doi: 10.1016/j.jim.2006.01.023

Yu Y, Ji H, Doudna JA, Leary JA (2005) Mass spectrometric analysis of the human 40S ribosomal subunit: native and HCV IRES-bound complexes. Protein science : a publication of the Protein Society 14:1438–46. doi: 10.1110/ps.041293005

Zecchinon L, Fett T, Vandenbergh P, Desmecht D (2006) Key roles of LFA-1 in leukocyte migration and immune response. Clinical and Applied Immunology Reviews 6:191–200. doi: 10.1016/j.cair.2006.09.003

Zehn D, Bevan MJ (2006) T cells with low avidity for a tissue-restricted antigen routinely evade central and peripheral tolerance and cause autoimmunity. Immunity 25:261–70. doi: 10.1016/j.immuni.2006.06.009

Zhang J, Shehabeldin A, da Cruz LA, et al. (1999) Antigen receptor-induced activation and cytoskeletal rearrangement are impaired in Wiskott-Aldrich syndrome protein-deficient lymphocytes. The Journal of experimental medicine 190:1329–42.

Zhao X, Guan J-L (2011) Focal adhesion kinase and its signaling pathways in cell migration and angiogenesis. Advanced drug delivery reviews 63:610–5. doi: 10.1016/j.addr.2010.11.001

Zhao Z, Manser E (2005) PAK and other Rho-associated kinases--effectors with surprisingly diverse mechanisms of regulation. The Biochemical journal 386:201–14. doi: 10.1042/BJ20041638

Zhou Q, Kee Y-S, Poirier CC, et al. (2010) 14-3-3 coordinates microtubules, Rac, and myosin II to control cell mechanics and cytokinesis. Current biology : CB 20:1881–9. doi: 10.1016/j.cub.2010.09.048

Zimmerman T, Blanco FJ (2008) Inhibitors targeting the LFA-1/ICAM-1 cell-adhesion interaction: design and mechanism of action. Current pharmaceutical design 14:2128–39.

(2008) Nastech Pharmaceutical Company, Inc.

APPENDIX

Appendix 1

Chapter 5 Supplementary Data

Appendix 1 Table 1: RACK1 IP Mass Spectrometry Results

Protein Name	RACK1 IP	Control IP	Mascot Score Data	No. of Matched Peptides
beta actin [Homo sapiens]	X		7318	615
cardiac muscle alpha actin 1 proprotein [Homo sapiens]	X		4995	429
gamma-actin [Homo sapiens]	X		4792	283
actin prepeptide [Homo sapiens]	X		4444	383
protein expressed in prostate, ovary, testis, and placenta 2 [Homo sapiens]	X		3950	227
actin, alpha, cardiac muscle, isoform CRA_b [Homo sapiens]	X		3497	261
Beta-actin-like protein 3 [Homo sapiens]	X		3192	107
actin, beta-like 2 [Homo sapiens]	X		3182	339
myosin, heavy polypeptide 9, non-muscle [Homo sapiens]	X		2035	214
guanine nucleotide binding protein (G protein), beta polypeptide 2-like 1 [Homo sapiens]	X		1078	76
myosin, heavy polypeptide 9, non-muscle [Homo sapiens]	X		1016	58
ribosomal protein L18 [Homo sapiens]	X		804	39
guanine nucleotide binding protein (G protein), beta polypeptide 2-like 1 [Homo sapiens]	X		773	55

polyadenylate binding protein II [Homo sapiens]	X		684	62
ribosomal protein S16 [Homo sapiens]	X		653	50
ribosomal protein S5 [Homo sapiens]	X		618	28
myosin, heavy polypeptide 14, isoform CRA_a [Homo sapiens]	X		573	62
myosin, heavy polypeptide 10, non-muscle [Homo sapiens]	X		559	58
ribosomal protein L18 [Homo sapiens]	X		530	21
ribosomal protein L23 [Homo sapiens]	X		528	23
heat shock 70kDa protein 8 isoform 1 [Homo sapiens]	X		501	30
myosin, light chain 12A, regulatory, non-sarcomeric [Homo sapiens]	X		484	27
guanine nucleotide binding protein (G protein), beta polypeptide 2-like 1 [Homo sapiens]	X		465	31
smooth muscle myosin heavy chain 11 isoform SM2B [Homo sapiens]	X		451	45
Ras-GTPase-activating protein SH3-domain-binding protein [Homo sapiens]	X		444	52
ribosomal protein S5 [Homo sapiens]	X		444	21
tubulin, beta, 2 [Homo sapiens]	X		426	22
testis-specific poly(A)-binding protein [Homo sapiens]	X		416	34
myosin, light chain 6, alkali, smooth muscle and non-muscle isoform 1 [Homo sapiens]	X		414	23
ribosomal protein L30 [Homo sapiens]	X		397	18
ribosomal protein S4, X-linked X isoform [Homo sapiens]	X		396	54
growth regulated nuclear 68 protein [Homo sapiens]	X		390	26
ribosomal protein S14 [Homo sapiens]	X		390	15

myosin, heavy polypeptide 9, non-muscle [Homo sapiens]	X		389	38
hCG2028724 [Homo sapiens]	X		388	41
ribosomal protein L7a [Homo sapiens]	X		388	37
heat shock 70kDa protein 8 isoform 1 [Homo sapiens]	X		386	21
keratin 1 [Homo sapiens]	X	X	385	21
ribosomal protein L4 [Homo sapiens]	X		381	37
beta-tubulin [Homo sapiens]	X		378	20
keratin 1 [Homo sapiens]	X	X	376	21
elongation factor Tu [Homo sapiens]	X		376	22
mutant beta-actin (beta'-actin) [Homo sapiens]	X		375	21
guanine nucleotide binding protein (G protein), beta polypeptide 2-like 1 [Homo sapiens]	X		366	23
lactate dehydrogenase A isoform 1 [Homo sapiens]	X		344	42
ribosomal protein L12 [Homo sapiens]	X		335	19
ribosomal protein L10, isoform CRA_e [Homo sapiens]	X		313	23
Q1Z 7F5 [Homo sapiens]	X		313	33
ribosomal protein S25 [Homo sapiens]	X		308	15
ribosomal protein S3a [Homo sapiens]	X		305	49
DDX17 [Homo sapiens]	X		296	16
nonmuscle myosin heavy chain (NMHC) [Homo sapiens]	X		293	21
Ras-GTPase-activating protein SH3-domain-binding protein [Homo sapiens]	X		292	35

ribosomal protein L7, isoform CRA_a [Homo sapiens]	X		286	34
ATP-dependent DNA helicase II, 70 kDa subunit [Homo sapiens]	X	X	279	32
growth regulated nuclear 68 protein [Homo sapiens]	X		273	25
similar to 60S ribosomal protein L7; similar to P18124 (PID:d133021) [Homo sapiens]	X		273	23
peroxiredoxin 1 [Homo sapiens]	X		272	38
myosin, light chain 12A, regulatory, non-sarcomeric [Homo sapiens]	X		270	12
Ig kappa chain [Homo sapiens]	X	X	268	7
poly A binding protein, cytoplasmic 4 isoform 2 [Homo sapiens]	X	X	267	28
heterogeneous nuclear ribonucleoprotein H1 [Homo sapiens]	X		258	14
heterogeneous nuclear ribonucleoprotein M isoform a [Homo sapiens]	X		255	28
M4 protein [Homo sapiens]	X		255	29
keratin 1 [Homo sapiens]	X	X	250	16
MYH14 protein [Homo sapiens]	X		247	11
tropomodulin 3 (ubiquitous) [Homo sapiens]	X		241	22
Ig kappa chain [Homo sapiens]	X		240	43
Q1Z 7F5 [Homo sapiens]	X		237	17
S3 ribosomal protein [Homo sapiens]	X		237	50
ribosomal protein S23 [Homo sapiens]	X		236	11
RNA binding motif protein 14 [Homo sapiens]	X		233	12
ribosomal protein S11 [Homo sapiens]	X		233	25

ribosomal protein S24 isoform c [Homo sapiens]	X		230	16
ribosomal protein L22 proprotein [Homo sapiens]	X		219	9
ribosomal protein S11 [Homo sapiens]	X		216	24
cytokeratin 9 [Homo sapiens]	X	X	216	11
keratin 1 [Homo sapiens]	X	X	214	13
ribosomal protein L18a [Homo sapiens]	X		214	9
ribosomal protein S13 [Homo sapiens]	X		209	28
cytokeratin 9 [Homo sapiens]	X	X	207	6
actin, beta-like 2 [Homo sapiens]	X		203	10
cytokeratin 9 [Homo sapiens]	X	X	200	32
M4 protein [Homo sapiens]	X		193	14
ribosomal protein S9 [Homo sapiens]	X		192	32
ribosomal protein S9 [Homo sapiens]	X		192	32
homology to rat ribosomal protein L23 [Homo sapiens]	X		191	7
ribosomal protein L24, isoform CRA_d [Homo sapiens]	X		191	13
RNA binding motif protein 14, isoform CRA_b [Homo sapiens]	X		189	10
ribosomal protein L13a [Homo sapiens]	X		186	29
heat shock-induced protein [Homo sapiens]	X		184	8
ribosomal protein L18a [Homo sapiens]	X		175	15
DDX17 [Homo sapiens]	X	X	174	17

F-actin capping protein beta subunit [Homo sapiens]	X		171	10
hCG2040224 [Homo sapiens]	X		171	17
homology to rat ribosomal protein L23 [Homo sapiens]	X		169	15
hCG40355, isoform CRA_a [Homo sapiens]	X		168	29
hCG21078 [Homo sapiens]	X		168	11
ribosomal protein L27a [Homo sapiens]	X		168	8
LDHAL6A protein [Homo sapiens]	X		161	4
actin-like protein [Homo sapiens]	X		158	137
ribosomal protein L8, isoform CRA_e [Homo sapiens]	X		158	14
ribosomal protein L8 [Homo sapiens]	X		158	16
ribosomal protein S2 [Homo sapiens]	X		158	16
ribosomal protein L3 [Homo sapiens]	X		157	19
ACTB protein [Homo sapiens]	X		157	16
hCG2016250, isoform CRA_a [Homo sapiens]	X		157	16
ribosomal protein L19 [Homo sapiens]	X		154	11
L21 ribosomal protein [Homo sapiens]	X		153	21
ribosomal protein L21 variant [Homo sapiens]	X		153	19
immunoglobulin kappa light chain variable region [Homo sapiens]	X	X	151	7
NF45 protein [Homo sapiens]	X		151	9
ARP3 actin-related protein 3 homolog [Homo sapiens]	X		147	25

testin isoform 1 [Homo sapiens]	X		144	12
enoyl-CoA hydratase/3-hydroxyacyl-CoA dehydrogenase alpha-subunit of trifunctional protein [Homo sapiens]	X		142	10
ribosomal protein S6 [Homo sapiens]	X		141	15
keratin 9 (epidermolytic palmoplantar keratoderma) [Homo sapiens]	X	X	140	7
PRO2044 [Homo sapiens]	X		139	3
albumin, isoform CRA_t [Homo sapiens]	X	X	139	8
ribosomal protein P2 [Homo sapiens]	X		136	6
hCG2025340, isoform CRA_a [Homo sapiens]	X		134	10
heat shock protein [Homo sapiens]	X		134	8
ribosomal protein [Homo sapiens]	X		134	27
ribosomal protein L12 [Homo sapiens]	X		131	9
ribosomal protein S10 [Homo sapiens]	X		129	13
60S ribosomal protein L36 [Homo sapiens]	X		128	8
ribosomal protein L13a [Homo sapiens]	X		127	23
ribosomal protein L14 [Homo sapiens]	X		125	6
RPL14 protein [Homo sapiens]	X		125	6
Unknown (protein for IMAGE:5426295) [Homo sapiens]	X		125	5
MYH14 protein [Homo sapiens]	X		124	10
Myosin heavy chain 14 [Homo sapiens]	X		124	11

prohibitin 2 isoform 2 [Homo sapiens]	X	X	123	13
hCG2040224 [Homo sapiens]	X		123	10
ribosomal protein L17 [Homo sapiens]	X		120	14
ribosomal protein S9 [Homo sapiens]	X		115	36
ribosomal protein S9 [Homo sapiens]	X		115	36
laminin-binding protein [Homo sapiens]	X		114	6
heterogeneous nuclear ribonucleoprotein K [Homo sapiens]	X		113	8
ribosomal protein L26 [Homo sapiens]	X		113	20
keratin 1 [Homo sapiens]	X	X	110	7
ribosomal protein S17 [Homo sapiens]	X		109	11
POTE-2 alpha-actin [Homo sapiens]	X		109	5
ribosomal protein S15a [Homo sapiens]	X		108	12
HNRPF protein [Homo sapiens]	X		107	8
DNA-binding protein B [Homo sapiens]	X		107	7
Myosin heavy chain (MHY11) (5'partial) [Homo sapiens]	X		106	10
histone H2B [Homo sapiens]	X		106	13
immunoglobulin kappa light chain variable region [Homo sapiens]	X	X	105	9
L21 ribosomal protein [Homo sapiens]	X		103	11
ribosomal protein L21 variant [Homo sapiens]	X		103	10
poly(A) binding protein, cytoplasmic 1-like 2A [Homo sapiens]	X	X	102	9

small GTP binding protein Rab7 [Homo sapiens]	X		100	11
poly(A) binding protein, cytoplasmic 1, isoform CRA_c [Homo sapiens]	X	X	99	7
ribosomal protein [Homo sapiens]	X		98	13
immunoglobulin light chain variable region [Homo sapiens]	X	X	98	5
ribosomal protein S9, isoform CRA_c [Homo sapiens]	X		97	22
Ig lambda,anti-Rh© [Homo sapiens]	X	X	96	9
ATP-dependent DNA helicase II [Homo sapiens]	X		96	5
ATPase family, AAA domain containing 3A [Homo sapiens]	X		95	16
ribosomal protein S19 [Homo sapiens]	X		93	23
RAB8B, member RAS oncogene family [Homo sapiens]	X		93	6
tyrosine 3/tryptophan 5 -monooxygenase activation protein, theta polypeptide 14-3-3θ [Homo sapiens]	X		92	12
ras-related C3 botulinum toxin substrate 2 precursor p21-rac3 [Homo sapiens]	X		92	8
cytokeratin 9 [Homo sapiens]	X	X	91	6
gelsolin isoform a precursor [Homo sapiens]	X		91	4
vimentin [Homo sapiens]	X		91	5
serum albumin [Homo sapiens]	X	X	90	6
ribosomal protein L9, isoform CRA_a [Homo sapiens]	X		90	6
RPL26 [Homo sapiens]	X		89	11
ribosomal protein L21 [Homo sapiens]	X		89	18

ribosomal protein L9 [Homo sapiens]	X		89	12
ribosomal protein L31 [Homo sapiens]	X		88	11
ribosomal protein S20 isoform 2 [Homo sapiens]	X		88	9
ribosomal protein L27 [Homo sapiens]	X		88	12
immunoglobulin kappa light chain [Homo sapiens]	X	X	87	7
epidermal cytokeratin 2 [Homo sapiens]	X	X	86	4
keratin 1b [Homo sapiens]	X	X	86	3
ribosomal protein L29 [Homo sapiens]	X		86	3
ribosomal protein L21, isoform CRA_e [Homo sapiens]	X		86	16
Zinc finger CCHC domain-containing protein 3 ZCCHC3 [Homo sapiens]	X		84	19
NY-REN-2 antigen [Homo sapiens]	X		84	8
ribosomal protein L27a [Homo sapiens]	X		84	2
NY-REN-2 antigen [Homo sapiens]	X		83	6
ribosomal protein L19 [Homo sapiens]	X		83	6
nucleolin [Homo sapiens]	X		83	6
cytokeratin 9 [Homo sapiens]	X	X	83	2
tyrosine 3/tryptophan 5 -monooxygenase activation protein, zeta polypeptide [Homo sapiens]	X		83	12
prohibitin [Homo sapiens]	X		83	4
heat shock-induced protein [Homo sapiens]	X		81	4
proteasome subunit p58 [Homo sapiens]	X		81	9

mitochondrial ATP synthase, O subunit precursor ATPM O [Homo sapiens]	X		81	4
ribosomal protein S10 [Homo sapiens]	X		81	10
Putative Ras-related protein Rab-1C [Homo sapiens]	X		80	5
RAB35, member RAS oncogene family isoform 1 [Homo sapiens]	X		80	5
Ras-related protein Rab-15 [Homo sapiens]	X		80	5
ribosomal protein L35 [Homo sapiens]	X		79	6
Gry-rbp [Homo sapiens]	X		79	10
heterogeneous nuclear ribonucleoprotein R isoform 2 [Homo sapiens]	X		78	6
mitochondrial ATP synthase, O subunit precursor [Homo sapiens]	X		78	4
epidermal cytokeratin 2 [Homo sapiens]	X	X	77	11
actin, beta-like 2 [Homo sapiens]	X		76	9
progesterone receptor membrane component 1 PGRMC1 [Homo sapiens]	X		76	1
peptidylprolyl isomerase B precursor [Homo sapiens]	X		76	6
actin related protein 2/3 complex subunit 3 [Homo sapiens]	X		76	8
Ras-GAP SH3 binding protein [Homo sapiens]	X		74	3
S3 ribosomal protein [Homo sapiens]	X		74	4
keratin 6B, isoform CRA_a [Homo sapiens]	X	X	74	6
capping protein (actin filament) muscle Z-line, beta [Homo sapiens]	X		74	3
S3 ribosomal protein [Homo sapiens]	X		73	5
F-actin capping protein beta subunit [Homo sapiens]	X		73	6

splicing factor proline/glutamine rich (polypyrimidine tract binding protein associated) [Homo sapiens]	X		72	3
GPI-anchored protein p137 [Homo sapiens]	X		72	2
poly(A) binding protein, cytoplasmic 1, isoform CRA_c [Homo sapiens]	X	X	72	12
hCG1639802 [Homo sapiens]	X		72	4
immunoglobulin light chain variable region [Homo sapiens]	X	X	72	2
FLJ00293 protein [Homo sapiens]	X		72	4
zinc finger protein 9 isoform 3 [Homo sapiens]	X		72	2
ribosomal protein L32 [Homo sapiens]	X		71	6
ELAV-like 1 [Homo sapiens]	X		70	11
alpha-tubulin [Homo sapiens]	X		70	4
PREDICTED: similar to protein expressed in prostate, ovary, testis, and placenta 2 isoform 2 [Homo sapiens]	X		70	10
serum albumin [Homo sapiens]	X	X	68	7
c-myc binding protein [Homo sapiens]	X		68	3
KH domain containing, RNA binding, signal transduction associated 1 [Homo sapiens]	X		67	10
unknown [Homo sapiens]	X		67	2
S3 ribosomal protein [Homo sapiens]	X		66	8
putative [Homo sapiens]	X		65	18
immunoglobulin lambda chain variable region [Homo sapiens]	X	X	65	4
Chain A, Crystal Structure Of Human Dead-Box Rna Helicase Ddx3x [Homo sapiens]	X	X	64	5

neuropolypeptide h3 RAF kinase inhibitor protein (RKIP) [Homo sapiens]	X		64	4
Phosphoglycerate mutase family member 5 (PGAM5) [Homo sapiens]	X		62	2
gamma subunit of CCT chaperonin [Homo sapiens]	X	X	62	9
keratin 6B, isoform CRA_a [Homo sapiens]	X	X	62	4
ribosomal protein L28 [Homo sapiens]	X		61	11
transformation upregulated nuclear protein [Homo sapiens]	X	X	60	7
heterogeneous nuclear ribonucleoprotein [Homo sapiens]	X		60	2
BBC1 [Homo sapiens]	X		60	6
putative [Homo sapiens]	X		60	27
ribosomal protein L13 [Homo sapiens]	X		60	13
ribosomal protein L36a-like protein [Homo sapiens]	X		58	8
ACTR2 protein [Homo sapiens]	X		58	11
TPM1 protein [Homo sapiens]	X		58	2
Chain C, Structure Of The Karyopherin Beta2-Ran Gppnhp Nuclear Transport Complex [Homo sapiens]	X		58	6
epidermal cytokeratin 2 [Homo sapiens]	X	X	57	3
TLS protein [Homo sapiens]	X		57	2
keratin 1 [Homo sapiens]	X	X	57	5
RAB13, member RAS oncogene family [Homo sapiens]	X		57	4
transcription factor A, mitochondrial precursor [Homo sapiens]	X		57	4

immunoglobulin kappa chain variable region [Homo sapiens]	X	X	56	11
tubulin, beta 4, isoform CRA_b [Homo sapiens]	X		55	4
hCG1781941 [Homo sapiens]	X		55	2
eukaryotic translation initiation factor 4A, isoform 2, isoform CRA_d [Homo sapiens]	X		54	2
myosin, heavy polypeptide 10, non-muscle [Homo sapiens]	X		54	10
ribosomal protein L29 [Homo sapiens]	X		53	3
HSPC173 (FARSB) [Homo sapiens]	X		52	6
immunoglobulin lambda light chain variable region [Homo sapiens]	X	X	52	7
immunoglobulin lambda light chain variable region [Homo sapiens]	X	X	52	7
Ig lambda chain V region (Zim) [Homo sapiens]	X	X	52	9
immunoglobulin lambda chain variable region [Homo sapiens]	X	X	52	6
immunoglobulin light chain lambda 6 [Homo sapiens]	X	X	52	6
immunoglobulin lambda chain variable region [Homo sapiens]	X	X	52	7
immunoglobulin light chain variable region [Homo sapiens]	X	X	52	6
immunoglobulin light chain variable region [Homo sapiens]	X	X	52	6
GTP-binding protein [Homo sapiens]	X		52	3
RAB43 protein [Homo sapiens]	X		52	3
rab-related GTP-binding protein [Homo sapiens]	X		52	2
RAB33B, member RAS oncogene family [Homo sapiens]	X		52	14
Zinc finger CCHC domain-containing protein 3 [Homo sapiens]	X		51	10

Ig light chain [Homo sapiens]	X	X	51	4
immunoglobulin lambda-3 surrogate light chain [Homo sapiens]	X	X	51	4
lambda 1 immunoglobulin light chain variable region [Homo sapiens]	X	X	51	4
immunoglobulin lambda light chain variable region [Homo sapiens]	X	X	51	4
immunoglobulin lambda light chain [Homo sapiens]	X	X	51	4
transgelin 2 [Homo sapiens]	X		51	12
macropain subunit delta [Homo sapiens]	X	X	51	2
ATP-dependent DNA helicase II, 70 kDa subunit [Homo sapiens]	X	X	50	6
WDR1 protein [Homo sapiens]	X		50	3
ribosomal protein L34 [Homo sapiens]	X		50	6
hCG1640974, isoform CRA_b [Homo sapiens]	X		50	5
adenylate kinase 2 isoform a (AK2) [Homo sapiens]	X		50	2
putative RNA binding protein KOC [Homo sapiens]	X		49	2
IGF-II mRNA-binding protein 2 [Homo sapiens]	X		49	2
histone cluster 3, H3 [Homo sapiens]	X		49	6
eukaryotic translation initiation factor 2, subunit 3 gamma, 52kDa [Homo sapiens]	X		49	4
eFI-2-gamma [Homo sapiens]	X		49	4
epidermal cytokeratin 2 [Homo sapiens]	X	X	49	4
immunoglobulin lambda-3 surrogate light chain [Homo sapiens]	X		49	7
protein NIG64 lambda,Bence-Jones [Homo sapiens]	X	X	49	6

immunoglobulin lambda chain variable region [Homo sapiens]	X	X	49	6
Zinc finger CCHC domain-containing protein 3 [Homo sapiens]	X		48	4
immunoglobulin lambda light chain variable region [Homo sapiens]	X	X	48	9
Ig lambda chain V region (Zim) [Homo sapiens]	X	X	48	12
immunoglobulin lambda light chain variable region [Homo sapiens]	X	X	48	9
immunoglobulin lambda chain variable region [Homo sapiens]	X	X	48	9
immunoglobulin lambda light chain variable region [Homo sapiens]	X	X	48	10
immunoglobulin light chain lambda 6 [Homo sapiens]	X	X	48	9
immunoglobulin lambda light chain variable region [Homo sapiens]	X	X	48	10
lambda 1 immunoglobulin light chain variable region [Homo sapiens]	X	X	48	9
immunoglobulin light chain variable region [Homo sapiens]	X	X	48	8
BM-010 (eIF-4a2) [Homo sapiens]	X		48	3
Cytokeratin-27 [Homo sapiens]	X	X	48	3
LSM12 homolog [Homo sapiens]	X		48	2
arginyl-tRNA synthetase (RARS2) [Homo sapiens]	X		47	10
ribosomal protein s6 [Homo sapiens]	X		47	3
small nuclear ribonucleoprotein polypeptide D3 (SNRPD3) [Homo sapiens]	X		47	4
eukaryotic initiation factor 4AII [Homo sapiens]	X		47	7
Chain J, 20s Proteasome [Homo sapiens]	X	X	47	2
Ig lambda chain V region (Zim) [Homo sapiens]	X	X	47	8

immunoglobulin lambda light chain variable region [Homo sapiens]	X	X	47	6
immunoglobulin lambda light chain variable region [Homo sapiens]	X	X	47	6
Ig lambda chain precursor [Homo sapiens]	X	X	47	5
immunoglobulin lambda light chain variable region [Homo sapiens]	X	X	47	5
immunoglobulin lambda chain variable region [Homo sapiens]	X	X	47	5
immunoglobulin light chain variable region [Homo sapiens]	X	X	47	5
TCR beta chain Vbeta 1S1A1N1-FADTQYF-Jbeta 2.3 [Homo sapiens]	X		46	2
ATP-dependent RNA helicase #46 [Homo sapiens]	X	X	46	4
Ras-GAP SH3 binding protein [Homo sapiens]	X		46	2
immunoglobulin kappa chain [Homo sapiens]	X	X	46	3
thyroglobulin autoantibody #26 light chain VJ region [Homo sapiens]	X		46	3
gamma subunit of CCT chaperonin [Homo sapiens]	X	X	45	2
mutant beta-actin (beta'-actin) [Homo sapiens]	X		45	1
ribosomal protein L17 [Homo sapiens]	X		45	9
heterogeneous nuclear ribonucleoprotein R isoform 2 [Homo sapiens]	X		45	7
Alpha-2-HS-glycoprotein chain B (AHSG) [Homo sapiens]	X		45	3
DNA-binding protein [Homo sapiens]	X		45	3
ribosomal protein L8 [Homo sapiens]	X		44	2
ribosomal protein L9 [Homo sapiens]	X		44	8
eukaryotic translation elongation factor 1 alpha 2 variant [Homo sapiens]	X		44	1

H1 histone family, member X [Homo sapiens]	X		44	1
tyrosine 3-monooxygenase/tryptophan 5-monooxygenase activation protein, beta polypeptide (14-3-3β) [Homo sapiens]	X		44	11
ribosomal protein L8 [Homo sapiens]	X		44	2
TLS protein [Homo sapiens]	X		43	3
myosin, heavy polypeptide 10, non-muscle [Homo sapiens]	X		43	11
leucine rich repeat containing 59 (LRRC59) [Homo sapiens]	X		43	4
coronin, actin binding protein, 1A [Homo sapiens]	X		43	3
hCG1642531 [Homo sapiens]	X		43	4
myosin, heavy polypeptide 9, non-muscle [Homo sapiens]	X		43	9
tubulin 5-beta [Homo sapiens]	X		43	4
splicing factor, arginine/serine-rich 3 [Homo sapiens]	X		43	4
epidermal cytokeratin 2 [Homo sapiens]	X	X	42	1
Gry-rbp [Homo sapiens]	X		42	7
Ig lambda chain precursor [Homo sapiens]	X	X	42	3
immunoglobulin light chain variable region [Homo sapiens]	X	X	42	3
elongation factor 1 alpha [Homo sapiens]	X		42	3
keratin 6B, isoform CRA_a [Homo sapiens]	X	X	41	7
hCG2043493 [Homo sapiens]	X		41	5
chaperonin (HSP60) [Homo sapiens]	X		41	4

immunoglobulin lambda-3 surrogate light chain [Homo sapiens]	X	X	41	5
immunoglobulin lambda chain variable region [Homo sapiens]	X	X	41	5
immunoglobulin lambda chain variable region [Homo sapiens]	X	X	41	5
putative RNA binding protein KOC [Homo sapiens]	X		41	8
myosin, heavy chain 7B, cardiac muscle, beta [Homo sapiens]	X		41	5
myosin, heavy polypeptide 13, skeletal muscle [Homo sapiens]	X		41	5
myosin heavy chain IIb [Homo sapiens]	X		41	4
myosin, heavy polypeptide 7, cardiac muscle, beta, isoform CRA_c [Homo sapiens]	X		41	3
ClpX caseinolytic protease X homolog precursor (CLPX) [Homo sapiens]	X		41	1
tyrosine 3/tryptophan 5 -monooxygenase activation protein, epsilon polypeptide (14-3-3ε) [Homo sapiens]	X		41	9
Ig kappa chain V-III region (Jh) [Homo sapiens]	X	X	41	3
immunoglobulin kappa chain variable region [Homo sapiens]	X		41	3
replication protein A1 (RPA1) [Homo sapiens]	X		40	5
signal sequence receptor gamma subunit (SSR3) [Homo sapiens]	X		40	4
poly A binding protein, cytoplasmic 4 isoform 2 [Homo sapiens]	X	X	40	2
heterogeneous nuclear ribonucleoprotein A2/B1 isoform A2 [Homo sapiens]	X		40	3
Fragile X mental retardation syndrome-related protein 1 FXR1 [Homo sapiens]	X		39	6
ribosomal protein L3-like [Homo sapiens]	X		39	4
ribosmal protein small subunit [Homo sapiens]	X		39	6

ribosomal protein S2 [Homo sapiens]	X		39	2
immunoglobulin kappa chain [Homo sapiens]	X	X	38	4
thyroglobulin autoantibody #26 light chain VJ region [Homo sapiens]	X	X	38	2
ALL1 fused gene from 5q31 (AF5Q31) [Homo sapiens]	X		38	4
RAP1B, member of RAS oncogene family precursor [Homo sapiens]	X		38	3
Ig kappa-chain V-J4-region precursor [Homo sapiens]	X		38	1
alpha-tubulin [Homo sapiens]	X		37	3
HDCMD47P (GSTK1) [Homo sapiens]	X		37	1
Polyadenylate-binding protein pseudogene 2 [Homo sapiens]	X	X	36	5
ribosomal protein L24 [Homo sapiens]	X		24	17
cytokeratin 9 [Homo sapiens]	X	X	11	5

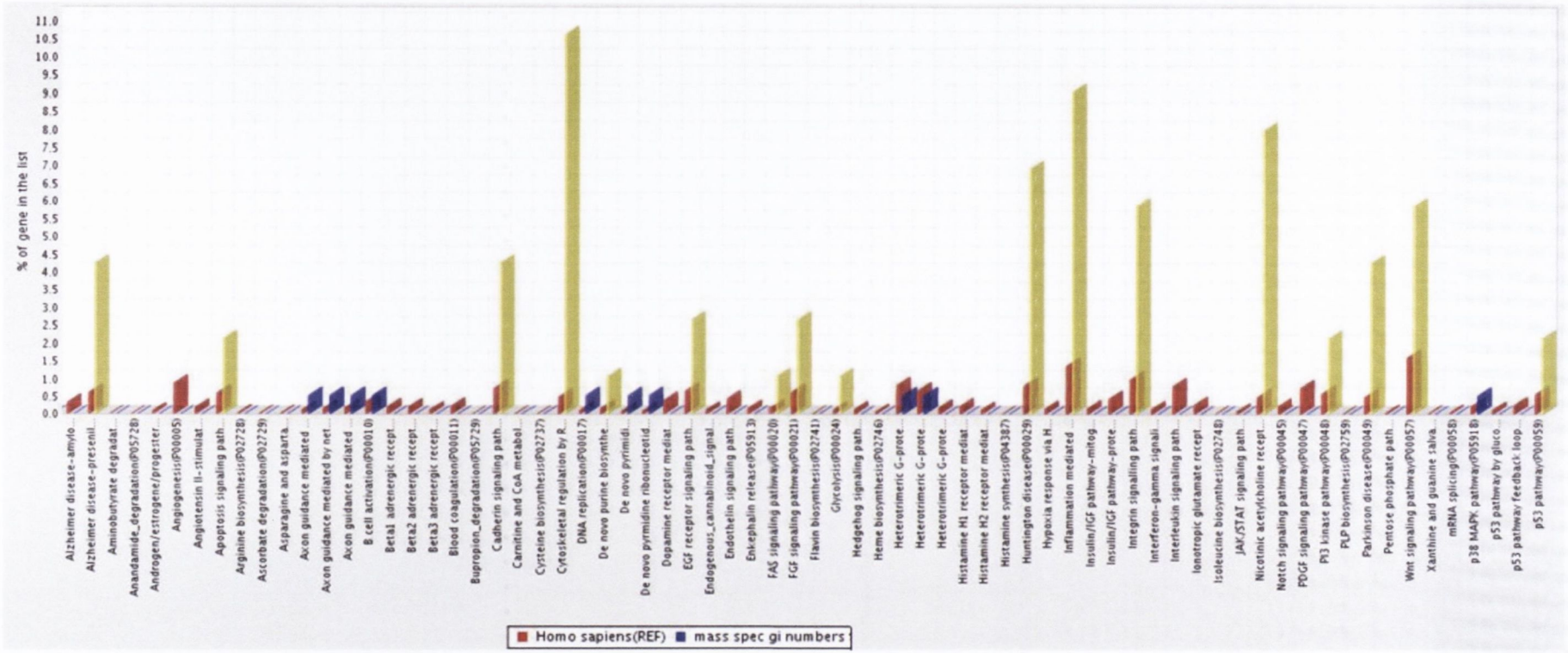

Appendix 1 Figure 1: Categorisation of proteins identified by mass spectrometry analysis of RACK1 immuno affinity purified proteins by Gene Ontology.

The accession numbers of gene products identified in mass spectrometry analysis were categorised based on molecular function using PANTHER Gene Ontology. The database was able to map 188 proteins from the analysis. The figure depicts the observed versus the expected frequency of genes in any category calculated from the *H. sapiens* reference genome. The yellow coloured bars represent categories which contain a statistically significantly ($p<0.05$) higher number of gene products from the RACK1 proteomics data compared to the expected amount.

Appendix 1 Table 2: Summary of RACK1 Proteomics Data

Signal Transduction	Cytoskeleton	Transcription Regulation	RNA maturation; protein biosynthesis and transport	Metabolic Enzymes	Other
RACK1	Tubulin (alpha, beta, gamma)	C-myc BP	RPL3	LDH	PRO2044
WDR1	Actin (alpha, beta, gamma)	DBPB	RPL7a	LDHAL6A	Albumin
14-3-3ε	Vimentin	DNA Helicase II	RPL8	PRDX1	Histone H1
14-3-3θ	NMHC-IIA (MYH9)	ZCCHC3	RPL4	ECHP	Histone H2B
14-3-3ζ	NMHC-IIB (MYH10)	ZNF9	RPL8	ATPM O	Histone H3
14-3-3β	NMHC-IIC (MYH14)	LRRC59	RPL9	AK2	AHSG
Ras-GAP SH2 Binding Protein	MYHC 7b	RPA1	RPL10	GSTK1	FLJ00293
Ras-GAP SH3 Binding Protein	MYHC 11		RPL12		AF5Q31
Prohibitin	MYHC 13		RLP13		Hsp60
Prohibitin 2	MLC 6		RPL13a		Hsp70
ATAD3A	MLC 12a		RPL14		
p21-Rac3	ARP 2/3		RPL17		
GPI-p137	TPM1		RPL18		
KHDRBS1*	TMOD3		RPL18a		
RKIP	LBP		RPL19		
PGAM5	Coronin		RPL21		
BBC1	F-actin capping protein		RPL22		
GTP-binding protein	F-actin capping protein (muscle Z-line)		RPL23		
TCR Vbeta chain	RAB35		RPL24		
	POTE-2 alpha-actin		RPL26		
	CENP-B		RPL27a		
	Gelsolin		RLP28		
	Nucleolin		RPL29		
	Transgelin 2		RPL32		
			RPL35		
			RPL36		
			RLP36a		
			RPS2		
			RPS3		
			RPS5		
			RPS6		
			RPS9		
			RPS10		
			RPS11		

			RPS13 RPS15a RPS16 RPS17 RPS19 RPS14 RPS23 RPS24 RPP2 RBM14 RAB8B RAB1B RAB1C RAB13 RAB15 RAB33b RAB43 RNA helicase p68 Proteasome subunit p58 EF-1α eIF-4A 2 eIF-2γ3 EF-Tu DDX17 hnRNP H1 hnRNP H2 hnRNP K hnRNP Ma hnRNP M4 NF45 NY-REN-2 GRY-RBP PGRMC1 PPIB SFPQ ELAVL1 KHDRBS1* TLS protein		

			FARSB IGF-II RBP LSM12 Homolog RARS2 SNRPD3 IGF2BP2 CLPX FXR1 SSR3 PABP PABP II		

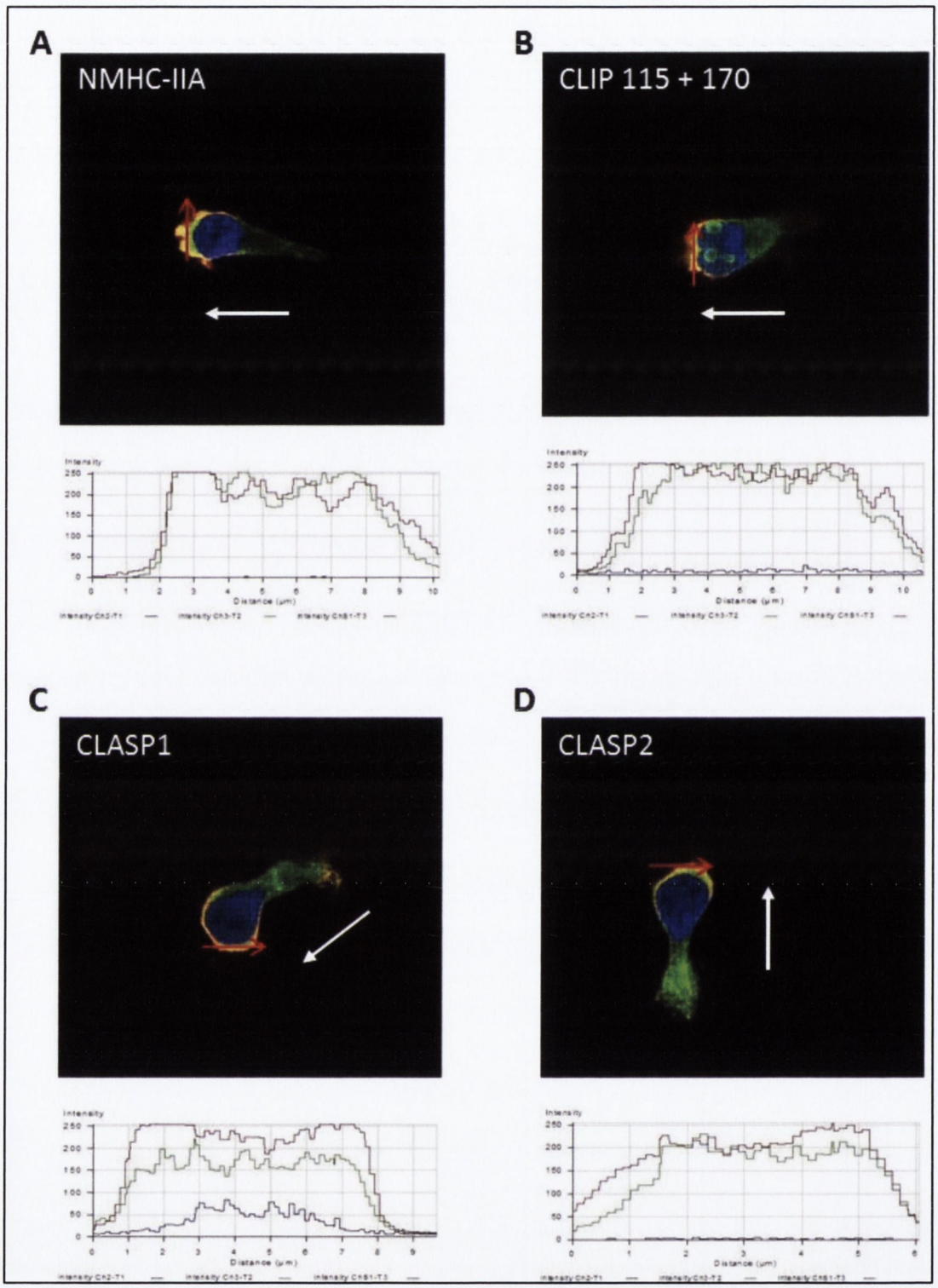

Appendix 1 Figure 2: Co-localisation of RACK1 with NMHC-IIA, CLIP-115 and -170, CLASP1 and CLASP2 at the leading edge of LFA-1-stimulated migrating T lymphocytes.

Co-localisation histograms of images acquired by confocal microscopy at 63X. Cells were stained with Hoechst nuclear stain and antibodies specific to RACK1 shown in red and NMHC-IIA (A), CLIP-115 and -170 (B), CLASP1 (C) and CLASP2 (D) shown in green. Red arrows indicate region of histogram data. White arrows indicate direction of cell migration.

Chapter 6 Supplementary Data

Appendix 1 Table 3: RACK1 Peptide Array Results

Peptide Sequence	Residue Start	Residue End	Interaction
MTEQMTLRGTLKGHNGWV	1	18	N
MTLRGTLKGHNGWVTQIA	5	23	N
GTLKGHNGWVTQIATTPQ	9	27	N
GHNGWVTQIATTPQFPDM	13	31	N
WVTQIATTPQFPDMILSA	17	35	N
IATTPQFPDMILSASRDK	21	39	N
PQFPDMILSASRDKTIIM	25	43	N
DMILSASRDKTIIMWKLT	29	47	N
SASRDKTIIMWKLTRDET	33	51	N
DKTIIMWKLTRDETNYGI	37	55	N
IMWKLTRDETNYGIPQRA	41	59	N
LTRDETNYGIPQRALRGH	45	63	N
ETNYGIPQRALRGHSHFV	49	67	N
GIPQRALRGHSHFVSDVV	53	71	N
RALRGHSHFVSDVVISSD	57	75	N
GHSHFVSDVVISSDGQFA	61	79	N
FVSDVVISSDGQFALSGS	65	83	N
VVISSDGQFALSGSWDGT	69	87	N
SDGQFALSGSWDGTLRLW	73	91	+
FALSGSWDGTLRLWDLTT	77	95	N
GSWDGTLRLWDLTTGTTT	81	99	N
GTLRLWDLTTGTTTRRFV	85	103	++
LWDLTTGTTTRRFVGHTK	89	107	++
TTGTTTRRFVGHTKDVLS	93	111	+

TTRRFVGHTKDVLSVAFS	97	115	+
FVGHTKDVLSVAFSSDNR	101	119	N
TKDVLSVAFSSDNRQIVS	105	123	N
LSVAFSSDNRQIVSGSRD	109	127	N
FSSDNRQIVSGSRDKTIK	113	131	++
NRQIVSGSRDKTIKLWNT	117	135	++
VSGSRDKTIKLWNTLGVC	121	139	++
RDKTIKLWNTLGVCKYTV	125	143	++
IKLWNTLGVCKYTVQDES	129	147	N
NTLGVCKYTVQDESHSEW	133	151	N
VCKYTVQDESHSEWVSCV	137	155	N
TVQDESHSEWVSCVRFSP	141	159	N
ESHSEWVSCVRFSPNSSN	145	163	N
EWVSCVRFSPNSSNPIIV	149	167	N
CVRFSPNSSNPIIVSCGW	153	171	N
SPNSSNPIIVSCGWDKLV	157	175	N
SNPIIVSCGWDKLVKVWN	161	179	++
IVSCGWDKLVKVWNLANC	165	183	++
GWDKLVKVWNLANCKLKT	169	187	+++
LVKVWNLANCKLKTNHIG	173	191	++
WNLANCKLKTNHIGHTGY	177	195	++
NCKLKTNHIGHTGYLNTV	181	199	++
KTNHIGHTGYLNTVTVSP	185	203	N
IGHTGYLNTVTVSPDGSL	189	207	N
GYLNTVTVSPDGSLCASG	193	211	N
TVTVSPDGSLCASGGKDG	197	215	N
SPDGSLCASGGKDGQAML	201	219	N

SLCASGGKDGQAMLWDLN	205	223	N
SGGKDGQAMLWDLNEGKH	209	227	N
DGQAMLWDLNEGKHLYTL	213	231	N
MLWDLNEGKHLYTLDGGD	217	235	N
LNEGKHLYTLDGGDIINA	221	239	N
KHLYTLDGGDIINALCFS	225	243	N
TLDGGDIINALCFSPNRY	229	247	N
GDIINALCFSPNRYWLCA	233	251	N
NALCFSPNRYWLCAATGP	237	255	N
FSPNRYWLCAATGPSIKI	241	259	N
RYWLCAATGPSIKIWDLE	245	263	N
CAATGPSIKIWDLEGKII	249	267	N
GPSIKIWDLEGKIIVDEL	253	271	N
KIWDLEGKIIVDELKQEV	257	275	N
LEGKIIVDELKQEVISTS	261	279	N
IIVDELKQEVISTSSKAE	265	283	N
ELKQEVISTSSKAEPPQC	269	287	N
EVISTSSKAEPPQCTSLA	273	291	N
TSSKAEPPQCTSLAWSAD	277	295	N
AEPPQCTSLAWSADGQTL	281	299	N
QCTSLAWSADGQTLFAGY	285	303	N
LAWSADGQTLFAGYTDNL	289	307	N
ADGQTLFAGYTDNLVRVW	293	311	N
TLFAGYTDNLVRVWQVTI	297	315	N
GYTDNLVRVWQVTIGTR	301	319	N

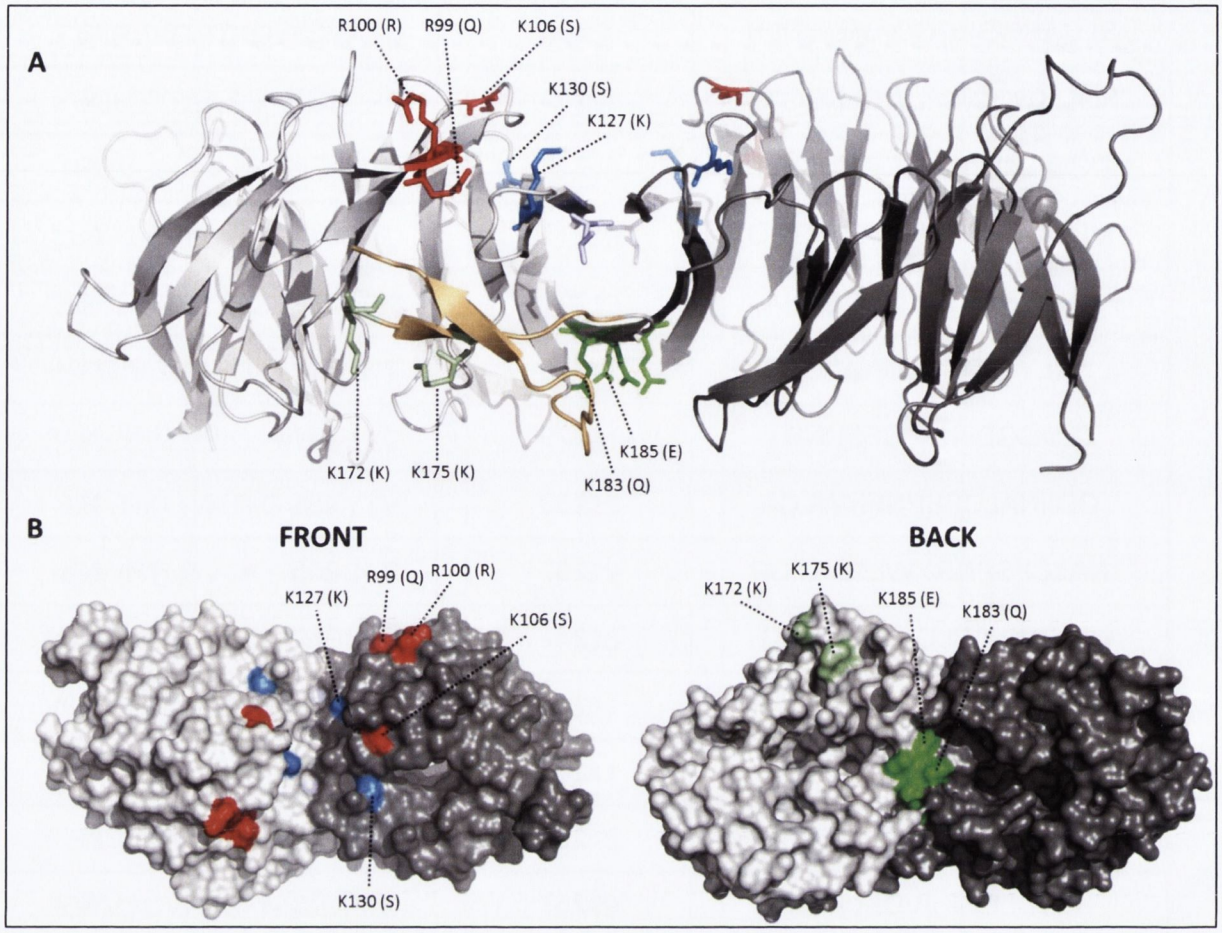

Appendix 1 Figure 3: Presentation of the key residues implicated in the NMHC-IIA interaction on the RACK1 homodimer.

(A) Structure of the dimeric yeast RACK1 ortholog, Asc1, shown in ribbon format with the extruded blade WD4 hairpin (orange). This is likely to be a flexible motif and could position K^{172} and K^{175} proximal to R^{99} and R^{100} on blade WD2. (B) Front and back structure of the dimeric yeast RACK1 ortholog, Asc1, shown with surface rendering with one protomer in light grey and the other in dark grey. The positions of key residues implicated in the interaction with NMHC-IIA are mapped onto the dark grey protomer as marked. The extruded hairpin of blade WD4 in the darker protomer is disordered in the crystal structure; hence, the apparent asymmetry and absence of one pair of K^{172}/K^{175} residues.

Appendix 2

Sources of Reagents and Antibodies

Appendix 2 Table 4: Reagents

S.N.	Reagents	Source	Cat. No.
1.	Developer Solution	AGFA	G153 A+ B
2.	Fixer Solution	AGFA	G354
3.	Bio-Rad protein assay kit	Bio-Rad	500-0001
4.	Dithiothreitol (DTT)	Bio-Rad	161-0611
5.	Marvel	Chivers Ireland, Ltd.	Grocers
6.	Rho A Activation Assay Biochem Kit	Cytoskeleton	BK036
7.	Costar 6.5mm diameter inserts	Corning, Inc.	3415
8.	Anti-fade mounting medium for immunofluorescence	Dako	S3023
9.	RACK1 siGenome siRNA	Dharmacon	M-006876-01-0005
10.	Non-targeting siGenome siRNA	Dharmacon	D-001206-13-05
11.	Pre-stained Molecular Weight Markers	GE Healthcare	RPN800E
12.	pCR8/GW/TOPO vector kit (Spectinomycin resistant)	Invitrogen	K250020
13.	Phalloidin Fluorescein Isothiocyanate Labelled	Invitrogen	A22283
14.	Hoechst nuclear stain	Invitrogen	H3569
15.	Gibco RPMI 1640 + HEPES	Invitrogen	52400-025
16.	Gibco Dulbecco's Modified Eagle Medium (DMEM)	Invitrogen	11966-025
17.	Gibco Fetal Bovine Serum (FBS)	Invitrogen	16140-071
18.	Gibco HEPES buffer	Invitrogen	15630-080
19.	Gibco PBS pH 7.2 1X Cation-Free	Invitrogen	20012-027
20.	Gibco PBS tablets (PBS)	Invitrogen	00-3002

21.	DNA ladder 1kb+	Invitrogen	10787-018
22.	Competent E. coli (TOP10)	Invitrogen	C4040-03
23.	Gateway LR Clonase II enzyme mix	Invitrogen	11791-020
24.	Dynal Dynabeads Protein G kit	Invitrogen	100-07D
25.	DynaMag Magnetic Rack-2	Invitrogen	123-21D
26.	5X DNA loading dye	Qiagen	239901
27.	0.05% Trypsin-EDTA 1X	Invitrogen	25300-054
28.	Amaxa Nucleofector Kit	Lonza	VCA-1001
29.	Amaxa Nucleofector Kit Human T Cell	Lonza	VCA-1002
30.	Millicell Hanging Cell Culture Insert , polyethylene terephthalate 5µm	Millipore	PIMP15R48
31.	Millicell Hanging Cell Culture Insert , polyethylene terephthalate 3µm	Millipore	PISP15L04
32.	Methanol	Merck	1060071000
33.	Ethanol	Merck	8187601000
34.	Acetone	Merck	8222511000
35.	Ingenio® Electroporation Solution	Mirus Bio	MIR 50117
36.	SphI	New England Biolabs	R0182S
37.	BmtI	New England Biolabs	R0658S
38.	Phusion Taq High-Fidelity PCR Master Mix	New England Biolabs	M0531L
39.	Plasticwares	Nunc	
40.	Lymphoprep®	Nycomed	1114547
41.	Matrical 96 well glass bottom plate (.17mm)	PAA	MGB096-1-2-LG-L
42.	SDF-1α (CXCL12)	PeproTech	500-P87A
43.	IL-2	PeproTech	200-02
44.	Plasmid Mini Prep Kit	Qiagen	12123

45.	QIAfilter Plasmid Midi Kit	Qiagen	12243
46.	QIAprep Spin Miniprep Kit	Qiagen	27104
47.	Qiafilter Plasmid Maxi Kit	Qiagen	12662
48.	Qiaquick Gel Extraction Kit	Qiagen	28704
49.	Human recombinant ICAM-1Fc (rICAM-1)	R&D Systems	720-IC-050
50.	Interleukin-2 (IL-2)	R&D Systems	202-IL-010
51.	Agar	Sigma	A5054
52.	Coomassie Brilliant Blue G-250	Sigma	B0770
53.	Anti-FLAG M2 Magnetic Beads	Sigma	M8823
54.	Isobutanol	Sigma	58448
55.	FLAG peptide	Sigma	F3290
56.	pCMV (Ampicillin resistance)	Sigma	E7398
57.	Sodium Chloride (NaCl)	Sigma	S-7653
58.	Magnesium Chloride ($MgCl_2$)	Sigma	7786-30-3
59.	Sodium Fluoride (NaF)	Sigma	S-7920
60.	Calcium Chloride	Sigma	C1016
61.	Chloroform	Sigma	C2432
62.	Sodium orthovanadate (Na_3VO_4)	Sigma	S-6508
63.	Ethylenediaminetetraacetic acid (EDTA)	Sigma	100933T
64.	Ethylene glycol tetraacetic acid (EGTA)	Sigma	E0396
65.	Phenylmethylsulfonylfluoride (PMSF)	Sigma	P7626
66.	Leupeptin	Sigma	L8511
67.	Sodium dodecyl sulphate (SDS)	Sigma	L-5750
68.	Phorbol 12-myristate 13-acetate (PMA)	Sigma	P8139
69.	Phytohaemagglutin (PHA)	Sigma	L-2769
70.	Paraformaldehyde (PFA)	Sigma	P6148
71.	Sodium bicarbonate (Na_2CO_3)	Sigma	S5761
72.	Sodium pyrophosphate decahydrate	Sigma	223168
73.	Chloroquine	Sigma	C6628

74.	Ethidium bromide	Sigma	E7637
75.	Bovine Serum Albumin (BSA)	Sigma	A2153
76.	Glycerol	Sigma	G5516
77.	Agarose (low melting)	Sigma	A9414
78.	Triton X-100	Sigma	X100
79.	Igepal (Nonidet P-40)	Sigma	CA-630
80.	Trizma Base (Tris)	Sigma	T-1503
81.	Glycine	Sigma	G8898
82.	Bromophenol Blue	Sigma	B-0126
83.	Dimethyl Sulphoxide (DMSO)	Sigma	D2438
84.	Poly-L lysine	Sigma	P4707
85.	Tween-20	Sigma	P1379
86.	Ammonium persulphate (APS)	Sigma	A3678
87.	*N,N,N',N'*-Tetramethylethylenediamine (TEMED)	Sigma	T-9281
88.	Coomassie R-250	Sigma	27816
89.	Kodak® light sensitive film	Sigma	F1274
90.	Hydrogen Peroxide	Sigma	516813
91.	Penicillin-Streptomycin Solution (Antibiotics)	Sigma	P4333
92.	Cytochalasin D	Sigma	C8273
93.	Nocodazole	Sigma	M1404
94.	Cell permeable Hoechst nuclear stain	Sigma	33342
95.	2X HEPES Buffer	Sigma	51558
96.	SOC Medium	Sigma	S1797
97.	LB Broth	Sigma	L3022
98.	Unstained Molecular Weight Markers	Sigma	SDS6H2
99.	Spectinomycin	Sigma	S4014
100.	Ampicillin	Sigma	A0166
101.	BDH Chemicals Acrylamide-bisacrylamide solution, Acrylogel (30%)	Sigma	A3699

102.	pFLAG-CMV™-2 Expression Vector	Sigma	E7033
103.	Fermentas 10X Tris-Borate-EDTA (TBE)	Thermo Scientific	B52
104.	Lab-Tek II Chamber slide (Nunc)	Thermo Scientific	154534
105.	BDH Chemicals Hydrochloric acid (HCL)	VWR	101254H
106.	PVDF membrane	VWR	66543

Appendix 2 Table 5: Antibodies

S.N.	Antibodies	Source	Cat No.
1.	Mouse monoclonal anti-CD3 (SP7)	Abcam	ab16669
2.	Mouse monoclonal L-plastin	Abcam	ab3290
3.	Mouse monoclonal IgM anti-RACK1	BD Transduction	610177
4.	Rabbit Antibody anti-NMHCIIA	Biomedical Technologies, Inc.	BT-567
5.	Goat anti-mouse IgG polyclonal antibody HRP conjugated	Cell Signalling	7074
6.	Goat anti-rabbit IgG polyclonal antibody HRP conjugated	Cell Signalling	7076
7.	Rabbit Phospho specific (Thr18/Ser19) Myosin Light Chain antibody	Cell Signalling	3674
8.	Rabbit Phospho specific (ser19) Myosin Light Chain antibody	Cell Signalling	3671
9.	Rabbit Regulatory Myosin Light Chain antibody	Cell Signalling	3672
10.	Mouse monoclonal anti-Rho A antibody	Cytoskeleton	ARH03
11.	Rabbit anti-mouse IgG	DAKO	Z0259
12.	Goat anti-mouse IgM Fab Fragment	Jackson ImmunoResearch	115-007-020
13.	AlexaFluor goat anti-mouse 488	Molecular Probes	A-11001
14.	AlexaFluor goat anti-rabbit 546	Molecular Probes	A-11003

15.	AlexaFluor goat anti-rabbit 488	Molecular Probes	A-11008
16.	Mouse anti-LFA-1 (clone SPVL7, mAb to the α–chain of LFA-1)	Monosan	MON1020-1
17.	Mouse monoclonal anti-PDLIM2	Patrick Kiely, UL, Ireland	----------
18.	PE-conjugated mouse monoclonal anti-CXCR4 (clone 12G5)	R&D Systems	FAB170P
19.	Rabbit Phospho specific (ser19) Myosin Light Chain antibody	Rockland	600-401-416
20.	Rabbit polyclonal anti-PKC ζ (C-20)	Santa Cruz	sc-216
21.	Normal Rabbit IgG	Santa Cruz	sc2027
22.	Normal Mouse IgG	Santa Cruz	sc3881
23.	Mouse IgM Control (clone MOPC-104E)	Sigma	M5909
24.	Rabbit Monoclonal Antibody Anti-FLAG (Clone M2)	Sigma	F7425
25.	Goat anti-mouse IgG	Sigma	M8642
26.	Rabbit polyclonal anti-actin	Sigma	A2066
27.	Mouse monoclonal anti-α-tubulin (Clone DM1A)	Sigma	T6199
28.	Mouse monoclonal anti-acetylated tubulin (Clone 6-11B-1)	Sigma	T6793
29.	Mouse monoclonal anti-tyrosinated tubulin (Clone TUB-1A2)	Sigma	T9028
30.	Goat anti-human IgG (Fc specific)	Sigma	I2136
31.	Mouse monoclonal anti-phosphotyrosine (Clone 4G10)	Upstate	05-321

Addresses

Abcam: Abcam, Cambridge, MA, USA.

Biomedical Technologies, Inc.: Staughton, MA, USA.

BDH Chemicals: BDH, VWR International Ltd., England.

BD Transduction: Heidelberg, Germany.

Bio-Rad: Bio-Rad Laboratories GmbH, München, Germany.

Cell Signalling Technology: Cell Signalling Technology, Danvers, MA, USA.

Chemicon: Millipore Corporation, Billerica, MA, USA.

Chivers Ireland Ltd.: Chivers Ireland Ltd., Dublin 5, Ireland.

Corning Inc.: Corning Life sciences, Lowell, MA, USA

Dako: Dako A/S, Denmark.

Gibco (Invitrogen): Carlsbad, CA, USA.

Invitrogen: Carlsbad, CA, USA.

Mirus Bio LLC: Madison, WI USA

Molecular Probes: Invitrogen Corporation, CA, USA.

Monosan: Sanbio, Uden, Netherlands.

New England Biolabs: Ipswich, MA, USA.

Nunc: Thermo Fisher Scientific (Nunc GmbH & Co. KG), Langenselbold, Germany.

Nycomed: Nycomed Pharma AS, Norway.

Pepro Tech, Inc.: Rocky Hill, NJ, USA.

Promega: Promega, Madison, WI, USA.

R&D Systems: R&D Systems, MN, USA.

Rockland Immunochemicals, Inc.: Philadelphia, Pennsylvania, USA

Santa Cruz Biotechnology, Inc.: Santa Cruz, CA, USA

Sigma Aldrich: Sigma Chemicals Company, St Louis, MO, USA.

Upstate: Upstate, Lake Placid, NY, USA.

VWR International LLC: West Chester, Pennsylvania, USA.

Zymed Laboratories (Invitrogen): Carlsbad, CA, USA.

Appendix 3

REAGENTS AND BUFFERS

A. Cell Culture Reagents

Complete Cell Culture Medium - HuT78 T cells

RPMI 1640 + HEPES (25.03 mM) + L-Glutamine (2.05 mM)	500 ml
Heat inactivated foetal bovine serum (FBS)	50 ml
Sodium bicarbonate solution (7.5%)	10 ml
Sodium pyruvate solution (100 mM)	5 ml
Penicillin-Streptomycin solution	5 ml

Complete Cell Culture Medium – Jurkat T cells

RPMI 1640 + HEPES (25.03 mM) + L-Glutamine (2.05 mM)	500 ml
Heat inactivated foetal bovine serum (FBS)	50 ml
Penicillin-Streptomycin solution	5 ml

Complete Cell Culture Medium – PBT cells

RPMI 1640 + HEPES (25.03 mM) + L-Glutamine (2.05 mM)	500 ml
Heat inactivated FBS	50 ml
Penicillin-Streptomycin solution	10 ml

Cell Cryopreservation Medium

FBS	9 ml
Dimethylsulfoxide (DMSO)	1 ml

Phosphate-Buffered saline (PBS) 1X

PBS tablets (Gibco)	5 g

Each 5 g tablet dissolved in 500 ml distilled water and sterilised by autoclaving.

PHEM Buffer

PIPES	60 mM
HEPES (pH 7.4)	25 nM
EGTA	10 nM
$MgCl_2$	20 mM

The pH was adjusted to pH 6.9 with dilute HCl and was stored at 4°C.

Paraformaldehyde – fixation reagent (3%)

Paraformaldehyde	2 g
PBS	50 ml

While heating to dissolve paraformaldehyde we ensured not to not exceed 56°C, so as to avoid resulting reagent autofluorescence.

Luria Bertani (LB) Broth

LB Broth powder	2 g

2 g of LB broth powder was added to 400ml distilled water and sterilised by autoclaving. Indicated antibiotics were diluted 1:1000 and added after broth was cooled.

Luria Bertani (LB) Broth + Agar

LB Broth powder	2 g
Agar powder	5 g

2 g of LB broth powder and 5 g of agar powder was added to 400ml distilled water and sterilised by autoclaving. Indicated antibiotics were added at 1:1000 dilution after broth was cooled. The solution was then poured into plates and stored at 4°C.

B. Cell Lysis Reagents

Cell Lysis Buffer 1

Tris-HCl (pH 7.4)	20 mM
$MgCl_2$	1.5 mM
EGTA	5 mM
EDTA	5 mM

Sodium pyrophosphate	5 mM
Sodium fluoride	5 mM
β-glycerophosphate	50 mM
Triton X-100	1% (v/v)
Na_3VO_4	1 mM
Phenylmethylsulphonyl fluoride	1 mM
Leupeptin	10 μg/ml

N.B. Protease and phosphatase inhibitors were added fresh before lysis.

Cell Lysis Buffer 2

Tris-HCl (pH 7.4)	20 mM
$MgCl_2$	1.5 mM
EGTA	5 mM
EDTA	5 mM
Sodium pyrophosphate	5 mM
Sodium fluoride	5 mM
Nonidet P40 (Igepal)	1% (v/v)
Na_3VO_4	1 mM
Phenylmethylsulphonyl fluoride	1 mM
Leupeptin	10 μg/ml

N.B. Protease and phosphatase inhibitors were added fresh before lysis. For IP of cell lysates for mass spectrometry experiments, the cell lysis buffer was used with 1% NP-40 or 0.5% Digitonin.

RIPA Buffer

Tris-HCL (pH 7.2)	50 mM
NaCl	150 mM
Nonidet P-40 (Igepal)	1% (v/v)
Sodium deoxycholate	0.5% (w/v)
SDS	1% (w/v)
EDTA	1 mM
EGTA	1 mM
Sodium fluoride	50 mM
Phenylmethylsulphonyl fluoride	2 mM
Leupeptin	10 μg/ml

N.B. Protease and phosphatase inhibitors are added fresh before lysis.

RACK1 Cell Lysis Buffer

Tris-HCL (pH 7.2)	50 mM
NaCl	150 mM
Nonidet P-40 (Igepal)	1% (v/v)
Na_3VO_4	1 mM
Phenylmethylsulphonyl fluoride	1 mM
Leupeptin	10 μg/ml

N.B. Protease and phosphatase inhibitors were added fresh before lysis.

High Salt Buffer

Tris-HCL (pH 7.2)	50 mM
NaCl	300 mM
Nonidet P-40 (Igepal)	0.5% (v/v)
EDTA (pH 7.4)	1mM
Na_3VO_4	1 mM
Phenylmethylsulphonyl fluoride	1 mM
Leupeptin	10 μg/ml

N.B. Protease and phosphatase inhibitors were added fresh before lysis.

Activated Sodium Orthovanadate (Na_3VO_4)

A 100 mM solution of Na_3VO_4 was prepared in 100 ml distilled water. The pH was adjusted to 10.0 to give a yellow colour. The solution was boiled until it turned colourless and allowed to cool to room temperature. The pH was readjusted to 10.0 and the sample was boiled and allowed to cool (this step was repeated a number of times) until the solution remained colourless and the pH stabilised at 10.0. The solution was aliquoted and stored at -20°C.

2X SDS Sample Buffer

Trizma	3.03 g
Glycerol	40 ml
SDS powder	8 g
Bromophenol blue	0.004 g
distilled water	215 ml

N.B. The following was combined: 1.51 g Trizma, 20 ml Glycerol, 35 ml distilled water and the pH was adjusted to pH 6.8 and then 8g SDS, 0.004g bromophenol blue, and distilled water to 180ml was added. The buffer was stored at room temperature. DTT

was added to final concentration of 100 mM immediately before use. This solution was added to the lysate to give a final concentration of 1X.

C. SDS-PAGE Reagents

Appendix 3 Table 6: Components of the resolving gel solution for SDS-PAGE

Component	**6% gel**	**8% gel**	**10 % gel**	**12 % gel**
Distilled water	10.6 ml	9.3 ml	7.9 ml	6.6 ml
1.5 M Tris-HCl; pH 8.8	5.0 ml	5.0 ml	5.0 ml	5.0 ml
10 % w/v SDS	200 µl	200 µl	200 µl	200 µl
10 % w/v APS	200 µl	200 µl	200 µl	200 µl
TEMED	16 µl	12 µl	8 µl	8 µl
30 % Polyacrylamide	4.0 ml	5.3 ml	6.7 ml	8.0 ml
Total	**20 ml**	**20 ml**	**20 ml**	**20 ml**

Appendix 3 Table 7: Components of the stacking gel solution for SDS-PAGE

Component	**5% gel**
Distilled water	6.8 ml
1.5 M Tris-HCl; pH 8.8	1.25 ml
10 % w/v SDS	100 µl
10 % w/v APS	100 µl
TEMED	10 ml
30 % Polyacrylamide	1.7 ml
Total	**10 ml**

D. Western Blot Buffers

HRP Development Solution

100 mM Tris-HCl (pH 8.5)	12 mls
30% Hydrogen Peroxide	7.2 µl
250 mM luminol	60 µl
90 mM 4 Iodophenylboronic acid in DMSO	266 µl

The solution was made fresh immediately before putting on blot and is enough for one mini Western blot membrane. All stocks were stored at room temperature in foil to protect from light.

Western Blot Stripping Buffer

SDS	2 % (w/v)
Tris-HCl (pH 6.8)	50 mM
2-Mercaptoethanol	100 mM

Membranes for immunoblot were stripped of probing antibodies by submerging blot in stripping buffer and heating to 50°C, incubating for up to 45 minutes with some agitation in fume hood, and washing extensively in TBS/T. The membrane was then immersed in blocking buffer or 1 hour at room temperature and re-probed for another protein of interest or loading control (e.g. actin).

10% Ammonium persulphate (APS)

APS	0.1 g
Deionised water	1.0 ml

Make up fresh before use.

E. High Content Analysis

Appendix 3 Table 8: IN Cell Parameters (Adapted from Product User Manual, 2006)

Parameter	Definition
Cell Count	The number of targets contained within the region of interest.
Cell Area	The area is calculated by counting pixels inside target outline borders, not including the border itself.
Cell Perimeter	The length of the target's outer boundary.
Cell Elongation	Mean ratio of the short axis of the cell to the long axis of the cell. If the value is 1 then the object is centre-symmetric (not elongated). Short and long axes are orthogonal and do not necessarily pass through the shape centre of gravity.
Cell Gyration Radius	Average radius of the shape.
Nuclear Displacement	The distance between the nucleus's and the cell's centres of gravity, normalised by the gyration radius of the nucleus.
Cell1 Form Factor	Mean cell roundness index. The standard estimate of circularity relates perimeter length to area; the measurement varies from 0 to 1, with 1 being a perfect circle.
Cell Intensity	Average intensity of pixels within the cytoplasm region.
Nuclear Intensity	Average intensity of pixels within the nucleus.
Intensity (N + C)	Average fluorescence intensity of pixels in whole cell (nucleus + cytoplasm).
I x A (nucleus + cell)	The amount of light emitted by the whole cell. It is equal to cytoplasm average intensity multiplied by cell area.
Cell/Background Intensity	Ratio of cytoplasm to local background intensity values.
Intensity Spreading	Intensity-based descriptor allowing estimation of the extent of intensity concentration near the boundary of the cell.
Cell Intensity CV	Describes the coefficient of variation of the fluorescence intensity of pixels within the cytoplasm.